Molecular markers associated with resistance to combined CDK4/6 inhibitor and endocrine therapy in advanced ER+ breast cancer

Kindt, Charlotte Karup

DOI:
10.21996/zs9n-7y36

Publication date:
2023

Document version:
Final published version

SDU
Syddansk Universitet

Department of Molecular Medicine
Cancer and Inflammation Research

Charlotte Karup Kindt

PhD Thesis

Molecular markers associated with resistance to combined CDK4/6 inhibitor and endocrine therapy in advanced ER+ breast cancer

April 2023

Supervisor

Professor Dr. Henrik J. Dtizel, MD, Ph.D., DMSc
Department of Molecular Medicine
Cancer and Inflammation Research
University of Southern Denmark

Co-supervisors

Carla L. Alves, Ph.D., Post.doc.
Department of Molecular Medicine
Cancer and Inflammation Research
University of Southern Denmark

Annette Raskov Kodahl, MD, Ph.D.
Department of Oncology
Odense University Hospital

Assessment committee

Professor Jesper Nylandsted, Ph.D. (Chair)
Department of Molecular Medicine
Cancer and Inflammation Research
University of Southern Denmark

Professor Mårten Fernö, Ph.D
Division of Oncology and Pathology
Department of Clinical Sciences
Lund University

Clinical Associate Professor Iben Kümler, MD, Ph.D., consultant
Department of Oncology
Herlev University Hospital

Preface and acknowledgements

The work in this thesis was performed under the supervision of Prof. Dr. Henrik Ditzel, Postdoc. Dr. Annette Raskov Kodahl, and Postdoc. Carla Alves at the Ditzel laboratory in the Department of Molecular Medicine, Faculty of Health Science, University of Southern Denmark, Odense. The work was carried out between March 2019 and April 2024.

I am grateful to my supervisor Henrik Ditzel for giving me the opportunity to join his research group and for providing scientific guidance throughout the project. I also want to express my gratitude to my co-supervisors Annette Raskov Kodahl and Carla Alves for their invaluable support and assistance. Annette, thank you for your help in navigating the clinical world and optimizing patient enrollment in the project. Without your contributions, there would be no patient samples to analyze. And Carla, your expertise with in vitro data and daily guidance were essential to the success of this project.

I would also like to acknowledge the co-authors of the manuscripts included in this thesis for their valuable contributions. Special thanks go to Sidse Ehmsen for her assistance in project planning and clinical data collection. This project would not have been possible without her support.

I am also grateful to the entire Ditzel group for creating a supportive and enjoyable work environment. The technicians in the group, especially Lene Johansen, deserve a special thanks for their assistance in the laboratory.

Lastly, I would like to thank my friends and family, particularly Thorbjørn, for their unwavering support and patience. I am grateful to my parents and in-laws for their help during stressful times, to Sofie for proofreading, and to Ida for reminding me of what really matters.

Charlotte Karup Kindt
April 2023

Manuscripts included in the thesis

Manuscript 1
Charlotte Karup Kindt, Sidse Ehmsen, Sofie Traynor, Monique F. Hundebøl, Lene E. Johansen, Martin Bak, Elsa Arbajian, Johan Staaf, Henrik Ditzel, Carla Alves. *RET inhibition overcomes resistance to combined CDK4/6 inhibitors and endocrine therapy in ER+ breast cancer.* In preparation.

Manuscript 2
Charlotte Karup Kindt, Carla Alves, Sidse Ehmsen, Amalie Kragh, Thomas Reinert, Marianne Vogsen, Annette Raskov Kodahl, Jeanette Dupont Jensen, Dilan Ardik, Rasmus Koefod Petersen, Johan Staaf, Henrik Ditzel. *Genomic alterations associated with CDK4/6 inhibitor resistance and serial circulating tumor DNA monitoring in CDK4/6 inhibitor treated patients with advanced estrogen receptor-positive breast cancer.* In preparation.

Contents

Summary

Breast cancer is the leading cause of cancer-related deaths among women worldwide, with the estrogen receptor-positive (ER+) subtype accounting for 70% of cases. Patients with primary ER+ breast cancer are treated with endocrine therapy, while those with metastatic disease receive combined CDK4/6 inhibitor (CDK4/6i) and endocrine therapy. Although this therapy has improved clinical outcomes, resistance is inevitable, and optimal subsequent therapy is unclear. Therefore, metastatic breast cancer remains an incurable disease. This Ph.D. project aimed to identify possible resistance mechanisms and monitor disease progression in patients receiving combined CDK4/6i and endocrine therapy for advanced ER+ breast cancer.

The investigation into resistance mechanisms was tackled using two distinct methods. By using cell lines that were resistant to combined CDK4/6i and endocrine therapy, manuscript 1 identified high RET expression to be associated with CDK4/6i and endocrine therapy resistance in ER+ breast cancer. Furthermore, targeting RET with a specific inhibitor significantly reduced cellular growth of resistant cell lines.

Manuscript 2 performed sequencing on paired tumor and blood samples before and after therapy, and this revealed pathogenic *TP53* and *PIK3CA* mutations as potential mutations associated with resistance. Copy number variations of genes such as *PDK1*, were more common. Serial analysis of circulating tumor DNA for mutant *PIK3CA* revealed disease progression before clinical evidence in three of six patients 4-17 months prior to diagnosis of progression.

Collectively, our study suggests that RET inhibition in combination with CDK4/6i and endocrine therapy may be a promising therapeutic approach for advanced ER+ breast cancer patients who experience disease progression. Additionally, the use of serial circulating tumor DNA analysis could lead to earlier identification of progressive disease and be used for real-time monitoring of combined CDK4/6i and endocrine therapy response.

Dansk resume

Brystkræft er den førende årsag til kræftrelaterede dødsfald blandt kvinder verden over, og østrogenfølsom brystkræft udgør 70 % af alle tilfælde. Patienter med primær østrogenfølsom brystkræft er kandidater til endokrin behandling, mens patienter med metastatisk sygdom tilbydes CDK4/6-hæmmer kombineret med endokrin behandling. Selvom denne form for behandling sikrer en forsinkelse af sygdomsprogressionen, er resistens uundgåelig, og det er uklart, hvad den optimale efterfølgende behandling er. Dermed er metastatisk brystkræft stadig en uhelbredelig sygdom. Målet med dette Ph.d.-projekt er at identificere resistensmekanismer og overvåge sygdomsspredning i patienter, der modtager kombineret CDK4/6-hæmmer og endokrin behandling for metastatisk østrogenfølsom brystkræft.

I manuskript 1 undersøgte vi resistensmekanismer mod kombineret CDK4/6-hæmmer og endokrin behandling. Vi brugte genekspressionsdata fra cellelinjer, der var resistente mod behandlingen, og vi identificerede et højt RET-udtryk, hvilket kunne være skyld i resistens mod kombineret CDK4/6-hæmmer og endokrin behandling. Når RET blev inhiberet med en RET-specifik hæmmer, blev resistente cellelinjers vækst signifikant reduceret.

I manuskript 2 evaluerede vi genomiske ændringer, herunder mutationer og copy number-forandringer. Vi udførte sekventering af parrede tumor og blodprøver taget før og efter kombineret CDK4/6-hæmmer og endokrin behandling. Dette afslørede patogene *TP53* og *PIK3CA* mutationer og copy number-forandringer i *PDK1*, der kunne være potentiel årsag til resistensen. Analyse af muteret *PIK3CA* i cirkulerende tumor DNA fra serielle blodprøver, taget under behandling med kombineret CDK4/6-hæmmer og endokrin behandling, afslørede sygdomsprogression i tre ud af seks patienter 4-17 måneder, før progression blev diagnosticeret med en PET-scanning.

Samlet indikerer dette studie, at en RET-hæmmer muligvis er en lovende behandling for patienter med metastatisk østrogenfølsom brystkræft, der oplever progression på CDK4/6-hæmmer og endokrin behandling. Derudover kan genomisk analyse af tumorer og blodprøver potentielt identificere patient-specifikke mutationer, der kan bruges til seriel analyse af cirkulerende tumor DNA. Dette kan føre til overvågning af sygdomsspredning og tidligere opdagelse af progression blandt patienter, der modtager kombineret CDK4/6-hæmmer og endokrin behandling.

Overall goal and specific aims of the project

This Ph.D. project has an overall goal of determining possible resistance mechanisms towards combined CDK4/6i and endocrine therapy while identifying genomic alterations that can be used to monitor disease progression over time in blood samples of patients receiving this treatment. The following specific aims will be addressed:

I. Investigating the role of the RET protein in resistance towards combined CDK4/6i and endocrine therapy, with a primary focus on breast cancer cell lines.

II. Identifying genetic alterations that could potentially be associated with resistance towards combined CDK4/6i and endocrine therapy in both tumor and blood samples from patients with advanced ER+ breast cancer.

III. Examining whether these genetic alterations can be used to monitor disease progression over time in serial blood samples from patients undergoing combined CDK4/6i and endocrine therapy.

Chapter 1: Breast cancer subtypes and therapy

Breast cancer is the most common cause of cancer related deaths in women in 2020 (1, 2). It accounts for 2.3 million cases each year and approximately 685,000 deaths worldwide (1, 2). In Denmark approximately one in ten women will be diagnosed with breast cancer before the age of 75 and every year the disease causes around 1000 deaths (1).

Breast cancer subtypes

Breast cancer is a very diverse disease, and several research groups have made an effort to improve responsiveness to treatment by subdividing it into subtypes. Perou and Sørlie presented 4 subtypes of breast cancer based on microarray analysis of 65 breast cancer samples in 2000 (3). These were: ER+/luminal-like, basal-like, human epithelial growth factor receptor 2 positive (HER2+), and normal breast. Further studies showed that the luminal-like subtype can be divided further into two subtypes called luminal A and luminal B. Luminal A has a greater expression of ER-related genes and luminal B expresses more proliferative genes (4, 5). In 2007 a fifth subgroup was identified, when the claudin-low breast cancer was characterized (6), which is similar to basal-like tumors but with a different molecular profiling (7). Since these subtypes were described, it has been shown that molecular profiling is clinically relevant with significant differences in overall survival (OS) and response to chemotherapy (4, 8). Although several other techniques to evaluate subgroups have been described, immunohistochemical staining of tumor tissue to evaluate hormone receptor status is the golden standard in classification of the tumor (9-11). The classification into these subgroups rely on the three receptors: ER, progesterone receptor (PR) and HER2. These constructed subgroups consist of luminal A (ER+ or PR+ and HER-), luminal B (ER+ or PR+ and HER+), HER2 (ER- and PR- and HER2+) and basal (ER- and PR- and HER2-) (10, 12, 13). Basal is also referred to as triple negative. Overall, ER is expressed in 70-80% of breast cancer tumors (luminal subtype) (14), and HER2 enriched and triple negative subtypes represent 10-15% and 10% of breast cancers respectively (15). These are associated with a poorer overall prognosis than luminal cancers (16). Recent studies have shown that patients with tumors determined as HER2- benefit from treatment with trastuzumab deruxtecan which is based on an anti-HER2 monoclonal antibody. Even though they are deemed HER2- the more appropriate name is HER2-low since most of them express low amounts of HER2 receptor (17). Thus, the old classification system might be deemed obsolete as new treatments arrive.

Treatment

Treatment decision is based on tumor morphology, tumor grade, tumor size, nodal involvement, the expression of the abovementioned different receptors and expression of proliferation markers (e.g. Ki67) (18). Patients who present with early breast cancer is initially offered breast-conserving surgery, followed by adjuvant therapy based on the subtype of cancer (18). Patients with ER+ breast cancer is offered endocrine therapy - alone for luminal A cancers and following chemotherapy for luminal B cancers (18).
ER+ breast cancer is dependent on ER signaling to promote growth and cell proliferation. When estrogens, such as 17β-estradiol, binds to the ER, it promotes homodimerization, which results in its translocation to the nucleus of the cell (Figure 1). Here it binds directly with parts of the DNA called estrogen-response elements and this attracts various co-regulators and thus acts as a transcription factor which induces the transcription of different growth factors (19). This is important in the normal setting where estrogens play and important role in growth and development of female mammary and reproductive physiology, but in ER+ breast cancer it has been shown to play a vital role in tumorigenesis (20).
Endocrine therapy consists of four different groups: selective estrogen receptor modulators (SERMs), selective estrogen receptor downregulators (SERDs), aromatase inhibitors (AIs), and ovarian function suppression (OFS). The basic mechanisms of function for SERDS and SERMS can be seen in figure 1. Introducing endocrine therapy has prolonged the progression-free survival but approximately 30% of breast cancer patients experience relapse over time, and resistance towards endocrine treatment remains a major clinical challenge (21, 22).

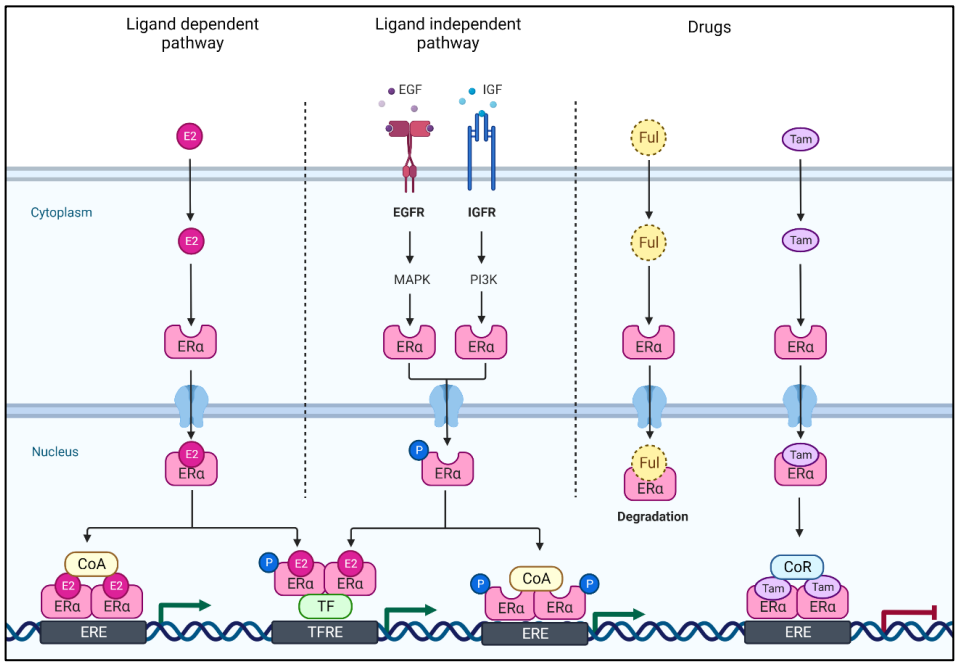

Figure 1: Estrogen signalling in ER+ breast cancer and mechanisms of action of the SERD fulvestrant (ful) and the SERM tamoxifen (Tam). CoA: Steroid receptor Coactivator, CoR: steroid receptor Corepressor, E2: Estradiol, ER: Estrogen receptor, ERE: Estrogen receptor response element, TF: transcription factor. Adapted from "Estrogen Receptor Signaling", by BioRender.com (2023)

SERMs are estrogen receptor antagonists that compete with estrogen and modulate ER activity. When binding to the ER, it induces a conformational change different to what estrogen induces, thus changing which co-regulators bind to the homodimer. As a result, the activation of the receptor is blocked (23). The most widely used SERM is Tamoxifen. This is antagonistic in breast tissue, but has an agonistic effect in the uterus, bone and the heart (24). This drug has been used for over 30 years as an adjuvant therapy in pre- and postmenopausal women. It has been shown to significantly reduce breast cancer recurrence and mortality in patients with early breast cancer (25).

Post-menopausal women that present with early ER+ breast cancer are offered AI therapy (e.g. letrozole). This binds to the aromatase enzyme that is responsible for synthesizing estrogen from adrenal steroids in the post-menopausal setting (26). OFS is given to pre-menopausal women to prevent the release of estrogen from the ovaries. This can be done by surgery, radiation or drug adinistration and is also given in combination with either a SERM or an AI (27).

The most commonly used SERD is fulvestrant, which is approved for use in post-menopausal women with metastatic ER+ breast cancer after progression on earlier treatment with another endocrine therapy such as tamoxifen. It induces degradation by binding to ER, and inhibiting the dimerization and nuclear localization (Figure 1) (28).

Fulvestrant is also given in combination with a CDK4/6 inhibitor (CDK4/6i) (palbociclib, ribociclib or abemaciclib) to pre-and post-menopausal women who have progressed on prior endocrine therapy monotherapy (29-31). The addition of a CDK4/6i in this metastatic setting increased progression free survival (PFS) from 4.6 months to 9.5 months in patients with metastatic ER+ breast cancer who received placebo and fulvestrant or combined palbociclib and fulvestrant therapy, respectively (32, 33). CDK4/6 plays a key role in the progression from the G1 phase to S phase in the cell cycle. They interact with cyclin D, and hyperphosphorylates the retinoblastoma (Rb) protein, which leads to its inactivation and the release of transcription factors that allow progression to the S phase (34). CDK4/6is inhibits the CDK4/6 kinases, and thus arrest the cells in G1 phase. CDK4/6is are also approved in combination with an AI as first-line treatment for postmenopausal women with advanced ER+ breast cancer (35-37). In the first-line metastatic setting the PFS ranges from 23.8-28.8 months when treated with combined CDK4/6i and endocrine therapy (38-40).

A study has recently compared ribociclib and palbociclib, and the conclusion was that OS and quality-adjusted life years was significantly longer with ribociclib, which therefore is the first choice for first-line treatment in postmenopausal women with advanced ER+ breast cancer (41). Importantly, palbociclib has failed to show significant OS benefit, which riboclib has shown a consistent OS benefit that is independent from the menopausal status (42, 43). In table 1 there is an overview of the clinical trials conducted with different CDK4/6i and endocrine therapies.

Table 1: Efficacy of CDK4/6 inhibitors in* ER+*, HER2-negative* advanced breast cancer *phase III trials. *Adapted from (53)*

				Median PFS in months			Median OS in months		
	Study name	ET partner	Sample size	With CDK4/6i	Without CDK4/6i	Statistically Significant as per protokol	With CDK4/6i	Without CDK4/6i	Statistically Significant as per protokol
ET +/- Abemaciclib	MONARCH-2 (30, 45)	Fulvestrant	669	16.4	9.3	yes	45.8	37.3	yes
	MONARCH-3 (38, 46)	AI	493	28.2	14.8	yes	67.1	54.5	final analysis not yet reported
ET +/- palbociclib	PALOMA-2 (35, 43)	AI	666	24.8	14.5	yes	53.9	52.1	no
	PALOMA-3 (32, 52)	Fulvestrant	521	9.5	4.6	yes	34.9	28	no
ET +/- ribociclib	MONALEESA 2 (47, 48)	AI	668	25.3	16	yes	63.9	51.4	yes
	MONALEESA 3 (49, 42)	Fulvestrant	726	20.5	12.8	yes	53.7	41.5	yes
	MONALEESA 7 (50, 51)	OFS + Tamoxifen or fulvestrant	672	23.8	13	yes	58.7	48	yes

AI: Aromatase inhibitor, ET: endocrine therapy, OFS: ovarian function suppression, OS: overall survival, PFS: progression free survival.

References

1. Estimated cancer incidence, mortality and prevalence worldwide in 2020 https://gco.iarc.fr/today/data/factsheets/cancers/20-Breast-fact-sheet.pdf: International Agency for Research on Cancer and World Health Orginization; 2020 [
2. Sung H, et al. Global Cancer Statistics 2020: GLOBOCAN Estimates of Incidence and Mortality Worldwide for 36 Cancers in 185 Countries. CA: A Cancer Journal for Clinicians. 2021;71(3):209-49.
3. Perou CM, et al. Molecular portraits of human breast tumours. Nature. 2000;406(6797):747-52.
4. Sørlie T, et al. Gene expression patterns of breast carcinomas distinguish tumor subclasses with clinical implications. Proc Natl Acad Sci U S A. 2001;98(19):10869-74.
5. Sorlie T, et al. Repeated observation of breast tumor subtypes in independent gene expression data sets. Proc Natl Acad Sci U S A. 2003;100(14):8418-23.
6. Herschkowitz JI, et al. Identification of conserved gene expression features between murine mammary carcinoma models and human breast tumors. Genome Biol. 2007;8(5):R76.
7. Prat A, et al. Phenotypic and molecular characterization of the claudin-low intrinsic subtype of breast cancer. Breast Cancer Research. 2010;12(5):R68.
8. Rouzier R, et al. Breast Cancer Molecular Subtypes Respond Differently to Preoperative Chemotherapy. Clinical Cancer Research. 2005;11(16):5678-85.
9. Livasy CA, et al. Phenotypic evaluation of the basal-like subtype of invasive breast carcinoma. Modern Pathology. 2006;19(2):264-71.
10. Nguyen PL, et al. Breast Cancer Subtype Approximated by Estrogen Receptor, Progesterone Receptor, and HER-2 Is Associated With Local and Distant Recurrence After Breast-Conserving Therapy. Journal of Clinical Oncology. 2008;26(14):2373-8.
11. Dominici LS, et al. Impact of Breast Cancer Subtypes on Local-Regional Outcomes. Current Breast Cancer Reports. 2010;2(2):107-13.
12. Fragomeni SM, et al. Molecular Subtypes and Local-Regional Control of Breast Cancer. Surgical Oncology Clinics of North America. 2018;27(1):95-120.
13. Goldhirsch A, et al. Personalizing the treatment of women with early breast cancer: highlights of the St Gallen International Expert Consensus on the Primary Therapy of Early Breast Cancer 2013. Annals of Oncology. 2013;24(9):2206-23.
14. Keen JC, Davidson NE. The biology of breast carcinoma. Cancer. 2003;97(S3):825-33.
15. Harbeck N, et al. Breast cancer. Nature Reviews Disease Primers. 2019;5(1):66.
16. Cheang MC, et al. Ki67 index, HER2 status, and prognosis of patients with luminal B breast cancer. J Natl Cancer Inst. 2009;101(10):736-50.
17. Modi S, et al. Trastuzumab Deruxtecan in Previously Treated HER2-Low Advanced Breast Cancer. New England Journal of Medicine. 2022;387(1):9-20.
18. Cardoso F, et al. Early breast cancer: ESMO Clinical Practice Guidelines for diagnosis, treatment and follow-up†. Annals of Oncology. 2019;30(8):1194-220.
19. Yaşar P, et al. Molecular mechanism of estrogen-estrogen receptor signaling. Reprod Med Biol. 2017;16(1):4-20.
20. Holst F, et al. Estrogen receptor alpha (ESR1) gene amplification is frequent in breast cancer. Nat Genet. 2007;39(5):655-60.
21. Pan H, et al. 20-Year Risks of Breast-Cancer Recurrence after Stopping Endocrine Therapy at 5 Years. New England Journal of Medicine. 2017;377(19):1836-46.
22. Colleoni M, et al. Annual Hazard Rates of Recurrence for Breast Cancer During 24 Years of Follow-Up: Results From the International Breast Cancer Study Group Trials I to V. J Clin Oncol. 2016;34(9):927-35.
23. Romano A, et al. Identification of novel ER-alpha target genes in breast cancer cells: gene- and cell-selective co-regulator recruitment at target promoters determines the response to 17beta-estradiol and tamoxifen. Mol Cell Endocrinol. 2010;314(1):90-100.
24. Jordan VC. Tamoxifen: catalyst for the change to targeted therapy. Eur J Cancer. 2008;44(1):30-8.
25. Effects of chemotherapy and hormonal therapy for early breast cancer on recurrence and 15-year survival: an overview of the randomised trials. Lancet. 2005;365(9472):1687-717.
26. Johnston SR, Dowsett M. Aromatase inhibitors for breast cancer: lessons from the laboratory. Nat Rev Cancer. 2003;3(11):821-31.

27. Scharl A, Salterberg A. Significance of Ovarian Function Suppression in Endocrine Therapy for Breast Cancer in Pre-Menopausal Women. Geburtshilfe Frauenheilkd. 2016;76(5):516-24.
28. Ozyurt R, Ozpolat B. Molecular Mechanisms of Anti-Estrogen Therapy Resistance and Novel Targeted Therapies. Cancers (Basel). 2022;14(21).
29. Turner NC, et al. Palbociclib in Hormone-Receptor–Positive Advanced Breast Cancer. New England Journal of Medicine. 2015;373(3):209-19.
30. George W. Sledge J, et al. MONARCH 2: Abemaciclib in Combination With Fulvestrant in Women With HR+/HER2− Advanced Breast Cancer Who Had Progressed While Receiving Endocrine Therapy. Journal of Clinical Oncology. 2017;35(25):2875-84.
31. Im S-A, et al. Overall Survival with Ribociclib plus Endocrine Therapy in Breast Cancer. New England Journal of Medicine. 2019;381(4):307-16.
32. Cristofanilli M, et al. Fulvestrant plus palbociclib versus fulvestrant plus placebo for treatment of hormone-receptor-positive, HER2-negative metastatic breast cancer that progressed on previous endocrine therapy (PALOMA-3): final analysis of the multicentre, double-blind, phase 3 randomised controlled trial. Lancet Oncol. 2016;17(4):425-39.
33. Loibl S, et al. Palbociclib Combined with Fulvestrant in Premenopausal Women with Advanced Breast Cancer and Prior Progression on Endocrine Therapy: PALOMA-3 Results. Oncologist. 2017;22(9):1028-38.
34. Lundberg AS, Weinberg RA. Control of the cell cycle and apoptosis. Eur J Cancer. 1999;35(14):1886-94.
35. Finn RS, et al. Palbociclib and Letrozole in Advanced Breast Cancer. New England Journal of Medicine. 2016;375(20):1925-36.
36. Hortobagyi GN, et al. Ribociclib as First-Line Therapy for HR-Positive, Advanced Breast Cancer. New England Journal of Medicine. 2016;375(18):1738-48.
37. Goetz MP, et al. MONARCH 3: Abemaciclib As Initial Therapy for Advanced Breast Cancer. Journal of Clinical Oncology. 2017;35(32):3638-46.
38. Johnston S, et al. MONARCH 3 final PFS: a randomized study of abemaciclib as initial therapy for advanced breast cancer. NPJ Breast Cancer. 2019;5:5.
39. Rugo HS, et al. Palbociclib plus letrozole as first-line therapy in estrogen receptor-positive/human epidermal growth factor receptor 2-negative advanced breast cancer with extended follow-up. Breast Cancer Res Treat. 2019;174(3):719-29.
40. Tripathy D, et al. Ribociclib plus endocrine therapy for premenopausal women with hormone-receptor-positive, advanced breast cancer (MONALEESA-7): a randomised phase 3 trial. Lancet Oncol. 2018;19(7):904-15.
41. Cameron DA, et al. 206 (PB-030) Poster - Cost-effectiveness of first-line ribociclib use vs palbociclib in the treatment of postmenopausal women with HR+/HER2− advanced breast cancer: analysis based on final OS results of MONALEESA-2 and PALOMA-2. European Journal of Cancer. 2022;175:S67.
42. Slamon DJ, et al. Ribociclib plus fulvestrant for postmenopausal women with hormone receptor-positive, human epidermal growth factor receptor 2-negative advanced breast cancer in the phase III randomized MONALEESA-3 trial: updated overall survival. Annals of Oncology. 2021;32(8):1015-24.
43. Finn RS, et al. Overall survival (OS) with first-line palbociclib plus letrozole (PAL+LET) versus placebo plus letrozole (PBO+LET) in women with estrogen receptor–positive/human epidermal growth factor receptor 2–negative advanced breast cancer (ER+/HER2− ABC): Analyses from PALOMA-2. Journal of Clinical Oncology. 2022;40(17_suppl):LBA1003-LBA.
44. Cardoso F, et al. 5th ESO-ESMO international consensus guidelines for advanced breast cancer (ABC 5). Ann Oncol. 2020;31(12):1623-49.
45. Sledge GWT, M.; Neven, P.; Sohn, J.; Inoue, K.; Pivot, X.; Okera, M.; Masuda, N.; Kaufman, P.A.; Koh, H.; et al. Final Final Overall Survival Analysis of MONARCH-2: A Phase 3 trial of Abemaciclib Plus Fulvestrant in Patients with Hormone Receptor-positive, Human Epidermal Growth Factor Receptor 2-Negative Advanced Breast Cancer. 2022 San Antonio Breast Cancer Symposium; 6-10 December; San Antonio, Tx, USA2022.
46. Goetz MP, et al. LBA15 MONARCH 3: Interim overall survival (OS) results of abemaciclib plus a nonsteroidal aromatase inhibitor (NSAI) in patients (pts) with HR+, HER2- advanced breast cancer (ABC). Annals of Oncology. 2022;33:S1384.

47. Hortobagyi GN, et al. Updated results from MONALEESA-2, a phase III trial of first-line ribociclib plus letrozole versus placebo plus letrozole in hormone receptor-positive, HER2-negative advanced breast cancer. Annals of Oncology. 2018;29(7):1541-7.
48. Hortobagyi GN, et al. Overall Survival with Ribociclib plus Letrozole in Advanced Breast Cancer. New England Journal of Medicine. 2022;386(10):942-50.
49. Slamon DJ, et al. Phase III Randomized Study of Ribociclib and Fulvestrant in Hormone Receptor–Positive, Human Epidermal Growth Factor Receptor 2–Negative Advanced Breast Cancer: MONALEESA-3. Journal of Clinical Oncology. 2018;36(24):2465-72.
50. Tripathy D, et al. Ribociclib plus endocrine therapy for premenopausal women with hormone-receptor-positive, advanced breast cancer (MONALEESA-7): a randomised phase 3 trial. The Lancet Oncology. 2018;19(7):904-15.
51. Lu YS, et al. Updated Overall Survival of Ribociclib plus Endocrine Therapy versus Endocrine Therapy Alone in Pre- and Perimenopausal Patients with HR+/HER2- Advanced Breast Cancer in MONALEESA-7: A Phase III Randomized Clinical Trial. Clin Cancer Res. 2022;28(5):851-9.
52. Turner NC, et al. Overall Survival with Palbociclib and Fulvestrant in Advanced Breast Cancer. New England Journal of Medicine. 2018;379(20):1926-36.
53. Nabieva N, Fasching PA. CDK4/6 Inhibitors-Overcoming Endocrine Resistance Is the Standard in Patients with Hormone Receptor-Positive Breast Cancer. Cancers (Basel). 2023;15(6).

Chapter 2: Resistance to therapy

Resistance to endocrine therapy

Although endocrine treatment is the backbone for ER+ breast cancers, 30% of patients will develop either de novo or acquired resistance towards the treatment (1). Modification of the ER and a change in sensitivity to estrogen are the main mechanisms of endocrine resistance. Mutations in the gene encoding the ER (ESR1), truncated isoforms of ER, and loss of ER makes the tumor growth independent of ER signaling and thus the tumor cells develop resistance to endocrine therapy (2-6). Loss of ER is the cause of endocrine resistance in up to 20 % of cases (7). Growth factor signaling pathways that facilitate cell proliferation has also been shown to be the cause of resistance, by cross talk with the ER as seen on figure 1. These pathways include PI3K/AKT/mTOR, RAF/MEK/ERK, and HER2 pathways (8-10). Upregulation of HER2 is assumed to serve as an alternative survival pathway in the cells, and this can happen by either gene amplification or overexpression of HER2 (11, 12). Gain-of-function mutations in the PI3KCA gene or loss of PTEN can be the cause of activation of the PI3K/AKT/mTOR pathway (13-17), just like activating AKT mutations has been linked to worse prognosis in patients treated with endocrine therapy (18, 19). Furthermore, cyclin D is upregulated in 58% of luminal B cancers and 29% of luminal A cancers and is strongly connected to endocrine resistance (20, 21). Importantly, Rb protein remains functional during the development of endocrine resistance thus, these tumors are rendered responsive to CDK4/6i (22). The clinical success of CDK4/6i suggest that endocrine-resistant tumors maintain sensitivity to CDK4/6i, especially when combined with endocrine therapy. In the PALOMA-3 trial fulvestrant plus palbociclib improved the PFS of endocrine resistant tumors with and without activating ESR1 mutations, indicating that CDK4/6i are effective independent of ER mutation status (23).

RET protein

RET (REarranged during Transfection) is a receptor tyrosine kinase, which is dependent on RET is composed of an extracellular domain, a cysteine-rich region, a single pass transmembrane domain, and a cytoplasmic region with a split tyrosine kinase domain (24). It does not directly bind its ligands but depend on the glial-derived neutrophic factor (GDNF) receptor α family (GFRα 1-4) coreceptors. GFRα forms homodimers that are recruited by specific GDNF family of ligands (GFLs) into a complex that activates RET homodimers leading to autophosphorylation of the tyrosine kinase domain (25). Activa-

tion of RET leads to activation of the MAPK/ERK, JAK/STAT and PI3K/AKT pathways leading to proliferation, survival, and migration (26, 27). RET has a complicated relationship with the ER, since it is a transcriptional target of ER but ER is also downstream of RET since RET activation has been shown to induce ER phosphorylation (28, 29). RET expression has been associated with tamoxifen and AI resistance in ER+ breast cancers (28, 30), and targeting RET potentiated the effect of tamoxifen, demonstrating greater reduction in tumor growth compared to single agent therapy in ER+ breast cancer cells (31). The RET inhibitor NVP-AST487 in combination with the AI letrozole was effective in inhibiting breast cancer cell line motility and growth (32). The effect of RET activation in AI and tamoxifen resistance is believed to be through estrogen-independent activation of ER transcriptional activity via the MAPK/ERK and PI3K/AKT pathways, where mTOR might play a key role (28, 30). Furthermore, another study have shown that overexpression of the RET ligand GDNF can cause resistance towards endocrine treatment in ER+ breast cancer cell lines (33). In thyroid carcinoma and non-small cell lung cancer constitutively active RET fusion proteins have been identified in 30% and 2% of patients respectively (34-36). Activating RET mutations are found in up to 70% of medullary thyroid carcinoma, but all RET alterations are rare in breast cancer. The selective RET inhibitor (RETi) selpercatinib was approved for the use in advanced NSCLC and PTC with RET fusion proteins and in MTC with activating RET mutations. Selbercatinib is effective towards RET fusions, mutant RET, and wildtype RET. Although RET has been associated with endocrine resistance in ER+ breast cancer, the role in resistance towards combined CDK4/6i and endocrine therapy has not been detailed.

Resistance to CDK4/6i

Metastatic breast cancer is an incurable disease with a median OS of 3 years and a 5-year survival of only 25% (37). A minority of metastatic ER+ breast cancer are so-called intrinsic resistant towards the treatment and relapse will occur within the first 3-6 months in 15% of patients receiving CDK4/6i with AIs and about 30% of patients receiving combined CDK4/6i an fulvestrant (38, 39), whereas 70% of the patients have PFS for 40 months (40-42).

The cyclin D-CDK4/6-retinoblastoma (Rb) axis is important for the progression through the cell cycle, specifically when cells move from G1 to S-phase. In quiescent cells, the Rb protein is hypophosphorylated and bound to E2F transcription factors. When mitogenic signals occur for the cells to enter the cell cycle, leading to the expression of cyclin D, which competes with CDK2 to bind to CDK4/6. The active cyclin D-CDK4/6 complexes phosphorylate Rb, which then releases the E2F transcription factors, who are respon-

sible for the transcription of factors which drive S phase entry (43). ER+ breast cancer is highly dependent on this pathway, since ER induces expression of cyclin D, leading to active cyclin D-CDK4/6 complexes thus inducing growth and proliferation of ER+ cells. Therefore, CDK4/6is are most efficient in ER+ breast cancer compared to other breast cancer subtypes (44). Furthermore, pre-clinical studies have shown that changes in cell cycle regulation was essential for cells to become resistant to fulvestrant (45). CDK4/6i binds to the ATP binding site of CDK4/6 and inhibits the kinase activity and halts the cells in G1 phase.

Acquired resistance towards CDK4/6i has been described to be caused by many different mechanisms in preclinical models (46, 47). CDK4/6i alone result in G0/G1 cell cycle arrest but in some ER+ breast cancer cell models the S-phase entry markers and Rb phosphorylation returned within days (46, 48). This effect was attenuated by the addition of a PI3K inhibitor (46), an mTOR1/2 inhibitor (49), and importantly endocrine therapy (50). Multiple mechanisms have been described to explain resistance, including loss or mutation in Rb, changes in CDK4/6 and CDK2 signaling, and activation of various growth signaling pathways (see figure 2):

Rb is the main target of CDK4/6i, and thus mutations in Rb have been observed in both pre-clinical models and patients (40, 46, 51), and in the PALOMA-3 trial polyclonal Rb mutations were identified in 4.7% of patients receiving combined CDK4/6i and endocrine therapy and in no patients receiving endocrine therapy alone (52). ER+ breast cancer patients with a loss of heterozygosity of the RB signature, which comprises several genes involved in the cell cycle such as *Rb*, *Myc*, *E2F1*, and *CDK6*, in their pre-treatment blood samples are likely to experience lower PFS when treated with combined CDK4/6i and endocrine therapy (53, 54).

Amplification of CDK6 has been identified as a mechanism of resistance towards CDK4/6i and endocrine therapy (55, 56). Furthermore, the amplification of cyclin D has also been shown to be implicated in resistance (47).

Cyclin E-CDK2 complexes further phosphorylates Rb following cyclin D-CDK4/6 complexes in the normal state, but when CDK4/6i inhibits the initial phosphorylation of Rb endogenous levels of cyclin E-CDK2 complexes cannot prime Rb. Additionally, cyclin E1 and E2 are transcriptional targets of E2F, thus the levels of these drops when CDK4/6i are present (57). CDK2 is inhibited by $p21^{Waf1/Cip1}$ and $p27^{Kip1}$ which are transcriptionally driven by TP53 (57). In CDK4/6i resistance cyclin E1, E2, and CDK2 has been described to be upregulated. Either via *CCNE1* gene (coding for cyclin E1) amplification and *CCNE2* gene (coding for cyclin E2) amplification (46, 47, 58). It can also be through TP53 and $p21^{Waf1/Cip1}$ and $p27^{Kip1}$. If these are either nonfunctional or low, they do not

inhibit CDK2, which then can drive phosphorylation of Rb (59). Mutations in either TP53 or its regulators MDM2 or MDM4 have been observed in ER+ breast cancer resistant to CDK4/6i (56, 60), although some TP53-mutant cell lines are still sensitive to CDK4/6i (61).

Growth regulatory pathways control Rb, CDK4/6, and CDK2 to upregulate cell growth and cell cycle progression, and it is therefore not surprising that these pathways can be involved in resistance towards CDK4/6i. FGFR1/2 amplification and activating HER2 mutations have been shown in resistance towards combined CDK4/6i and fulvestrant therapy, but the mechanisms behind this is not fully understood (60, 62), although they might activate parallel CDK4/6-independent pathways promoting proliferation. FGFR1/2 amplifications or activating mutations have been identified in 14 of 34 patients after progression on CDK4/6i and endocrine therapy (62), and FGFR1 amplification identified in

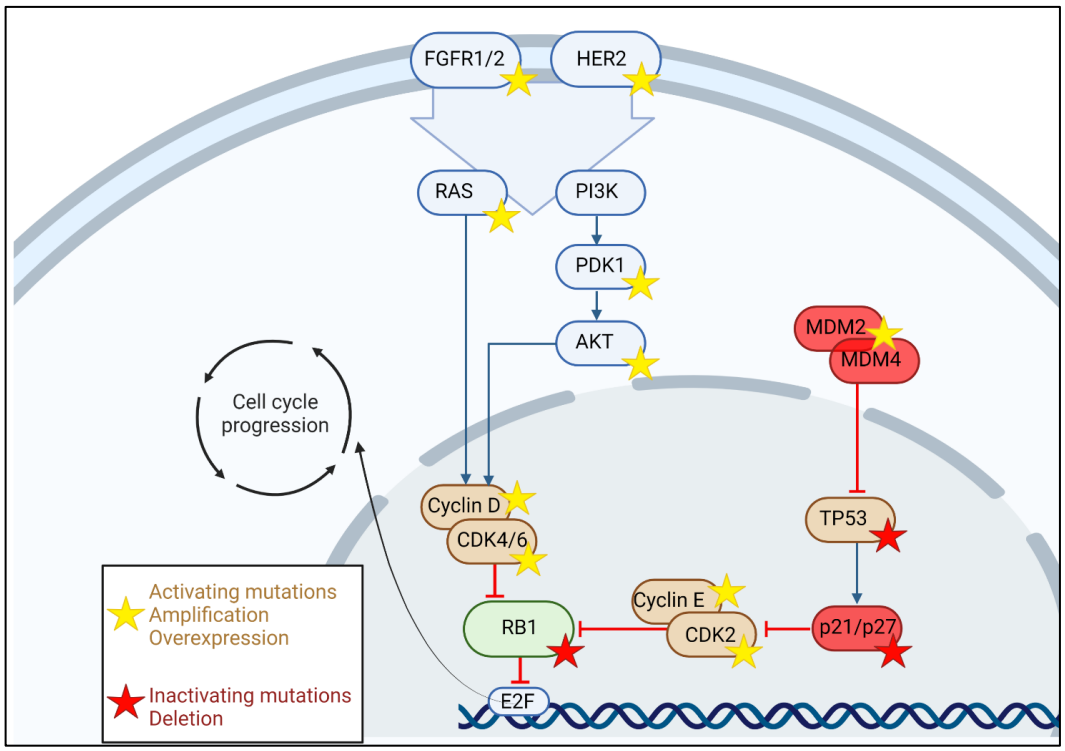

Figure 2: Resistance mechanisms to combined CDK4/6i and endocrine therapy. See text for further information. Created with BioRender.com

patient plasma is a predictor of poor prognosis of CDK4/6i in combination with endocrine treatment (63), but this has also been observed as a resistance towards endocrine treatment alone (64, 65). Alterations in the RAS/ERK and PI3K/AKT pathways has been observed, and specific mutations, overexpression, or constitutive activation of AKT1 and AKT3 has been shown to correlate with CDK4/6i resistance (46, 52, 60, 66). Furthermore, triple combinations of CDK4/6i, endocrine therapy and either a PI3K inhibitor or

AKT inhibitor are efficient in preclinical resistant models (46, 66), which shows that there is some dependency on this pathway in the resistant setting. The PI3K pathway kinase, PDK1 has been shown to be highly expressed in ribociclib resistant cells compared to ribociclib sensitive cells (67).

To detect resistance towards treatment tumor monitoring is crucial. This is based on imaging techniques, usually CE-CT or PET-CT, performed every 2-3 months. However, these techniques have several limitations, such as late detection of resistance and non-objective analysis of data. Techniques that more readily monitor tumor size in real time are desirable. Tissue biopsy is generally not a suitable approach for frequent monitoring of disease because it is an invasive procedure that may cause distress and complications for the patient. Furthermore, due to intratumor heterogeneity, the tissue of a biopsy might not be representative of the entire tumor. It may also be impossible to retrieve a tumor biopsy due to the location of the tumor.

References

1. Osborne CK, Schiff R. Mechanisms of endocrine resistance in breast cancer. Annu Rev Med. 2011;62:233-47.
2. Toy W, et al. ESR1 ligand-binding domain mutations in hormone-resistant breast cancer. Nature Genetics. 2013;45(12):1439-45.
3. Robinson DR, et al. Activating ESR1 mutations in hormone-resistant metastatic breast cancer. Nat Genet. 2013;45(12):1446-51.
4. Reinert T, et al. Implications of ESR1 Mutations in Hormone Receptor-Positive Breast Cancer. Curr Treat Options Oncol. 2018;19(5):24.
5. Fanning SW, et al. Estrogen receptor alpha somatic mutations Y537S and D538G confer breast cancer endocrine resistance by stabilizing the activating function-2 binding conformation. Elife. 2016;5.
6. Angus L, et al. ESR1 mutations: Moving towards guiding treatment decision-making in metastatic breast cancer patients. Cancer Treat Rev. 2017;52:33-40.
7. Gutierrez MC, et al. Molecular changes in tamoxifen-resistant breast cancer: relationship between estrogen receptor, HER-2, and p38 mitogen-activated protein kinase. J Clin Oncol. 2005;23(11):2469-76.
8. Miller TW, et al. Hyperactivation of phosphatidylinositol-3 kinase promotes escape from hormone dependence in estrogen receptor-positive human breast cancer. J Clin Invest. 2010;120(7):2406-13.
9. Tokunaga E, et al. Activation of PI3K/Akt signaling and hormone resistance in breast cancer. Breast Cancer. 2006;13(2):137-44.
10. Bosch A, et al. PI3K inhibition results in enhanced estrogen receptor function and dependence in hormone receptor-positive breast cancer. Sci Transl Med. 2015;7(283):283ra51.
11. Lipton A, et al. Serum HER-2/neu conversion to positive at the time of disease progression in patients with breast carcinoma on hormone therapy. Cancer. 2005;104(2):257-63.
12. Meng S, et al. HER-2 gene amplification can be acquired as breast cancer progresses. Proc Natl Acad Sci U S A. 2004;101(25):9393-8.
13. Clark AS, et al. Constitutive and inducible Akt activity promotes resistance to chemotherapy, trastuzumab, or tamoxifen in breast cancer cells. Mol Cancer Ther. 2002;1(9):707-17.
14. Kirkegaard T, et al. AKT activation predicts outcome in breast cancer patients treated with tamoxifen. J Pathol. 2005;207(2):139-46.
15. Shoman N, et al. Reduced PTEN expression predicts relapse in patients with breast carcinoma treated by tamoxifen. Mod Pathol. 2005;18(2):250-9.
16. Huang D, et al. PIK3CA mutations contribute to fulvestrant resistance in ER-positive breast cancer. Am J Transl Res. 2019;11(9):6055-65.
17. Cristofanilli M, et al. Fulvestrant plus palbociclib versus fulvestrant plus placebo for treatment of hormone-receptor-positive, HER2-negative metastatic breast cancer that progressed on previous endocrine therapy (PALOMA-3): final analysis of the multicentre, double-blind, phase 3 randomised controlled trial. Lancet Oncol. 2016;17(4):425-39.
18. Pérez-Tenorio G, Stål O. Activation of AKT/PKB in breast cancer predicts a worse outcome among endocrine treated patients. Br J Cancer. 2002;86(4):540-5.
19. Tokunaga E, et al. The association between Akt activation and resistance to hormone therapy in metastatic breast cancer. Eur J Cancer. 2006;42(5):629-35.
20. Comprehensive molecular portraits of human breast tumours. Nature. 2012;490(7418):61-70.

21. Jirström K, et al. Adverse effect of adjuvant tamoxifen in premenopausal breast cancer with cyclin D1 gene amplification. Cancer Res. 2005;65(17):8009-16.
22. Musgrove EA, et al. Cyclin D as a therapeutic target in cancer. Nature Reviews Cancer. 2011;11(8):558-72.
23. Fribbens C, et al. Plasma ESR1 Mutations and the Treatment of Estrogen Receptor–Positive Advanced Breast Cancer. Journal of Clinical Oncology. 2016;34(25):2961-8.
24. Gattelli A, et al. Ret Receptor Has Distinct Alterations and Functions in Breast Cancer. J Mammary Gland Biol Neoplasia. 2020;25(1):13-26.
25. Ibáñez CF. Structure and physiology of the RET receptor tyrosine kinase. Cold Spring Harb Perspect Biol. 2013;5(2).
26. Mulligan LM. RET revisited: expanding the oncogenic portfolio. Nat Rev Cancer. 2014;14(3):173-86.
27. Gattelli A, et al. Ret inhibition decreases growth and metastatic potential of estrogen receptor positive breast cancer cells. EMBO Mol Med. 2013;5(9):1335-50.
28. Plaza-Menacho I, et al. Targeting the receptor tyrosine kinase RET sensitizes breast cancer cells to tamoxifen treatment and reveals a role for RET in endocrine resistance. Oncogene. 2010;29(33):4648-57.
29. Boulay A, et al. The Ret receptor tyrosine kinase pathway functionally interacts with the ERalpha pathway in breast cancer. Cancer Res. 2008;68(10):3743-51.
30. Morandi A, et al. GDNF-RET signaling in ER-positive breast cancers is a key determinant of response and resistance to aromatase inhibitors. Cancer Res. 2013;73(12):3783-95.
31. Spanheimer PM, et al. Inhibition of RET increases the efficacy of antiestrogen and is a novel treatment strategy for luminal breast cancer. Clin Cancer Res. 2014;20(8):2115-25.
32. Andreucci E, et al. Targeting the receptor tyrosine kinase RET in combination with aromatase inhibitors in ER positive breast cancer xenografts. Oncotarget. 2016;7(49):80543-53.
33. Horibata S, et al. ER-positive breast cancer cells are poised for RET-mediated endocrine resistance. PloS one. 2018;13:e0194023.
34. Kondo T, et al. Pathogenetic mechanisms in thyroid follicular-cell neoplasia. Nature Reviews Cancer. 2006;6(4):292-306.
35. Richardson DS, et al. Transcript level modulates the inherent oncogenicity of RET/PTC oncoproteins. Cancer Res. 2009;69(11):4861-9.
36. Wang R, et al. RET Fusions Define a Unique Molecular and Clinicopathologic Subtype of Non–Small-Cell Lung Cancer. Journal of Clinical Oncology. 2012;30(35):4352-9.
37. Cardoso F, et al. 5th ESO-ESMO international consensus guidelines for advanced breast cancer (ABC 5). Ann Oncol. 2020;31(12):1623-49.
38. Guarducci C, et al. Mechanisms of Resistance to CDK4/6 Inhibitors in Breast Cancer and Potential Biomarkers of Response. Breast Care. 2017;12(5):304-8.
39. McCartney A, et al. Mechanisms of Resistance to CDK4/6 Inhibitors: Potential Implications and Biomarkers for Clinical Practice. Frontiers in Oncology. 2019;9.
40. Condorelli R, et al. Polyclonal RB1 mutations and acquired resistance to CDK 4/6 inhibitors in patients with metastatic breast cancer. Ann Oncol. 2018;29(3):640-5.
41. Portman N, et al. Overcoming CDK4/6 inhibitor resistance in ER-positive breast cancer. Endocrine-Related Cancer. 2019;26(1):R15-R30.
42. Finn RS, et al. Palbociclib and Letrozole in Advanced Breast Cancer. New England Journal of Medicine. 2016;375(20):1925-36.
43. Bertoli C, et al. Control of cell cycle transcription during G1 and S phases. Nat Rev Mol Cell Biol. 2013;14(8):518-28.

44. Finn RS, et al. PD 0332991, a selective cyclin D kinase 4/6 inhibitor, preferentially inhibits proliferation of luminal estrogen receptor-positive human breast cancer cell lines in vitro. Breast Cancer Research. 2009;11(5):R77.
45. Kaminska K, et al. Distinct mechanisms of resistance to fulvestrant treatment dictate level of ER independence and selective response to CDK inhibitors in metastatic breast cancer. Breast Cancer Research. 2021;23(1):26.
46. Herrera-Abreu MT, et al. Early Adaptation and Acquired Resistance to CDK4/6 Inhibition in Estrogen Receptor-Positive Breast Cancer. Cancer Res. 2016;76(8):2301-13.
47. Martin L-A, et al. Abstract P3-03-09: Resistance to palbociclib depends on multiple targetable mechanisms highlighting the potential of drug holidays and drug switching to improve therapeutic outcome. Cancer Research. 2017;77(4_Supplement):P3-03-9-P3--9.
48. Fry DW, et al. Specific inhibition of cyclin-dependent kinase 4/6 by PD 0332991 and associated antitumor activity in human tumor xenografts. Molecular Cancer Therapeutics. 2004;3(11):1427-38.
49. Michaloglou C, et al. Combined Inhibition of mTOR and CDK4/6 Is Required for Optimal Blockade of E2F Function and Long-term Growth Inhibition in Estrogen Receptor-positive Breast Cancer. Mol Cancer Ther. 2018;17(5):908-20.
50. Knudsen ES, Witkiewicz AK. Defining the transcriptional and biological response to CDK4/6 inhibition in relation to ER+/HER2- breast cancer. Oncotarget. 2016;7(43):69111-23.
51. Dean JL, et al. Therapeutic response to CDK4/6 inhibition in breast cancer defined by ex vivo analyses of human tumors. Cell Cycle. 2012;11(14):2756-61.
52. O'Leary B, et al. The Genetic Landscape and Clonal Evolution of Breast Cancer Resistance to Palbociclib plus Fulvestrant in the PALOMA-3 Trial. Cancer Discov. 2018;8(11):1390-403.
53. Prat A, et al. Circulating tumor DNA reveals complex biological features with clinical relevance in metastatic breast cancer. Nature Communications. 2023;14(1):1157.
54. Malorni L, et al. A gene expression signature of retinoblastoma loss-of-function is a predictive biomarker of resistance to palbociclib in breast cancer cell lines and is prognostic in patients with ER positive early breast cancer. Oncotarget. 2016;7(42):68012-22.
55. Yang C, et al. Acquired CDK6 amplification promotes breast cancer resistance to CDK4/6 inhibitors and loss of ER signaling and dependence. Oncogene. 2017;36(16):2255-64.
56. Li Z, et al. Loss of the FAT1 Tumor Suppressor Promotes Resistance to CDK4/6 Inhibitors via the Hippo Pathway. Cancer Cell. 2018;34(6):893-905.e8.
57. Caldon CE, et al. Estrogen Regulation of Cyclin E2 Requires Cyclin D1 but Not c-Myc. Molecular and Cellular Biology. 2009;29(17):4623-39.
58. Guerrero-Zotano Á, et al. CCNE1 and PLK1 mediates resistance to palbociclib in HR+/HER2- metastatic breast cancer. Clin Cancer Res. 2023.
59. Vilgelm AE, et al. MDM2 antagonists overcome intrinsic resistance to CDK4/6 inhibition by inducing p21. Sci Transl Med. 2019;11(505).
60. Wander SA, et al. The Genomic Landscape of Intrinsic and Acquired Resistance to Cyclin-Dependent Kinase 4/6 Inhibitors in Patients with Hormone Receptor-Positive Metastatic Breast Cancer. Cancer Discov. 2020;10(8):1174-93.
61. Gong X, et al. Genomic Aberrations that Activate D-type Cyclins Are Associated with Enhanced Sensitivity to the CDK4 and CDK6 Inhibitor Abemaciclib. Cancer Cell. 2017;32(6):761-76.e6.

62. Formisano L, et al. Aberrant FGFR signaling mediates resistance to CDK4/6 inhibitors in ER+ breast cancer. Nature Communications. 2019;10(1).
63. O'Leary B, et al. Genomic markers of early progression on fulvestrant with or without palbociclib for ER+ advanced breast cancer in the PALOMA-3 trial. Journal of Clinical Oncology. 2019;37(15_suppl):1010-.
64. Mao P, et al. Acquired FGFR and FGF Alterations Confer Resistance to Estrogen Receptor (ER) Targeted Therapy in ER+ Metastatic Breast Cancer. Clinical Cancer Research. 2020;26(22):5974-89.
65. Turner N, et al. FGFR1 amplification drives endocrine therapy resistance and is a therapeutic target in breast cancer. Cancer Res. 2010;70(5):2085-94.
66. Alves CL, et al. Co-targeting CDK4/6 and AKT with endocrine therapy prevents progression in CDK4/6 inhibitor and endocrine therapy-resistant breast cancer. Nat Commun. 2021;12(1):5112.
67. Jansen VM, et al. Kinome-Wide RNA Interference Screen Reveals a Role for PDK1 in Acquired Resistance to CDK4/6 Inhibition in ER-Positive Breast Cancer. Cancer Research. 2017;77(9):2488-99.

Chapter 3: Circulating tumor DNA

Circulating free DNA (cfDNA) is present in blood plasma, and consists of highly fragmented double-stranded DNA that are below 200 base pairs (1). cfDNA is derived mainly from apoptosis of normal cells in the hematopoietic lineage with low contribution from other tissues (2). cfDNA has a short half-life which suggests ongoing release from apoptotic cells and rapid degradation or filtration (3, 4). In cancer, circulating tumor DNA (ctDNA) is a part of cfDNA. The tumor releases fractions of DNA into the vascular system, but the amount of ctDNA depends on tumor stage, localization, and vascularization of the tumor (5, 6). The ctDNA fraction of cfDNA is usually quite small, it can be <0.01% but it can vary among patients with similar clinical characteristics, and even some patients with metastatic disease show very low amounts of ctDNA (5, 7, 8). In patients with localized breast cancer ctDNA fractions in the blood is lower than in metastatic breast cancer patients. In localized breast cancer patients only approximately 50% of patients will be ctDNA positive, while this number rises to approximately 85% in the metastatic setting (5, 9). Thus, the use of ctDNA in clinical oncology appears to have the biggest potential in the metastatic setting. Therapeutic response monitoring is especially important in metastatic breast cancer since progression is inevitable. Thus, it is crucial if the cancer is still responding to treatment or if it has progressed. Dawson and colleagues showed in 2013 that ctDNA provided the earliest measure of treatment response compared to standard imaging techniques (10).

In different cancers it has been shown that ctDNA can provide a comprehensive view of the tumor genome as it reflects DNA released from multiple tumor regions (11, 12). Several studies have shown concordance between mutations identified in matched blood and tumor sample types (13, 14). The issue in metastatic breast cancer, is that the amount of ctDNA might be very low and therefore, very sensitive techniques are required. But liquid biopsies have shown great promise for clinical applications in breast cancer such as residual disease monitoring (15-17), therapeutic response monitoring (10, 18), and mutation profiling (5, 13, 14). Residual disease monitoring requires a highly sensitive methods, as the amount of ctDNA in the plasma is very low following treatment in non-metastatic breast cancer patients. McDonald and colleagues developed the targeted digital sequencing (TARDIS) method in 2019 (15). They were able to detect ctDNA in all patients prior to treatment with a median allele frequency of 0.11% by multiplexed analysis of patient-specific cancer mutations and to follow the mutations in the blood samples from patients taken during treatment. They observed that patients who achieved

complete pathological response had lower ctDNA concentrations than patients with residual disease.

To detect ctDNA targeted quantification techniques such as BEAMing (beads, emulsion, amplification, and magnetics), ddPCR (droplet digital polymerase chain reaction), and TARDIS have been developed. These are specific techniques and are therefore only able to screen for known mutations and specific methylation sites with high sensitivity. These techniques display a sensitivity down to variants that represent 0.01% of genomic material (15, 19, 20). Targeted sequencing including TAM-seq (tagged amplicon deep sequencing), CAPP-Seq (cancer personalized profiling by deep sequencing), and AmpliSeq (amplicon sequencing). These techniques are less sensitive, but some are used in the clinical setting today. The Oncomine Breast cfDNA test is used to detect aberrations in a limited number of genes in breast cancer patients (21-23).

However, these targeted techniques can only detect a limited number of predefined mutations. Thus, the complex genetic heterogeneity in breast cancer might be lost. With massive next-generation sequencing (NGS) techniques a global analysis of CNA (copy number alteration), point mutations, and other genetic alterations can be identified using either whole genome or exome sequencing (WGS or WES) (24). The limitations of these include lower overall sensitivity and the need for higher concentrations of ctDNA. Thus, limiting the utility in patients with low ctDNA.

The issue with monitoring advanced breast cancer is that the most applicable approaches are the targeted ones since the broader approaches usually are not sensitive enough. However, due to the heterogenetic nature of the disease the targeted approaches need to be specific for each patient, which makes it time consuming and expensive. In patients treated with combined CDK4/6i and endocrine therapy there are not any resistance markers that are common for all patients. Therefore, individual tumor-lead approaches are ideal.

References

1. Snyder Matthew W, et al. Cell-free DNA Comprises an In Vivo Nucleosome Footprint that Informs Its Tissues-Of-Origin. Cell. 2016;164(1):57-68.
2. Lui YY, et al. Predominant Hematopoietic Origin of Cell-free DNA in Plasma and Serum after Sex-mismatched Bone Marrow Transplantation. Clinical Chemistry. 2002;48(3):421-7.
3. Lo YMD, et al. Rapid Clearance of Fetal DNA from Maternal Plasma. The American Journal of Human Genetics. 1999;64(1):218-24.
4. Diehl F, et al. Circulating mutant DNA to assess tumor dynamics. Nature Medicine. 2008;14(9):985-90.
5. Bettegowda C, et al. Detection of circulating tumor DNA in early- and late-stage human malignancies. Sci Transl Med. 2014;6(224):224ra24.
6. Abbosh C, et al. Phylogenetic ctDNA analysis depicts early-stage lung cancer evolution. Nature. 2017;545(7655):446-51.
7. Heitzer E, et al. Establishment of tumor-specific copy number alterations from plasma DNA of patients with cancer. Int J Cancer. 2013;133(2):346-56.
8. Heidary M, et al. The dynamic range of circulating tumor DNA in metastatic breast cancer. Breast Cancer Res. 2014;16(4):421.
9. Zhou Y, et al. Clinical factors associated with circulating tumor DNA (ctDNA) in primary breast cancer. Mol Oncol. 2019;13(5):1033-46.
10. Dawson SJ, et al. Analysis of circulating tumor DNA to monitor metastatic breast cancer. N Engl J Med. 2013;368(13):1199-209.
11. De Mattos-Arruda L, et al. Capturing intra-tumor genetic heterogeneity by de novo mutation profiling of circulating cell-free tumor DNA: a proof-of-principle. Ann Oncol. 2014;25(9):1729-35.
12. Chan KC, et al. Cancer genome scanning in plasma: detection of tumor-associated copy number aberrations, single-nucleotide variants, and tumoral heterogeneity by massively parallel sequencing. Clin Chem. 2013;59(1):211-24.
13. Phallen J, et al. Direct detection of early-stage cancers using circulating tumor DNA. Sci Transl Med. 2017;9(403).
14. Rothé F, et al. Plasma circulating tumor DNA as an alternative to metastatic biopsies for mutational analysis in breast cancer. Ann Oncol. 2014;25(10):1959-65.
15. McDonald BR, et al. Personalized circulating tumor DNA analysis to detect residual disease after neoadjuvant therapy in breast cancer. Sci Transl Med. 2019;11(504).
16. Olsson E, et al. Serial monitoring of circulating tumor DNA in patients with primary breast cancer for detection of occult metastatic disease. EMBO Mol Med. 2015;7(8):1034-47.
17. Garcia-Murillas I, et al. Mutation tracking in circulating tumor DNA predicts relapse in early breast cancer. Sci Transl Med. 2015;7(302):302ra133.
18. O'Leary B, et al. Early circulating tumor DNA dynamics and clonal selection with palbociclib and fulvestrant for breast cancer. Nat Commun. 2018;9(1):896.
19. Beaver JA, et al. Detection of cancer DNA in plasma of patients with early-stage breast cancer. Clin Cancer Res. 2014;20(10):2643-50.
20. Li M, et al. BEAMing up for detection and quantification of rare sequence variants. Nature Methods. 2006;3(2):95-7.
21. Forshew T, et al. Noninvasive Identification and Monitoring of Cancer Mutations by Targeted Deep Sequencing of Plasma DNA. Science Translational Medicine. 2012;4(136):136ra68-ra68.
22. Newman AM, et al. An ultrasensitive method for quantitating circulating tumor DNA with broad patient coverage. Nature Medicine. 2014;20(5):548-54.
23. Page K, et al. Circulating Tumor DNA Profiling From Breast Cancer Screening Through to Metastatic Disease. JCO Precis Oncol. 2021;5.
24. Imperial R, et al. Matched Whole-Genome Sequencing (WGS) and Whole-Exome Sequencing (WES) of Tumor Tissue with Circulating Tumor DNA (ctDNA) Analysis: Complementary Modalities in Clinical Practice. Cancers (Basel). 2019;11(9).

Chapter 4: Methodological considerations

In the following sections, I will provide a detailed overview of the benefits and drawbacks associated with the methods discussed in the two manuscripts.

Manuscript I

Cancer cell lines

To investigate drug resistance mechanisms, this study employed immortalized breast cancer cell lines that were made resistant to CDK4/6i and endocrine therapy via long-term exposure. The advantages of using such cell lines include ease of handling, characteristics resembling cancer, and the ability to provide quick, cost-effective high throughput analysis (1, 2). The establishment of cell lines resistant to combined CDK4/6i and endocrine therapy through treatment with fulvestrant and palbociclib for 2-4 months mimics the acquired drug resistance seen in metastatic ER+ breast cancer patients (3, 4). This technique has led to the identification of important biomarkers for clinical use. Cancer cell lines thus remain a crucial tool for understanding drug resistance mechanisms and developing new therapeutic strategies (5-7).

Despite the advantages of immortalized cancer cell lines, there are several limitations that need to be addressed. These include the lack of tissue architecture, interactions with other cell types, and the absence of the tumor microenvironment, which can all affect the expression profile and response to treatments (2). Therefore, research in immortalized cancer cell lines should be validated with clinical samples or more complex *in vitro* models such as 3D cell cultures or organoids, as well as *in vivo* studies. 3D models can either be prepared as suspension cultures on non-adherent plates, cultures in gel-like substances, or cultures on a scaffold. The cancer cells will form spheroid structures that resemble the physical and biochemical features of a solid tumor mass. They have shown similarity to cells growing *in vivo* with regards to gene expression, hypoxia, cell signaling, and similar drug responses to that of a solid tumor (8-10). Even closer to the clinical setting are organoids where cells are isolated from a patient with metastatic breast cancer, treated with combined CDK4/6i and endocrine therapy and cultured in 3D structures. The cells can be from either tumor tissue or blood samples. These organoids resemble the tumor in many ways including morphological, hormone receptor status, genotype, and drug response (11-13). By utilizing more complex models, such as 3D cultures or organoids, we can obtain a more accurate representation of the tumor environment and potentially identify new targets for therapeutic intervention. In this study, we validated our find-

ings in clinical samples from patients with metastatic breast cancer, and the next step will be to further validate the findings in an *in vivo* cancer model or organoids.

Functional assays

Several in vitro assays can be used to determine the effect of a treatment on cancer cell lines on characteristics such as cell proliferation and apoptosis. In this study we chose to analyze the effect on MCF7 and T47D cell lines following drug exposure or knockdown of RET using crystal violet (CV) colorimetric staining which determines cell growth. CV contains triarymethan dye, which binds to the DNA of cells that are attached to the plates. Cell growth is then determined by colorimetric measurement, which is proportional to the amount of stained DNA and thus the number of cells (14). CV staining is a quite simple, easy, and low-cost method to determine differences in grow rates between treated and untreated cells. The main limitation of CV staining is that it does not differentiate between viable, growth arrested, or if apoptotic cells adhere to the plate. To emphasize that the drug combination or knockdown affect the viability of the cell a CellTiter Blue (CTB) assay can be used. CTB assays contain a redox dye called resazurin which can be metabolized into a fluorescent end-product. The quantity of the generated fluorescent signal is proportional to the number of living cells, since non-viable cells lose metabolic capacity, and does not produce any fluorescence (14). Therefore, only the viable cells are detected by this assay. Importantly, if the drug interferes with metabolism of the cells the CTB assay is not a suitable assay, but this is not relevant in our case. CTB assay is not as easy and cheap as CV assay therefore, CV is often the first choice and if the effect of the drug or knockdown is clear using this assay it might not be necessary to perform other assays such as CTB.

Microarray and Western blotting

To evaluate which signaling pathways were affected by the knockdown of RET we chose to conduct a microarray analysis of the cell lines. This was chosen to do initially rather than Western blotting (WB) to gain a more comprehensive insight into the changes following knockdown. Microarray analysis is gene expression profiling which allow global analysis of multiple genes at the transcription level (15). The input is mRNA, which makes it possible to identify any changes in transcription following knockdown of RET. This method was previously used to describe that ER+ and ER- are different diseases at the transcriptome levels (16, 17). A limitation of this method is that it provides an average expression profile for each sample, and tumors consists of many different cell types and subclones, thus a microarray analysis will not be able to identify rare resistant clones

(18). We used the analysis on cell culture samples, which are much more homogenous than patient tumors and should therefore not limit this study. To validate the microarray findings WB analysis will be performed of the pathways that seems effected by RET knockdown. WB is a widely used technique for analyzing and characterizing protein expression. It can also be employed to identify protein expression involved in different signaling pathways and post-translational modifications such as phosphorylation. The phosphorylation or dephosphorylation of proteins is often involved in signaling pathways, and WB allows for monitoring of this process (19). However, the multistep nature of the technique and the subjective analysis of results increases the risk of errors and variations, which can reduce its reliability and reproducibility. In our study, WB was used to confirm the expression of RET in various cell lines and to verify the knockdown of RET at the protein level.

Manuscript II

Whole exome sequencing

The use of cancer cell lines to comprehend the mechanisms of therapy resistance is limited, which can be overcome by studying biological material from patients. This includes tumor cells that are directly obtained from the patient, and have interacted with the tumor microenvironment, making them representative of the tumor itself. Thus, our aim was to study molecular markers linked to resistance against combined CDK4/6i and endocrine therapy in advanced ER+ breast cancer, using biopsies obtained from patients prior to treatment and after progression. To diagnose patients with metastatic breast cancer, they often undergo a routine biopsy, and the tissue collected from this procedure is commonly preserved as formalin-fixed paraffin-embedded tissue (FFPE). The major limitation of patient material is the scarcity of the material, especially in the case of biopsies taken after progression, which are not routinely performed in the clinic. Physicians are reluctant to conduct invasive procedures that do not benefit the patient's treatment, especially if the patient has a poor performance status.

To gain insight into tumor biology and possible resistance mechanisms, we chose to do whole exome sequencing (WES) on the tumor samples. The advantages of WES over whole genome sequencing (WGS) are lower cost and simplification of variant analysis and data storage (20). Furthermore, more than 89% of variants reported to be pathogenic are found in the protein coding part of the genome, thus WES was preferrable to WGS (21). However, the use of WES also has limitations. For example, it cannot identify other potential mechanisms of resistance such as methylation patterns and differences in gene expression, which require whole genome bisulfite sequencing or RNA sequencing (22,

23). In our study, we chose to perform WES on tumor samples, ideally maintained as fresh frozen tissue. However, in cases where only formalin-fixed paraffin-embedded (FFPE) tissue was available, we used that instead. One major drawback of using FFPE tissue is that the extracted DNA is often damaged, leading to an increased error rate in variant calling. Despite this, multiple studies have shown that sequencing DNA from FFPE tissue is comparable to fresh frozen tissue, with a concordance of 70-90% (24-27). To minimize germline variant contamination and therefore increase sensitivity and specificity we sequenced matched peripheral blood leukocytes as normal tissue for each patient. Thus, we avoided false-positive variants with a high frequency.

TSO500

For some patients we did not obtain any tumor biopsies, and since this situation is likely to happen in the clinic, we opted to use ctDNA, which is less invasive and provides a more representative view of the tumor compared to a biopsy (28, 29). However, performing WES on ctDNA is technically challenging due to low tumor fractions in a high background of normal cfDNA. Mean read depth has been shown to be lower in cfDNA than in tumor-derived DNA, which can lead to inaccurate variant calling (30-32). To overcome this issue, we analyzed blood samples taken prior to combined CDK4/6i and endocrine therapy and following progression with the Illumina sequencing panel TruSight Oncology 500 (TSO500). This targeted sequencing panel covers 523 genes based on pan-cancer biomarkers and offers high read depth of predetermined genes, simpler data interpretation, and lower cost compared to WES. It is limiting our analysis, since it is only targeting 523 genes, and does not provide any information about epigenetic changes. We only selected a few patients as a pilot study for this analysis, as breast cancer is highly heterogenous, and pre-selected genes may not be altered in patient samples

Monitoring disease progression

To monitor disease progression during combined CDK4/6i and endocrine therapy, we aimed to use a tumor-guided approach due to the heterogeneity of breast cancer. We utilized data from WES on paired tumor samples and TSO500 results from paired blood samples to select mutations for identification in blood samples taken during treatment. Several methods exist for a tumor-guided approach, such as ddPCR, BEAMing, and SensiScreen, but they are time-consuming and require expertise. Thus, we collaborated with Pentabase, who have developed the SensiScreen technology and have experience in developing and testing assays. SensiScreen has a sensitivity of 0.25-1% in 50 ng wild type background and provides results within three hours after assay development. The

limitation of this approach is uncertainty about whether the monitored mutations represent the clone that will eventually grow upon CDK4/6 treatment. To implement in the clinic, multiple mutations representing most tumor cells for each patient should be followed. Alternatively, non-tumor-guided approaches, such as genome-wide profiling of copy-number instability or LIFE-CNA (liquid biopsy fragmentation, epigenetic signature and copy number alteration analysis) (33-35), could be used. These methods perform shallow-WGS (WGS with a low coverage of only 0.1-0.5X) on blood samples to quantify chromosomal instability, copy number alterations, and fragmentation. They have lower costs and do not require a biopsy prior to testing but require a somewhat high fraction of ctDNA in blood samples, which may be challenging in some metastatic breast cancer patients, expertise in bioinformatics and machine learning.

References

1. Burdall SE, et al. Breast cancer cell lines: friend or foe? Breast Cancer Res. 2003;5(2):89-95.
2. Vargo-Gogola T, Rosen JM. Modelling breast cancer: one size does not fit all. Nat Rev Cancer. 2007;7(9):659-72.
3. Lykkesfeldt AE, et al. Human breast cancer cell lines resistant to pure anti-estrogens are sensitive to tamoxifen treatment. Int J Cancer. 1995;61(4):529-34.
4. Kirkegaard T, et al. T47D breast cancer cells switch from ER/HER to HER/c-Src signaling upon acquiring resistance to the antiestrogen fulvestrant. Cancer Lett. 2014;344(1):90-100.
5. McDermott M, et al. In vitro Development of Chemotherapy and Targeted Therapy Drug-Resistant Cancer Cell Lines: A Practical Guide with Case Studies. Front Oncol. 2014;4:40.
6. Herrera-Abreu MT, et al. Early Adaptation and Acquired Resistance to CDK4/6 Inhibition in Estrogen Receptor-Positive Breast Cancer. Cancer Res. 2016;76(8):2301-13.
7. Alves CL, et al. High CDK6 Protects Cells from Fulvestrant-Mediated Apoptosis and is a Predictor of Resistance to Fulvestrant in Estrogen Receptor-Positive Metastatic Breast Cancer. Clin Cancer Res. 2016;22(22):5514-26.
8. Pampaloni F, et al. The third dimension bridges the gap between cell culture and live tissue. Nat Rev Mol Cell Biol. 2007;8(10):839-45.
9. Kapałczyńska M, et al. 2D and 3D cell cultures - a comparison of different types of cancer cell cultures. Arch Med Sci. 2018;14(4):910-9.
10. Imamura Y, et al. Comparison of 2D- and 3D-culture models as drug-testing platforms in breast cancer. Oncol Rep. 2015;33(4):1837-43.
11. Sachs N, et al. A Living Biobank of Breast Cancer Organoids Captures Disease Heterogeneity. Cell. 2018;172(1-2):373-86.e10.
12. Fujii M, et al. A Colorectal Tumor Organoid Library Demonstrates Progressive Loss of Niche Factor Requirements during Tumorigenesis. Cell Stem Cell. 2016;18(6):827-38.
13. van de Wetering M, et al. Prospective Derivation of a Living Organoid Biobank of Colorectal Cancer Patients. Cell. 2015;161(4):933-45.
14. Śliwka L, et al. The Comparison of MTT and CVS Assays for the Assessment of Anticancer Agent Interactions. PLoS One. 2016;11(5):e0155772.
15. Quackenbush J. Microarray analysis and tumor classification. N Engl J Med. 2006;354(23):2463-72.
16. Perou CM, et al. Molecular portraits of human breast tumours. Nature. 2000;406(6797):747-52.
17. Sørlie T, et al. Gene expression patterns of breast carcinomas distinguish tumor subclasses with clinical implications. Proc Natl Acad Sci U S A. 2001;98(19):10869-74.
18. Weigelt B, et al. Challenges translating breast cancer gene signatures into the clinic. Nat Rev Clin Oncol. 2011;9(1):58-64.
19. Day EK, et al. Cell signaling regulation by protein phosphorylation: a multivariate, heterogeneous, and context-dependent process. Curr Opin Biotechnol. 2016;40:185-92.
20. Wang Z, et al. The Role and Challenges of Exome Sequencing in Studies of Human Diseases. Frontiers in Genetics. 2013;4.
21. Barbitoff YA, et al. Systematic dissection of biases in whole-exome and whole-genome sequencing reveals major determinants of coding sequence coverage. Scientific Reports. 2020;10(1):2057.
22. Feng S, et al. Efficient and accurate determination of genome-wide DNA methylation patterns in Arabidopsis thaliana with enzymatic methyl sequencing. Epigenetics Chromatin. 2020;13(1):42.
23. Wang Y, et al. Changing Technologies of RNA Sequencing and Their Applications in Clinical Oncology. Front Oncol. 2020;10:447.
24. Astolfi A, et al. Whole exome sequencing (WES) on formalin-fixed, paraffin-embedded (FFPE) tumor tissue in gastrointestinal stromal tumors (GIST). BMC Genomics. 2015;16:892.
25. Kerick M, et al. Targeted high throughput sequencing in clinical cancer settings: formaldehyde fixed-paraffin embedded (FFPE) tumor tissues, input amount and tumor heterogeneity. BMC Med Genomics. 2011;4:68.
26. Yost SE, et al. Identification of high-confidence somatic mutations in whole genome sequence of formalin-fixed breast cancer specimens. Nucleic Acids Res. 2012;40(14):e107.
27. Hedegaard J, et al. Next-generation sequencing of RNA and DNA isolated from paired fresh-frozen and formalin-fixed paraffin-embedded samples of human cancer and normal tissue. PLoS One. 2014;9(5):e98187.

28. De Mattos-Arruda L, et al. Capturing intra-tumor genetic heterogeneity by de novo mutation profiling of circulating cell-free tumor DNA: a proof-of-principle. Ann Oncol. 2014;25(9):1729-35.
29. Rothé F, et al. Plasma circulating tumor DNA as an alternative to metastatic biopsies for mutational analysis in breast cancer. Ann Oncol. 2014;25(10):1959-65.
30. Bos MK, et al. Whole exome sequencing of cell-free DNA – A systematic review and Bayesian individual patient data meta-analysis. Cancer Treatment Reviews. 2020;83:101951.
31. Diefenbach RJ, et al. Analysis of the Whole-Exome Sequencing of Tumor and Circulating Tumor DNA in Metastatic Melanoma. Cancers. 2019;11(12):1905.
32. Wang Q, et al. Novel metrics to measure coverage in whole exome sequencing datasets reveal local and global non-uniformity. Scientific Reports. 2017;7(1):885.
33. Paracchini L, et al. Genome-wide Copy-number Alterations in Circulating Tumor DNA as a Novel Biomarker for Patients with High-grade Serous Ovarian Cancer. Clin Cancer Res. 2021;27(9):2549-59.
34. Hallermayr A, et al. Somatic copy number alteration and fragmentation analysis in circulating tumor DNA for cancer screening and treatment monitoring in colorectal cancer patients. Journal of Hematology & Oncology. 2022;15(1):125.
35. Prat A, et al. Circulating tumor DNA reveals complex biological features with clinical relevance in metastatic breast cancer. Nature Communications. 2023;14(1):1157.

Chapter 5: Manuscript 1

RET inhibition overcomes resistance to combined CDK4/6 inhibitors and endocrine therapy in ER+ breast cancer

Charlotte Karup Kindt[1], Sidse Ehmsen[1,2], Sofie Traynor[1], Monique F. Hundebøl[1], Lene E. Johansen[1], Martin Bak[3], Elsa Arbajian[4], Johan Staaf[4], Henrik Ditzel[1, 2], Carla Alves[1]
1: Department of Cancer and Inflammation Research, Institute of Molecular Medicine, University of Southern Denmark, Odense, Denmark
2: Department of Oncology, Odense University Hospital; Institute of Clinical Research, University of Southern Denmark, Odense, Denmark
3: Department of Pathology, Sydvestjysk Sygehus, Esbjerg, Denmark
4: Division of Oncology, Department of Clinical Sciences Lund, Lund University, Lund, Sweden.

Abstract
Combined CDK4/6 inhibitor (CDK4/6i) and endocrine therapy has a major impact on the outcome of patients with advanced estrogen receptor-positive (ER+) breast cancer. However, resistance to this treatment and thus disease progression remains a major clinical challenge. To address this, we performed global gene expression analysis and NGS RNA sequencing and identified RET expression to be associated with CDK4/6i and endocrine therapy resistance in ER+ breast cancer. We show that RET is upregulated in ER+ breast cancer cell lines resistant to combined CDK4/6i and fulvestrant and siRNA-mediated silence of RET in RET-high combined CDK4/6i- and fulvestrant-resistant cells reduced their growth, partially by affecting cell cycle regulators of the G2-M phase and E2F targets. Further, targeting RET with the FDA/EMA approved RET-selective inhibitor selpercatinib in combination with CDK4/6i and fulvestrant inhibited cellular growth of CDK4/6i- and fulvestrant-resistant cell lines, partially by blocking cell cycle progression. Importantly, analysis of RET expression in ER+ breast cancer patients treated with endocrine therapy showed that high RET expression correlates with poor clinical outcomes. Our findings suggest that RET inhibition in combination with CDK4/6i and endocrine therapy may represent a promising therapeutic approach for patients with advanced ER+ breast cancer who experience disease progression on combined CDK4/6i and endocrine therapy.

Introduction

Breast cancer (BC) remains the most common cancer and second cause of cancer related death in women worldwide (1). Although there has been a substantial improvement in available therapies and clinical outcome, metastatic breast cancer is considered incurable (2). Estrogen receptor-positive (ER+) breast cancer comprises approximately 70% of all breast cancers and is dependent on the ER pathway for proliferation and survival. Therefore inhibition of the ER pathway is an effective treatment strategy in this patient population (3). However, resistance to endocrine treatment remains a major clinical challenge (4). Several studies have shown that endocrine resistance mechanisms depend on alterations of cell cycle regulators, which led to the development of cyclin dependent kinases 4 and 6 (CDK4/6) inhibitors in ER+ breast cancer (5-8). CDK4/6 plays a key role in the control of G1-S phase progression in the cell cycle by interacting with cyclin D and subsequently hyperphosphorylating the retinoblastoma (Rb) protein, which leads to its inactivation and release of transcription factors that allow progression to the cell cycle S-phase (9). CDK4/6 inhibitors (CDK4/6i), including ribociclib, palbociclib, and abemaciclib inhibit the CDK4/6 kinases, and thus arrest the cells in G1 phase. Clinical studies have shown that treatment with CDK4/6i in combination with endocrine therapy improved progression free survival (PFS) and overall survival (OS) compared to endocrine therapy alone in patients with ER+ advanced breast cancer. This resulted in the approval of CDK4/6i for ER+ advanced breast cancer as first-line treatment in combination with an aromatiase inhibitor (AI) (3, 10, 11), and as second-line therapy in combination with the selective estrogen-receptor degrader (SERD) fulvestrant following initial AI monotherapy (12-14). Recently, the CDK4/6i abemaciclib has also been approved for high-risk patients with early stage ER+ breast cancer (15). Despite favourable outcomes the development of resistance to combined CDK4/6i and endocrine therapy is inevitable, and 70% of patients with advanced ER+ breast cancer will experience progressive disease after 40 months (3, 16, 17). Understanding resistance mechanisms to combined CDK4/6i and endocrine therapy and identification of optimal treatment option following progression on combined CDK4/6i and endocrine therapy is currently areas of intense research.

The RET (REarranged during Transfection) proto-oncogene is a receptor tyrosine kinase and RET hyperactivation is observed associated with several cancer types. RET is composed of an extracellular domain, a cysteine-rich region, a single pass transmembrane domain, and a cytoplasmic region with a split tyrosine kinase domain. It does not directly bind its ligands but depend on the glial-derived neutrophic factor (GDNF) receptor α family (GFRα 1-4) coreceptors. GFRα forms homodimers that are recruited by specific GDNF family of ligands (GFLs) into a complex that activates RET homodimers leading to

autophosphorylation of the tyrosine kinase domain (18). Activation of RET leads to activation of the MAPK/ERK, JAK/STAT and PI3K-AKT pathways leading to proliferation, survival, and migration (19, 20).

Regarding breast cancer, increased levels of RET have been observed in breast tumors compared to surrounding healthy tissue (21, 22). Furthermore, RET expression correlates with ER expression in breast cancer cell lines and tumor specimens (23). Multiple studies have shown that ER induces the expression of RET, which led to the activation of downstream signalling pathways, including the MAPK/ERK, JAK/STAT, and PI3K-AKT pathways. Conversely, RET has been shown to enhance estrogen-mediated proliferation (23, 24). Overexpression of RET alone, has been shown to increase ER+ breast cancer incidences in mice (25). RET expression has been associated with tamoxifen and AI resistance in ER+ breast cancers (21, 26), and targeting RET with the multikinase inhibitor vandetanib potentiated the effect of tamoxifen, demonstrating greater reduction in tumor growth compared to single agent therapy in ER+ breast cancer cells (27). The RET inhibitor NVP-AST487 in combination with the AI letrozole was effective in inhibiting breast cancer cell line motility and growth (28). It has been shown that RET activation promotes AI and tamoxifen resistance through estrogen-independent activation of ER transcriptional activity via the MAPK/ERK and PI3K/AKT pathways, where mTOR might play a key role (21, 26).

In papillary thyroid carcinoma (PTC) and non-small cell lung cancer (NSCLC), RET fusion proteins, which are constitutively active and contribute in tumor growth, have been identified in 13-43% (29) and 2% of patients, respectively (29-31). In addition, up to 70% of medullary thyroid cancers (MTC) show activating RET mutations but RET alterations are rare in breast cancer (32-34). In 2020 the European Medicines Agency (EMA) and the Food and Drug Agency (FDA) approved the use of a RET-selective inhibitor (RETi) selpercatinib in RET fusion-positive advanced NSCLC and PTC, and in RET-mutant MTC (35, 36). Selpercatinib is effective towards RET-wildtype, -mutant, and -fusion protein (37). Although RET has been associated with ER+ breast cancer tumorigenesis and endocrine treatment response (23, 24, 27), the role of RET in the mechanisms of resistance to combined fulvestrant and CDK4/6i has not been evaluated.

In this article we show that RET overexpression is associated with resistance to combined CDK4/6i and fulvestrant treatment in ER+ breast cancer cell lines, and inhibition of RET by siRNA-mediated knockdown or treatment with the tyrosine kinase inhibitor selpercatinib impaired growth of combined fulvestrant and CDK4/6i-resistant cell by inhibiting, at least in part, cell cycle progression. Finally, we show that clinical ER+ breast can-

cer samples expressing high mRNA levels of RET correlated with poor clinical outcome following endocrine therapy.

Methods

Cell lines and anti-tumor agents

The original MCF7 and T47D cell lines were obtained from the Breast Cancer Task Force Cell Culture Bank, Mason Research Institute. The MCF-7-derived cell line MPF-R was developed by extended treatment with fulvestrant (100 nM) and CDK4/6 inhibitor (CDK4/6i) palbociclib (150-200nM). Cells were maintained in phenol red-free Dulbecco's Modified Eagle Medium (DMEM/F12; Gibco) supplemented with 1 % glutamine (Gibco), 1% heat-inactivated fetal bovine serum (FBS; Sigma-Aldrich), and 6 ng/mL insulin (Sigma-Aldrich) supplemented with 100nM of fulvestrant and 200 nM CDK4/6i. MCF-7 cells grown in parallel with MPF-R cells without treatment in the media were designated M-S and remain sensitive to drug treatment.

T47D cells were maintained in Roswell Park Memorial Institute (RPMI) 1640 medium (Gibco) without phenol red, supplemented with 1% glutamine (Gibco), 5% heat-inactivated FBS (Sigma-Aldrich), and 8 µg/mL insulin (Sigma-Aldrich). T47D-derived fulvestrant and CDK4/6i resistant cell line TPF-R was established by long term treatment with 100 nM fulvestrant and 150-200 nM of CDK4/6i. T47D-sensitive cells grown in parallel with TPF-R were designated T-S and were maintained in the same medium as TPF-R cells without treatment. All cells were kept in humidified atmosphere of 5% CO_2 at 37 °C and underwent mycoplasma testing (Lonza) before the described experiments. Fulvestrant (ICI 182,780, Tocris) was dissolved in 96% ethanol, CDK4/6i palbociclib isothiocyanate (HY-A0065, MedChemExpress) was dissolved in water, RET inhibitor selpercatinib (also known as LOXO-292, HY-114370, MedChemExpress) was dissolved in DMSO (Sigma-Aldrich). The concentrations of CDK4/6i and RET inhibitor to be used for in vitro experiments were determined based on the IC50 for each cell line model.

Western Blotting

Whole-cell extracts were obtained using RIPA buffer (50 mM Tris HCl (pH 8), 150 mM NaCl (pH 8), 1% IgePAL 630, 0.5% sodium deoxycholate, 0.1% SDS) containing protease and phosphatase inhibitor cocktail (Thermo Scientific). Protein concentration of the lysate samples was determined using Pierce BCA Protein Assay kit (Thermo Fisher Scientific) and the optical density (OD) was measured at 562 nm in the microplate reader Paradigm (Beckman Coulter). Protein (10-45 µg) was loaded on a 4-20% SDS-PAGE gel (Bio-Rad) under reducing conditions and electroblotted onto a PVDF transfer membrane

(Bio-Rad). Membranes were blocked in Tris-buffered Saline (TBS), 0.1 % Tween-20 (Sigma-Aldrich) containing 5% non-fat dry milk powder (Sigma-Aldrich) for one hour at room temperature. The following antibodies were used according to the manufacturers protocol: anti-RET (3223S, Cell Signaling, 1:250-1:1000) and anti-GAPDH (sc-32233,Santa Cruz Biotechnology, 1:20000, (loading control)). Secondary antibodies horseradish peroxidase (HRP)-conjugated goat anti-mouse (P0447, Dako, 1:5000) and HRP-conjugated goat anti-rabbit (P0448, Dako, 1:5000) were incubated in blocking buffer for one hour at room temperature. Membranes were developed with SuperSignal^{tm} West Pico PLUS chemiluminescent Substrate (Thermo Scientific) and visualized on a ChemiDoc MP imaging system (Bio-Rad).

RET-specific siRNA mediated knockdown

RET gene knockdown was performed using two different RET-specific siRNAs (RET_15, SI04950554 and RET_17, SI05089756) both from Qiagen and a nontargeting scrambled (control) siRNA used as the universal negative control (SIC001, Sigma-Aldrich). Chemical transfection was performed in M-S, MPF-R, T-S, and TPF-R cell lines with Lipofectamine 3000 transfection reagent (15282465, ThermoFisher Scientific) in Opti-MEM medium (Gibco) according to manufacturer's instructions. Efficiency was evaluated at the mRNA level 48 hours after transfection by qPCR, and at the protein level 96 hours after transfection with Western blotting. The effect of siRNA mediated knockdown of RET on cell growth was evaluated with crystal violet assay at 24, 48, 96 and 144 hours after transfection.

RNA extraction, cDNA synthesis, quantitative real-time PCR (RT-qPCR)

TRI reagent® (Sigma Aldrich) was used for total RNA extraction and cDNA synthesis was performed using random deoxynucleic acid hexamers and reverse transcriptase (Fermentas). Quantitative real-time OCR (RT-qPCR) was performed using SYBR Green PCR Mastermix (Applied Biosystems) according to the manufacturer's instructions. The primers used were: *RET* (QT00047985, transcript ID: ENST00000355710, amplicon length 120, Qiagen) and *PUM1* (QT00029421, transcript ID: ENST00000257075, amplicon length 73, Qiagen) was used as a reference gene. The RT-qPCR reactions were performed using a StepOnePlus system (Applied Biosystems) and data were analyzed with StepOne Software. All reactions were conducted in triplicates and the data were analyzed using the delta-delta CT method (38).

Global gene expression and microarray analysis

Global gene expression analysis was performed on RNA purified from the parental cell line MCF7 (M-S) and MCF-7-derived fulvestrant-resistant cell line (MF-R) and combined palbociclib and fulvestrant resistant cell line (MPF-R) using Affymetrix Gene Chip Human Genome U133 plus 2.0. Cells were grown to reach 70-80% confluency and RNA was extracted using TRIzol™ Reagent according to manufacturer's instructions. Data were analyzed using Transcriptome Analysis Console (TAC) software (ThermoFisher). Genes from the dataset that exhibited two-fold or greater alteration in expression with a false discovery rate (FDR) < 0.05 cut-off and $p < 0.05$ with one-way ANOVA were considered significantly regulated. Gene Set Enrichment Analysis (GSEA 4.3.2) was performed to identify the gene sets enriched in the resistant cells.

RNA sequencing

To perform RNA-sequencing exon-spanning primers were designed, and the primer sequences are available upon request. For RNA sequencing, RNA from three independent experiments were prepared for sequencing on the Illumina NovaSeq 6000 platform using the NEBNext Poly(A) mRNA Magnetic Isolation Module (New England Biolabs, E7490L) and the NEBNext Ultra II DNA Library Prep Kit for Illumina (New England Biolabs, E7645L) with unique dual indexes according to the manufacturer´s instructions. The quality of raw sequencing reads was assessed using FASTQC (Babraham Bioinformatics) and adaptor sequences were removed using the FASTX toolkit. Trimmed Reads were aligned to the human genome (hg38) using the Spliced Transcripts Alignment to a Reference (STAR) software with default parameters (39). Tags in exons were counted using iRNA-seq (40) and differential expression (FDR-adjusted $p < 0.05$) between three independent replicates of sensitive cell line and double-resistant cell line samples was determined using DESeq2 (41). Differentially expressed genes were defined as those having FDR ≤ 0.05 and a log2 fold change > 1.0 in either direction. To identify candidate fusion transcripts from the sequence data, fusion calling was performed on the fastq files using FusionCatcher version 1.33 (42), STAR-fusion version 1.11.0 (43), and Arriba version 2.3.0 (44), with default settings. The GRCh38/hg38 build was used as the human reference genome.

Cell growth assay

Cells were seeded at 20,000-50,000 cells/well in 96-well plates and allowed to attach for 24 hours before drugs or vehicles were added. Evaluation of cell growth was performed using crystal violet-based colorimetric assay, where cells were incubated with a crystal violet staining solution for 5 minutes at room temperature followed by three washes in

ddH2O and overnight drying. Cellular crystal violet was extracted by incubation with a 0.1 M citrate buffer (29.41 g sodium citrate dissolved in 50% water and 50% ethanol, pH=6) for 30 minutes at room temperature on a shaker. The OD was analyzed at 570 nm in a Paradigm microplate reader (Beckman Coulter) and SoftMax pro 7.0.2 software.

Statistical analysis

All Statistical analyses were performed using GraphPad Prism v.9.4.0 software. One-way analysis of variance (ANOVA) and two-tailed t-test were used to determine statistical significance among data for the *in vitro* studies (as indicated in the figure legends). Survival curves for the clinical data were generated by Kaplan-Meier estimates, where log-rank test was applied to evaluate the correlation between the expression levels of RET and the PFS. The Cox proportional hazard regression model was used to calculate the hazard ratio (HR) of PFS by RET expression and clinicopathological characteristics using the univariate model. *p*-values were defined as follows: *p<0.05, **p<0.01, *** p<0.001, and **** p<0.0001.

Study approval

The immunohistochemical study was approved by the Ethics committee of the Region of Southern Denmark (approval no S-2008-0115) and the Danish Data Protection Agency. All patient samples were collected in compliance with informed consent policy and coded to maintain patient confidentiality.

KM plotter

The web tool Kaplan-Meier (KM) plotter (45) was used to generate survival curves for ER+ breast cancer patients based on mRNA expression (gene chip) of *RET*. All datasets available in KM plotter were included in the analysis. The inclusion criteria for the sample selection were: ER status positive by IHC, HER2 status negative by array, and previous treatment with endocrine therapy. These criteria were independent of pathological characteristics such as grade, lymph node status, and previous chemotherapy. The JetSet optimal probe was selected for *RET* (probe ID 211,421) and the best performing threshold was selected as the cut-off to evaluate the correlation of *RET* expression and clinical outcome. Relapse-free survival (RFS) and overall survival (OS) were used as endpoints.

Clinical samples and endpoints

Formalin-fixed, paraffin-embedded (FFPE), metastatic tumor lesions from ER+ advanced breast cancer patients treated with combined CDK4/6i and endocrine therapy were ob-

tained from the Department of Pathology at Odense University Hospital (OUH) (n= 115). Inclusion criteria were patients with ER+ advanced breast cancer treated with combined CDK4/6i and endocrine therapy in the metastatic setting who had undergone surgery or biopsy at OUH, who included complete clinical information and pathological verification that the metastatic lesion was of breast cancer origin. Cut-off for ER positivity was ≥1%. Exclusion criteria were insufficient tumor material in the FFPE block and metastatic biopsy only available after starting treatment with combined CDK4/6i (palbociclib or ribociclib) and endocrine therapy (letrozole or fulvestrant). These criteria yielded n = 83 patients. Progression-free survival (PFS) was defined as the time from starting treatment with combined CDK4/6i and endocrine therapy until disease progression or death.

Immunohistochemistry

FFPE blocks of patient metastatic lesions were sectioned at 4 µM with a microtome and mounted on ChemMateTM Capillary GAP slides (Dako, Glostrup, Denmark). Sections were dried at 60 °C, deparaffinized, hydrated and endogenous activity was blocked. Epitope unmasking was performed by boiling sections in T-EG solution. The following primary antibody was used: RET. Primary antibody binding for anti-RET was detected with Optiview-DAB (8-8), EnV, FLEX/HRB+ Rabbit LINK 15-30 for anti-RET. The clinical samples were evaluated by an experienced breast pathologist in a blinded setup. RET were primarily expressed in the cytoplasm. The intensity of the staining was recorded on a semi quantitative scale 0-3 with 0 meaning absolutely no reaction and 3 as the most intense staining. The cut-off value for high (intensity ≥ 2) vs. low (intensity < 2) was determined based on the survival significance.

Results

RET is upregulated in ER+ BC cells resistant to combined CDK4/6i and fulvestrant

To investigate the resistance mechanisms to combined CDK4/6i and fulvestrant, we used two ER+ breast cancer cell line models, MCF7 and T47D, to develop cells resistant to combined CDK4/6i and fulvestrant (MPF-R and TPF-R, respectively). Growth of the two resistant cell lines, MPF-R and TPF-R was not inhibited by combined CDK4/6i and fulvestrant, or any of the two drugs alone, while growth of the corresponding sensitive cell lines M-S and T-S, respectively, was significantly inhibited by all three treatments (Figure 1A). To ensure that the resistance mechanism was related to combined CDK4/6i and fulvestrant and not to fulvestrant alone we evaluated gene expression alterations in the combined palbociclib and fulvestrant resistant cell lines compared to the respective cell lines resistant to fulvestrant alone (MF-R). Using RNA-sequencing we identified a

total of 1103 genes (523 upregulated and 580 downregulated) that exhibited significantly altered expression (fold-change ≥2, FDR<0.05, Wald significance test $p < 0.05$) in MPF-R versus MF-R, in TPF-R versus TF-R a total of 1041 genes (600 upregulated and 441 downregulated) that exhibited significantly altered expression (fold-change ≥2,

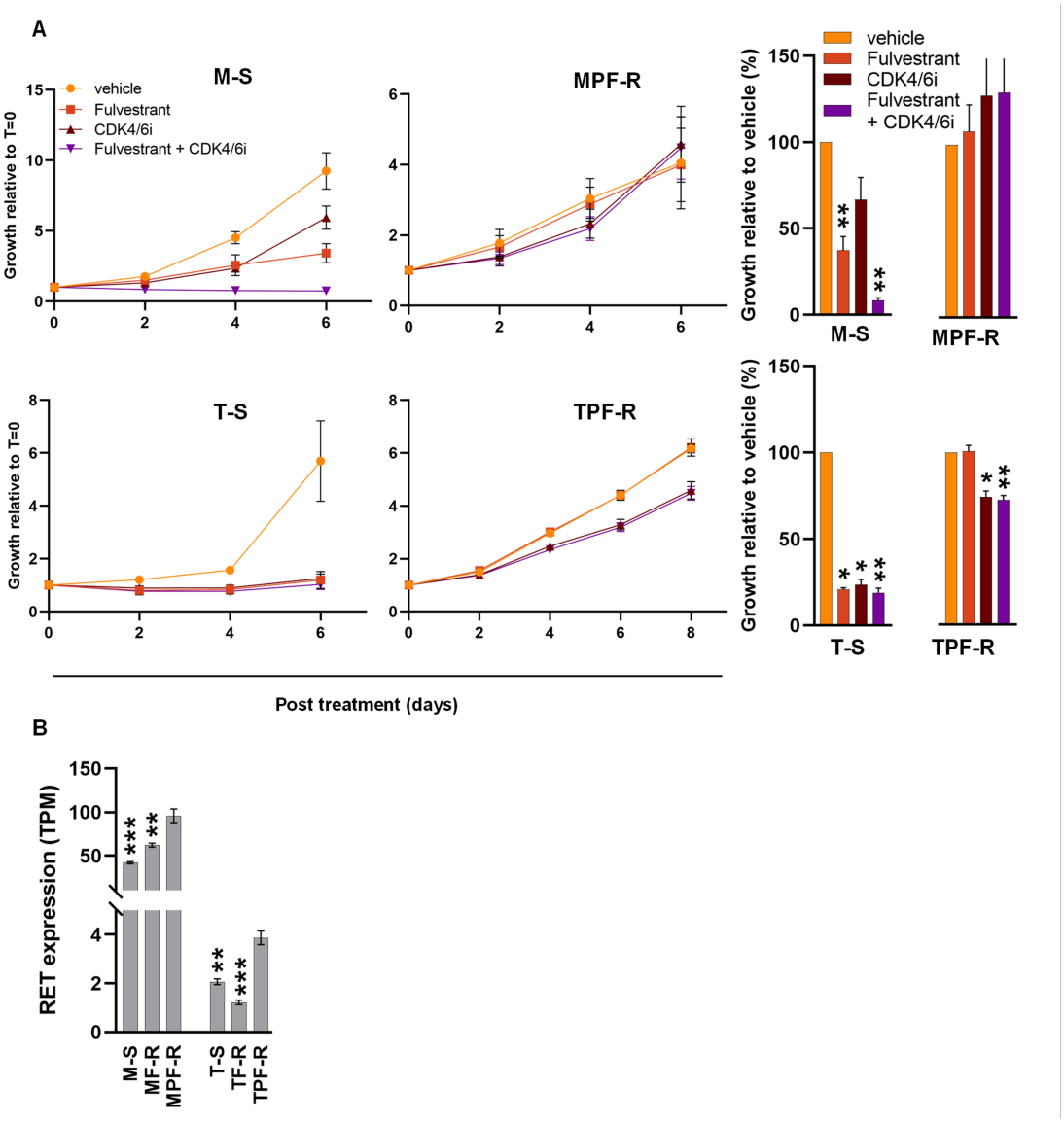

Figure 1: MPF-R and TPF-R cell lines were resistant towards combined CDK4/6i and endocrine therapy.
*A) Evaluation of cell growth of combined palbociclib and fulvestrant resistant (MPF-R and TPF-R) cells and the sensitive M-S and T-S cells by crystal violet colorimetric assay. Cell growth assay was performed over 6 days with fulvestrant (100 nM) and CDK4/6i (100 nM) alone or combined. Growth at day 6 is represented by columns. The data represent independent experiments in triplicates ±SEM. Asterisk indicate significant differences in one-way ANOVA tests at day 6 (*0.01 < p < 0.05 and **0.001 < p < 0.01). B) Evaluation of RET expression in ER+ BC cell lines. Combined palbociclib and fulvestrant resistant cells (MPF-R and TPF-R), fulvestrant resistant cells (MF-R and TF-R), and sensitive cells (M-S and T-S) using RNA sequencing. TPM = transcripts per million. The data represent independent experiments in triplicates ±SEM. Asterisk indicate significant differences between double resistant cells and their concordant sensitive and fulvestrant resistant in students t- test (*0.01 < p < 0.05, **0.001 < p < 0.01) and ***0.0001< p <0.001*

FDR<0.05, Wald significance test $p < 0.05$). Among the most upregulated genes (? Fold) in MPF-R versus MF-R and TPF-R versus TF-R, RET was identified. Next, to evaluate the expression level of RET in all cell lines and to evaluate whether RET-fusions could be identified we performed NGS RNA sequencing of MPF-R, TPF-R, MF-R, TF-R, M-S and T-S. This showed that RET was higher expressed in MPF-R compared to MF-R and M-S cells (Figure 1B). Furthermore, overexpression of RET was also observed in the T47D-derived TPF-R versus TPF-R and T-S cells (Figure 1B). Notably, RET expression is much higher in the MCF7-derived cells than in the T47D-derived cells, in agreement with previous reported (26), suggest a more important role for RET in MCF-7 cells. Although higher in the MCF7-derived cells, RET expression ratios in MPF-R versus M-S and TPF-R versus T-S were 2.3 and 1.9, respectively, and thus comparable. While *RET* fusions have been widely described in NSCLC and PTC, no fusion transcripts involving the *RET* gene were identified in any of the four ER+ BC cell lines using the three fusion callers (Fusioncatcher, STAR-fusion, and Arriba).

To further validate the overexpression of RET in combined fulvestrant and CDK4/6i resistant cells, qPCR and Western blotting were performed, and overexpression of RET on the mRNA and protein levels was confirmed (Figure 2A/B). Together, our findings support a significant upregulation of RET in two cell line models resistant to combined CDK4/6i and fulvestrant.

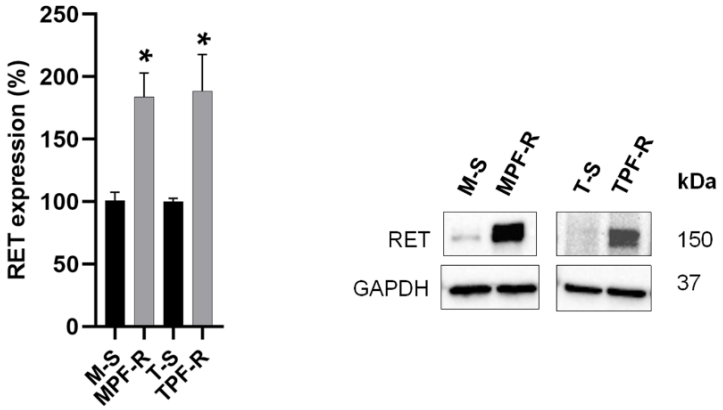

Figure 2: RET overexpressed in double fulvestrant and palbociclib resistant cell lines. Expression of RET was evaluated using qPCR and Western blotting. *A) Quantitative RT-PCR verifying the gene expression alterations of RET. The expression was normalized using PUM1 gene and shown as relative expression in MPF-R vs. M-S and TPF-R vs T-S cells. Data represents three independent experiments ±SEM. Asterisk indicate significant differences in students t- test (*0.01 < p < 0.05). B) Western blotting analysis of lysates from M-S, MPF-R, T-S, and TPF-R cells. GAPDH was used as loading control. A representative for three biological replicates is shown.*

RET-specific siRNA-mediated knockdown impairs growth of combined CDK4/6i and fulvestrant-resistant ER+ BC cells

To investigate the role of RET in the mechanism of resistance to combined CDK4/6i and fulvestrant, we performed gene knockdown by using two specific siRNAs targeting RET (RET15 and RET17) and a scrambled siRNA (control). RET was efficiently silenced in both MCF-7- and T47D-derived sensitive and resistance cell lines when using the individual and pooled RET-siRNAs compared with the control siRNA, as determined by quantitative RT-PCR and Western blotting (Figure 3A and B). It was not possible to visualize the RET knockdown in T-S cells by Western blotting due to the extremely low levels of RET in these cells.

Silencing of RET did not affect the growth of sensitive M-S cells compared to the control, as assessed by crystal violet assay (Figure 3C). In contrast, the growth of MPR-F (in absence of CDK4/6i and fulvestrant) was significantly reduced after RET knockdown compared to the control siRNA (Figure 3C), indicating that the resistant MPF-R cells, but not the sensitive counterparts, are dependent on the expression of RET for proliferation and growth. This supports that RET may has a key role in the mechanisms of resistance to combined CDK4/6i and fulvestrant therapy in the MCF-7-derived cell model. The same effect on cell growth upon RET siRNA-mediated knockdown was not observed in TPF-R cells (in absence of CDK4/6i and fulvestrant), which may be due to the significant lower level of RET in these cells.

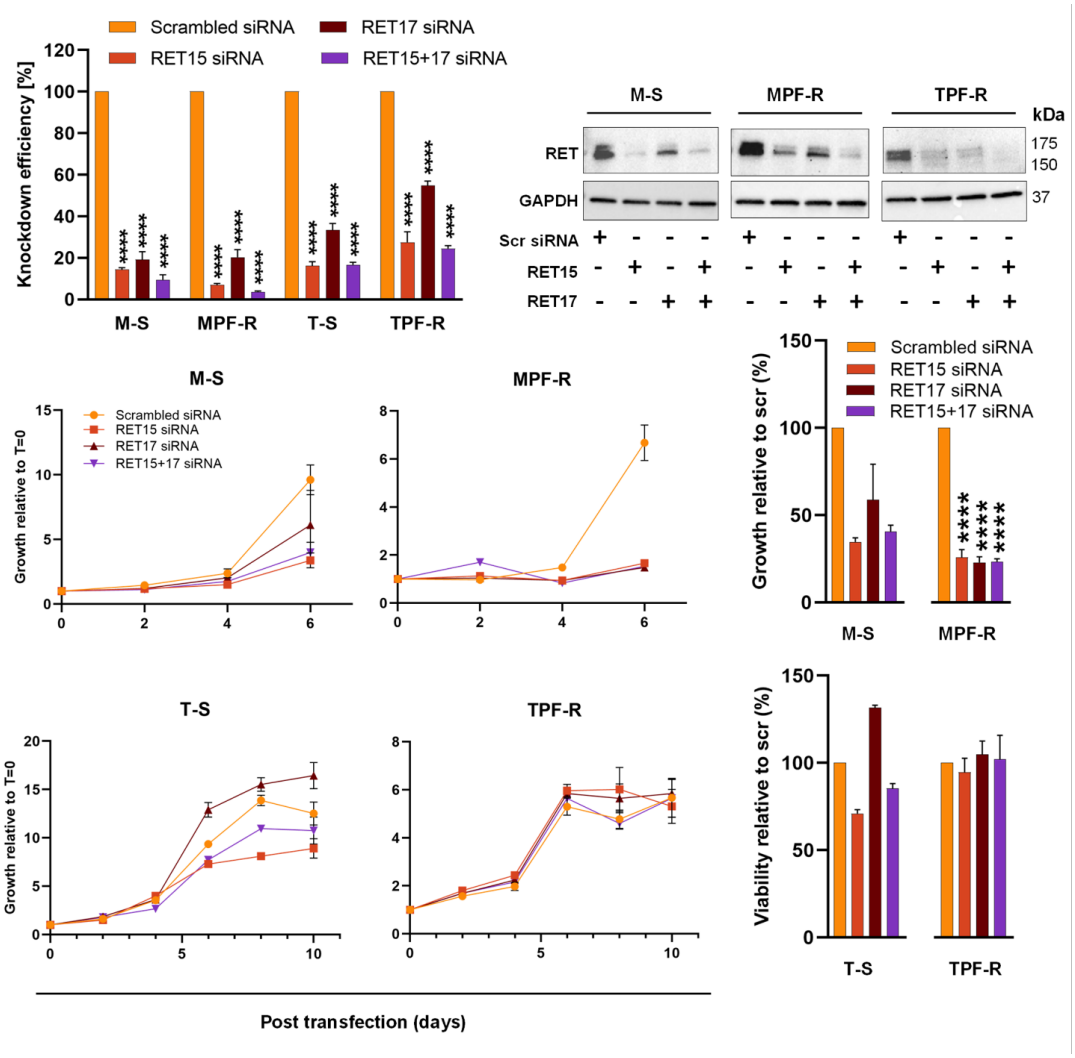

Figure 3: RET-specific siRNA mediated knockdown is effective in all cell lines on RNA and protein level. The efficiency of RET silencing in fulvestrant and CDK4/6i resistant cell lines (MPF-R and TPF-R) and their parental sensitive cell lines (M-S and T-S respectively) transfected with two different RET-specific siRNAs (RET15 and RET17) or scrambled siRNA (control). A) Quantitative RT-PCR verifying reduction of RET mRNA level 48 h post-transfection with RET-specific siRNA. The expression was normalized using PUM1 gene. The knockdown efficiency is represented as average percentage compared to control (scr) of triplicates mean ± SEM. B) Western blot validation of protein level 96 h post-transfection with RET-specific siRNAs. GAPDH was used as protein loading control. C) Cell growth at different time points following Ret-specific siRNA transfection, as assessed by crystal violet assay. Columns show cell growth at day 6 and 10 for MCF7 derived cell lines and T47D derived cell lines respectively. Scrambled siRNA: control siRNA, RET15 and RET17: two different RET-specific siRNAs. RET15+17: combination of both RET-specific siRNAs. Asterisks indicate significant differences in one-way ANOVA test (**p < 0.0001).**

RET is a driver of cell cycle progression in combined CDK4/6i and fulvestrant resistant ER+ BC cells

To identify which pathways were altered following silencing of *RET* we performed gene expression analysis on MPF-R and TPF-R cells transfected with RET-siRNA compared to cells transfected with controls siRNA. Remarkably, alterations in regulators of cell cycle, particularly regulators of G2-M phase and E2F targets, were identified as top significantly enriched gene-datasets by gene set enrichment analysis (GSEA) in control-siRNA compared to RET-siRNA treated MPF-R and TPF-R cells (supplementary Figure 1 and 2). In both MCF7- and T47D-derived resistant cells, *RET* knockdown is significantly correlated with reduced expression of genes of regulators of late phase cell cycle transition.

The specific RET inhibitor selpercatinib in combination with CDK4/6i and fulvestrant inhibits growth of combined CDK4/6i and fulvestrant-resistant ER+ BC cells

To evaluate whether we could pharmacologically overcome resistance to combined CDK4/6i and fulvestrant, we examined whether treatment with a specific inhibitor of RET, selpercatinib, alone or in combination with CDK4/6i and/or fulvestrant could inhibit growth of MPF-R and TPF-R cells resistant towards CDK4/6i and fulvestrant.

RET inhibition resensitized resistant MPF-R and TPF-R cells to combined CDK4/6i and fulvestrant treatment (Figure 4C and 4D). Indeed, treatment with the triple combination including fulvestrant, CDK4/6i, and RETi significantly reduced growth of MPF-R cells compared to combined CDK4/6i and fulvestrant. Furthermore, triple therapy more efficiently inhibited growth of TPF-R cells compared to the dual therapy with fulvestrant and RETi, although the difference did not reach statistical significance. Interestingly, the dual combination with RETi and either fulvestrant or CDK4/6i reduced MPF-R and TPF-R cells growth more efficiently than combined CDK4/6i and fulvestrant (Figure 4B). These data further indicate that BC ER+ cells use RET upregulation as a mean to acquire resistance to combined CDK4/6i and endocrine therapy.

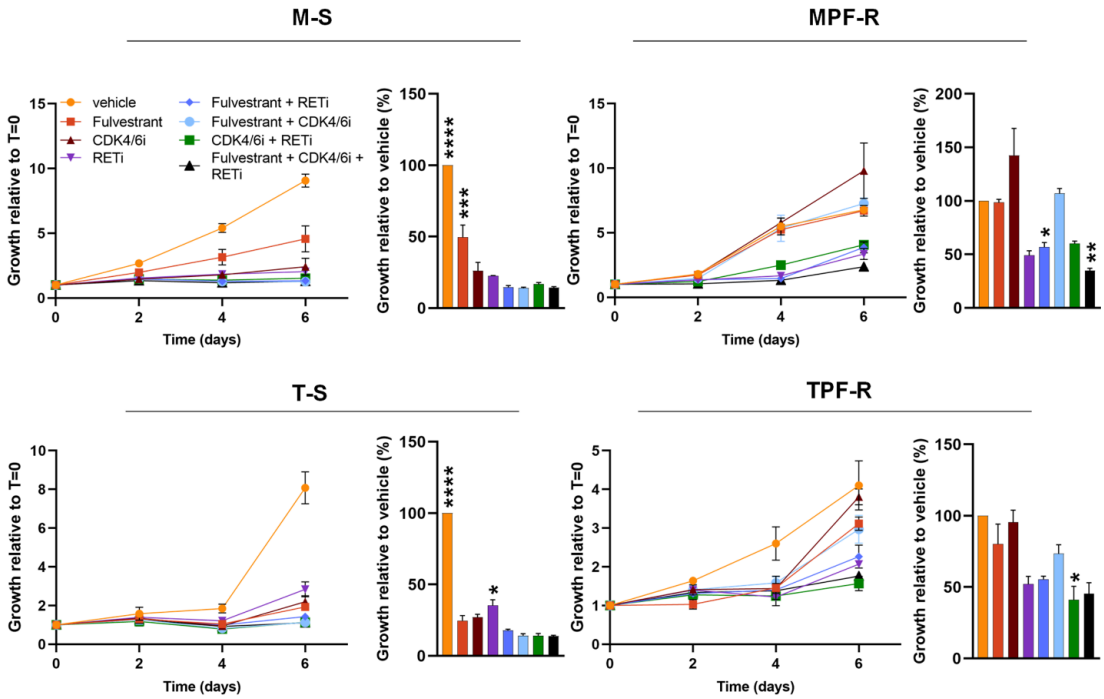

Figure 4: RETi resensitizes TPF-R and MPF-R to CDK4/6i and fulvestrant treatment. *Cell growth assays were performed over 6 days of treatment with fulvestrant (100nM), CDK4/6i (200 nM) and RETi (5μM) alone or different combinations as assessed by crystal violet. Growth at day 6 is represented by columns. The data represents the mean of three biological replicates ± SEM. Asterisks indicate significant differences in one-way ANOVA tests at day 6. Means are compared to the mean of the standard combined CDK4/6i and fulvestrant therapy (*0.01 < p < 0.05, **0.001 < p < 0.01, ***0.0001 < p < 0.001, and ****p < 0.0001).*

High expression of RET correlates with poor clinical outcome in ER+ HER2- patients treated with endocrine therapy

Finally, we evaluated the clinical relevance of RET by assessing the correlation between RET expression and clinical outcome in ER+ breast cancer patients. Firstly, we used the web-based tool Kaplan-Meier plotter (46) to access the correlation between *RET* mRNA expression and overall survival (OS) and relapse-free survival (RFS) in a cohort of ER+ BC patients receiving endocrine treatment in the primary setting. High RET expression significantly correlated with shorter OS (n=189, p=0.0504, HR=1.92; Figure 5A) in ER+, HER2- BC patients who have been treated with endocrine therapy. Estimated 10-year survival was 70% for patients with high expression of RET and 85% for patients with low expression of RET (Figure 5A). High RET expression was also associated with shorter RFS (n=1201, p=0.054, HR=1.3; Figure 5B). Median time to relapse was 15 years (180 months) in the high-RET group, whereas the median time to progression in the low-RET group was 16 years (200 months) (Figure 5B).

Next, we evaluated the clinical relevance of RET as a biomarker of response/resistance to combined CDK4/6i and endocrine therapy in a cohort of ER+ advanced BC patients. The expression levels of RET were evaluated in full sections of metastatic lesions before treatment with combined CDK4/6i and endocrine therapy. The survival analysis indicated no correlation between RET-high (intensity ≥2) or RET-low (intensity <2) levels and progression-free survival (PFS; *p*=0.278, Figure 6).

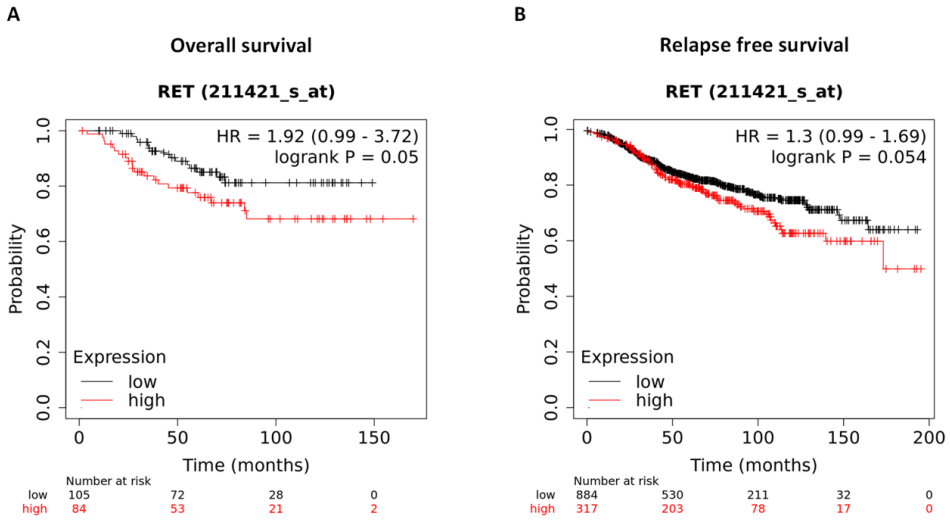

Figure 5: High RET expression correlates with shorter overall survival in ER+ BC patients who have undergone endocrine treatment. *Kaplan-Meier survival curves for OS (A) and RFS (B) for RET expression by KM plotter analysis.*

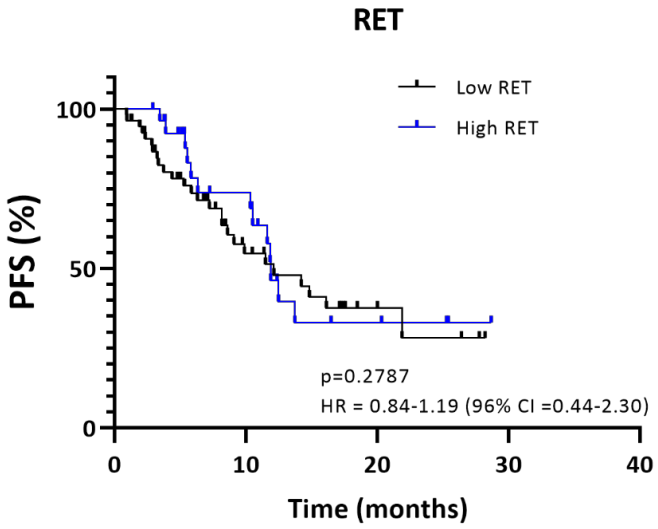

Figure 6: RET expression is not associated with progression free survival (PFS) in patients with metastatic ER+ breast cancer treated with combined CDK4/6i and endocrine therapy. *Kaplan-Meier survival curves evaluating PFS according to RET score in ER+ metastatic lesions from breast cancer patient. The cutoff values used: Low RET: 0-1, High RET: ≥2. A two-sided p-value calculated using Log-rank testing is shown.*

Discussion

Although combined CDK4/6i and endocrine therapy has significantly improved outcome of patients with advanced ER+ BC, progression is inevitable and thus, new therapeutic strategies to overcome treatment resistance are urgently needed. In this study, we show that RET is upregulated in breast cancer cell lines resistant to combined CDK4/6i and endocrine therapy and inhibition of RET, either by siRNA-mediated knockdown or with the RET-specific inhibitor selpercatinib, alone or in combination with CDK4/6i and/or fulvestrant reduces growth of combined CDK4/6i and fulvestrant-resistant ER+ breast cancer cell lines. To our knowledge, our study is the first to suggests an association between RET overexpression and induction of cell-cycle progression, which likely contributes to resistance to combined CDK4/6i and endocrine therapy.

Recently, the RETi selpercatinib has been approved for use in NSCLC, PTC, and MTC patients with *RET* activating fusions or mutations. We examined the CDK4/6i- and fulvestrant- resistant cell lines for RET fusions using RNA-sequencing, but none were found. Since the drug also has effect on RET-wildtype tumors, it may also be useful in patients with RET overexpressing cancers. Following resistance towards combined CDK4/6i and endocrine therapy, RETi could be added to the combination treatment or administered in combination with endocrine therapy alone. Importantly, results from a recent clinical trial evaluating the multikinase inhibitor lenvatinib (with potent activity

against RET) in combination with AI letrozole showed manageable toxicity profile and promising efficacy in ER+ advanced breast cancer patients heavily pretreated, including in patients who progressed on previous combined CDK4/6i and endocrine therapy (47). Previous studies have shown that RET induces estrogen independent ERα phosphorylation and expression of ER target genes in ER+ breast cancer cells (21, 48). Overexpression of RET or its ligand GDNF has been associated with resistance to ER-targeted treatment with tamoxifen, through activation of the RAS/RAF/MEK/ERK or the mTOR/P70S6K pathway. This is consistent with our findings, that RET induces growth and proliferation during combined CDK4/6i and endocrine therapy, though we have not yet evaluated alterations of PI3K and ERK following RET knockdown. In our study, we found that RET silencing using RET-specific siRNAs significantly inhibited growth of MCF7-derived ER+ breast cancer cells resistant to combined CDK4/6i and endocrine therapy (MPF-R). This effect was not observed in either the sensitive cell lines M-S or T-S, but also not in the T47D-derived double-resistant cell line (TPF-R). Although TPF-R showed an increase in RET expression compared to the sensitive paternal T-S cell line, the amount of RET was significantly lower than in MPF-R, as shown by Western Blotting and RNA-seq. These data suggest that RET overexpression is a key regulator of resistance to combined CDK4/6i and endocrine therapy in MCF7-derived, but not in T47D-derived resistant cells. The difference in effect of RET silencing in the two CDK4/6i and endocrine therapy resistant cell lines MPF-R and TPF-R might be due to the difference in the activation of the PI3K/AKT/mTOR and RAS/RAF/MEK/ERK pathways in MCF-7 and T47D parental cells. Indeed, increased AKT and ERK activation has been observed in MCF7-derived fulvestrant-resistant cell line (MF-R) due to a reliance on HER2 receptors for growth compared to the sensitive parental cell line, but this was not observed in the T47D-derived fulvestrant-resistant cell line (TF-R) (49-51). Since RET activates the RAS–MAPK and PI3K–AKT pathways in breast cancer cell lines, this might suggest that cell lines less dependent on these pathways for growth will also respond less to RET inhibition. Nevertheless, siRNA-mediated silencing of RET was associated with a significant decrease in the activation of pathways involved in late-stage cell cycle control. This indicates that RET plays a role in this stage of cell cycle progression, which have not been reported previously. Earlier studies have shown that RET upregulate the transcription of cyclin D1, leading to cell cycle progression, and tamoxifen resistance, but this effect was blocked by the addition of a CDK4/6i (52). In our study we do not observe a decrease in cyclin D1 following RET silencing, but the most pronounced effect of silencing RET was on the late stages of cell cycle progression, in which cyclin D1 is not in-

volved in. Further, analysis on the effect of CDK4/6i and endocrine therapy following RET silencing is ongoing.

Finally, we show in our study that high levels of RET significantly correlated with shorter overall survival in patients with ER+ breast cancer who received any type of endocrine therapy. These findings concur with other studies showing increased RET expression in metastatic ER+ breast cancer following endocrine therapy and in samples from AI resistant patients (21, 26), and with the observation that RET play a role in resistance to endocrine therapy (21, 26, 48). However, there was no significant correlation between RET expression level and PFS of ER+ advanced breast cancer patients treated with combined CDK4/6i and endocrine therapy. These findings suggest that, although RET overexpression may be involved in the mechanisms of acquired resistance to CDK4/6i and endocrine therapy, there is likely not potential for RET as a biomarker of response to this treatment in pretreated samples.

In conclusion, RET overexpression appears to contribute to resistance to combined CDK4/6i and endocrine therapy in ER+ breast cancer by promoting cell cycle progression. RET inhibition could be a potential strategy for patients who develop resistance to CDK4/6i and endocrine therapy.

Acknowledgements

We thank Lone Christiansen at the Department of Pathology, Odense University Hospital, for excellent technical assistance with the immunohistochemistry.

Conflicts of interest

The authors declare no potential conflicts of interest.

Data availability

The gene expression data generated during the study are publicly available in the gene expression omnibus (GEO) database under the accession number GSE228637. Survival analyses and immunohistochemistry data are not publicly available to protect patient privacy but will be made available to authorized researchers who have an approved Institutional Review Board application and have obtained approval from the Regional Committees on Health Research Ethics for Southern Denmark. Please contact the corresponding author with data access requests. All other datasets generated during the study will be made available upon reasonable request to the corresponding author, Dr. Henrik Ditzel, email address: hditzel@health.sdu.dk. Uncropped Western blots are part of the supplementary information.

Supplementary figures

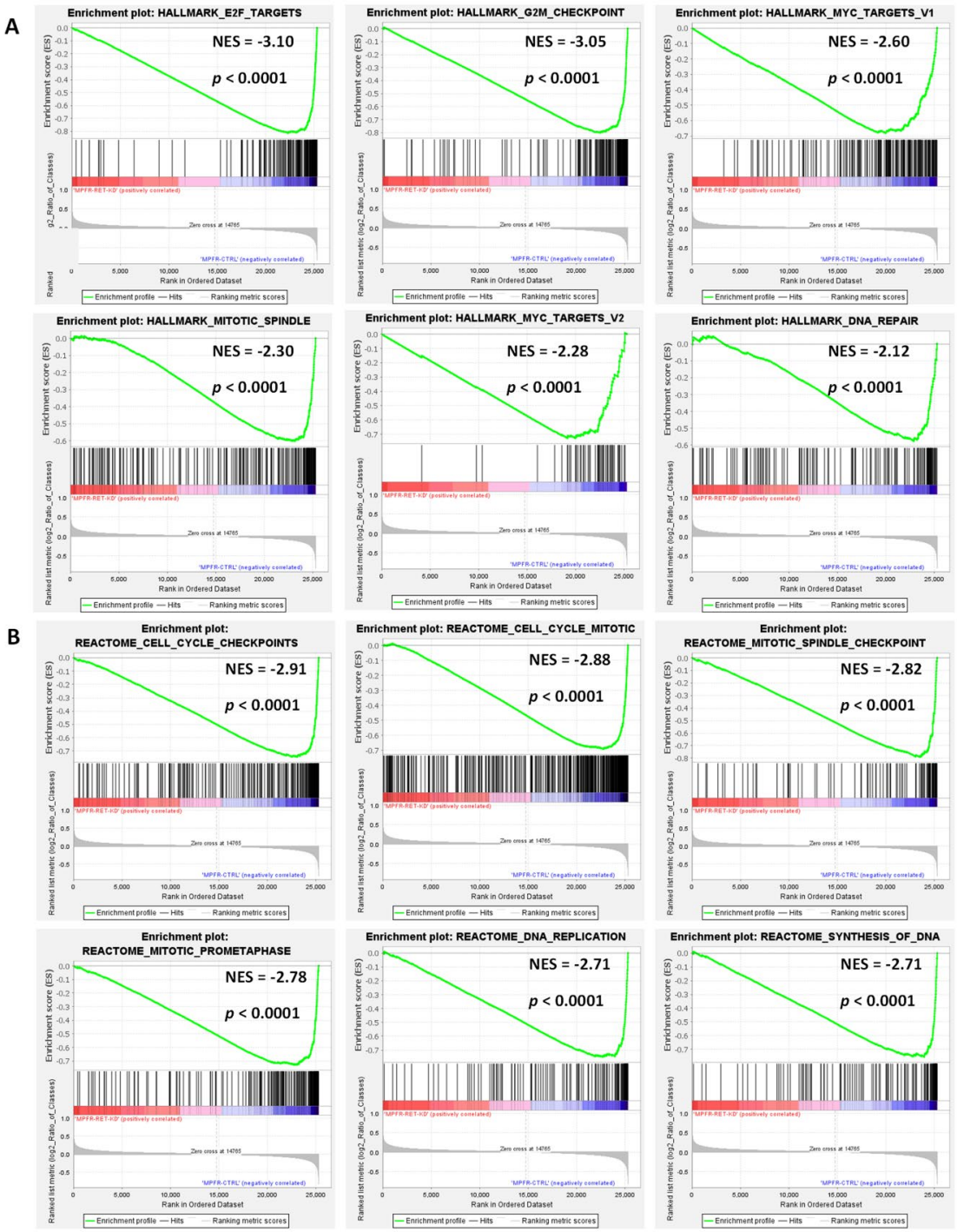

Supplementary Figure 1: GSEA enrichment plots for MPF-R cells treated with RET-specific siRNA versus MPF-R cells treated with control siRNA. *A) Enrichment plots made from Hallmark genes, B) Enrichment plots made from Reactome genes. Genes involved in E2F, G2M checkpoint, MYC targets, mitotic Spindle, DNA repair, cell cycle checkpoints, mitotic spindle, prometaphase, DNA replication, and synthesis of DNA are downregulated when RET is silenced.*

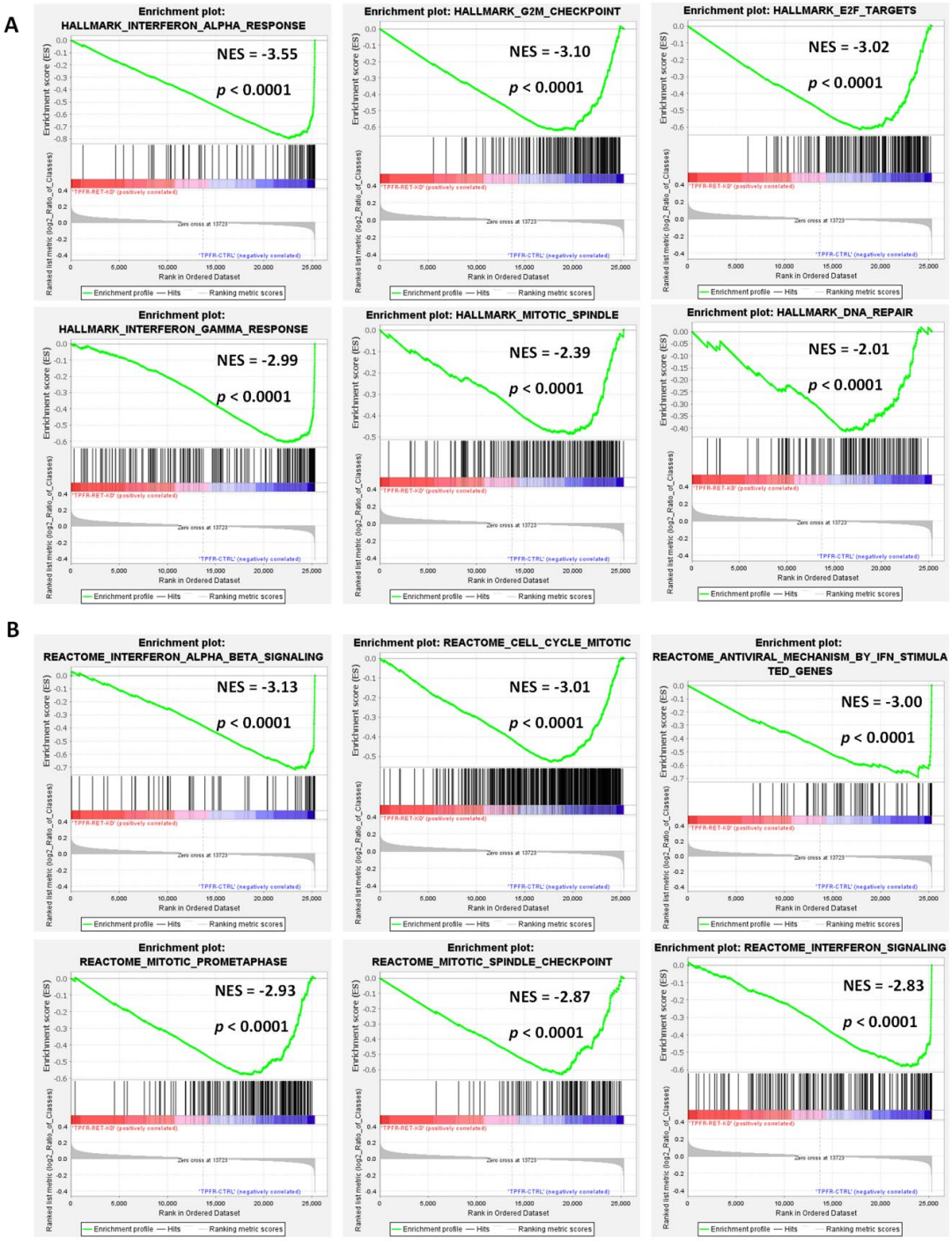

Supplementary Figure 2: GSEA enrichment plots for TPF-R cells treated with RET-specific siRNA versus TPF-R cells treated with control siRNA. *A) Enrichment plots made from Hallmark genes, B) Enrichment plots made from Reactome genes. Genes involved in G2M checkpoint, E2F targets, mitotic spindle, DNA repair, cell cycle mitotic, prometaphase, and mitotic spindle checkpoint are downregulated when RET is silenced.*

A

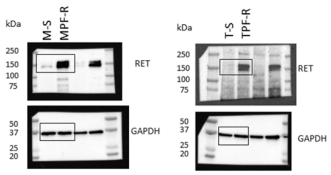

B

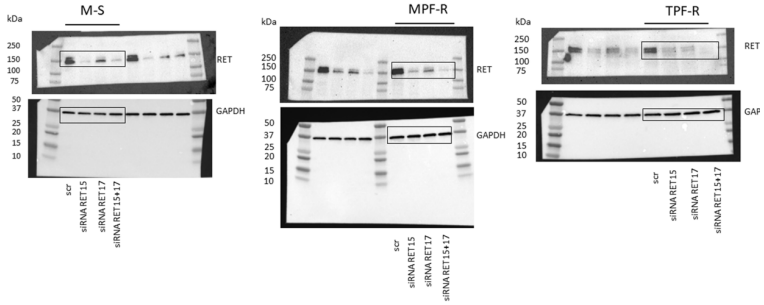

Supplementary Figure 3: Uncropped Western Blot of ER+ cell lines. *A) RET expression and GAPDH expression in M-S, MPF-R, T-S, and TPF-R. B) RET expression following silencing of RET in M-S, MPF-R and TPF-R. siRNAs: scr: unspecific control siRNA, RET15 and RET17: RET-specific siRNAs.*

References

1. Siegel RL, et al. Cancer statistics, 2022. CA: A Cancer Journal for Clinicians. 2022;72(1):7-33.
2. Sung H, et al. Global Cancer Statistics 2020: GLOBOCAN Estimates of Incidence and Mortality Worldwide for 36 Cancers in 185 Countries. CA: A Cancer Journal for Clinicians. 2021;71(3):209-49.
3. Finn RS, et al. Palbociclib and Letrozole in Advanced Breast Cancer. New England Journal of Medicine. 2016;375(20):1925-36.
4. Pan H, et al. 20-Year Risks of Breast-Cancer Recurrence after Stopping Endocrine Therapy at 5 Years. New England Journal of Medicine. 2017;377(19):1836-46.
5. Varma H, et al. Functional Ablation of pRb Activates Cdk2 and Causes Antiestrogen Resistance in Human Breast Cancer Cells. PLOS ONE. 2007;2(12):e1256.
6. Finn RS, et al. PD 0332991, a selective cyclin D kinase 4/6 inhibitor, preferentially inhibits proliferation of luminal estrogen receptor-positive human breast cancer cell lines in vitro. Breast Cancer Research. 2009;11(5):R77.
7. Markey MP, et al. Loss of the retinoblastoma tumor suppressor: differential action on transcriptional programs related to cell cycle control and immune function. Oncogene. 2007;26(43):6307-18.
8. Thangavel C, et al. Therapeutically activating RB: reestablishing cell cycle control in endocrine therapy-resistant breast cancer. Endocrine-Related Cancer. 2011;18(3):333-45.
9. Lundberg AS, Weinberg RA. Control of the cell cycle and apoptosis. Eur J Cancer. 1999;35(14):1886-94.
10. Hortobagyi GN, et al. Ribociclib as First-Line Therapy for HR-Positive, Advanced Breast Cancer. New England Journal of Medicine. 2016;375(18):1738-48.
11. Goetz MP, et al. MONARCH 3: Abemaciclib As Initial Therapy for Advanced Breast Cancer. Journal of Clinical Oncology. 2017;35(32):3638-46.
12. Turner NC, et al. Palbociclib in Hormone-Receptor–Positive Advanced Breast Cancer. New England Journal of Medicine. 2015;373(3):209-19.
13. George W. Sledge J, et al. MONARCH 2: Abemaciclib in Combination With Fulvestrant in Women With HR+/HER2− Advanced Breast Cancer Who Had Progressed While Receiving Endocrine Therapy. Journal of Clinical Oncology. 2017;35(25):2875-84.
14. Im S-A, et al. Overall Survival with Ribociclib plus Endocrine Therapy in Breast Cancer. New England Journal of Medicine. 2019;381(4):307-16.
15. Johnston SRD, et al. Abemaciclib plus endocrine therapy for hormone receptor-positive, HER2-negative, node-positive, high-risk early breast cancer (monarchE): results from a preplanned interim analysis of a randomised, open-label, phase 3 trial. The Lancet Oncology. 2023;24(1):77-90.
16. Condorelli R, et al. Polyclonal RB1 mutations and acquired resistance to CDK 4/6 inhibitors in patients with metastatic breast cancer. Ann Oncol. 2018;29(3):640-5.
17. Portman N, et al. Overcoming CDK4/6 inhibitor resistance in ER-positive breast cancer. Endocrine-Related Cancer. 2019;26(1):R15-R30.
18. Ibáñez CF. Structure and physiology of the RET receptor tyrosine kinase. Cold Spring Harb Perspect Biol. 2013;5(2).
19. Gattelli A, et al. Ret Receptor Has Distinct Alterations and Functions in Breast Cancer. J Mammary Gland Biol Neoplasia. 2020;25(1):13-26.
20. Mulligan LM. RET revisited: expanding the oncogenic portfolio. Nat Rev Cancer. 2014;14(3):173-86.
21. Plaza-Menacho I, et al. Targeting the receptor tyrosine kinase RET sensitizes breast cancer cells to tamoxifen treatment and reveals a role for RET in endocrine resistance. Oncogene. 2010;29(33):4648-57.
22. Kothari V, et al. Outlier Kinase Expression by RNA Sequencing as Targets for Precision Therapy. Cancer Discovery. 2013;3(3):280-93.
23. Wang C, et al. The rearranged during transfection/papillary thyroid carcinoma tyrosine kinase is an estrogen-dependent gene required for the growth of estrogen receptor positive breast cancer cells. Breast Cancer Research and Treatment. 2012;133(2):487-500.
24. Boulay A, et al. The Ret receptor tyrosine kinase pathway functionally interacts with the ERalpha pathway in breast cancer. Cancer Res. 2008;68(10):3743-51.
25. Gattelli A, et al. Chronic expression of wild-type Ret receptor in the mammary gland induces luminal tumors that are sensitive to Ret inhibition. Oncogene. 2018;37(29):4046-54.

26. Morandi A, et al. GDNF-RET signaling in ER-positive breast cancers is a key determinant of response and resistance to aromatase inhibitors. Cancer Res. 2013;73(12):3783-95.
27. Spanheimer PM, et al. Inhibition of RET increases the efficacy of antiestrogen and is a novel treatment strategy for luminal breast cancer. Clin Cancer Res. 2014;20(8):2115-25.
28. Andreucci E, et al. Targeting the receptor tyrosine kinase RET in combination with aromatase inhibitors in ER positive breast cancer xenografts. Oncotarget. 2016;7(49):80543-53.
29. Richardson DS, et al. Transcript level modulates the inherent oncogenicity of RET/PTC oncoproteins. Cancer Res. 2009;69(11):4861-9.
30. Kondo T, et al. Pathogenetic mechanisms in thyroid follicular-cell neoplasia. Nature Reviews Cancer. 2006;6(4):292-306.
31. Wang R, et al. RET Fusions Define a Unique Molecular and Clinicopathologic Subtype of Non–Small-Cell Lung Cancer. Journal of Clinical Oncology. 2012;30(35):4352-9.
32. Paratala BS, et al. RET rearrangements are actionable alterations in breast cancer. Nat Commun. 2018;9(1):4821.
33. Unger K, et al. Novel gene rearrangements in transformed breast cells identified by high-resolution breakpoint analysis of chromosomal aberrations. Endocr Relat Cancer. 2010;17(1):87-98.
34. Kato S, et al. RET Aberrations in Diverse Cancers: Next-Generation Sequencing of 4,871 Patients. Clinical Cancer Research. 2017;23(8):1988-97.
35. Della Corte CM, Morgillo F. Rethinking treatment for RET-altered lung and thyroid cancers: selpercatinib approval by the EMA. ESMO Open. 2021;6(1).
36. Bradford D, et al. FDA Approval Summary: Selpercatinib for the Treatment of Lung and Thyroid Cancers with RET Gene Mutations or Fusions. Clin Cancer Res. 2021;27(8):2130-5.
37. Subbiah V, et al. Selective RET kinase inhibition for patients with RET-altered cancers. Ann Oncol. 2018;29(8):1869-76.
38. Livak KJ, Schmittgen TD. Analysis of Relative Gene Expression Data Using Real-Time Quantitative PCR and the 2−ΔΔCT Method. Methods. 2001;25(4):402-8.
39. Dobin A, et al. STAR: ultrafast universal RNA-seq aligner. Bioinformatics. 2013;29(1):15-21.
40. Madsen JG, et al. iRNA-seq: computational method for genome-wide assessment of acute transcriptional regulation from total RNA-seq data. Nucleic Acids Res. 2015;43(6):e40.
41. Love MI, et al. Moderated estimation of fold change and dispersion for RNA-seq data with DESeq2. Genome Biol. 2014;15(12):550.
42. Nicorici D, et al. FusionCatcher – a tool for finding somatic fusion genes in paired-end RNA-sequencing data. bioRxiv. 2014:011650.
43. Haas BJ, et al. Accuracy assessment of fusion transcript detection via read-mapping and de novo fusion transcript assembly-based methods. Genome Biology. 2019;20(1):213.
44. Uhrig S, et al. Accurate and efficient detection of gene fusions from RNA sequencing data. Genome Res. 2021;31(3):448-60.
45. Lánczky A, Győrffy B. Web-Based Survival Analysis Tool Tailored for Medical Research (KMplot): Development and Implementation. J Med Internet Res. 2021;23(7):e27633.
46. Győrffy B. Survival analysis across the entire transcriptome identifies biomarkers with the highest prognostic power in breast cancer. Computational and Structural Biotechnology Journal. 2021;19:4101-9.
47. Lim JSJ, et al. Phase Ib/II Dose Expansion Study of Lenvatinib Combined with Letrozole in Postmenopausal Women with Hormone Receptor–Positive Breast Cancer. Clinical Cancer Research. 2022;28(11):2248-56.
48. Zheng ZZ, et al. Super-enhancer-controlled positive feedback loop BRD4/ERα-RET-ERα promotes ERα-positive breast cancer. Nucleic Acids Res. 2022;50(18):10230-48.
49. Frogne T, et al. Antiestrogen-resistant human breast cancer cells require activated protein kinase B/Akt for growth. Endocrine Related Cancer. 2005;12(3):599.
50. Frogne T, et al. Activation of ErbB3, EGFR and Erk is essential for growth of human breast cancer cell lines with acquired resistance to fulvestrant. Breast Cancer Research and Treatment. 2009;114(2):263-75.
51. Kirkegaard T, et al. T47D breast cancer cells switch from ER/HER to HER/c-Src signaling upon acquiring resistance to the antiestrogen fulvestrant. Cancer Lett. 2014;344(1):90-100.
52. Marks BA, et al. GDNF-RET signaling and EGR1 form a positive feedback loop that promotes tamoxifen resistance via cyclin D1. BMC Cancer. 2023;23(1):138.

Chapter 6: Manuscript 2

Genomic alterations associated with CDK4/6 inhibitor resistance and serial circulating tumor DNA monitoring in CDK4/6 inhibitor treated patients with advanced estrogen receptor-positive breast cancer

Charlotte Karup Kindt[1], Carla Alves[1], Sidse Ehmsen[1,2], Amalie Kragh[2], Thomas Reinert[3], Marianne Vogsen[2], Annette Raskov Kodahl[2], Jeanette Dupont Jensen[2], Dilan Ardik[4], Rasmus Koefod Petersen[4], Johan Staaf[5], Henrik Ditzel[1,2]

1: Department of Cancer and Inflammation Research, Institute of Molecular Medicine, University of Southern Denmark, Odense, Denmark
2: Department of Oncology, Odense University Hospital; Institute of Clinical Research, University of Southern Denmark, Odense, Denmark
3: Department of Clinical Medicine, Aarhus University, Denmark
4: PentaBase Aps, Odense, Denmark
5: Division of Oncology, Department of Clinical Sciences Lund, Lund University, Lund, Sweden.

Abstract
Combined CDK4/6 inhibitor (CDK4/6i) and endocrine therapy significantly improves outcome of patients with advanced estrogen receptor-positive breast cancer, but drug resistance and thus disease progression inevitably occur. To identify genomic alterations associated with combined CDK4/6i and endocrine resistance, we performed whole exome sequencing or targeted sequencing of paired tumor or blood samples taken prior to combined CDK4/6i and endocrine therapy and on progression. Although only few or no mutations in potential driver genes associated with resistance were generally identified in the individual patients, a few known or novel alterations potentially associated with resistance were identified. Some of the genomic alterations identified by sequencing were also used to follow disease progression in serial blood samples of circulating tumor DNA (ctDNA). Serial ctDNA analysis for mutant *PIK3CA* (n=30) in six patients with advanced ER+ breast cancer treated with combined CDK4/6i, and endocrine therapy revealed progression in five of six patients. Rising levels of mutant *PIK3CA* ctDNA were in three cases observed 13, 4, and 17 months, respectively, prior to the PET-CT revealing clinical disease progression. Our data adds to the growing evidence indicating the possible utilizing serial ctDNA analysis for real-time monitoring of CDK4/6i response and earlier identification of progressive disease.

Introduction

Advanced estrogen receptor-positive (ER+) breast cancer is a severe disease but remarkable advancements in the treatment has occurred over the past decade (1). Notably, the addition of cyclin-dependent kinase 4/6 inhibitors (CDK4/6i) to endocrine therapy in the metastatic setting has shown impressive improvement of progression-free survival (PFS) and overall survival (OS) for patients who have progressed on previous endocrine therapy (2). CDK4/6i extended PFS from 4.6 to 9.5 months as second-line therapy in combination with the estrogen receptor degrader fulvestrant, and from 23.8 to 28.8 months as first-line therapy in combination with aromatase inhibitors (3-5). Unfortunately, resistance to this treatment is inevitable and multiple molecular mechanisms have been reported. Among these, loss of *RB* and *RB* mutations have been detected in both pre-clinical studies and metastatic biopsies from patients after progression on CDK4/6i, although infrequently (6-8). Furthermore, alterations in growth regulatory pathways controlling cell proliferation and cell cycle progression, such as *FGFR1/2* amplification and activating *HER2* mutations, have also been described in tumor samples following progression on CDK4/6i and endocrine therapy (9, 10). Moreover, alterations in regulators of G1-S phase transition of the cell cycle, including CDK4/6 and CDK2, as well as abnormal activation of various growth factor receptor signaling pathways, such as the PI3K/AKT and RAS/ERK pathways, have also been proposed as resistance mechanisms to CDK4/6i and endocrine therapy in pre-clinical studies (6-9, 11, 12). Thus, there is a need to better understand the mechanism underlying resistance to combined CDK4/6i and endocrine therapy using clinical samples and identify better therapeutic strategies upon disease progression. Additionally, improved real-time monitoring of treatment response/disease progression is required as assessment of treatment response through serial radiographic images is associated with suboptimal detection sensitivity and inconsistencies in tumor size measurements (13, 14).

Tumor tissue biopsies have been the gold standard for clinical genomic testing; however, the invasive nature of tumor biopsies has sparked interest in non-invasive liquid biopsies. Circulating free DNA (cfDNA) is released into the blood stream due to cellular breakdown by necrosis and apoptosis. Circulating tumor DNA (ctDNA) is often detected in blood samples of cancer patients (15), and the amounts often correlate with tumor size, stage, localization, and vascularization (16, 17), although some liquid biopsies from metastatic disease exhibit unexpected low fraction of ctDNA (18, 19). Indeed, the fraction of cfDNA consisting of ctDNA can be lower than 0.01 % posing a challenge in the reliable and accurate detection of alterations in ctDNA, which require highly specialized technologies (20).

In the present study, we investigated genomic alterations in paired ER+ metastatic breast cancer lesions prior to treatment initiation with combined CDK4/6i and endocrine therapy and following progression as well as ctDNA prior to treatment initiation, during treatment and at disease progression. To this end, we performed whole-exome sequencing (WES) or targeted sequencing to identify alterations associated with treatment resistance as well as other genomic alterations that could be used to monitor disease progression in ctDNA isolated from blood samples. Thus, allowing improved informed treatment decisions for patients with metastatic ER+ breast cancer.
Our results show that most of the genetic alterations found between samples before and after treatment with combined CDK4/6i and endocrine therapy were rare and distinct for each patient, while several copy number variations were shared between some patients. The most frequent acquired oncogenic alterations observed were *PIK3CA* and *TP53* mutations, and *PDK1* amplification. Finally, we show that analysis of *PIK3CA* mutations in ctDNA can be used to detect metastatic breast cancer progression earlier than standard radiographic methods.

Methods

Study population

Eighty ER+ advanced breast cancer patients were enrolled in this retrospective study. Inclusion criteria were patients ≥18 years old, with histologically confirmed ER+ inoperable metastatic breast cancer, eligible for combined CDK4/6i and endocrine therapy and no prior treatment with a CDK4/6i. All patients provided written informed consent for participation in the study, and collection, storage, and genomic analysis of biopsies and blood samples. Patients were followed up until disease progression, death, or end of the observational period (January 30th 2023). The study protocol was approved by the Ethical Committee Region of Southern Denmark (project-ID: S-20170154) and the Danish Data Protection Agency and was conducted in accordance with the Helsinki declaration.

Sample collection and processing

A baseline core-needle biopsy and/or blood sample was taken before starting treatment with combined CDK4/6i and endocrine therapy, as part of the routine clinical diagnostic protocol and was preferably stored as fresh frozen material. If this was not possible, formalin-fixed paraffin-embedded (FFPE) tissue was used. During treatment with combined CDK4/6i and endocrine therapy, blood samples were collected approximately every 12 weeks. A final blood sample and in few cases (n=5) a tissue biopsy were collected at the end point (disease progression).

Approximately 18 mL of venous blood was extracted at each timepoint and collected in 10 ml Streck Cell-free DNA BCT blood collection tubes (Streck, cat. No.: 230244). Blood was processed within 2 h after the collection. Centrifugation at 1600g for 10 minutes at 20°C was performed to separate plasma from the peripheral blood cells. The supernatant was transferred into 2 mL microcentrifuge tubes followed by a second centrifugation at 3000g for 20 minutes at 20°C to remove any remaining contaminants. Plasma was immediately aliquoted in 4x1.5 mL tubes and stored at -80°C until DNA extraction. Approximately 6 mL plasma was obtained from each patient per timepoint.

DNA extraction

DNA was extracted from FFPE and fresh frozen tissue samples using the Maxwell RSC instrument (Promega, Madison, WI, USA). The Maxwell RSC FFPE and Tissue DNA Kit (Promega, cat. No.: AS1450 and AS1610) were used on the instrument for different tissue types, according to the manufacturer's instructions. DNA was stored at -80°C until further use.

cfDNA was isolated from 3 ml aliquots of plasma using the QIAamp circulating nucleic acid kit (Qiagen, cat. No.: 55114) according to manufacturer's instructions and eluted with 60-75µL elution buffer into 1.5 mL DNA low binding tubes.

All DNA was quantified using the Qubit dsDNA HS Assay (Thermo Fisher Scientific, cat. No.: Q33231) together with the Qubit 3.0 Fluorometer (Thermo Fisher Scientific, Waltham, MA, USA). Following extraction and quantification DNA was stored at -80°C until further analysis.

Whole exome sequencing (WES)

WES was performed at the Department of Molecular Medicine, Aarhus University Hospital on matched tumor DNA (derived from primary fresh frozen and FFPE tissue) and buffy coat DNA. Libraries of tumor and matching germline DNA were prepared using 50 ng DNA and captured by Twist Comprehensive Exome with custom spike-ins, sequenced on the Illumina NovaSeq 6000 platform to an average coverage of 413x (range: 148-515x) (supplementary Table 1). The custom spike-ins consisted of 1042 SNP sites located throughout the genome. Raw sequencing data (FastQ files) were prepared using bcl2fastq2 (v2.20.0.422) and quality checked using FastQC (v0.11.5). Adapters were removed using cutadapt (v3.0). The trimmed tumor and germline samples were treated according to the GATK best practices. Reads were mapped to the hg38 reference genome using bwa-mem (v0.7.17) and PCR duplicates were marked for filtering in the downstream analysis using Picard MarkDuplicates (v2.23.3).

Somatic variants were called using GATK (v4.1.9.0), Mutect2, and Strelka2 (v2.9.10). Final somatic VCF file contained Mutect2 calls within 10bp of targeted regions. Only non-filtered (PASS) variants were included. Furthermore, variants in coding regions (repeat masked regions excluded) identified by Mutect2 that did not pass the built-in filters were reintroduced if they were identified with high confidence using Strelka. Germline variants were called using the GATK HaplotypeCaller. The SNVs were functionally annotated using snpEff (v5.1) (21).

As a quality control for all samples captured by the Twist Comprehensive Exome tumor and germline alignments were checked using allele counts for 1042 ID SNP sites. Briefly, genotype analysis of the 1042 fingerprint SNP sites served as a control for DNA contamination or sample and/or barcode mix-ups. Samples were flagged and eliminated in situations where the average minor allele frequency at homozygous sites in a patient-matched normal was observed to be >1%. Samples with more than 55% heterozygous SNP sites were eliminated as such percentages indicate large-scale contamination of DNA from another individual.

Somatic copy number were called with CNVkit (v0.9.9). Somatic structural variants with Delly2 (v0.8.6) and SvABA (v1.1.0). Copy numbera of three or more and unique in the baseline or progression sample were included. MSI status estimated with MSIsensor (v0.5) and mutational signatures estimated with deconstructSigs (v1.8.0.1). Furthermore, tumor purity was estimated using PurBayes (v1.3).

TruSight Oncology (TSO) 500 HT gene panel

TSO500 analysis was performed at the Center for Genomic Medicine at Rigshospitalet, Copenhagen. DNA libraries were prepared from 10 ng DNA and hybridized using the TruSight Oncology (TSO) 500 HT gene panel (Illumina) and subsequently, sequenced on the Illumina NovaSeq6000 platform to an average coverage of 1493x (range: 761-1960x) (Supplementary Table 2). The Illumina TSO500 analysis pipeline was applied on the ctDNA samples to estimate the Tumor Mutational Burden (TMB), hotspot mutations, and gene amplifications (fold change > 2.2 according to manufactures guidelines). Pairwise comparison between baseline blood samples and progression blood samples were made and a list of unique mutations found only in baseline and only in progression were generated along with a list of common variants found both in baseline and progression blood samples. These variants were reported (supplementary table). Mutations were investigated using literature and relevant databases (Catalogue of Somatic Mutations in Cancer, COSMIC (22), accessed in October 2022).

The SensiScreen® *PIK3CA*

The RT-PCR-based SensiScreen® *PIK3CA* liquid kits (Pentabase Aps) can be used for the detection of p.E542K (cat. No.: 5585/5591), p.E545K (cat. No.: 5586/5600), and p. H1047R (cat. No.: 5587/5590) mutations in the *PIK3CA* in ctDNA from liquid biopsies. SensiScreen® *PIK3CA* liquid assays were developed essentially as described for tumor tissue analysis (23, 24). The oligos used in the SensiScreen® *PIK3CA* liquid kits are modified with intercalating nucleic acids (INAs®), also referred to as pentabases. Modified oligos include primers, probes, and BaseBlockers™, where the BaseBlockers™ particularly block amplification of wildtype DNA as described previously (24). The SensiScreen® *PIK3CA* liquid kits also contain a reference assay amplifying part of the *PIK3CA* gene by means of allele unspecific primers and a green fluorescent HydrolEasy™ probe. In addition, all reactions include an internal control assay containing allele-independent primers and a HEX-labelled HydrolEasy™ probe targeting the *CYP450* gene, that does not interfere with amplification of the primary assays.

Evaluation of the SensiScreen® *PIK3CA* liquid assay was performed in 25µL total reaction volumes. The thermocycling conditions used were: 2 min of initial activation of the hotstart Taq-polymerase at 95°C, followed by 45 cycles of a 2-step PCR with a 15 sec denaturation step at 94°C and a 60 sec annealing and elongation step at 60°C. Fluorescence was measured during or at the end of each elongation step. To make data analysis independent of the type of instrument used, the threshold was defined as 10% of the signal strength of the reference assay at cycle 45. Samples were considered valid when $29 < Ct_{ref} \leq 40$ and positive for mutation when $Ct_{assay} < 40$. Mutations are quantified and represented as a variant allele frequency (VAF) calculated as the total number of molecules with a given mutation divided by the total number of mutants plus wild-type molecules. To define lead time for ctDNA analysis, we set the following criteria: sample is positive for mutation in consecutive samples from initial rise until progression and lead time is calculated from the initial rise in VAF of assay to clinical progression.

Results

Patients' characteristics

As of the data retrieval cut-off on January 30, 2023, plasma and tumor samples had been collected from 86 patients (Figure 1). Among them, patients with paired tumor biopsies taken before combined CDK4/6i and endocrine therapy initiation and after disease progression (N=5) were selected for whole-exome sequencing (WES). Tumors from patients who only had tissue sample taken prior to combined CDK4/6i and endocrine therapy (N=35) were also analyzed by WES, but the data from these have not yet

been analyzed. Additionally, among the patients who did not have pre- or post- tumor tissue, but only blood (N=46), five were randomly selected based on the following criteria: a blood sample taken at baseline and progression, and at least one blood sample taken during treatment. The remaining tumor and blood samples will be analyzed after this initial pilot study.

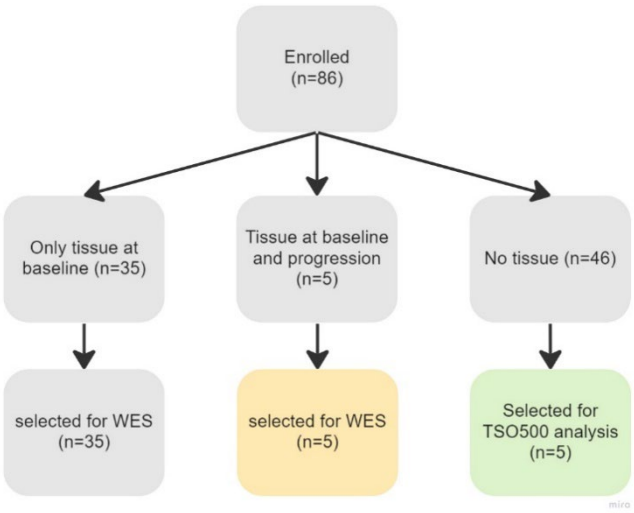

Figure 1: Flowchart of the study population. *TSO500: Trusight oncology 500 panel from Illumina, WES: Whole exome sequencing*

All 10 patients included had blood samples taken at baseline, during treatment, and at progression. All patients were clinically ER+ and HER2- and have progressed on combined CDK4/6i and endocrine therapy, with a median time to progression of 17 months (Table 1). Six patients presented with more than two metastases at the time of diagnosis. The majority of the patients received combined CDK4/6i and endocrine therapy as first-line treatment in the metastatic setting, while two patients received combined CDK4/6i and endocrine therapy as second-line following endocrine monotherapy. Palbociclib was the most common CDK4/6i used, but one patient changed from ribociclib to palbociclib due to side effects. The most common endocrine therapy given in combination with CDK4/6i was letrozole. None of the patients showed primary resistance to combined CDK4/6i and endocrine therapy, defined as disease progression within the first six months of treatment in the metastatic setting.

Table 2: Patient characteristics of the dataset at baseline. *Relapse time describes time between first diagnosis with primary disease to relapse.*

Patients, n		10
Age at time of diagnosis, years (mean, range)		68 (50-78)
	pre-menopausal	2
	post-menopausal	8
Relapse time, years (mean, range)		9 (0-27)
	<5 years	4
	5-10 years	3
	>10 years	3
Metastatic sites		
	1	4
	2	4
	≥3	2
Site		
	Visceral	8
	Non-visceral	10
Previous therapy in the metastatic setting		
	Chemotherapy	0
	Hormonal therapy	2
	Other	0
CDK4/6i line of therapy		
	1	8
	≥2	2
Type of CDK4/6i		
	Palbociclib	8
	Ribociclib	3
	Abemaciclib	0
Type of HT associated to CDK4/6i		
	Tamoxifen	0
	Fulvestrant	3
	Letrozole	7
Progression on CDK4/6i		
	Yes	10
	No	0
Time to progression, months (mean , range)		17 (8-33)
	< 12 months	3
	12-24 months	5
	> 24 months	2

Note: relapse time describes the time between first diagnosis with primary disease and relapse. n=11 for type of CDK4/6 since one patient changed due to side effects. HER2: human epidermal growth receptor 2, HT: hormonal therapy

DNA isolation and analysis

DNA was successfully extracted from all 10 tumor biopsies and 10 blood samples. From the 10 tumor biopsies, 50 ng was used to perform WES. Nine of the 10 samples were successfully sequenced (Supplementary Table 1) and one sample was contaminated and discarded. Therefore patient 11 only had WES on tumor tissue biopsied at progres-

sion. ctDNA from all 10 blood samples were successfully sequenced using TSO500 (supplementary Table 2).

Tumor and ctDNA genomic profiling reveals alterations potentially associated with resistance to combined CDK4/6i and endocrine therapy

To identify genomic alterations associated with resistance to combined CDK4/6i and endocrine therapy, we conducted a pairwise comparison of the WES data from tissue biopsies obtained prior to treatment (baseline sample) and after disease progression. All single nucleotide variants (SNVs) found at baseline and progression samples for each patient (N=4) are describe in supplementary material (Table 3-6). SNVs with variant allele frequency (VAF) ≥ 0.3 that were unique to either the baseline or progression sample are shown in Figure 2A. Of all SNV's 66% were missense mutations (45/68), while stop gain and frameshift mutations comprised both of 7% of SNVs (5/68). Although patients 1-3 showed a considerable increase in mutations in the progression sample, none were pathogenic except for the *PIK3CA* p. E542K mutation detected in patient 4, a known driver mutation found in various cancer types (25).

For patients without available tissue samples, we compared ctDNA obtained at baseline and after disease progression using targeted genomic sequencing with TSO500 (Figure 2B). All SNVs found at baseline and progression samples for each patient (N=5) are described in detail in supplementary material (Table 7-8). SNVs that were unique to either the baseline or progression sample are shown in Figure 2B. Patients 7 and 8 had 20 and 18 SNVs in baseline and following progression, respectively. Missense SNVs comprised the majority (51%, 18/35), while frameshift SNVs comprised of 20% (7/35) (Figure 2B). Four likely pathogenic mutations were identified, but two in patients 6 were present in both the baseline and progression sample (*TP53* p. R282W and *ESR1* p.D538G mutations) and thus not associated with resistance to combined CDK4/6i and endocrine therapy. In patient 5, a *TP53* mutation (p. R282W) and a *PIK3CA* (p. E545K) mutation were identified solely in the progression sample, suggesting they may have emerged during treatment and contributed to resistance.

Next, we investigated copy number alterations that were three or more and which were unique in the progression sample (Figure 2C). Among genes that are associated with tumor growth, we observed that *PDK1* was amplified in the progression samples of patients 1, 3, and 4. Patient 3 also showed amplification of *FGFR1/2*. Patients 2 and 4 showed amplifications of *TOP1, AURKA,* and *SRC*. *PDGFRB* was amplified in patients 1 and 2, while *PDGFRA* was amplified in patients 3 and 4. In general, there were more common amplifications between patients compared to SNVs.

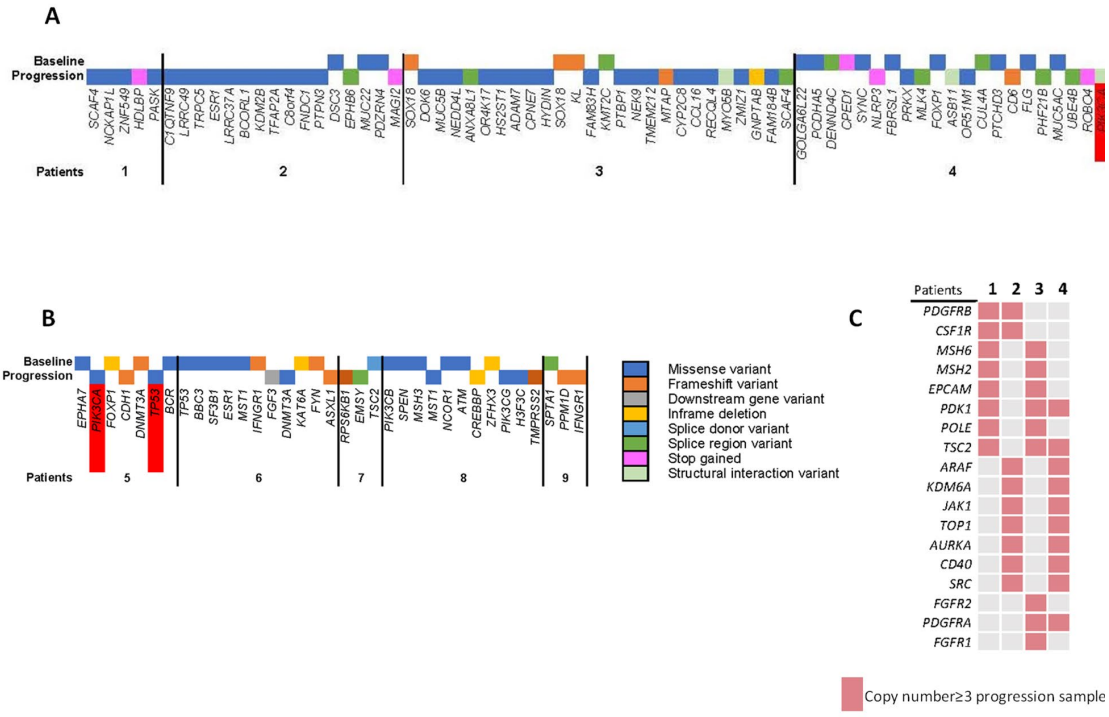

Figure 2: Unique variations identified in either baseline or progression sample. A) Mutations identified by WES of tumor samples from baseline or progression in patients 1-4. B) Mutations identified by TSO500 analysis of blood samples from baseline or progression in patients 5-9.C) Amplifications uniquely identified in the progression samples of patients 1-4. Red highlight: pathogenic mutation

Furthermore, we investigated alterations detected in tumor DNA and ctDNA before initiating treatment and that exhibited marked change in VAFs following treatment, and thus may potentially be involved in resistance to combined CDK4/6i and endocrine therapy (Figure 3). The VAF of alterations associated with resistance is expected to increase during treatment, indicating the selective growth of the resistant subclones. We selected mutations from the WES data analysis that showed a (VAFprogression/VAFbaseline) > 1.5, except for *PIK3CA* mutations, which were included regardless of the ratio. All mutations identified by TSO500 both in baseline and after progression samples were included. Although, many of the alterations identified were unchanged or had a modest in-

crease or decrease in VAF between baseline and progression samples, we observed a marked VAF increase of a *SLIT2* mutation (in patient 1) and of the VAF of *IL10RA, GNB1L, P4HB,* and *ESPNL* mutations in patient 2. In patient 3, there is a marked VAF increase of *PADI6, SIRT6, PIM3,* and *TP53* mutations. Notably, the identified *TP53* mutation (p. F270C) was likely pathogenic. VAF of *TUBGCP6* and *CASC3* mutations showed a marked increase after progression in patient 4 and VAF of *KAT6A* mutation showed an increase in patient 6. The alterations identified in the remaining patients (7, 8 and 9) showed either constant or decreased VAF. The most pronounced decreases in VAF were observed in a *NCOR1* mutation (patient 7), and *CBL* and *KRAS* (p. T50I, non-pathogenic) mutations in patient 8. Patients 2, 3, and 8 exhibited pathogenic *PIK3CA* mutations, but with similar frequency in the baseline and progression sample. The pathogenic *ERBB2* mutation (p. D769Y) was identified in patient 9, but it did not show a change in frequency between the baseline and progression samples.

Collectively, these findings suggest that the majority of the alterations observed in solid and liquid biopsies were specific for the individual patient and generally not observed in known cancer drivers, although some patient's tumors acquired driver mutations in *TP53* and *PIK3CA* after progression and these alterations may be associated with resistance to combined CDK4/6i and endocrine therapy.

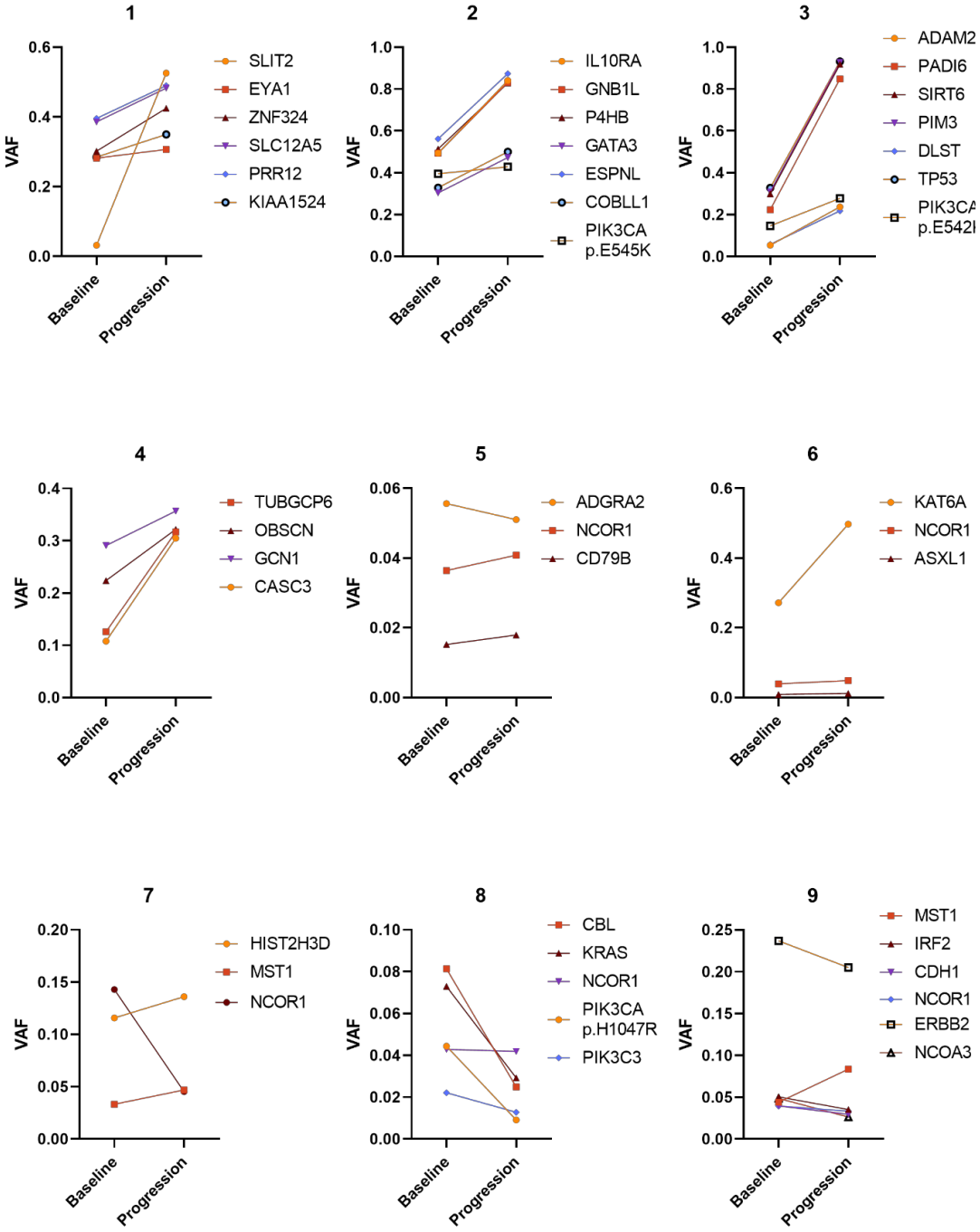

Figure 3: Mutations found in both baseline and progression samples. *Mutations called in patients 1-4 using WES of tumor samples. Mutations called in patients 5-9 using TSO500 analysis of blood samples. VAF: Variant allele frequency.*

PIK3CA mutations can be used to monitor disease progression in serial blood samples of circulating tumor DNA (ctDNA)

As *PIK3CA* mutations were detected in 5 out of the nine paired samples (56%, both in pre and post samples) as well as in one patient (patient 11) with only tumor sample at progression, we sought to determine whether we could use these mutations to track dis-

ease progression through blood samples collected during treatment. To monitor *PIK3CA* mutations in the blood samples we used the SensiScreen® liquid *PIK3CA* kit that has been shown to exhibit a very high sensitivity and specificity (Pentabase, Odense, Denmark).

Overall, we observed increased VAF of *PIK3CA*-mutation in the later part of the treatment with combined CDK4/6i and endocrine therapy in five out of six (83%) patients included (Figure 4). Notably, an increase in VAF of the identified *PIK3CA* mutations were detected 17, 4 and 13 months before progression was diagnosed using PET-CT in patients 2, 3 and 11, respectively. We also observed one case (patient 8) where *PIK3CA* mutation frequency was high in the baseline, then decreased, but had only minimally increased in the progression sample, suggesting that the *PIK3CA* mutation was not expressed in the expanding clones of the metastasis. In patient 4, the *PIK3CA* mutation could not be identified in any of the blood samples despite it being called by WES in the tumor sample obtained at progression. Notably, the baseline and progression biopsies were obtained five years prior to combined CDK4/6i and endocrine therapy and one year after progression.

Discussion

Combined CDK4/6i and endocrine therapy has significantly improved the outcome of patients with metastatic ER+ breast cancer. However, patients will inevitably develop resistance and therefore, knowledge of resistance mechanisms and strategies to monitor treatment response more intensely are needed. Circumventing the limitations of tissue biopsies newly developed liquid biopsy approaches have the potential to uncover resistance mechanisms and identify disease progression at an earlier timepoint than when using standard imaging techniques.

In this study we show that a few potential pathogenic mutations specific for the individual patient were observed after disease progression on combined CDK4/6i and endocrine therapy, whereas several gene amplifications were common among some patients. Assessment of *PIK3CA* mutations in ctDNA from blood samples collected before, during and after treatment, identified disease progression in five of six patients, and in three of these patients, detection of disease progression was 4-17 months earlier than diagnosis of disease progression by PET-CT.

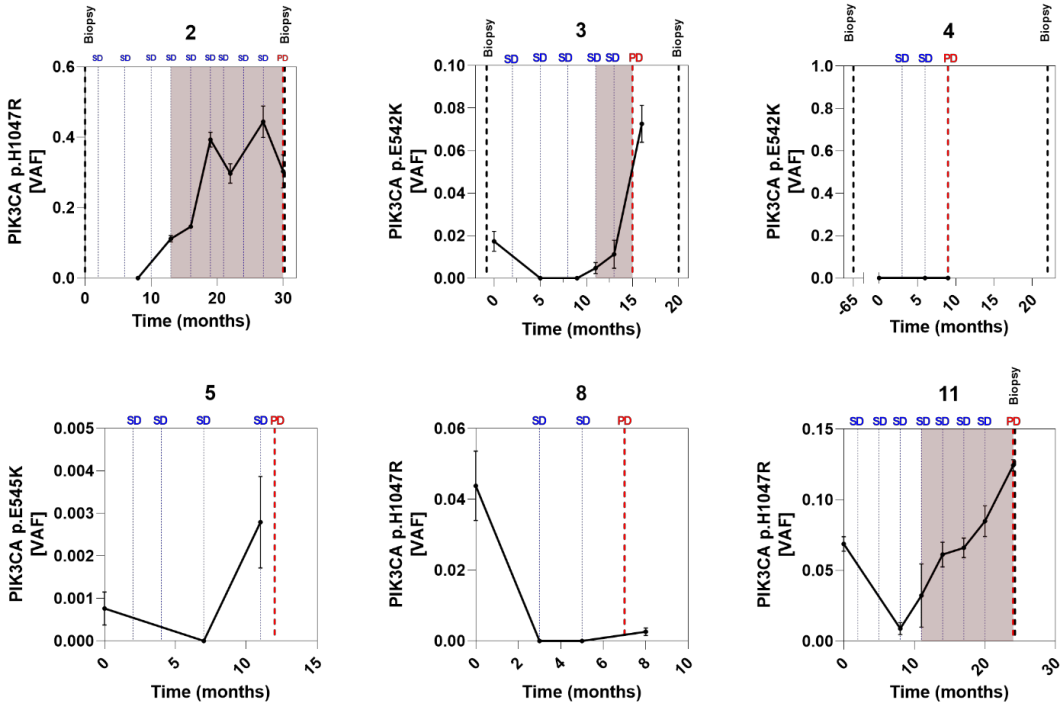

Figure 4: Alteration in VAF of PIK3CA mutations identified in blood samples from patients treated with combined CDK4/6i and endocrine therapy. *Treatment was initiated at time=0 and continued until progression was diagnosed. Patients 2, 3, and 4 had WES performed on tumor biopsies from before treatment and after progression on combined CDK4/6i and endocrine therapy. Patients 5 and 8 had TSO analysis of blood samples taken before treatment and after progression on combined CDK4/6i and endocrine therapy. Patient 11 had WES performed on tumor biopsy taken after progression on CDK4/6i and endocrine therapy. Data are shown as mean of VAF ±SEM. Grey area: Lead time from positive ctDNA sample until progression was diagnosed with PET-CT. VAF: Variant allele frequency. SD: stable disease. PD: progressive disease.*

Our findings concur with previous studies showing that common pathogenic mutations associated with resistance to combined CDK4/6i and endocrine therapy among different patients are rare. Although multiple SNPs were identified by WES and TSO500 in tumor and ctDNA, respectively, only few *PIK3CA* and *TP53* pathogenic mutations were found. *PIK3CA* mutations were present both at baseline and progression but their VAF was substantially higher at progression blood samples in four patients. These findings could suggest that this mutation represented a small clone at baseline, which was able to grow and expand under treatment selective pressure. Thus, *PIK3CA* mutations might provide a growth advantage during combined CDK4/6i and endocrine therapy. *RB* mutations have been identified in blood samples of 4.7% of patients in PALOMA-3 trial following progression on combined CDK4/6i and endocrine therapy (8). However, in our study we did not find alterations in key cell cycle regulators, such as *RB,* after progression of CDK4/6i and endocrine therapy. Furthermore, common gene amplifications, including *PDK1*, *TSC2*, and *PDGFRA/B*, were observed across different patients by WES in tumor

samples. *PDK1* is a key activator of the PI3K/AKT pathway, and this protein has been suggested to play a role in resistance to CDK4/6i (26). We also found *PIK3CA* mutations, which have been extensively investigated in studies of CDK4/6i resistance, but they have not been consistently associated with clinical outcome in patients with advanced ER+ breast cancer treated with combined CDK4/6i and endocrine therapy in clinical trials (27-29). Moreover, we found *AURKA* amplifications which has also been implicated in resistance to combined CDK4/6i and endocrine therapy (9). We further observed amplifications in *PDGFRB, PDGFRA, ARAF, KDM6A, TOP1* and *SRC* which have all been reported to promote proliferation and migration of breast cancer cells (30-35). Finally, we found amplification of *FGFR1/2*, which has also been previously described to be altered, including gene amplification and mutations, in blood samples in 14 of 34 patients after progression on combined CDK4/6i and endocrine therapy (10). Thus, it appears that CNVs may play an important role in resistance to combined CDK4/6i and endocrine therapy (36-38).

Additionally, we show that *PIK3CA* mutations can be used to monitor disease progression in ctDNA from blood samples using the SensiScreen liquid *PIK3CA* kit. Notably, approximately 40% of ER+ breast cancer patients harbor a *PIK3CA* mutation, with p. E545K, E542K, and H1047R mutations accounting for 80% of all *PIK3CA* mutations (39-41). These alterations have been shown to occur early and appear to be clonal (42), which is supported by previous studies showing concordant *PIK3CA* status in paired primary and metastatic tumor (43). Using WES and TSO500, we identified *PIK3CA* mutations in five of nine patients, both in the baseline and progression samples (N=3) or only at progression (N=2) on combined CDK4/6i and endocrine therapy. Importantly, the SensiScreen liquid *PIK3CA* assay detected *PIK3CA* mutations in the baseline blood sample 4 of 5 patients which suggests that the *PIK3CA* mutations are clonal. In patient 2 the *PIK3CA* mutation was identified by WES in both baseline and progression tumor sample, while it was not identified in the first blood sample accessible for analysis with SensiScreen® liquid *PIK3CA* kit. However, this blood sample was collected 11 months after starting treatment with combined CDK4/6i and endocrine therapy and thus this might a result of inhibition of cancer growth by the treatment. Only one patient did not show *PIK3CA* mutations in the blood samples at any timepoint even though it was found in the progression tumor sample, which is fact was collected approximately one year after progression was diagnosed by PET-CT which suggests that this *PIK3CA* mutation may have been acquired later and thus were not clonal in this patient. Most importantly, an increase of VAF for *PIK3CA* mutations were observed in 3 of 6 patients earlier that clinical progression as determined by PET-CT imaging, which supports the clinical use-

fulness of measuring ctDNA in liquid biopsies to monitor treatment response. Earlier detection of progression on combined CDK4/6 inhibitor and endocrine therapy in samples harboring *PIK3CA* mutations may improve the timing for switching therapy, such as to the PI3K inhibitor, alpelisib, in combination with endocrine therapy, which is FDA approved, but not yet approved in Denmark (40).

In conclusion, our findings contribute to the increasing body of evidence that supports the potential use of serial ctDNA analysis of clonal variations, such as *PIK3CA* mutations, for the real-time monitoring of CDK4/6i response and earlier detection of progressive disease. Additionally, our findings suggest that analysis of SNPs and CNVs holds potential in understanding the mechanisms underlying resistance to combined CDK4/6i and endocrine therapy.

ACKNOWLEDGEMENTS

We thank Lone Christiansen and Helle Wohlleben, at the Department of Pathology, Odense University Hospital, for excellent technical assistance with sectioning, the technical staff at Department of Oncology, R lab, for blood sample collection, molecular biologist Lise Barlebo Ahlborn, Center for Genomic Medicine, Righospitalet for advice regarding the TSO500 analysis,

The study was supported by grants from The Danish Cancer Society (H.J.D.), Pink Tribute (H.J.D.), Academy of Geriatric Cancer Research (AgeCare) (H.J.D.), Agnes and Poul Friis' foundation (C.K.K), Else and Mogens Wedell-Wedellborgs foundation (C.K.K), Fabrikant Einar Willumsens Foundation(C.K.K), Fonden til Lægevidenskabens fremme (C.K.K), Grosserer L.F. Foghts Foundation (C.K.K) and the Region of Southern Denmark (C.K.K)

Supplementary figures

Table 1: Whole exome sequencing data from patients 1-4 and 11.

Patient	Sample	Type	Input [ng]	CapturePanel	Tumor Coverage	Normal Coverage	SNVs	SNVs impact=High	Indels	Mutational Load	TMB	notes
1	Baseline	FF	50	Twist Exome 2.0	515	208	133	9	6	139	3.34	
1	Progression	FF	50	Twist Exome 2.0	436	208	197	15	14	211	5.06	
2	Baseline	FF	50	Twist Exome 2.0	455	219	79	10	8	88	2.11	
2	Progression	FF	50	Twist Exome 2.0	408	219	97	9	6	105	2.52	
3	Baseline	FFPE	50	Twist Exome 2.0	332	218	11344	416	94	11539	276.91	
3	Progression	FF	50	Twist Exome 2.0	497	218	596	82	77	681	16.34	
4	Baseline	FFPE	50	Twist Exome 2.0	148	264	7519	755	59	7584	182	
4	Progression	FF	50	Twist Exome 2.0	459	264	368	61	55	427	10.25	
11	Baseline	FF	50	Twist Exome 2.0	1	225						Contaminated
11	Progression	FF	50	Twist Exome 2.0	463	224	70	10	13	83	1.99	

FF: Fresh frozen tissue, FFPE: Formalin-fixed paraffin-embedded tissue, SNV: Single nucleotide variant, Indel: insertions/deletions, TMB: tumor mutational burden

Table 3: TSO500 data from patients 5-9.

Patient	Sample	Median coverage	Variant calling pipeline	SNVs	TMB	MSI
5	Baseline	1832	TSO500	20	0.8	4.03
5	Progression	761	TSO500	19	1.6	2.48
6	Baseline	1960	TSO500	27	1.6	3.23
6	Progression	1478	TSO500	17	0	3.23
7	Baseline	1354	TSO500	20	0.9	4.71
7	Progression	1485	TSO500	18	0.8	4.84
8	Baseline	1308	TSO500	20	3.2	3.23
8	Progression	1606	TSO500	18	3.2	3.23
9	Baseline	1198	TSO500	21	1.6	0.81
9	Progression	1950	TSO500	22	2.4	0.81

SNV: Single nucleotide variant, TMB: tumor mutational burden, MSI: Microsatellite instability

Supplementary Table 3: Variants in patient 1. Identified by WES. Green: shared mutations between tumor at baseline and tumor at progression.

Yellow: unique mutations to baseline tumor. Blue: Unique mutations to progression tumor

Chrom	POS	REF	ALT	Gene	c_change	p_change	Effect	Impact	AF_baseline	AF_progression	Ratio
chr1	20727609	C	G	SH2D5	c.88-6G>C	.	intron	LOW	0.432	0.466	1.08
chr1	220162249	C	A	RAB3GAP2	c.3174G>T	p.Trp1058Cys	missense_variant	MODERATE	0.288	0.289	1.00
chr1	91274773	C	G	HFM1	c.3625G>C	p.Glu1209Gln	missense_variant	MODERATE	0.28	0.275	0.98
chr1	204987504	G	A	NFASC	c.2557G>A	p.Gly853Arg	missense_variant	MODERATE	0.328	0.312	0.95
chr1	204449280	G	A	PIK3CB	c.2251C>T	p.Arg751Trp	missense_variant	MODERATE	0.306	0.269	0.88
chr2	159350356	T	C	BAZ2B	c.4215A>G	p.Gly1405Gly	synonymous variant	LOW	0.284	0.335	1.18
chr2	208442379	C	T	PTH2R	c.427C>T	p.Arg143Cys	missense_variant	MODERATE	0.277	0.302	1.09
chr2	53897959	G	C	PSME4	c.3517C>G	p.Leu1173Val	missense_variant	MODERATE	0.287	0.308	1.07
chr2	178551707	C	T	TTN	c.91193G>A	p.Arg30398His	missense_variant	MODERATE	0.296	0.314	1.06
chr2	166204354	TTTTACCCCTGGTCGAGGAATTGGCTTTTGTGGCTTCTTGG	T	SCN9A	c.4436_4470+5delCCAAGAAGCCACAAAAGCCAATTCCTCGACCAGGGGTAAA	p.Ser1479fs	frameshift	HIGH	0.173	0.183	1.06
chr2	54644488	G	A	SPTBN1	c.4171G>A	p.Asp1391Asn	missense_variant	MODERATE	0.314	0.314	1.00
chr2	135920577	T	C	DARS	c.835A>G	p.Thr279Ala	missense_variant	MODERATE	0.295	0.277	0.94
chr3	108569402	T	C	KIAA1524	c.1100A>G	p.Lys367Arg	missense_variant	MODERATE	0.285	0.35	1.23
chr3	50364754	A	C	CACNA2D2	c.3365T>G	p.Val1122Gly	missense_variant	MODERATE	0.258	0.288	1.12
chr3	43348375	T	C	SNRK	c.2116T>C	p.Phe706Leu	missense_variant	MODERATE	0.324	0.358	1.10
chr3	49686750	C	T	MST1	c.781G>A	p.Glu261Lys	missense_variant	MODERATE	0.286	0.311	1.09
chr3	65379382	G	GC	MAGI1	c.2873dupG	p.Ser959fs	frameshift_variant	HIGH	0.316	0.32	1.01
chr4	20550850	C	T	SLIT2	c.2513C>T	.	structural_interaction_variant	HIGH	0.032	0.526	16.44
chr4	152953526	A	T	FHDC1	c.526A>T	p.Met176Leu	missense_variant	MODERATE	0.299	0.337	1.13
chr4	89895509	C	T	MMRN1	c.538C>T	p.Arg180Trp	missense_variant	MODERATE	0.28	0.295	1.05
chr4	148260107	G	A	NR3C2	c.1768C>T	p.Arg590*	stop_gained	HIGH	0.302	0.3	0.99
chr5	138573801	T	C	HSPA9	c.190A>G	p.Asn64Asp	missense_variant	MODERATE	0.277	0.329	1.19
chr5	173323358	G	A	STC2	c.367C>T	p.Arg123Trp	missense_variant	MODERATE	0.301	0.348	1.16
chr5	177091787	A	T	FGFR4	c.706A>T	p.Asn236Tyr	missense_variant	MODERATE	0.305	0.348	1.14
chr5	140632586	G	C	CD14	c.398C>G	p.Pro133Arg	missense_variant	MODERATE	0.299	0.319	1.07
chr6	144459285	G	A	UTRN	c.2638G>A	p.Asp880Asn	missense_variant	MODERATE	0.312	0.361	1.16
chr6	135189794	C	G	MYB	c.217C>G	p.Arg73Gly	missense_variant	MODERATE	0.285	0.321	1.13
chr6	159779742	C	T	TCP1	c.1339G>A	p.Val447Ile	missense_variant	MODERATE	0.295	0.325	1.10
chr6	44248670	CTT	C	HSP90AB1	c.44_45delTT	p.Phe15fs	frameshift_variant	HIGH	0.296	0.315	1.06
chr6	166164637	G	T	T	c.698C>A	p.Pro233His	missense_variant	MODERATE	0.31	0.329	1.06
chr6	26056404	G	C	HIST1H1C	c.25C>G	p.Pro9Ala	missense_variant	MODERATE	0.284	0.297	1.05
chr6	151351920	G	A	AKAP12	c.3529G>A	p.Val1177Ile	missense_variant	MODERATE	0.288	0.3	1.04
chr6	159780068	C	T	TCP1	c.1117G>A	p.Ala373Thr	missense_variant	MODERATE	0.277	0.285	1.03
chr6	134028836	C	T	SLC2A12	c.989G>A	p.Ser330Asn	missense_variant	MODERATE	0.308	0.309	1.00
chr6	30922492	A	G	VARS2	c.2065A>G	p.Met689Val	missense_variant	MODERATE	0.312	0.313	1.00
chr6	26204885	A	G	HIST1H4E	c.241A>G	p.Thr81Ala	missense_variant	MODERATE	0.3	0.285	0.95
chr6	82216255	TA	T	IBTK	c.1427-6delT	.	intron	LOW	0.365	0.328	0.90
chr7	76440580	G	C	ZP3	c.1029G>C	p.Trp343Cys	missense_variant	MODERATE	0.295	0.318	1.08
chr7	64707389	G	A	ZNF107	c.1292G>A	p.Gly431Asp	missense_variant	MODERATE	0.295	0.312	1.06
chr7	26184978	A	T	NFE2L3	c.1280A>T	p.His427Leu	missense_variant	MODERATE	0.332	0.351	1.06
chr7	101196083	C	T	MOGAT3	c.889G>A	p.Val297Ile	missense_variant	MODERATE	0.312	0.31	0.99
chr7	26185205	C	G	NFE2L3	c.1507C>G	p.Gln503Glu	missense_variant	MODERATE	0.313	0.295	0.94
chr8	141434020	G	A	MROH5	c.3895C>T	p.Arg1299Trp	missense_variant	MODERATE	0.423	0.472	1.12
chr8	71321750	G	T	EYA1	c.402C>A	p.Tyr134*	stop_gained	HIGH	0.282	0.307	1.09
chr9	79721834	G	T	TLE4	c.2028G>T	p.Arg676Ser	missense_variant	MODERATE	0.452	0.508	1.12
chr9	137080826	G	T	UAP1L1	c.1316G>T	p.Gly439Val	missense_variant	MODERATE	0.639	0.657	1.03
chr10	122088576	C	G	TACC2	c.5558C>G	p.Ala1853Gly	missense_variant	MODERATE	0.27	0.305	1.13
chr10	8073911	C	CG	GATA3	c.1224dupG	p.Pro409fs	frameshift_variant	HIGH	0.326	0.345	1.06
chr10	133465521	G	A	SCART1	n.3954G>A	.	non coding	MODIFIER	0.298	0.302	1.01
chr10	70873423	G	A	SGPL1	c.1132G>A	p.Val378Ile	missense_variant	MODERATE	0.326	0.309	0.95
chr11	46728135	G	T	F2	c.1270G>T	p.Val424Leu	missense_variant	MODERATE	0.307	0.359	1.17
chr11	55812155	C	T	OR5L1	c.689C>T	p.Ser230Phe	missense_variant	MODERATE	0.442	0.511	1.16
chr11	5709493	G	A	TRIM22	c.1342G>A	p.Asp448Asn	missense_variant	MODERATE	0.293	0.304	1.04
chr11	9423146	A	G	IPO7	c.1041+6A>G	.	intron	LOW	0.384	0.383	1.00
chr11	5737243	G	A	OR56B1	c.727G>A	p.Ala243Thr	missense_variant	MODERATE	0.322	0.306	0.95
chr12	21334640	T	C	SLCO1A2	c.8A>G	p.Glu3Gly	missense_variant	MODERATE	0.259	0.303	1.17
chr12	10801630	T	G	TAS2R7	c.941A>C	p.Gln314Pro	missense_variant	MODERATE	0.297	0.342	1.15
chr12	33426277	C	T	SYT10	c.370G>A	p.Val124Ile	missense_variant	MODERATE	0.292	0.329	1.13
chr12	12244626	G	A	LRP6	c.85C>T	.	structural_interaction_variant	HIGH	0.301	0.298	0.99
chr14	104780214	C	T	AKT1	c.49G>A	p.Glu17Lys	missense_variant	MODERATE	0.276	0.333	1.21
chr14	104952489	C	T	AHNAK2	c.2962G>A	p.Asp988Asn	missense_variant	MODERATE	0.298	0.34	1.14
chr14	21426250	G	C	CHD8	c.1602-8C>G	.	intron	LOW	0.316	0.336	1.06
chr14	99174888	C	T	BCL11B	c.1948G>A	p.Ala650Thr	missense_variant	MODERATE	0.343	0.323	0.94
chr15	72474967	C	A	ARIH1	c.328C>A	p.Leu110Ile	missense_variant	MODERATE	0.516	0.487	0.94
chr16	58516554	C	A	SETD6	c.553C>A	p.Arg185Ser	missense_variant	MODERATE	0.268	0.316	1.18
chr16	1256366	A	C	TPSD1	c.82+4A>C	.	intron	LOW	0.142	0.156	1.10
chr16	15004179	C	T	PDXDC1	c.243-8C>T	.	intron	LOW	0.157	0.161	1.03
chr17	5354465	C	G	RABEP1	c.1070C>G	p.Ser357Cys	missense_variant	MODERATE	0.435	0.483	1.11
chr17	39424693	G	A	MED1	c.785C>T	p.Thr262Ile	missense_variant	MODERATE	0.338	0.37	1.09
chr17	35925523	T	A	RDM1	c.391A>T	p.Ile131Phe	missense_variant	MODERATE	0.482	0.481	1.00
chr17	81665464	G	C	OXLD1	c.181C>G	p.His61Asp	missense_variant	MODERATE	0.257	0.215	0.84
chr19	58471957	G	A	ZNF324	c.1465G>A	p.Ala489Thr	missense_variant	MODERATE	0.302	0.425	1.41
chr19	49625524	C	T	PRR12	c.6028C>T	p.Arg2010Trp	missense_variant	MODERATE	0.396	0.49	1.24
chr19	55732003	A	G	NLRP9	c.1828T>C	p.Ser610Pro	missense_variant	MODERATE	0.472	0.516	1.09
chr20	46040601	C	A	SLC12A5	c.910C>A	p.Pro304Thr	missense_variant	MODERATE	0.386	0.483	1.25
chr20	4857060	C	G	SLC23A2	c.1865G>C	p.Ser622Thr	missense_variant	MODERATE	0.238	0.263	1.11
chr20	44159693	T	C	JPH2	c.1094A>G	p.Lys365Arg	missense_variant	MODERATE	0.26	0.281	1.08
chr20	63570752	T	G	HELZ2	c.395A>C	p.Asp132Ala	missense_variant	MODERATE	0.289	0.295	1.02
chr22	30292689	G	C	TBC1D10A	c.1234C>G	p.Gln412Glu	missense_variant	MODERATE	0.422	0.483	1.14
chr22	50744172	C	T	ACR	c.677C>T	p.Ala226Val	missense_variant	MODERATE	0.458	0.477	1.04

Chrom	POS	REF	ALT	Gene	c_Change	p_Change	Effect	Impact	AF_Tumor	AF_BC
chr1	95246550	G	T	RWDD3	c.582G>T	p.Leu194Phe	missense_variant	MODERATE	0.121	0.008688
chr7	17834172	T	C	SNX13	c.1477A>G	p.Met493Val	missense_variant	MODERATE	0.076	0.006786
chr13	108210521	G	T	LIG4	c.748C>A	.	structural_interaction_variant	HIGH	0.078	0.005072
chr17	12896440	T	G	ARHGAP44	c.127T>G	p.Ser43Ala	missense_variant	MODERATE	0.243	0.005664
chr19	32999660	T	C	RHPN2	c.1151A>G	p.Gln384Arg	missense_variant	MODERATE	0.162	0.024
chr1	202735514	G	A	KDM5B	c.3446C>T	p.Pro1149Leu	missense_variant	MODERATE	0.205	0.005025
chr1	202735516	C	G	KDM5B	c.3444G>C	p.Leu1148Phe	missense_variant	MODERATE	0.205	0.00504
chr1	202735505	T	A	KDM5B	c.3455A>T	p.Lys1152Met	missense_variant	MODERATE	0.201	0.00507
chr1	206195830	G	A	FAM72A	c.277C>T	p.Leu93Phe	missense_variant	MODERATE	0.058	0.007586
chr2	241264590	G	T	HDLBP	c.92C>A	p.Ser31*	stop_gained	HIGH	0.32	0.006834
chr2	241124079	C	T	PASK	c.2774G>A	p.Cys925Tyr	missense_variant	MODERATE	0.314	0.003519
chr2	241491522	C	A	FARP2	c.2630C>A	p.Pro877His	missense_variant	MODERATE	0.295	0.004184
chr2	135920511	C	T	DARS	c.901G>A	p.Glu301Lys	missense_variant	MODERATE	0.279	0.00856
chr3	184291106	G	A	ECE2	c.2255G>A	p.Arg752Gln	missense_variant	MODERATE	0.05	0.003477
chr4	161500101	T	C	FSTL5	c.1373A>G	p.Tyr458Cys	missense_variant	MODERATE	0.264	0.008449
chr5	50763109	TCACTTCTGAGACACTTTTAAATTATCCCTTTTCATCA	T	PARP8	c.424-38_424-2delCACTTCTGAGACACTTTTAAATTATCCCTTTTCATCA	.	intron	HIGH	0.252	0.007766
chr5	98873719	C	T	CHD1	c.3445G>A	p.Asp1149Asn	missense_variant	MODERATE	0.224	0.00874
chr5	140808896	C	T	PCDHA4	c.1709C>T	p.Ala570Val	missense_variant	MODERATE	0.077	0.003971
chr6	30730569	A	G	FLOT1	c.952-4T>C	.	intron	LOW	0.243	0.003678
chr6	30741874	G	C	FLOT1	c.44-7C>G	.	intron	LOW	0.206	0.003733
chr6	152098785	T	G	ESR1	c.1613T>G	p.Leu538Arg	missense_variant	MODERATE	0.238	0.003381
chr6	152098791	A	G	ESR1	c.1619A>G	p.Asp540Gly	missense_variant	MODERATE	0.061	0.003323
chr7	142866555	G	C	EPHB6	c.1537G>C	p.Asp513His	missense_variant	MODERATE	0.182	0.003489
chr7	48274390	A	C	ABCA13	c.4724A>C	p.Glu1575Ala	missense_variant	MODERATE	0.096	0.005086
chr7	48272307	T	A	ABCA13	c.2641T>A	p.Trp881Arg	missense_variant	MODERATE	0.092	0.006485
chr7	48275844	C	T	ABCA13	c.6178C>T	p.Pro2060Ser	missense_variant	MODERATE	0.076	0.006672
chr7	34143322	G	A	BMPER	c.1838G>A	p.Gly613Asp	missense_variant	MODERATE	0.055	0.005299
chr8	144392817	G	A	ADCK5	c.1562G>A	p.Arg521Gln	missense_variant	MODERATE	0.069	0.002974
chr9	131150325	CAA	C	NUP214	c.2044_2045delAA	p.Lys682fs	frameshift_variant	HIGH	0.187	0.006763
chr9	121759993	T	C	DAB2IP	c.640T>C	p.Tyr214His	missense_variant	MODERATE	0.184	0.00342
chr11	8100512	G	A	TUB	c.1291G>A	p.Val431Ile	missense_variant	MODERATE	0.264	0.005041
chr11	75797160	A	G	DGAT2	c.637A>G	p.Ile213Val	missense_variant	MODERATE	0.052	0.006509
chr12	54519284	A	G	NCKAP1L	c.1577A>G	p.Asp526Gly	missense_variant	MODERATE	0.369	0.005362
chr12	129074212	A	G	TMEM132D	c.2963T>C	p.Ile988Thr	missense_variant	MODERATE	0.174	0.003403
chr14	93183757	A	C	MOAP1	c.486T>G	p.Tyr162*	stop_gained	HIGH	0.251	0.002886
chr16	22527961	C	G	NPIPB5	c.533C>G	p.Thr178Ser	missense_variant	MODERATE	0.18	0.091
chr17	69302845	T	C	ABCA5	c.992A>G	p.Glu331Gly	missense_variant	MODERATE	0.087	0.009332
chr18	3086135	T	C	MYOM1	c.4154A>G	p.Lys1385Arg	missense_variant	MODERATE	0.225	0.007852
chr19	57538682	A	G	ZNF549	c.1678A>G	p.Ser560Gly	missense_variant	MODERATE	0.322	0.004166
chr19	42370828	C	G	MEGF8	c.7133C>G	p.Thr2378Ser	missense_variant	MODERATE	0.143	0.029
chr20	47672210	G	GT	SULF2	c.1563dupA	p.Leu522fs	frameshift_variant	HIGH	0.057	0.00593
chr21	31706343	C	G	SCAF4	c.45G>C	p.Met15Ile	missense_variant	MODERATE	0.453	0.005762
chrX	141897463	T	G	MAGEC3	c.1705T>G	p.Trp569Gly	missense_variant	MODERATE	0.059	0.003379
chrX	141897466	G	A	MAGEC3	c.1708G>A	p.Glu570Lys	missense_variant	MODERATE	0.059	0.003334

Supplementary Table 4: Variants in patient 2. Identified by WES. Green: shared mutations between tumor at baseline and tumor at progresion.

Yellow: unique mutations to baseline tumor. Blue: Unique mutations to progression tumor

CHROM	POS	REF	ALT	GENE	c_change	p_change	Effect	Impact	AF_baseline	AF_progression	Ratio
chr1	1291567	AGAGCTGGGCTGGGCCC	A	SCNN1D	c.2367_2382delGAGCTGGGCTGGGCCC	p.Glu789fs	frameshift_variant	HIGH	0.354	0.465	1.31
chr1	112456676	G	T	CTTNBP2NL	c.1184G>T	p.Gly395Val	missense_variant	MODERATE	0.358	0.455	1.27
chr1	247949407	G	T	OR2L8	c.550G>T	p.Val184Leu	missense_variant	MODERATE	0.369	0.456	1.24
chr1	212872812	A	T	FLVCR1	c.1018A>T	p.Thr340Ser	missense_variant	MODERATE	0.38	0.459	1.21
chr1	145747989	A	G	RNF115	c.783+6T>C		ice_region_variant&intron_vari	LOW	0.369	0.418	1.13
chr2	238117033	C	T	ESPNL	c.986C>T	p.Pro329Leu	inse_variant&splice_region_va	MODERATE	0.562	0.874	1.56
chr2	164695204	C	T	COBLL1	c.2503G>A	p.Gly835Ser	missense_variant	MODERATE	0.329	0.5	1.52
chr2	141049099	C	T	LRP1B	c.1676G>A	p.Arg559His	missense_variant	MODERATE	0.346	0.435	1.26
chr3	184577088	G	A	EPHB3	c.1259G>A	p.Arg420His	missense_variant	MODERATE	0.193	0.246	1.27
chr3	160438041	G	A	TRIM59	c.1143G>C	p.Lys381Asn	missense_variant	MODERATE	0.393	0.457	1.16
chr3	179218303	G	A	PIK3CA	c.1633G>A	.	protein_protein_contact	HIGH	0.395	0.429	1.09
chr3	132477971	TA	T	DNAJC13	c.2565-6delA		ice_region_variant&intron_vari	LOW	0.042	0.041	0.98
chr4	186534252	G	A	MTNR1A	c.490C>T	p.Arg164Cys	missense_variant	MODERATE	0.317	0.432	1.36
chr4	30920365	A	T	PCDH7	c.3387A>T	p.Glu1129Asp	missense_variant	MODERATE	0.359	0.448	1.25
chr4	103145659	A	T	CENPE	c.4436T>A	p.Leu1479His	missense_variant	MODERATE	0.353	0.438	1.24
chr4	186084752	G	T	TLR3	c.2594G>T	p.Cys865Phe	missense_variant	MODERATE	0.365	0.436	1.19
chr4	73058211	C	T	COX18	c.914G>A	p.Arg305His	missense_variant	MODERATE	0.341	0.399	1.17
chr5	41018702	C	A	MROH2B	c.2662G>T	p.Glu888*	stop_gained	HIGH	0.315	0.467	1.48
chr5	56815713	C	T	MAP3K1	c.1140C>T	p.Ala476Val	missense_variant	MODERATE	0.413	0.556	1.35
chr5	102950768	G	T	PAM	c.853G>T	p.Ala285Ser	missense_variant	MODERATE	0.242	0.299	1.24
chr5	132814558	G	A	SOWAHA	c.937G>A	p.Glu313Lys	missense_variant	MODERATE	0.532	0.635	1.19
chr5	172669821	C	T	NEURL1B	c.68C>T	p.Pro23Leu	missense_variant	MODERATE	0.291	0.345	1.19
chr5	112828889	C	T	APC	c.1660C>T	p.Arg554*	stop_gained	HIGH	0.236	0.244	1.03
chr6	145955162	T	C	SMIM1	c.161A>G	p.Tyr54Cys	missense_variant	MODERATE	0.359	0.441	1.23
chr6	111589863	C	T	REV3L	c.6931G>A	p.Asp2311Asn	missense_variant	MODERATE	0.364	0.431	1.18
chr10	8058473	C	A	GATA3	c.410C>A	p.Ser137*	stop_gained	HIGH	0.304	0.473	1.56
chr10	45826486	A	T	AGAP4	c.1490T>A	p.Leu497His	missense_variant	MODERATE	0.145	0.192	1.32
chr11	117993387	C	T	IL10RA	c.514C>T	p.Arg172Cys	missense_variant	MODERATE	0.494	0.841	1.70
chr11	61006634	C	G	CD6	c.110G>C	p.Trp37Ser	missense_variant	MODERATE	0.412	0.451	1.09
chr13	30713844	G	A	ALOX5AP	c.116+3G>A		ice_region_variant&intron_vari	LOW	0.038	0.043	1.13
chr14	39177651	TC	T	PNN	c.388delC	p.Gln130fs	frameshift_variant	HIGH	0.309	0.453	1.47
chr14	81499619	C	G	SEL1L	c.821G>C	p.Ser274Th	missense_variant	MODERATE	0.225	0.31	1.38
chr16	31436755	G	A	ZNF843	c.95C>T	p.Pro32Leu	missense_variant	MODERATE	0.355	0.469	1.32
chr17	81844022	T	C	P4HB	c.1517A>G	p.Asp506Gly	missense_variant	MODERATE	0.514	0.829	1.61
chr17	78561774	T	G	DNAH17	c.1776C>A	p.Ser592Arg	missense_variant	MODERATE	0.637	0.883	1.39
chr17	35766511	C	T	MMP28	c.1552G>A	p.Ala518Thr	missense_variant	MODERATE	0.475	0.605	1.27
chr17	63485267	GT	AG	ACE	c.1953_1954delGTinsAG	p.Phe652Val	missense_variant	MODERATE	0.258	0.276	1.07
chr18	36602669	C	A	FHOD3	c.719-5C>A	.	ice_region_variant&intron_vari	LOW	0.306	0.439	1.43
chr18	346546	G	A	COLEC12	c.1076C>T	p.Thr359Met	missense_variant	MODERATE	0.365	0.422	1.16
chr19	48955721	G	T	BAX	c.121G>T	p.Glu41*	stop_gained	HIGH	0.315	0.455	1.44
chr19	54574336	G	C	LILRA2	c.106G>C	p.Gly36Arg	missense_variant	MODERATE	0.245	0.338	1.38
chr19	19714405	C	T	ZNF14	c.864>G	p.Tyr29Cys	missense_variant	MODERATE	0.341	0.408	1.20
chr19	33148880	G	A	WDR88	c.649G>A	p.Glu217Lys	missense_variant	MODERATE	0.339	0.368	1.09
chr21	37238554	C	G	DSCR3	c.257G>C	p.Ser86Thr	missense_variant	MODERATE	0.353	0.396	1.12
chr22	19788873	C	G	GNB1L	c.820G>A	p.Asp274Asn	missense_variant	MODERATE	0.494	0.832	1.68

Chrom	POS	REF	ALT	Gene	c_Change	p_Change	Effect	Impact	AF_Tumor	AF_BC
chr1	152220479	C	A	HRNR	c.1150G>T	p.Ala384Ser	missense_variant	MODERATE	0.072	0.002622
chr3	63912684	GGCAGGA	G	ATXN7	c.113_118delAGCAGC	.Gln38_Gln39del	disruptive_inframe_deletion	MODERATE	0.066	0.029
chr5	75593932	G	A	POLK	c.1411G>A	p.Ala471Thr	missense_variant	MODERATE	0.09	0.0051
chr6	31027815	A	C	MUC22	c.2393C>A	p.Thr798Asn	missense_variant	MODERATE	0.138	0.002484
chr6	110210777	C	T	CDC40	c.701C>T	p.Pro234Leu	missense_variant	MODERATE	0.138	0.011
chr7	121928159	G	T	PTPRZ1	c.62G>T	p.Trp21Leu	missense_variant	MODERATE	0.052	0.007691
chr11	14519020	C	T	PDHA1	c.43G>A	p.Asp15Asn	missense_variant	MODERATE	0.06	0.007519
chr12	41509851	G	A	PDZRN4	c.1141G>A	p.Asp381Asn	missense_variant	MODERATE	0.314	0.009274
chr14	37592014	CCGTTCT	C	FOXA1	c.764_769delAGAACG	Glu255_Asn256d	disruptive_inframe_deletion	MODERATE	0.09	0.002858
chr18	31022443	G	A	DSC3	c.835C>T	p.Arg279Cys	missense_variant	MODERATE	0.351	0.004353
chr20	21162367	G	T	KI2	c.902G>T	p.Gly301Val	missense_variant	MODERATE	0.26	0.004213
chr20	35226890	GGGC	G	MMP24	c.170_172delCGG	p.Ala57del	disruptive_inframe_deletion	MODERATE	0.142	0.056
chrX	1403309	C	A	ASMTL	c.1826G>T	p.Gly609Val	missense_variant	MODERATE	0.092	0.002357
chrX	141907182	A	T	MAGEC1	c.1778A>T	p.His593Leu	missense_variant	MODERATE	0.086	0.00253
chrX	13043787	C	A	FAM9C	c.3G>T	p.Met1?	start_lost	HIGH	0.065	0.003251
chr1	30908466	CCAG	C	SDC3	c.118_120delCTG	p.Leu40del	onservative_inframe_deletion	MODERATE	0.092	0.035
chr6	152098791	A	G	ESR1	c.1619A>G	p.Asp540Gly	missense_variant	MODERATE	0.471	0.002978
chr6	10410084	C	G	TFAP2A	c.297G>C	p.Gln99His	missense_variant	MODERATE	0.438	0.003689
chr6	159232407	G	A	FNDC1	c.1895G>A	p.Arg632His	missense_variant	MODERATE	0.41	0.00331
chr7	142867074	C	T	EPHB6	c.1750+6G>T		ice_region_variant&intron_vari	LOW	0.342	0.003986
chr7	78194913	C	A	MAGI2	c.2230G>T	p.Glu744*	stop_gained	HIGH	0.071	0.005656
chr8	40153795	C	G	C8orf4	c.263C>G	p.Thr88Arg	missense_variant	MODERATE	0.411	0.004572
chr8	7950105	A	T	ZNF7058	c.2127>A	p.Val726Glu	missense_variant	MODERATE	0.248	0.011
chr8	66666537	T	C	VCPIP1	c.422A>G	p.Lys141Arg	missense_variant	MODERATE	0.082	0.00341
chr9	109454574	C	G	PTPN3	c.290G>C	p.Gly97Ala	inse_variant&splice_region_va	MODERATE	0.38	0.004833
chr12	121445409	T	G	KDM2B	c.1969C>A	p.Pro657Thr	missense_variant	MODERATE	0.441	0.004948
chr13	24321155	T	G	C1QTNF9	c.389T>G	p.Val130Gly	missense_variant	MODERATE	0.563	0.066
chr15	70963796	T	C	LRRC49	c.800T>C	p.Val267Ala	missense_variant	MODERATE	0.507	0.008538
chr15	33644424	C	A	RYR3	c.3670C>A	p.Pro1224Thr	missense_variant	MODERATE	0.05	0.004553
chr17	46331410	T	C	LRRC37A	c.4133T>C	p.Leu1378Pro	missense_variant	MODERATE	0.459	0.038
chr17	36435221	G	A	TBC1D3K	c.387+4C>T		ice_region_variant&intron_vari	LOW	0.298	0.009519
chrX	113912668	G	A	TRPC5	c.523C>T	p.Arg175Cys	missense_variant	MODERATE	0.472	0.002856
chrX	130013830	C	G	BCORL1	c.1058C>G	p.Pro353Arg	missense_variant	MODERATE	0.443	0.002992

Supplementary table 5: Variants in patient 3. Identified by WES. Green: shared mutations between tumor at baseline and tumor at progresion.

Yellow: unique mutations to baseline tumor. Blue: Unique mutations to progression tumor

CHROM	POS	REF	ALT	GENE	c_change	p_change	Effect	Impact	AF_baseline	AF_progression	Ratio
chr1	111727422	G	A	FAM212B	c.440C>T	p.Ser147Phe	missense_variant	MODERATE	0.06	0.3	5.00
chr1	17375431	C	T	PADI6	c.299C>T	p.Ser100Leu	missense_variant	MODERATE	0.224	0.849	3.79
chr1	247841110	T	G	OR11L1	c.787A>C	p.Ser263Arg	missense_variant	MODERATE	0.199	0.736	3.70
chr1	5277673	G	A	FLVCR1	c.850G>A	p.Val284Ile	missense_variant	MODERATE	0.051	0.177	3.47
chr1	180916407	A	C	KIAA1614	c.3044>C	p.Ser102Arg	missense_variant	MODERATE	0.084	0.264	3.14
chr1	39523075	C	A	BMP8A	c.1017C>A	p.Asp339Glu	missense_variant	MODERATE	0.175	0.549	3.14
chr1	113651083	C	T	MAGI3	c.2227T>C	p.Ile775Th	missense_variant	MODERATE	0.111	0.314	2.83
chr1	31699814	G	A	COL16A1	c.265C>T	p.Arg89*	ıp_gained&splice_region_vari	HIGH	0.149	0.41	2.75
chr1	244863927	GGCGGCCTCCTCTCCTCCATCGGGCCCGAGTCGGCCGCCCCC	G	HNRNPU	c.339_380delGGGGGCGCGCCGACTCGGGCCCGATGGAGGAGGAGGAGCCGC	Gly114_Ala127d	disruptive_inframe_deletion	MODERATE	0.136	0.373	2.74
chr1	15260273	C	T	PAMEF5	c.339G>T	p.Trp113Cys	missense_variant	MODERATE	0.155	0.425	2.74
chr1	114097765	A	C	SYT6	c.1222T>G	p.Trp408Gly	missense_variant	MODERATE	0.112	0.304	2.71
chr1	12847805	G	C	HNRNPCL1	c.485C>G	p.Ser162Cys	missense_variant	MODERATE	0.135	0.362	2.68
chr1	160681466	G	C	CD48	c.388C>G	p.Pro130Ala	inse_variant&splice_region_va	MODERATE	0.136	0.27	1.55
chr1	25826682	T	A	MTFR1L	c.3077>A	p.Ser1037Th	missense_variant	MODERATE	0.101	0.25	2.48
chr1	185989519	A	C	HMCN1	c.3080A>C	p.Lys1027Thr	missense_variant	MODERATE	0.138	0.31	2.25
chr1	154328120	T	G	ATP8B2	c.787>G	p.Ile263Met	missense_variant	MODERATE	0.131	0.258	1.97
chr1	206913894	GCTTCAGAGTAA	G	FCMR	c.227_237delTTACTCTGAAG	p.Val76fs	frameshift_variant	HIGH	0.059	0.11	1.86
chr1	203045370	G	A	PPFIA4	c.669C>A	p.Glu223Gly	_region_variant&synonymous_	LOW	0.277	0.483	1.74
chr1	155478609	G	T	ASH1L	c.4265C>A	p.Leu1421Ile	missense_variant	MODERATE	0.073	0.126	1.73
chr1	223802620	AGCTCAAGTGCACCAATGTGCCAC	A	SSP1	c.1226_1248delTCAAGTGCACCAATGTGCCACGC	p.Leu409fs	frameshift_variant	HIGH	0.199	0.322	1.62
chr1	47801574	G	A	TRABD2B	c.712C>T	p.Arg238Trp	missense_variant	MODERATE	0.181	0.292	1.61
chr1	152613865	C	T	LCE3B	c.55C>T	p.Pro19Ser	missense_variant	MODERATE	0.063	0.098	1.56
chr1	223122089	C	T	TLR5	c.943A>T	p.Lys315*	stop_gained	HIGH	0.132	0.2	1.52
chr1	174525574	G	A	RABGAP1L	c.970G>A	p.Glu324Lys	missense_variant	MODERATE	0.093	0.138	1.48
chr1	46035963	C	A	MAST2	c.5315C>A	p.Thr1772Asn	missense_variant	MODERATE	0.205	0.3	1.46
chr1	223802652	A	G	DISP1	c.1225A>G	p.Thr409Ala	missense_variant	MODERATE	0.242	0.352	1.45
chr1	206648063	G	C	DYRK3	c.865G>C	p.Glu289Gln	missense_variant	MODERATE	0.086	0.116	1.35
chr1	58782539	G	C	JUN	c.532C>G	p.Pro178Ala	missense_variant	MODERATE	0.141	0.187	1.33
chr1	151344435	G	A	RFX5	c.455G>C	p.Gly152Ala	missense_variant	MODERATE	0.403	0.499	1.24
chr1	228318955	G	A	OBSCN	c.17074G>A	p.Asp5692Asn	missense_variant	MODERATE	0.193	0.137	0.71
chr1	116389451	G	A	ATP1A1	c.767G>A	p.Gly256Asp	missense_variant	MODERATE	0.198	0.122	0.62
chr1	45608025	C	A	NASP	c.1114C>A	p.Pro372Thr	missense_variant	MODERATE	0.102	0.036	0.35
chr1	165565782	G	A	NBPF1	c.2918C>T	p.Ala973Val	missense_variant	MODERATE	0.817	0.195	0.24
chr1	140385944	G	A	LRP1B	c.10480C>T	p.Arg3494Trp	missense_variant	MODERATE	0.116	0.478	4.12
chr2	74457581	A	G	INO80B	c.788G>A	p.Gly263Glu	missense_variant	MODERATE	0.08	0.21	2.63
chr2	233772332	G	A	UGT1A8	c.1366G>A	p.Val456Met	missense_variant	MODERATE	0.086	0.199	2.31
chr2	27239785	G	T	CAD	c.5483G>T	p.Ser1828Ile	missense_variant	MODERATE	0.203	0.453	2.23
chr2	216100279	C	T	TMEM169	c.631G>C	p.Val211Leu	missense_variant	MODERATE	0.095	0.205	2.16
chr2	200604071	G	A	AOX1	c.643G>A	p.Glu215Lys	missense_variant	MODERATE	0.164	0.349	2.13
chr2	178664684	G	A	TTN	c.36172C>T	p.Leu12058Phe	missense_variant	MODERATE	0.087	0.185	2.13
chr2	44715286	G	A	CAMKMT	c.557-1G>A	.	ıe_acceptor_variant&intron_va	HIGH	0.215	0.456	2.12
chr2	112567978	G	C	POLR1B	c.1872G>C	p.Glu624Asp	missense_variant	MODERATE	0.1	0.208	2.08
chr2	205121745	C	T	PARD3B	c.961C>T	p.Pro321Ser	missense_variant	MODERATE	0.194	0.395	2.04
chr2	233483366	T	G	DGKD	c.2663T>G	p.Val888Gly	missense_variant	MODERATE	0.186	0.353	1.90
chr2	206751043	A	T	MDH1B	c.943A>T	p.Ser315Cys	missense_variant	MODERATE	0.096	0.179	1.86
chr2	219515272	G	T	ASIC4	c.929G>T	p.Ser310Ile	missense_variant	MODERATE	0.22	0.375	1.70
chr2	73813901	G	T	C2orf78	c.522G>T	p.Met174Ile	missense_variant	MODERATE	0.204	0.344	1.69
chr2	101266729	G	C	CNOT11	c.1088C>G	p.Thr363Ser	missense_variant	MODERATE	0.102	0.162	1.59
chr2	17932167	G	T	KCNS3	c.1159G>T	p.Ala387Ser	missense_variant	MODERATE	0.203	0.282	1.39
chr2	201387760	C	TGGCAACT	TRAK2	c.1638_1639insTGCCAGTTGCCAGTT	Ala547insCysGln	tonservative_inframe_insertion	MODERATE	0.123	0.168	1.37
chr2	43675778	TC	CT	C1GALT1C1L	c.544_545delGAinsAG	p.Glu182Arg	missense_variant	MODERATE	0.192	0.173	0.90
chr3	47006423	G	C	NBEAL2	c.7108G>C	p.Asp2370His	missense_variant	MODERATE	0.091	0.579	6.36
chr3	48631270	G	C	SLC26A6	c.940C>G	p.Leu314Val	missense_variant	MODERATE	0.119	0.618	5.19
chr3	126898786	C	T	PLXNA1	c.1193G>T	p.Ser398Leu	inse_variant&splice_region_va	MODERATE	0.099	0.493	4.98
chr3	157261160	T	A	VEPH1	c.2476A>T	p.Ser826Cys	missense_variant	MODERATE	0.173	0.531	3.07
chr3	128408244	G	A	EEF5EC	c.1776G>A	p.Met592Ile	missense_variant	MODERATE	0.18	0.534	2.97
chr3	170128851	C	G	PHC3	c.1621G>C	p.Glu541Gln	missense_variant	MODERATE	0.148	0.35	2.36
chr3	52492100	C	T	NISCH	c.4133C>T	p.Ser1378Phe	missense_variant	MODERATE	0.126	0.28	2.22
chr3	156516311	A	G	KCNAB1	c.907A>G	p.Ile303Val	missense_variant	MODERATE	0.065	0.144	2.22
chr3	122699485	A	T	PARP14	c.931A>T	p.Lys311*	stop_gained	HIGH	0.077	0.148	1.92
chr3	179218294	G	A	PIK3CA	c.1624G>A	.	protein_protein_contact	HIGH	0.146	0.278	1.90
chr3	185218242	T	C	EHHADH	c.464-2A>G	.	ıe_acceptor_variant&intron_va	HIGH	0.052	0.095	1.83
chr3	78636074	A	T	ROBO1	c.3072T>A	p.Asp1024Glu	missense_variant	MODERATE	0.168	0.298	1.77
chr3	184372764	C	T	TIPIP2	c.1231G>A	p.Ala411Thr	missense_variant	MODERATE	0.158	0.255	1.61
chr3	138946088	G	A	FOXL2	c.635C>T	p.Pro212Leu	missense_variant	MODERATE	0.082	0.13	1.59
chr3	195295888	C	T	ACAP2	c.1492G>A	p.Glu498Lys	missense_variant	MODERATE	0.164	0.23	1.40
chr3	189320777	A	G	TPEG1	c.785A>G	p.Asn262Ser	missense_variant	MODERATE	0.256	0.32	1.25
chr3	119613115	G	T	PLA1A	c.661G>T	p.Asp221Tyr	missense_variant	MODERATE	0.13	0.153	1.18
chr3	194431202	C	T	ATP13A3	c.2446G>A	p.Asp816Asn	missense_variant	MODERATE	0.093	0.087	0.94
chr3	196584143	G	C	FBXO45	c.686G>C	p.Arg229Thr	missense_variant	MODERATE	0.169	0.133	0.79
chr3	149163914	G	C	HPS3	c.2554G>C	p.Asp852His	missense_variant	MODERATE	0.21	0.155	0.74
chr3	170038987	A	T	GPR160	c.-249A>T	ITR_premature_start_codon_ga	LOW	0.162	0.112	0.69
chr3	193435725	C	T	ATP13A4	c.2692G>A	p.Val898Ile	missense_variant	MODERATE	0.1	0.062	0.62
chr4	154542233	G	T	PLRG1	c.641C>A	p.Pro214His	missense_variant	MODERATE	0.093	0.302	3.25
chr4	147909766	G	C	ARHGAP10	c.1151G>C	p.Arg384Thr	missense_variant	MODERATE	0.085	0.247	2.91
chr4	107687153	G	A	PAPSS1	c.436C>T	.	structural_interaction_variant	HIGH	0.102	0.287	2.81
chr4	121686353	GTACAGTGCCTC	G	ANXA5	c.17_28delGAGGCACTGTGA	.	structural_interaction_variant	HIGH	0.096	0.255	2.66
chr4	182681939	G	A	TENM3	c.1960G>A	p.Gly654Ser	missense_variant	MODERATE	0.107	0.268	2.50
chr4	121686368	A	AATTAGG	ANXA5	c.13_14insCCTAAT	.Ile5delinsProTerfinedS	onservative_inframe_ir	HIGH	0.109	0.258	2.37
chr4	99343025	C	G	ADH1C	c.598G>C	p.Gly200Arg	missense_variant	MODERATE	0.065	0.141	2.17
chr4	70689857	G	C	UTP3	c.1180G>C	p.Glu394Gln	missense_variant	MODERATE	0.175	0.378	2.16
chr4	40944930	C	G	APBB2	c.979G>C	p.Asp327His	missense_variant	MODERATE	0.098	0.161	1.64
chr4	41981966	G	T	DCAF4L1	c.1746T>T	p.Lys582Asn	missense_variant	MODERATE	0.192	0.301	1.57
chr4	73155766	T	A	ANKRD17	c.865A>T	p.Met289Leu	missense_variant	MODERATE	0.104	0.139	1.34
chr5	23510034	G	T	PRDM9	c.301+7G>T	.	ice_region_variant&intron_vari	LOW	0.072	0.388	5.39
chr5	151064976	T	G	TNIP1	c.120A>C	p.Gln40His	missense_variant	MODERATE	0.136	0.485	3.57
chr5	33441142	CGGTGAGCAAACTT	C	TARS	c.57+4_57+16delAGCAAACTTGGTG	.	ice_region_variant&intron_vari	LOW	0.062	0.175	2.82
chr5	126914968	TGAAGTGGCA	T	MARCH3	c.346_354delTGCCACTTC	.Cys116_Phe118d	onservative_inframe_deletion	MODERATE	0.069	0.182	2.64
chr5	140796400	C	G	PCDHA2	c.1526C>T	p.Ser509Leu	missense_variant	MODERATE	0.148	0.375	2.53
chr5	122423037	G	C	SNCAIP	c.441G>C	p.Gln147His	missense_variant	MODERATE	0.154	0.384	2.49
chr5	168753033	C	G	SLIT3	c.1895G>C	p.Arg632Thr	missense_variant	MODERATE	0.069	0.144	2.09
chr5	36136399	C	A	LMBR1D2	c.657G>T	p.Arg219Ser	missense_variant	MODERATE	0.091	0.148	1.63
chr5	134854913	C	T	C5orf24	c.13G>T	p.Val5Phe	missense_variant	MODERATE	0.101	0.131	1.30
chr5	161873163	GG	TT	GABRA1	c.302_303delGGinsTT	p.Arg101Ile	missense_variant	MODERATE	0.284	0.301	1.06
chr5	434396	GGTGTGGCTGGGGGGCA	G	AHR8	c.1726_1741delTGGCTGGGGGCCAGTG	p.Trp576fs	frameshift_variant	HIGH	0.157	0.112	0.71
chr6	10876482	T	C	GCM2	c.419A>G	p.Asn140Ser	missense_variant	MODERATE	0.031	0.182	5.87
chr6	35870947	G	T	SRPK1	c.764C>A	p.Pro255His	missense_variant	MODERATE	0.13	0.475	3.65
chr6	38949500	C	T	DNAH8	c.12178C>G	p.Pro4060Ala	missense_variant	MODERATE	0.152	0.342	2.25
chr6	158978347	C	T	RSPH3	c.1286-1G>A	.	ıe_acceptor_variant&intron_va	HIGH	0.167	0.369	2.21
chr6	29725144	G	T	HLA-F-4	c.724G>T	p.Gly242Trp	missense_variant	MODERATE	0.184	0.385	2.09
chr6	17799337	C	T	KIF13A	c.2719G>A	p.Val907Met	missense_variant	MODERATE	0.084	0.158	1.88
chr6	39322449	A	G	KCNK16	c.327C>C	p.Ile317Thr	missense_variant	MODERATE	0.102	0.169	1.66
chr6	125922739	A	C	NCOA7	c.2428A>C	p.Thr810Pro	missense_variant	MODERATE	0.27	0.396	1.47

chr7	88153220		G	C	ADAM22	c.1682-1G>C	-	splice_acceptor_variant&intron_var	HIGH	0.054	0.237	4.39
chr7	100107601		G	T	TAF6	c.1790C>A	p.Ala597Asp	missense_variant	MODERATE	0.063	0.244	3.87
chr7	87509341		TGAC	T	ABCB1	c.3420_3422delGTC	p.Ser1141del	disruptive_inframe_deletion	MODERATE	0.12	0.408	3.40
chr7	73840554		G	A	WBSCR27	c.253-5C>T	-	splice_region_variant&intron_vari	LOW	0.069	0.223	3.23
chr7	142874958		C	G	TRPV6	c.1352G>C	p.Gly451Ala	missense_variant	MODERATE	0.101	0.296	2.93
chr7	99858868		CCAGAATTCCAA	C	CYP3A43	c.835_845delCAGAATTCCAA	p.Gln279fs	frameshift_variant	HIGH	0.068	0.186	2.74
chr7	142866181		G	C	EPHB6	c.1327G>C	p.Glu443Gln	missense_variant	MODERATE	0.121	0.309	2.55
chr7	47368719		C	A	TNS3	c.1927G>T	p.Val643Phe	missense_variant	MODERATE	0.095	0.226	2.38
chr7	123119317		A	G	SLC13A1	c.1456G>T	p.Glu486*	stop_gained	HIGH	0.142	0.332	2.34
chr7	128716849		G	T	FAM71F1	c.286G>T	p.Ala96Ser	missense_variant	MODERATE	0.095	0.216	2.27
chr7	64220164	TAAGAGAATTCATACTGGAGAGAAACCATACA	T	ZNF735	c.1116_1146delGAGAATTCATACTGGAGAGAAACCATACAAA	p.Lys372fs	frameshift_variant	HIGH	0.083	0.179	2.16
chr7	82758689		C	A	PCLO	c.15315G>T	p.Lys5105Asn	missense_variant	MODERATE	0.089	0.175	1.97
chr7	102178587		T	A	CUX1	c.980T>A	p.Leu327Gln	missense_variant	MODERATE	0.12	0.2	1.67
chr7	1058133		GC	CG	GPR146	c.618_619delGCinsCG	p.Leu207Val	missense_variant	MODERATE	0.276	0.361	1.31
chr7	26196962		A	G	HNRNPA2B1	c.356T>C	p.Ile119Thr	missense_variant	MODERATE	0.313	0.381	1.22
chr7	20742879		C	T	ABCB5	c.3027C>T	p.Asp1009Asp	region_variant&synonymous_	LOW	0.316	0.325	1.03
chr7	6026906		G	T	EIF2AK1	c.1586C>A	p.Thr529Lys	missense_variant	MODERATE	0.161	0.16	0.99
chr8	134602083		G	A	ZFAT	c.1636G>T	p.Asp546Tyr	missense_variant	MODERATE	0.258	0.636	2.47
chr8	38836273		T	A	TACC1	c.1825T>A	p.Leu609Ile	missense_variant	MODERATE	0.314	0.604	1.92
chr8	144804130		CT	C	ZNF517	c.1668delT	p.Val567fs	frameshift_variant	HIGH	0.112	0.169	1.51
chr8	144804133		GT	G	ZNF517	c.1671delT	p.Ala58fs	frameshift_variant	HIGH	0.112	0.169	1.51
chr8	144475233		G	T	FOXH1	c.203C>A	p.Pro68His	missense_variant	MODERATE	0.148	0.159	1.07
chr8	60742598		C	T	CHD7	c.1166C>T	p.Thr389Ile	missense_variant	MODERATE	0.077	0.068	0.88
chr9	15860954		G	T	ORF13J	c.848C>A	p.Thr283Asn	missense_variant	MODERATE	0.086	0.31	3.60
chr9	104809529		A	T	ABCA1	c.4211T>A	p.Leu1404His	missense_variant	MODERATE	0.063	0.219	3.48
chr9	112817816		G	A	SNX30	c.459+1G>A	-	splice_donor_variant&intron_vari	HIGH	0.257	0.633	2.46
chr9	74840146		G	A	TRPM6	c.4220>T	p.Ser1411Leu	missense_variant	MODERATE	0.12	0.268	2.23
chr9	133102043	GTCCCCGCTGC	G	RALGDS	c.2096_2105delGCAGCGGGGA	p.Ser699fs	frameshift_variant	HIGH	0.08	0.178	2.23
chr9	32448897	G	A	ACO1	c.2372G>A	p.Gly791Glu	inse_variant&splice_region_va	MODERATE	0.08	0.168	2.10
chr9	35305864	G	C	UNC13B	c.762-4603G>C	-	sequence_feature	MODERATE	0.175	0.344	1.97
chr9	104570006	T	G	OR13C8	c.839T>G	p.Ile280Ser	missense_variant	MODERATE	0.121	0.21	1.74
chr9	32542010	C	T	TOPORS	c.2515G>A	p.Glu839Lys	missense_variant	MODERATE	0.201	0.193	0.96
chr10	46549410	ACTGCATGACAGCCGCGAGTGGCCCCTCCGGCC	A	GPRIN2	c.1294_1326delGGCCGGAGGGGGCCACTGCGGGCTGTCATGCAG	Gly432_Gln442dconservative_inframe_deletion	MODERATE	0.031	0.08	2.58
chr10	103246504		T	A	RPEL1	c.508T>A	p.Leu170Met	missense_variant	MODERATE	0.172	0.318	1.85
chr10	103607562		C	G	SH3PXD2A	c.2572G>C	p.Glu858Gln	missense_variant	MODERATE	0.163	0.291	1.79
chr10	129840247		T	G	EBF3	c.1622A>C	p.Gln541Pro	inse_variant&splice_region_va	MODERATE	0.195	0.327	1.68
chr10	93793308		G	A	LG11	c.796G>A	p.Ala266Asn	missense_variant	MODERATE	0.146	0.203	1.39
chr11	5709115		C	A	TRIM22	c.964C>A	p.Gln322Lys	missense_variant	MODERATE	0.203	0.326	1.61
chr11	5352120	GTCTTGTTGGACTTTCTCA	G	OR51B6	c.616_633delTTGTTGGACTTTCTCATC	Leu206_Ile211dconservative_inframe_deletion	MODERATE	0.084	0.26	3.10
chr11	92866804		T	A	FAT3	c.11722T>A	p.Ser3908Thr	missense_variant	MODERATE	0.082	0.252	3.07
chr11	6634003		C	G	OCH1	c.2004G>C	p.Met668Ile	missense_variant	MODERATE	0.092	0.265	2.88
chr11	3660260		G	T	ART1	c.741G>T	p.Glu247Asp	missense_variant	MODERATE	0.098	0.275	2.81
chr11	92354667		A	C	FAT3	c.2555A>C	p.Gln852Pro	missense_variant	MODERATE	0.083	0.214	2.58
chr11	10773249		G	A	CTR9	c.2703G>C	p.Lys901Asn	missense_variant	MODERATE	0.119	0.292	2.45
chr11	124626471		A	T	TBRG1	c.455-2A>T	-	splice_acceptor_variant&intron_vari	HIGH	0.116	0.27	2.33
chr11	83466777		T	A	DLG2	c.2660A>T	p.Lys887Met	missense_variant	MODERATE	0.095	0.2	2.11
chr11	63974673		G	C	CD6BA	c.-80>A	-	5_prime_UTR_premature_start_codon_ga	LOW	0.233	0.481	2.06
chr11	14505197		G	A	PSMA1	c.805C>T	p.His269Tyr	missense_variant	MODERATE	0.211	0.403	1.91
chr11	72237763		C	G	INPPL1	c.3519G>C	p.Ile1173Met	missense_variant	MODERATE	0.09	0.165	1.83
chr11	83166684		G	A	PCF11	c.1787G>A	p.Arg596Lys	missense_variant	MODERATE	0.276	0.506	1.83
chr11	62666846		G	C	METTL12	c.518G>C	p.Gly173Ala	missense_variant	MODERATE	0.27	0.478	1.77
chr11	73975064		A	T	UCP2	c.873T>A	p.Tyr291*	stop_gained	HIGH	0.289	0.458	1.58
chr11	100623726		G	A	GAL3L3	c.921G>A	-	sequence_feature	MODERATE	0.105	0.37	3.52
chr12	123315543		C	T	SBNO1	c.3048+5G>A	-	splice_region_variant&intron_vari	LOW	0.208	0.605	2.91
chr12	129075038		C	T	TMEM132D	c.2137G>A	p.Val713Ile	missense_variant	MODERATE	0.326	0.942	2.89
chr12	6845588		C	T	GNB3	c.702C>T	p.Phe234Phe	region_variant&synonymous_	LOW	0.073	0.209	2.86
chr12	110033913		C	A	ANKRD13A	c.1465C>A	p.Gln488Lys	missense_variant	MODERATE	0.13	0.369	2.84
chr12	157656		G	A	IQSEC3	c.2405G>A	p.Arg802Gln	missense_variant	MODERATE	0.163	0.453	2.78
chr12	110515154		T	G	RAD9B	c.593T>G	p.Met198Arg	inse_variant&splice_region_va	MODERATE	0.212	0.581	2.74
chr12	109796519		GC	G	TRPV4	c.1332+5delG	-	splice_region_variant&intron_vari	LOW	0.215	0.554	2.58
chr12	40473164		G	A	MUC19	c.5725G>A	p.Ala1909Thr	missense_variant	MODERATE	0.197	0.444	2.25
chr12	50177645		C	A	LIMA1	c.1702G>T	p.Val568Phe	missense_variant	MODERATE	0.428	0.922	2.15
chr12	57627670		G	T	B4GALNT1	c.1332C>A	p.Asp444Glu	missense_variant	MODERATE	0.449	0.848	1.89
chr12	21477945	TTTAAG	T	RECQL	c.720_724delCTTAA	p.Leu241fs	frameshift_variant	HIGH	0.075	0.138	1.84
chr12	56350126	G	A	STAT2	c.1180C>T	p.Gln394*	stop_gained	HIGH	0.164	0.214	1.30
chr12	25037998	A	T	LOC645177	c.1978A>T	p.Lys660*	stop_gained	HIGH	0.241	0.311	1.29
chr12	14466549	G	C	ATF7IP	c.2845G>C	p.Asp948His	missense_variant	MODERATE	0.205	0.21	1.02
chr13	23334320	C	A	SACS	c.9556G>T	p.Asp3186Tyr	missense_variant	MODERATE	0.081	0.153	1.89
chr13	59810810	C	A	DIAPH3	c.3141G>T	p.Lys1047Asn	missense_variant	MODERATE	0.108	0.203	1.88
chr13	24316597	C	T	LTB4R	c.946C>T	p.Arg316Cys	missense_variant	MODERATE	0.04	0.217	5.43
chr14	44506421	C	A	FSCB	c.567G>T	p.Lys189Asn	missense_variant	MODERATE	0.069	0.264	3.83
chr14	74901173	TCAGTCTGCCATCCTCGGGGATGCATGG	T	DLST	c.1170_1195delGTCTGCCATCCTCGGGGATGCATGGCA	p.Gln390fs	frameshift_variant	HIGH	0.058	0.218	3.76
chr14	33774528	T	G	NPAS3	c.1044T>G	p.Asn348Lys	inse_variant&splice_region_va	MODERATE	0.16	0.572	3.58
chr14	77859279	G	A	ADCK1	c.423G>A	p.Glu141Glu	region_variant&synonymous_	LOW	0.103	0.323	3.14
chr14	77859281	TACCC	T	ADCK1	c.423+6_423+9delCACC	-	splice_region_variant&intron_vari	LOW	0.103	0.323	3.14
chr14	56802064	G	C	OTX2	c.565C>G	p.Gln189Glu	missense_variant	MODERATE	0.192	0.547	2.85
chr14	91974746	G	A	TRIP11	c.5458-3C>T	-	splice_region_variant&intron_vari	LOW	0.242	0.549	2.27
chr14	21394040	C	G	OHD8	c.5755G>C	p.Glu1919Gln	missense_variant	MODERATE	0.113	0.226	2.00
chr14	23428957	C	T	MYH7	c.1405G>A	p.Asp469Asn	inse_variant&splice_region_va	MODERATE	0.118	0.232	1.97
chr15	33543669	G	T	RYR3	c.6940>T	p.Glu2312*	stop_gained	HIGH	0.177	0.451	2.55
chr15	32636415	AACTCTTTGGAGCCTGATATTATGGTAGAAAAGTC	A	ARHGAP21A	c.1645_1678delTCTTTGGAGCCTGATATTATGGTAGAAAAGTCAC	p.Ser549fs	frameshift_variant	HIGH	0.146	0.35	2.40
chr15	41816605	C	G	MAP1B1	c.1558C>G	p.His520Asp	missense_variant	MODERATE	0.187	0.443	2.37
chr15	40220754	C	T	BUB1B	c.3148C>T	p.Gln1050*	stop_gained	HIGH	0.219	0.478	2.18
chr15	71812134	C	A	NR2E3	c.529C>A	p.Leu177Ile	missense_variant	MODERATE	0.074	0.142	1.92
chr15	88860376	G	C	ACAN	c.6883G>C	p.Glu2295Gln	missense_variant	MODERATE	0.086	0.155	1.80
chr15	65026889	C	T	MTFMT	c.361G>A	p.Gly121Arg	missense_variant	MODERATE	0.065	0.111	1.71
chr15	88873940	G	C	ACAN	c.7432C>G	p.Glu2478Gln	missense_variant	MODERATE	0.176	0.772	1.34
chr15	60385987	CAACTTGCAAAAATTATATAAAGTGAAAGTGATAT	C	ANXA2	c.102+7_102+40delATATCACTTTCACTTTATATAATTTTTGCAAGTT	-	splice_region_variant&intron_vari	LOW	0.098	0.121	1.23
chr16	57028297	T	C	NLRC5	c.2160-5T>C	-	splice_region_variant&intron_vari	LOW	0.132	0.871	6.60
chr16	406398	G	C	DECR2	c.201+1G>C	-	splice_donor_variant&intron_vari	HIGH	0.099	0.355	3.59
chr16	50291851	C	G	ADCY7	c.491C>G	p.Ser164Cys	missense_variant	MODERATE	0.186	0.598	3.22
chr16	66935463	C	G	CES2	c.20C>G	p.Ser7Cys	missense_variant	MODERATE	0.079	0.196	2.48
chr16	30418351	A	G	ZNF771	c.938A>G	p.Glu313Gly	missense_variant	MODERATE	0.075	0.177	2.36
chr16	66386806	T	C	CDH5	c.211-3T>C	-	splice_region_variant&intron_vari	LOW	0.226	0.427	1.89
chr16	17541287	C	G	XYLT1	c.1453G>C	p.Glu485Gln	missense_variant	MODERATE	0.18	0.315	1.75
chr16	31086066	T	C	PRSS53	c.781A>G	p.Thr261Ala	missense_variant	MODERATE	0.084	0.144	1.71
chr16	20471658	T	A	ACSM2A	c.863T>A	p.Leu288*	stop_gained	HIGH	0.094	0.155	1.65
chr16	10907253	G	C	CIITA	c.1764G>C	p.Met588Ile	missense_variant	MODERATE	0.194	0.296	1.53
chr16	8904524	G	T	USP7	c.1615C>A	-	structural_interaction_variant	HIGH	0.1	0.135	1.35
chr16	1511113	G	T	IFT140	c.4220C>A	p.Pro1407His	missense_variant	MODERATE	0.192	0.217	1.13
chr17	45242114	C	T	FMNL1	c.1853C>T	p.Ala618Val	missense_variant	MODERATE	0.17	0.601	3.54
chr17	44385619	C	T	ITGA2B	c.5006G>A	p.Gly1669Asp	missense_variant	MODERATE	0.21	0.623	2.97
chr17	7673811	A	C	TP53	c.809T>G	p.Phe270Cys	missense_variant	MODERATE	0.328	0.932	2.84
chr17	79835222	C	A	CBX4	c.420G>T	p.Lys140Asn	missense_variant	MODERATE	0.182	0.475	2.61
chr17	7804165	A	T	TNRC6C	c.103A>T	p.Ser35Cys	missense_variant	MODERATE	0.096	0.244	2.54
chr17	74795529	C	A	TMEM104	c.533C>A	p.Ala178Asp	missense_variant	MODERATE	0.091	0.229	2.52
chr17	64213866	C	G	TEX2	c.352G>C	p.Glu118Gln	missense_variant	MODERATE	0.171	0.381	2.23
chr17	58275693	C	A	MPO	c.1214G>T	p.Arg405Leu	missense_variant	MODERATE	0.257	0.569	2.21
chr17	36940810	G	C	LHX1	c.598G>C	p.Ala200Pro	missense_variant	MODERATE	0.279	0.594	2.13
chr17	44353864	C	T	FAM171A2	c.2350G>A	p.Glu784Lys	missense_variant	MODERATE	0.285	59	2.07
chr18	3673674	A	T	FHOD3	c.3446A>T	p.Glu1149Val	missense_variant	MODERATE	0.256	0.733	2.86
chr18	45852592	G	C	EPG5	c.7615C>G	p.Gln2539Glu	missense_variant	MODERATE	0.22	0.46	2.09
chr18	9258930	CAGTA	C	ANKRD12	c.5664+5_5664+8delGTAA	-	splice_region_variant&intron_vari	LOW	0.427	0.543	1.27
chr19	3783846	C	T	MATK	c.5530>A	p.Val1858Met	missense_variant	MODERATE	0.083	0.315	3.80
chr19	50482243	G	C	EMC10	c.773G>C	p.Gly258Ala	missense_variant	MODERATE	0.09	0.287	3.19
chr19	4179103	A	G	SIRT6	c.377+1G>T	-	splice_donor_variant&intron_vari	HIGH	0.3	0.919	3.06
chr19	23932603	TATAAG	T	ZNF726	c.494_498delTAAGA	p.Ile165fs	frameshift_variant	HIGH	0.139	0.394	2.83
chr19	407613	A	T	C2CD4C	c.749T>A	p.Val250Glu	missense_variant	MODERATE	0.111	0.31	2.79
chr19	7558998	C	T	PNPLA6	c.3576G>C	p.Lys1192Asn	missense_variant	MODERATE	0.107	0.298	2.79
chr19	18617103	G	T	TMEM59L	c.664+1G>T	-	splice_donor_variant&intron_vari	HIGH	0.069	0.189	2.74
chr19	2433902	G	A	LMNB2	c.1406C>T	p.Ser469Leu	missense_variant	MODERATE	0.111	0.301	2.71
chr19	75724	A	G	MS5P	c.2680>A	p.Glu90Lys	missense_variant	MODERATE	0.246	0.603	2.45
chr19	48599208	G	T	SULT2B1	c.9000>T	-	structural_interaction_variant	HIGH	0.089	0.215	2.42
chr19	51945641	TAACAGTGCGTTCCA	T	ZNF613	c.1760_1773delACAGTGCGTTCCAA	p.Asn587fs	frameshift_variant	HIGH	0.102	0.246	2.41
chr19	40513561	G	A	SPTBN4	c.2765+7G>A	-	splice_region_variant&intron_vari	LOW	0.186	0.462	2.36
chr19	16847039	GC	G	SIN3B	c.654delC	p.Asn219fs	frameshift_variant	HIGH	0.132	0.296	2.24
chr19	19264783	A	C	TM6SF2	c.1015T>G	p.Cys339Gly	missense_variant	MODERATE	0.187	0.406	2.17
chr19	17285009	C	G	ANKLE1	c.1617C>G	p.Phe538Leu	missense_variant	MODERATE	0.148	0.32	2.16
chr19	16847039	GC	G	SIN3B	c.654delC	p.Asn219fs	frameshift_variant	HIGH	0.132	0.296	2.24
chr19	19264783	A	C	TM6SF2	c.1015T>G	p.Cys339Gly	missense_variant	MODERATE	0.187	0.406	2.17
chr19	17285009	C	G	ANKLE1	c.1617C>G	p.Phe538Leu	missense_variant	MODERATE	0.148	0.32	2.16
chr19	14473915	A	G	PTGER1	c.406T>C	p.Cys136Arg	missense_variant	MODERATE	0.164	0.337	2.05
chr19	23224025	G	T	ZNF724	n.355-7C>A	-	splice_region_variant&intron_vari	LOW	0.236	0.453	1.92
chr19	54426757	G	T	TTYH1	c.723D>T	p.Tyr241Cys	missense_variant	MODERATE	0.171	0.213	1.25
chr19	11335519	G	G	RAB3D	c.400G>C	-	structural_interaction_variant	HIGH	0.214	0.249	1.16
chr19	19569496	C	T	PBX4	c.721G>A	p.Glu241Lys	missense_variant	MODERATE	0.158	0.182	1.15
chr19	35675840	G	G	UPK1A	c.469C>G	p.Gln157Glu	inse_variant&splice_region_va	MODERATE	0.203	0.216	1.06
chr19	51746592	T	A	FPR1	c.403A>T	p.Asn135Tyr	missense_variant	MODERATE	0.2	0.193	0.97
chr19	12745515	G	A	ASNA1	c.448G>A	p.Glu150Lys	missense_variant	MODERATE	0.209	0.2	0.96
chr20	33068942	G	A	BPIFB3	c.1118G>A	p.Gly373Glu	missense_variant	MODERATE	0.222	0.489	2.20
chr20	34979793	TGG	T	MYH7B	c.458_459delGG	p.Trp153fs	frameshift_variant	HIGH	0.159	0.316	2.11
chr20	64074196	T	A	RGS19	c.410A>T	p.Glu137Val	missense_variant	MODERATE	0.22	0.427	1.94
chr20	62464079	C	A	GATA5	c.1051G>T	p.Glu351*	stop_gained	HIGH	0.226	0.391	1.73
chr20	54164511	C	T	CYP24A1	c.785G>A	p.Ser262Asn	missense_variant	MODERATE	0.223	0.369	1.65
chr20	25476305	C	T	NINL	c.2986G>A	p.Glu996Lys	missense_variant	MODERATE	0.08	0.115	1.44
chr20	271258	TG	T	C20orf96	c.1040delC	p.Pro347fs	frameshift_variant	HIGH	0.107	0.148	1.38
chr20	62320830	G	C	LAMA5	c.6557C>G	p.Pro2188Arg	missense_variant	MODERATE	0.367	0.419	1.14
chr20	63685590	C	G	RTEL1	c.1259C>G	p.Ser420Cys	missense_variant	MODERATE	0.132	0.098	0.74
chr21	46428437	G	A	PCNT	c.7537G>A	p.Asp2513Asn	missense_variant	MODERATE	0.063	0.122	1.94
chr22	49963117	A	G	PIM3	c.971A>G	p.Glu324Gly	missense_variant	MODERATE	0.309	0.928	3.00
chr22	45413984	G	T	RIBC2	c.980>T	p.Arg327Leu	missense_variant	MODERATE	0.1	0.269	2.69
chr22	37075209	ATGGTGATCCCGGCCG	A	TMPRSS6	c.1253_1267delCGGCCGGATCACCA	Thr418_Thr422dc	disruptive_inframe_deletion	MODERATE	0.108	0.266	2.46
chr22	26026894	C	A	MYO18B	c.6923C>A	p.Ala2308Glu	missense_variant	MODERATE	0.1	0.217	2.17
chr22	16591916	G	T	CCTBL2	c.635C>A	p.Thr212Lys	missense_variant	MODERATE	0.108	0.223	2.06
chr22	18608539	C	A	RIMBP3	c.2896G>T	p.Glu966*	stop_gained	HIGH	0.079	0.163	2.06
chr22	20446558	G	T	KLHL22	c.1424C>A	p.Thr475Lys	missense_variant	MODERATE	0.107	0.214	2.00
chr22	30112477	TTTATTTTCCC	T	HORMAD2	c.316-14_316-5delTTTCCCTTAT	-	splice_region_variant&intron_vari	LOW	0.143	0.167	1.17
chrX	103786601	G	A	PLP1	c.328G>A	p.Gly110Ser	missense_variant	MODERATE	0.109	0.519	4.76
chrX	119589456	A	T	NXF2	c.2014T>A	p.Tyr672Asn	missense_variant	MODERATE	0.078	0.312	4.00
chrX	154031235	C	G	MECP2	c.629G>C	p.Arg210Thr	missense_variant	MODERATE	0.064	0.225	3.52
chrX	154533611	C	T	G6PD	c.919G>A	p.Ala307Thr	missense_variant	MODERATE	0.063	0.198	3.14
chrX	65729644	G	T	MSN	c.399G>T	p.Lys133Asn	missense_variant	MODERATE	0.062	0.172	2.77
chrX	152956976	A	T	HS6ST2	c.779T>A	p.Val260Glu	missense_variant	MODERATE	0.182	0.491	2.70
chrX	151700555	C	T	PRRG3	c.218C>T	p.Pro73Leu	missense_variant	MODERATE	0.243	0.512	2.11
chrX	53602620	T	A	HUWE1	c.2915A>T	p.Gln972Leu	missense_variant	MODERATE	0.071	0.13	1.83
chrX	83508679	GCACCGAACCGTCTAT	G	EIF1PX	c.359_374delGCAACCGGTCTATCAC	p.Pro120fs	frameshift_variant	HIGH	0.25	0.174	1.39
chrX	152736905	A	C	MAGEA12	c.744A>C	p.Gln248His	missense_variant	MODERATE	0.084	0.115	1.37
chrX	48541332	G	A	TBC1D25	c.124-1G>A	-	splice_acceptor_variant&intron_va	HIGH	0.255	32	1.25
chrX	71812977	G	C	ACRC	c.2073G>C	p.Val691Leu	missense_variant	MODERATE	0.126	0.154	1.22

Chrom	POS	REF	ALT	Gene	c_Change	p_Change	Effect	Impact	AF_Tumor	AF_BC	
chr1	33036775	G	A	AK2	c.54C>T	-	structural_interaction_variant	HIGH	0.185	0.018	
chr1	212329231	G	T	PPP2R5A	c.278G>T	p.Ser93Ile	missense_variant	MODERATE	0.155	0.007686	
chr1	33036756	C	T	AK2	c.73G>A	p.Gly25Arg	missense_variant	MODERATE	0.115	0.013	
chr1	26558801	G	A	RPS6KA1	c.1112-6G>A	-	splice_region_variant&intron_vari	LOW	0.106	0.006488	
chr1	26342840	C	G	AIM1L	c.3118G>C	p.Val1040Leu	missense_variant	MODERATE	0.087	0.004035	
chr1	225412649	T	A	LBR	c.893-4A>T	-	splice_region_variant&intron_vari	LOW	0.086	0.011	
chr1	1507939	G	T	USP24	c.7139C>A	p.Pro2380His	missense_variant	MODERATE	0.085	0.006072	
chr1	102997096	C	T	COL11A1	c.2261G>A	p.Gly754Glu	missense_variant	MODERATE	0.083	0.006388	
chr1	212286204	G	C	PPP2R5A	c.94G>C	p.Ala32Pro	missense_variant	MODERATE	0.072	0.003479	
chr1	47417034	G	A	FOXE3	c.719G>A	p.Cys240Tyr	missense_variant	MODERATE	0.069	0.014	
chr1	99004655	G	A	PLPPR5	c.17C>T	p.Ala6Val	missense_variant	MODERATE	0.068	0.005882	
chr1	62444764	A	T	USP1	c.584A>T	p.Tyr195Phe	missense_variant	MODERATE	0.065	0.009745	
chr1	58539090	G	A	OMA1	c.205C>T	p.His69Tyr	missense_variant	MODERATE	0.062	0.003615	
chr1	99004646	G	A	LOC100129620	n.370+1G>A	-	splice_donor_variant&intron_vari	HIGH	0.06	0.005469	
chr1	205921760	T	TG	SLC26A9	c.1830dupC	p.Asn611fs	frameshift_variant	HIGH	0.06	0.003958	
chr1	220025153	T	C	EPRS	c.729A>G	-	sequence_feature	MODERATE	0.056	0.009274	
chr1	13392054	A	G	PRAMEF17	c.977A>G	p.His326Arg	missense_variant	MODERATE	0.052	0.006524	
chr1	26161902	G	A	FAM120D	c.6110>A	p.Gly2044Asp	missense_variant	MODERATE	0.052	0.007685	
chr1	217669050	G	A	SPATA17	c.258G>A	p.Met86Ile	missense_variant	MODERATE	0.052	0.009829	
chr1	6825088	G	A	CAMTA1	c.116-4G>A	-	splice_region_variant&intron_vari	LOW	0.051	0.007904	
chr1	235253674	C	T	ARID4B	c.2602>A	p.Ser87Asn	missense_variant	MODERATE	0.051	0.008354	
chr1	222724122	T	C	BROX	c.432T>C	-	structural_interaction_variant	HIGH	0.05	0.008404	
chr1	222724134	G	A	BROX	c.444G>A	-	structural_interaction_variant	HIGH	0.05	0.008475	
chr1	55565049	A	G	PPP4R3B	c.1936-8T>C	-	splice_region_variant&intron_vari	LOW	0.136	0.012	
chr1	43320443	T	A	THADA	c.4438+3A>T	-	splice_region_variant&intron_vari	LOW	0.121	0.00728	
chr2	169081682	T	G	DHRS9	c.281T>G	p.Ile94Ser	missense_variant	MODERATE	0.119	0.00445	
chr2	9207148	A	T	ASAP2	c.44A>T	p.His15Leu	missense_variant	MODERATE	0.112	0.006077	
chr2	32503034	A	G	BIRC6	c.9305-8A>G	-	splice_region_variant&intron_vari	LOW	0.089	0.00623	
chr2	172558725	GAAA	G	PDK1	c.216_218delAAA	p.Lys73del	disruptive_inframe_deletion	MODERATE	0.084	0.006229	
chr2	151642800	A	T	NEB	c.8230T>A	p.Leu2744Ile	missense_variant	MODERATE	0.08	0.005664	
chr2	61204387	T	C	USP34	c.9260-7A>G	-	splice_region_variant&intron_vari	LOW	0.079	0.00563	

chr2	31891996	A	G	MEMO1	c.576T>C	.	structural_interaction_variant	HIGH	0.071	0.008267
chr2	147923095	C	T	ACVR2A	c.1200C>T	.	structural_interaction_variant	HIGH	0.067	0.005682
chr2	101286185	G	A	RNF149	c.864-8G>T	.	ce_region_variant&intron_vari	LOW	0.067	0.007448
chr2	61208918	C	T	USP34	c.89000>A	p.Gly2967Glu	missense_variant	MODERATE	0.066	0.011
chr2	148765119	C	G	EPC2	c.1113C>G	p.His371Gln	missense_variant	MODERATE	0.066	0.008975
chr2	71369989	G	A	ZNF638	c.2249G>A	p.Gly750Glu	missense_variant	MODERATE	0.064	0.00957
chr2	151642848	C	T	NEB	c.81820>A	p.Asp2728Asn	missense_variant	MODERATE	0.062	0.006052
chr2	230793269	G	A	CAB39	c.336G>A	.	protein_protein_contact	HIGH	0.06	0.006118
chr2	208304321	G	A	PIKFYVE	c.1468+3G>A	.	ce_region_variant&intron_vari	LOW	0.06	0.005986
chr2	148470467	G	A	MBD5	c.2518+6G>A	.	ce_region_variant&intron_vari	LOW	0.056	0.006187
chr2	148771040	T	A	EPC2	c.1377-4T>A	.	ce_region_variant&intron_vari	LOW	0.056	0.004223
chr2	173191184	T	A	ZAK	c.582+7T>A	.	ce_region_variant&intron_vari	LOW	0.055	0.007433
chr2	148771184	A	C	EPC2	c.1517A>C	p.His506Pro	missense_variant	MODERATE	0.054	0.0047
chr2	144398929	T	C	ZEB2	c.2258A>G	p.Asn753Ser	missense_variant	MODERATE	0.052	0.0051
chr2	148469586	G	A	MBD5	c.1643G>A	p.Ser548Asn	missense_variant	MODERATE	0.052	0.003848
chr2	148469588	G	G	MBD5	c.1645A>G	p.Ser549Gly	missense_variant	MODERATE	0.052	0.003907
chr2	173955539	T	C	SP3	c.973A>G	p.Thr325Ala	missense_variant	MODERATE	0.052	0.004113
chr2	97812676	T	C	TMEM131	c.1691A>G	p.Asn5645Ser	missense_variant	MODERATE	0.05	0.006942
chr3	44305142	G	C	TOPA21	c.3865-5G>C	.	ce_region_variant&intron_vari	LOW	0.222	0.01
chr3	49358049	G	C	GPX1	c.230C>G	p.Pro77Arg	missense_variant	MODERATE	0.176	0.011
chr3	52521501	C	G	STAB1	c.6049C>G	p.His2017Asp	missense_variant	MODERATE	0.132	0.003622
chr3	49862112	A	C	GAMAV	c.160A>T	p.Lys54*	stop_gained	HIGH	0.118	0.004605
chr3	52766200	G	C	NEK4	c.536C>G	p.Ser179*	stop_gained	HIGH	0.111	0.005404
chr3	49929718	CGCGGGGCCCCGGCCCCCT	C	MON1A	c.151_168delAGGGGCCGGGGCCCCGC	p.Arg51_Arg56delconservative_inframe_deletion	MODERATE	0.11	0.002974
chr3	25632693	T	C	TOP2B	c.1113A>G	p.Gln371Gln	/region_variant&synonymous_	LOW	0.108	0.006714
chr3	121115062	A	G	ST8SP1	c.605+1A>G	.	ce_region_variant&intron_vari	LOW	0.108	0.008836
chr3	25632581	T	A	TOP2B	c.1116A>T	p.Val372Val	/region_variant&synonymous_	LOW	0.098	0.006087
chr3	50061990	GA	CT	RBM6	c.2468_2469delGAinsCT	p.Gly823Ala	missense_variant	MODERATE	0.094	0.008801
chr3	45095349	A	G	CCR1	c.1244T>C	p.Ile415Thr	nse_variant&splice_region_va	MODERATE	0.09	0.00769
chr3	105550258	T	G	ALCAM	c.1506T>G	p.Ala502Ala	/region_variant&synonymous_	LOW	0.085	0.007714
chr3	192799555	C	T	MB21D2	c.307G>A	p.Asp103Asn	missense_variant	MODERATE	0.085	0.004176
chr3	196803031	G	C	PAK2	c.303G>C	p.Gln101His	missense_variant	MODERATE	0.079	0.007753
chr3	44287845	G	A	TOPAZ1	c.3681+6G>A	.	ce_region_variant&intron_vari	LOW	0.073	0.009015
chr3	113285498	G	T	BOC	c.3099G>T	p.Gln1031His	missense_variant	MODERATE	0.073	0.00356
chr3	169780692	G	A	MYNN	c.1163A>G	p.Lys388Arg	missense_variant	MODERATE	0.069	0.006185
chr3	45732132	G	A	SACM1L	c.1081G>A	p.Glu361Lys	missense_variant	MODERATE	0.064	0.008257
chr3	171211203	C	A	TNIK	c.219G>T	p.Leu73Phe	missense_variant	MODERATE	0.064	0.005301
chr3	56647008	G	A	FAM208A	c.1729C>T	p.Pro577Ser	missense_variant	MODERATE	0.063	0.00571
chr3	57559879	G	A	PDE12	c.1705G>A	p.Ala569Thr	missense_variant	MODERATE	0.062	0.005324
chr3	138167197	C	G	DBR1	c.598G>C	p.Val200Leu	missense_variant	MODERATE	0.062	0.005632
chr3	129651557	A	G	TMCC1	c.1886T>C	p.Ile629Ala	missense_variant	MODERATE	0.061	0.004682
chr3	155936475	A	G	GMPS	c.1945A>G	p.Ile649Val	missense_variant	MODERATE	0.06	0.004979
chr3	180604976	A	C	TTC14	c.826A>C	p.Asn276His	missense_variant	MODERATE	0.056	0.006829
chr3	155922239	G	A	GMPS	c.1371G>A	.	sequence_feature	MODERATE	0.055	0.009056
chr3	142736493	A	G	TRPC1	c.287A>G	p.Asn96Ser	missense_variant	MODERATE	0.054	0.006279
chr3	57559706	A	G	PDE12	c.1532A>G	p.Asn511Ser	missense_variant	MODERATE	0.05	0.00458
chr4	143550046	AC	GT	SMARCA5	c.3035_3036delACinsGT	p.Asn1012Ser	missense_variant	MODERATE	0.106	0.014
chr4	185310671	A	G	NAA25	c.707G>A	p.Arg236Lys	missense_variant	MODERATE	0.093	0.004605
chr4	139376394	A	G	NAA15	c.1977A>G	.	sequence_feature	MODERATE	0.092	0.009091
chr4	173332198	C	G	HMGB2	c.512G>C	p.Gly171Ala	missense_variant	MODERATE	0.085	0.005051
chr4	15091649	C	T	LRBA	c.826G>A	p.Val276Ile	missense_variant	MODERATE	0.078	0.007758
chr4	138223212	C	T	SLC7A11	c.633G>A	p.Met211Ile	missense_variant	MODERATE	0.066	0.007429
chr4	158719227	CT	TG	PPID	c.285_286delAGinsCA	p.Glu96Lys	missense_variant	MODERATE	0.066	0.008816
chr4	39755683	T	C	UBE2K	c.243T>C	.	structural_interaction_variant	HIGH	0.061	0.005824
chr4	23828602	A	G	PPARGC1A	c.555T>C	p.Thr185Thr	/region_variant&synonymous_	LOW	0.061	0.006586
chr4	81137388	A	C	PRKG2	c.1634+5T>G	.	ce_region_variant&intron_vari	LOW	0.055	0.007663
chr4	112186689	A	T	C4orf32	c.154-4A>T	.	ce_region_variant&intron_vari	LOW	0.055	0.008393
chr4	128867965	G	A	JADE1	c.1613G>A	p.Arg538Lys	missense_variant	MODERATE	0.054	0.008537
chr4	83066508	T	C	COPS4	c.957T>C	.	structural_interaction_variant	HIGH	0.052	0.008696
chr4	83066514	C	T	COPS4	c.963C>T	.	structural_interaction_variant	HIGH	0.051	0.008929
chr4	121852989	A	T	BBS7	c.816T>A	p.Asp272Glu	missense_variant	MODERATE	0.051	0.008016
chr4	113318627	A	G	ANK2	c.2900+7A>G	.	ce_region_variant&intron_vari	LOW	0.05	0.012
chr4	6862394	A	G	KIAA0232	c.2012A>G	p.Asn671Ser	missense_variant	MODERATE	0.05	0.004386
chr5	66024322	A	G	ERBIN	c.689A>G	p.Lys230Arg	missense_variant	MODERATE	0.119	0.008011
chr5	95586732	T	A	ARSK	c.870T>A	p.Leu290Leu	/region_variant&synonymous_	LOW	0.095	0.011
chr5	142005007	G	C	GNPDA1	c.519C>G	.	structural_interaction_variant	HIGH	0.082	0.006245
chr5	73568293	C	T	UTP15	c.1490C>T	p.Pro50Leu	missense_variant	MODERATE	0.082	0.007243
chr5	40843224	C	G	CARD6	c.356C>G	p.Ser119Cys	missense_variant	MODERATE	0.073	0.004506
chr5	103097471	G	A	GIN1	c.851C>T	p.Pro284Leu	missense_variant	MODERATE	0.071	0.005507
chr5	87379796	A	G	RASA1	c.2549A>G	p.Asn850Ser	missense_variant	MODERATE	0.064	0.007973
chr5	65470801	C	T	ADAMTS6	c.439C>A	p.Ala147Thr	missense_variant	MODERATE	0.062	0.00964
chr5	87379783	A	G	RASA1	c.2536A>G	p.Thr846Ala	missense_variant	MODERATE	0.062	0.008076
chr5	115866720	TAAGA	T	AP3S1	c.121_124delAAGA	p.Lys41fs	frameshift_variant	HIGH	0.061	0.009125
chr5	142144564	A	C	NDFIP1	c.563-7A>C	.	ce_region_variant&intron_vari	LOW	0.06	0.009902
chr5	64369773	A	G	RNF180	c.1738A>G	p.Ile580Val	missense_variant	MODERATE	0.057	0.006432
chr5	138559959	C	G	HSPA9	c.1315G>C	.	structural_interaction_variant	HIGH	0.055	0.004483
chr5	177041771	T	C	ZNF346	c.355-7T>C	.	ce_region_variant&intron_vari	LOW	0.055	0.006652
chr5	73554866	C	T	ANKRA2	c.733G>A	p.Asp245Asn	missense_variant	MODERATE	0.052	0.011
chr5	94870496	A	G	MCTP1	c.2242-5T>C	.	ce_region_variant&intron_vari	LOW	0.05	0.00735
chr6	110892996	T	C	AMD1	c.795T>C	.	structural_interaction_variant	HIGH	0.132	0.005573
chr6	110892357	T	C	AMD1	c.529T>C	.	structural_interaction_variant	HIGH	0.107	0.004953
chr6	63646529	C	T	PHF3	c.-23C>T	TR_premature_start_codon_ga	LOW	0.078	0.01
chr6	33295146	CTCTGGGAATAATTATCCTCCTCGGAGAAAA	C	RGL2	c.1160_1189delTTTTCTCCGAGGAGGGATAATTATTCCAGA	.Ile387_Gln396delinframe_deletion	MODERATE	0.076	0.00271
chr6	106308471	A	G	ATG5	c.129T>C	.	structural_interaction_variant	HIGH	0.075	0.009537
chr6	106308474	T	G	ATG5	c.126A>C	.	structural_interaction_variant	HIGH	0.075	0.009693
chr6	111411493	T	C	REV3L	c.391A>G	p.Thr131Ala	missense_variant	MODERATE	0.071	0.01
chr6	104729773	G	A	HACE1	c.2628-9C>T	.	sequence_feature	LOW	0.063	0.011
chr6	1611129	C	G	FOXC1	c.684C>G	.	sequence_feature	MODERATE	0.061	0.01
chr6	110892930	C	T	AMD1	c.729C>T	.	structural_interaction_variant	HIGH	0.059	0.005675
chr6	110746177	C	A	CDK19	c.153G>T	p.Leu51Phe	missense_variant	MODERATE	0.058	0.009105
chr6	88614403	G	A	RNGTT	c.1507-8C>T	.	ce_region_variant&intron_vari	LOW	0.056	0.006629
chr6	1212811	C	A	HIVEP1	c.6128C>A	p.Ala2043Asp	missense_variant	MODERATE	0.056	0.005724
chr6	149572531	A	C	GINM1	c.205A>C	p.Ser69Arg	missense_variant	MODERATE	0.053	0.00637
chr6	158503746	G	T	TULP4	c.4083G>T	p.Glu1361Asp	missense_variant	MODERATE	0.053	0.003897
chr6	151373628	T	C	ZBTB2	c.10G>A	p.Ala4Thr	missense_variant	MODERATE	0.051	0.005458
chr6	90544548	A	G	MAP3K7	c.1291+4T>C	.	ce_region_variant&intron_vari	LOW	0.05	0.007577
chr6	143471065	G	A	PEX3	c.436G>A	p.Ala146Thr	missense_variant	MODERATE	0.05	0.008041
chr7	152235812	C	A	KMT2C	c.2769+5G>T	.	ce_region_variant&intron_vari	LOW	0.345	0.06
chr7	67067307	G	C	TYW1	c.1178G>C	p.Gly393Ala	missense_variant	MODERATE	0.147	0.011
chr7	101196334	CCTTAAGT	C	MOGAT3	c.717_723delACTTAAG	p.Lys241fs	frameshift_variant	HIGH	0.091	0.003866
chr7	127374171	T	C	ZNF800	c.1165A>G	p.Thr389Ala	missense_variant	MODERATE	0.09	0.005158
chr7	129858945	T	C	UBE2H	c.206-4A>G	.	ce_region_variant&intron_vari	LOW	0.075	0.009167
chr7	82916426	C	T	PCLO	c.11560G>A	p.Glu3854Lys	missense_variant	MODERATE	0.075	0.003298
chr7	131470861	G	A	MKLN1	c.1948G>A	p.Val650Met	missense_variant	MODERATE	0.074	0.008403
chr7	127374105	CAACTTT	C	ZNF800	c.1225_1230delAAAGTT	.Lys409_Val410deconservative_inframe_deletion	MODERATE	0.071	0.004659
chr7	39999499	T	G	CDK13	c.2181T>G	p.Thr727Thr	/region_variant&synonymous_	LOW	0.069	0.005746
chr7	93438129	G	GA	CALCR	c.966-4dupT	.	ce_region_variant&intron_vari	LOW	0.067	0.004416
chr7	87196714	C	A	TMEM243	c.279G>T	p.Lys93Asn	missense_variant	MODERATE	0.059	0.005607
chr7	116906278	A	G	CAPZA2	c.442A>G	p.Ile148Val	missense_variant	MODERATE	0.058	0.006993
chr7	77571194	G	T	PTPN12	c.208+8G>T	.	ce_region_variant&intron_vari	LOW	0.057	0.009133
chr7	87059434	G	A	KIAA1324L	c.80C>T	p.Pro27Leu	missense_variant	MODERATE	0.055	0.01
chr7	138581750	T	C	TRIM24	c.2772T>C	.	structural_interaction_variant	HIGH	0.054	0.006114
chr7	87059443	C	G	KIAA1324L	c.71G>C	p.Gly24Ala	missense_variant	MODERATE	0.054	0.011
chr7	39999356	G	A	CDK13	c.2043-5G>A	.	ce_region_variant&intron_vari	LOW	0.051	0.005303
chr7	108573307	G	A	DNAJB9	c.626G>A	p.Arg209Gln	missense_variant	MODERATE	0.051	0.005098
chr7	87059440	C	A	KIAA1324L	c.74G>T	p.Arg25Leu	missense_variant	MODERATE	0.05	0.01
chr8	144116225	C	T	WDR97	c.4801C>T	p.Arg1601Trp	missense_variant	MODERATE	0.117	0.005362
chr8	132175490	T	C	KCNQ3	c.896A>G	p.Glu299Gly	missense_variant	MODERATE	0.099	0.004489
chr8	80519225	G	A	ZBTB10	c.2313G>A	p.Val771Val	/region_variant&synonymous_	LOW	0.068	0.006107
chr8	52683668	G	C	RB1CC1	c.250C>G	p.Pro84Ala	missense_variant	MODERATE	0.059	0.00584
chr8	100705604	G	C	PABPC1	c.1672C>G	.	structural_interaction_variant	HIGH	0.055	0.005885
chr8	23246720	G	C	CHMP7	c.25G>C	p.Glu9Gln	missense_variant	MODERATE	0.055	0.004868
chr8	69588074	T	C	SULF1	c.567C>T	p.Asp189Asp	/region_variant&synonymous_	LOW	0.05	0.006977
chr8	17195530	T	A	ZDHHC2	c.279T>A	p.Asp93Glu	missense_variant	MODERATE	0.05	0.006797
chr9	68387464	G	A	PGM5	c.573G>A	p.Val191Val	/region_variant&synonymous_	LOW	0.165	0.018
chr9	131197740	G	C	NUP214	c.4246G>C	p.Val1416Leu	missense_variant	MODERATE	0.093	0.002545
chr9	74896482	T	C	CNNM1	c.989A>G	p.Lys330Arg	missense_variant	MODERATE	0.092	0.006718
chr9	26920219	C	T	PLAA	c.1197+8G>A	.	ce_region_variant&intron_vari	LOW	0.071	0.008787
chr9	122919811	T	C	ZBTB26	c.124A>G	p.Ile42Val	missense_variant	MODERATE	0.057	0.0057
chr9	136846956	G	A	C9orf172	c.2542G>A	p.Ala848Thr	missense_variant	MODERATE	0.055	0.007791
chr9	2181622	A	C	SMARCA2	c.4305A>C	p.Glu1435Asp	missense_variant	MODERATE	0.053	0.008425
chr9	19316523	G	A	DENND4C	c.1588+6G>A	.	ce_region_variant&intron_vari	LOW	0.05	0.006259
chr10	50811049	T	C	A1CF	c.1499A>G	p.Asn500Ser	missense_variant	MODERATE	0.119	0.006197
chr10	110781133	G	T	RBM20	c.524G>T	p.Ser175Ile	missense_variant	MODERATE	0.095	0.003035
chr10	73786034	T	G	ZSWIM8	c.156T>G	p.Asn52Lys	missense_variant	MODERATE	0.093	0.005919
chr10	15782148	A	C	FAM188A	c.1188+7T>G	.	ce_region_variant&intron_vari	LOW	0.089	0.007289
chr10	21617147	T	G	MLLT10	c.639T>G	p.Asp213Glu	missense_variant	MODERATE	0.087	0.01
chr10	84212262	T	A	CDHR1	c.1637T>A	p.Phe546Tyr	missense_variant	MODERATE	0.079	0.004142
chr10	133379402	G	A	PADI4	c.176G>A	p.Cys59Tyr	missense_variant	MODERATE	0.074	0.008944
chr10	91499113	A	G	HECTD2	c.1925A>G	p.Tyr642Cys	missense_variant	MODERATE	0.07	0.005587
chr10	51804673	T	C	PRKG1	c.681T>C	.	structural_interaction_variant	HIGH	0.068	0.007061
chr10	26748699	T	G	AB11	c.1398A>C	.	sequence_feature	MODERATE	0.065	0.005495
chr10	73474916	T	T	PPP3CB	c.523+3G>A	.	ce_region_variant&intron_vari	LOW	0.062	0.009181
chr10	51804598	A	G	PRKG1	c.606A>G	.	structural_interaction_variant	HIGH	0.061	0.006962
chr10	94497115	AT	GC	TBC1D12	c.1355_1356delATinsGC	p.Asn452Ser	missense_variant	MODERATE	0.061	0.009056
chr10	103990794	T	C	SLK	c.270T>C	.	structural_interaction_variant	HIGH	0.059	0.007176
chr10	94293501	A	G	PLCE1	c.5036-7G>A	.	ce_region_variant&intron_vari	LOW	0.058	0.008884
chr10	102919132	T	G	CNNM2	c.653T>G	p.Ser218Ala	missense_variant	MODERATE	0.058	0.003623
chr10	48401780	A	G	MAPK8	c.120A>G	p.Val40Val	/region_variant&synonymous_	LOW	0.054	0.008433
chr10	51804613	T	C	PRKG1	c.621T>C	.	structural_interaction_variant	HIGH	0.053	0.006355
chr10	117341046	T	A	PDZD8	c.929A>T	p.His310Leu	missense_variant	MODERATE	0.053	0.005435
chr10	43387680	T	A	MINPP1	c.205A>T	p.Met69Leu	missense_variant	MODERATE	0.051	0.003672
chr11	83163675	C	T	PCF11	c.319-4C>T	.	ce_region_variant&intron_vari	LOW	0.138	0.01
chr11	59615498	CCCG	C	OSBP	c.164_166delCGG	p.Ala55del	disruptive_inframe_deletion	MODERATE	0.124	0.023
chr11	76454745	A	T	EMSY	c.246-4A>T	.	ce_region_variant&intron_vari	LOW	0.116	0.009622
chr11	83161456	C	T	PCF11	c.318+4C>T	.	ce_region_variant&intron_vari	LOW	0.114	0.009546
chr11	35685250	T	TAG	TRIM44	c.670-9_670-8insAG	.	ce_region_variant&intron_vari	LOW	0.102	0.005638
chr11	112087851	C	A	SDHD	c.53-6C>A	.	ce_region_variant&intron_vari	LOW	0.101	0.006174
chr11	128462375	C	T	ETS1	c.1444G>A	p.Asp482Asn	missense_variant	MODERATE	0.1	0.005513
chr11	65113555	C	G	TM7SF2	c.564C>G	p.Phe188Leu	missense_variant	MODERATE	0.098	0.005322
chr11	119580055	G	C	ARHGAP20	c.2891C>G	p.Ser964Cys	missense_variant	MODERATE	0.095	0.004147
chr11	103083256	A	G	DCUN1D5	c.249T>C	p.Asn83Asn	/region_variant&synonymous_	LOW	0.078	0.008745
chr11	76523148	T	C	EMSY	c.1730-7T>C	.	ce_region_variant&intron_vari	LOW	0.067	0.006531
chr11	64751346	G	C	PYGM	c.1948C>G	p.Arg650Gly	missense_variant	MODERATE	0.061	0.004417
chr11	118759988	C	T	DDX6	c.798G>A	.	structural_interaction_variant	HIGH	0.057	0.006732
chr11	6956530	G	A	ZNF215	c.1553G>A	p.Ter518Ter	stop_retained_variant	LOW	0.054	0.008146
chr11	124611719	G	A	PANX3	c.163G>A	p.Ala55Thr	missense_variant	MODERATE	0.051	0.013
chr11	32955419	A	G	QSER1	c.4230+7A>G	.	ce_region_variant&intron_vari	LOW	0.05	0.01
chr12	6537688	T	C	GAPDH	c.630T>C	.	sequence_feature	MODERATE	0.243	0.003984
chr12	116006416	A	G	MED13L	c.2239-5T>C	.	ce_region_variant&intron_vari	LOW	0.106	0.006661
chr12	31103996	T	C	DUSP16	c.2876T>C	p.Val959Ala	missense_variant	MODERATE	0.102	0.004857
chr12	65328601	T	C	MSRB3	c.282T>C	p.Phe94Phe	/region_variant&synonymous_	LOW	0.092	0.008159
chr12	55365235	T	A	OR6C75	c.125T>A	p.Ile42Asn	missense_variant	MODERATE	0.088	0.004044
chr12	110702001	G	C	PPP1CC	c.947C>G	p.Ala316Gly	missense_variant	MODERATE	0.081	0.006442
chr12	96280884	A	G	CDK17	c.1458T>C	p.Ser486Ser	/region_variant&synonymous_	LOW	0.08	0.009148
chr12	105126318	A	G	KIAA1033	c.994A>G	p.Ile332Val	missense_variant	MODERATE	0.074	0.009346
chr12	76815196	A	T	ZNF217	c.594A>T	.	structural_interaction_variant	HIGH	0.071	0.008369
chr12	56751154	A	G	PRIM1	c.145T>C	.	structural_interaction_variant	HIGH	0.065	0.008582
chr12	25104003	C	T	LRMP	c.997-6C>T	.	ce_region_variant&intron_vari	LOW	0.065	0.008855
chr12	110722648	G	T	PPP1CC	c.571C>A	.	structural_interaction_variant	HIGH	0.064	0.004765
chr12	121330642	A	C	ANAPC5	c.1063T>G	p.Ser355Ala	missense_variant	MODERATE	0.06	0.004436
chr12	121330639	C	G	ANAPC5	c.1066G>C	p.Asp356His	missense_variant	MODERATE	0.058	0.004444
chr12	39367974	C	T	KIF21A	c.5096G>A	p.Ser1706Asn	missense_variant	MODERATE	0.057	0.006229
chr12	93411052	C	T	UBE2N	c.277+1G>A	.	ice_donor_variant&intron_vari	HIGH	0.055	0.003697
chr12	70329415	T	C	CNOT2	c.239-8T>C	.	ce_region_variant&intron_vari	LOW	0.054	0.006811
chr12	16032662	A	G	DERA	c.750+8A>G	.	ce_region_variant&intron_vari	LOW	0.053	0.007874
chr12	122483482	A	T	ZCHC8	c.583T>A	p.Ser195Thr	missense_variant	MODERATE	0.053	0.006696
chr12	69694447	A	G	BEST3	c.170T>C	p.Val57Ala	missense_variant	MODERATE	0.051	0.007901
chr12	95485958	C	T	METAP2	c.405G>T	.	structural_interaction_variant	HIGH	0.05	0.005975
chr13	24447125	T	C	PARP4	c.3176A>G	p.Gln1059Arg	missense_variant	MODERATE	0.292	0.06
chr13	19426473	AT	GA	TPTE2	c.1346_1347delATinsTC	p.Tyr449Phe	missense_variant	MODERATE	0.097	0.007149

chr13	51383745	A	G	INTS6	c.895-4T>C	.	ice_region_variant&intron_vari	LOW	0.083	0.008394
chr13	97391340	G	A	MBNL2	c.1013G>A	p.Ser338Asn	missense_variant	MODERATE	0.083	0.007121
chr13	19426481	T	C	TPTE2	c.1339A>G	p.Asn447Asp	missense_variant	MODERATE	0.067	0.007699
chr13	24478255	G	T	PARP4	c.1470C>A	p.His490Gln	missense_variant	MODERATE	0.063	0.015
chr13	20083777	G	A	ZMYM2	c.3941+1G>A	.	ice_donor_variant&intron_vari	HIGH	0.053	0.00738
chr13	45401078	C	T	SLC25A30	c.614+5G>A	.	ice_region_variant&intron_vari	LOW	0.053	0.008304
chr14	57219306	AGATAATTTG	A	EXOC5	c.1526+7_1526+15delCAAATTATC	.	ice_region_variant&intron_vari	LOW	0.11	0.009868
chr14	44903253	A	G	C14orf28	c.571A>G	p.Asn191Asp	missense_variant	MODERATE	0.069	0.006063
chr14	60008123	G	A	LRRC9	n.3299G>A	.	n_coding_transcript_exon_varia	MODIFIER	0.067	0.007634
chr14	95130161	T	G	DICER1	c.4704A>C	p.Asn1577Thr	missense_variant	MODERATE	0.062	0.006995
chr14	63376112	A	G	PPP2R5E	c.1305-4T>C	.	ice_region_variant&intron_vari	LOW	0.061	0.011
chr14	31157202	A	G	HECTD1	c.1724T>C	p.Ile575Thr	missense_variant	MODERATE	0.06	0.007121
chr14	99501375	G	C	CCNK	c.537A>G	.	protein_protein_contact	HIGH	0.058	0.006555
chr14	49893904	T	C	ARF6	c.168T>C	.	structural_interaction_variant	HIGH	0.057	0.004373
chr14	53051901	T	A	DDHD1	c.2464A>T	p.Asn822Tyr	missense_variant	MODERATE	0.057	0.007991
chr14	96534485	A	G	PAPOLA	c.837-6A>G	.	ice_region_variant&intron_vari	LOW	0.056	0.005584
chr14	56585035	A	G	TMEM260	c.192+3A>G	.	ice_region_variant&intron_vari	LOW	0.052	0.007457
chr14	35109900	G	A	PPP2R3C	c.323C>T	p.Thr108Ile	missense_variant	MODERATE	0.052	0.007813
chr14	52768912	T	G	STYX	c.577T>G	p.Ser193Ala	missense_variant	MODERATE	0.052	0.008664
chr14	55169562	A	G	DLGAP5	c.1388-3C>T	.	ice_region_variant&intron_vari	LOW	0.051	0.011
chr14	32093928	C	T	ARHGAP5	c.3259C>T	p.Pro1087Ser	missense_variant	MODERATE	0.051	0.003701
chr15	60511232	C	T	RORA	c.913G>A	p.Gly305Lys	missense_variant	MODERATE	0.174	0.005895
chr15	41195862	A	G	EXD1	c.640-7T>C	.	ice_region_variant&intron_vari	LOW	0.168	0.007759
chr15	60511322	C	T	RORA	c.823G>A	p.Glu275Lys	missense_variant	MODERATE	0.141	0.004306
chr15	60511403	C	G	RORA	c.742G>C	p.Asp248His	missense_variant	MODERATE	0.129	0.00372
chr15	36697395	G	C	C15orf41	c.544+5G>C	.	ice_region_variant&intron_vari	LOW	0.112	0.005711
chr15	68153591	A	C	PIAS1	c.836A>C	p.Asn279Thr	nse_variant&splice_region_va	MODERATE	0.105	0.009049
chr15	71991235	T	A	MYO9A	c.1590A>T	p.Thr530Thr	_region_variant&synonymous_	LOW	0.102	0.01
chr15	71914467	T	A	MYO9A	c.2588A>G	p.Lys863Arg	missense_variant	MODERATE	0.099	0.006437
chr15	31487555	G	C	OTUD7A	c.1162C>G	p.Leu388Val	missense_variant	MODERATE	0.09	0.003701
chr15	60511463	C	tTTTTACAA	RORA	TACTACTAATATTACTGTTGCAAAGCAGCTGTTGTAAAATAATAGACTTCTCCCTACAA	p.Glu228fs	frameshift_variant	HIGH	0.076	0.003842
chr15	52650019	T	C	MAP6	c.582T>C	.	sequence_feature	MODERATE	0.071	0.00885
chr15	41669348	G	A	MGA	c.4546G>A	p.Val1521Ile	missense_variant	MODERATE	0.069	0.003689
chr15	58627863	G	A	ADAM10	c.1197C>T	.	sequence_feature	MODERATE	0.061	0.008475
chr15	89211868	G	C	RLBP1	c.559C>G	p.Leu187Val	missense_variant	MODERATE	0.054	0.005403
chr15	52046619	T	C	MAPK6	c.159T>C	.	structural_interaction_variant	HIGH	0.052	0.005484
chr15	45270199	G	A	SLC28A2	c.1571G>A	p.Arg524Lys	missense_variant	MODERATE	0.05	0.005626
chr15	75873477	G	A	UBE2Q2	c.497G>A	p.Ser166Asn	missense_variant	MODERATE	0.05	0.007353
chr16	88435170	T	C	ZNF469	c.7616C>T	p.Ser2539Phe	missense_variant	MODERATE	0.11	0.002829
chr16	9764636	G	A	GRIN2A	c.2908C>T	p.Arg970Trp	missense_variant	MODERATE	0.098	0.003444
chr16	50792671	T	C	CYLD	c.2316T>C	.	structural_interaction_variant	HIGH	0.085	0.00773
chr16	58549737	C	T	CNOT1	c.3504G>A	.	structural_interaction_variant	HIGH	0.078	0.005995
chr16	53692367	G	A	RPGRIP1L	c.231-3C>T	.	ice_region_variant&intron_vari	LOW	0.064	0.00704
chr16	4885285	C	T	PPL	c.3370G>A	p.Ala1124Thr	missense_variant	MODERATE	0.062	0.002924
chr16	5090129	C	T	EEF2KMT	c.697G>A	p.Val233Ile	missense_variant	MODERATE	0.06	0.007596
chr16	5090135	C	T	EEF2KMT	c.691G>A	p.Ala231Thr	missense_variant	MODERATE	0.058	0.007222
chr16	75577330	A	G	GABARAPL2	c.315A>G	.	structural_interaction_variant	HIGH	0.055	0.006419
chr16	57528882	T	C	CCDC102A	c.1960>A	p.Asp656Asn	missense_variant	MODERATE	0.055	0.015
chr17	47157001	A	T	CDC27	c.754T>A	p.Ser252Thr	missense_variant	MODERATE	0.154	0.017
chr17	16426710	TCCCCACCCCAGCACCGA	T	TRPV2	c.1096-10_1102delCCCACCCCAGCACCGAC	p.His366fs	_acceptor_variant&splice_regi	HIGH	0.096	0.003988
chr17	67160254	A	G	HELZ	c.2177+7T>C	.	ice_region_variant&intron_vari	LOW	0.076	0.006997
chr17	62035499	T	C	MED13	c.580A>G	p.Ile194Val	missense_variant	MODERATE	0.072	0.00663
chr17	62010613	C	T	MED13	c.1904G>A	p.Ser635Asn	missense_variant	MODERATE	0.058	0.005103
chr17	39285473	T	C	FBXL20	c.494+5A>G	.	ice_region_variant&intron_vari	LOW	0.055	0.01
chr17	29287384	C	T	NUP192	c.6100>A	p.Glu2004Ser	missense_variant	MODERATE	0.055	0.004965
chr17	31252981	A	G	NF1	c.4154A>G	p.Lys1385Arg	missense_variant	MODERATE	0.053	0.006519
chr17	62035613	A	T	MED13	c.471-5T>A	.	ice_region_variant&intron_vari	LOW	0.051	0.008056
chr17	18865846	A	G	PRPSAP2	c.13A>G	p.Thr5Ala	missense_variant	MODERATE	0.05	0.009009
chr17	64500024	G	C	DDX5	c.1744C>G	p.Pro582Ala	missense_variant	MODERATE	0.05	0.003524
chr18	62715985	C	T	PHLPP1	c.3020C>T	p.Pro1010Leu	missense_variant	MODERATE	0.087	0.02
chr18	79113289	A	G	ATP9B	c.493A>G	p.Ile165Val	missense_variant	MODERATE	0.083	0.007224
chr18	79113291	A	G	ATP9B	c.495A>G	p.Ile165Met	missense_variant	MODERATE	0.083	0.007203
chr18	13069859	AAT	A	CEP192	c.5174+7_5174+8delTA	.	ice_region_variant&intron_vari	LOW	0.078	0.007235
chr18	21768644	A	G	MIB1	c.4236>A	.	structural_interaction_variant	HIGH	0.053	0.015
chr19	8261925	C	T	CERS4	c.1006-5C>T	.	ice_region_variant&intron_vari	LOW	0.125	0.003347
chr19	48485764	TTCGGGGAATCAATTC	T	LMTK3	c.4464_*8delGAATTGATTCCCCGA	l488_Ter1490delilost&conservative_inframe_del	HIGH	0.088	0.004025
chr19	41756834	C	T	CEACAM6	c.29C>T	p.Thr10Ile	missense_variant	MODERATE	0.08	0.006961
chr19	18211183	C	T	PDE4C	c.1885G>A	p.Asp629Asn	missense_variant	MODERATE	0.076	0.004699
chr19	3982273	T	C	EEF2	c.764A>G	p.Asp255Gly	missense_variant	MODERATE	0.06	0.005588
chr19	54729499	T	A	KIR3DL3	c.662A>T	p.Tyr221Phe	missense_variant	MODERATE	0.055	0.005215
chr20	64049372	CGGGGCGCGGCGGGCGCGGCG	C	SOX18	c.126_144delCGCCGCGCCCCGCCGCGCCC	p.Ala43fs	frameshift_variant	HIGH	0.736	0.072
chr20	2752399	C	T	EBF4	c.1382C>T	p.Ala461Val	missense_variant	MODERATE	0.086	0.018
chr20	21389266	T	C	XRN2	c.3022-7T>C	.	ice_region_variant&intron_vari	LOW	0.063	0.01
chr20	21389328	A	G	XRN2	c.3077A>G	p.Asn1026Ser	missense_variant	MODERATE	0.054	0.00921
chr21	31266230	C	T	TIAM1	c.743G>A	p.Gly248Glu	missense_variant	MODERATE	0.143	0.003377
chr21	39270041	T	C	BRWD1	c.1396-8A>G	.	ice_region_variant&intron_vari	LOW	0.068	0.008101
chr21	44697431	C	G	KRTAP10-12	c.230C>G	p.Thr77Ser	missense_variant	MODERATE	0.062	0.001705
chr21	30592561	A	C	KRTAP6-3	c.116A>C	p.Tyr39Ser	missense_variant	MODERATE	0.058	0.002702
chr21	43800570	C	A	RRP1	c.945C>A	p.Ser315Arg	missense_variant	MODERATE	0.058	0.004286
chr22	31604922	C	A	SF1	c.2031C>A	p.Ser677Arg	missense_variant	MODERATE	0.114	0.005893
chr22	23894929	G	A	MIF	c.266G>A	p.Arg89His	missense_variant	MODERATE	0.099	0.002882
chr22	28719434	G	T	CHEK2	c.773C>A	p.Ala258Glu	missense_variant	MODERATE	0.077	0.01
chr22	31602237	T	G	SF1	c.1570T>G	p.Ser524Ala	missense_variant	MODERATE	0.065	0.004035
chr22	31602259	T	C	SF1	c.1592T>C	p.Phe531Ser	missense_variant	MODERATE	0.056	0.003946
chr22	23894837	G	C	MIF	c.174G>C	.	structural_interaction_variant	HIGH	0.055	0.002711
chrX	13038440	A	G	GPR119	c.80-T	p.Ser3Leu	missense_variant	MODERATE	0.182	0.004698
chrX	24810734	T	C	POLA1	c.3006T>C	.	structural_interaction_variant	HIGH	0.124	0.007639
chrX	150598588	A	C	MTM1	c.137-4A>C	.	ice_region_variant&intron_vari	LOW	0.111	0.007924
chrX	150598593	C	A	MTM1	c.138C>A	p.Asp46Glu	nse_variant&splice_region_va	MODERATE	0.101	0.007665
chrX	23379756	A	T	PTCHD1	c.517A>T	p.Ile173Phe	missense_variant	MODERATE	0.084	0.002989
chrX	20016125	T	C	MAP7D2	c.1613A>G	p.Glu538Gly	missense_variant	MODERATE	0.079	0.004762
chrX	35971936	C	T	CFAP47	c.2225C>T	p.Thr742Ile	missense_variant	MODERATE	0.077	0.005551
chrX	124051374	A	G	STAG2	c.1176A>G	.	structural_interaction_variant	HIGH	0.075	0.006672
chrX	109375948	G	A	GUCY2F	c.3278C>T	p.Ala1093Val	missense_variant	MODERATE	0.068	0.004472
chrX	30843027	C	G	TAB3	c.1827G>C	p.Met609Ile	missense_variant	MODERATE	0.065	0.006082
chrX	85957971	G	A	CHM	c.824C>T	p.Pro275Leu	missense_variant	MODERATE	0.061	0.008721
chrX	118443688	G	A	WDR44	c.2512+1G>A	.	ice_donor_variant&intron_vari	HIGH	0.058	0.006318
chrX	30843011	T	G	TAB3	c.1843A>C	p.Asn615His	missense_variant	MODERATE	0.058	0.005819
chrX	135556283	C	T	INTS6L	c.1175T>C	p.Val392Ala	missense_variant	MODERATE	0.058	0.007537
chrX	124063877	G	A	STAG2	c.1851G>A	.	structural_interaction_variant	HIGH	0.053	0.00446
chrX	13040876	G	A	FAM9C	c.215-4C>T	.	ice_region_variant&intron_vari	LOW	0.052	0.009622
chrX	101625180	C	T	ARMCX3	c.201C>T	.	sequence_feature	MODERATE	0.052	0.002365
chrX	120428545	A	G	LAMP2	c.1175T>C	p.Val392Ala	missense_variant	MODERATE	0.051	0.004066
chr1	87092559	A	T	HS2ST1	c.478A>T	p.Ile160Phe	missense_variant	MODERATE	0.5	0.018
chr1	999740	C	G	HES4	c.234G>C	p.Glu78Asp	missense_variant	MODERATE	0.284	0.003433
chr1	43443781	G	C	SZT2	c.8639C>G	p.Pro2880Arg	missense_variant	MODERATE	0.268	0.00513
chr1	54716626	GT	CA	TTC4	c.138_139delGTinsCA	p.MetSer46IleThr	missense_variant	MODERATE	0.213	0.005773
chr1	63323437	G	T	FOXD3	c.379G>T	p.Ala127Ser	missense_variant	MODERATE	0.198	0.004606
chr1	56886102	G	C	CBA	c.1031C>G	p.Ser344Cys	missense_variant	MODERATE	0.184	0.004389
chr1	37554042	G	C	SNIP1	c.188C>G	p.Ser63Trp	missense_variant	MODERATE	0.172	0.003767
chr1	171542211	C	G	PRRC2C	c.4739C>G	p.Ser1580*	stop_gained	HIGH	0.151	0.008408
chr1	107324529	T	C	NTN G1	c.496C>T	p.Ser166Phe	missense_variant	MODERATE	0.144	0.003398
chr1	32668375	A	T	RBBP4	c.461A>T	.	structural_interaction_variant	HIGH	0.142	0.006853
chr1	66361682	G	C	PDE4B	c.909G>C	p.Gln303His	missense_variant	MODERATE	0.141	0.007173
chr1	196746000	G	A	CFH	c.3493+1G>A	.	ice_donor_variant&intron_vari	HIGH	0.134	0.005319
chr1	160553417	A	G	CD84	c.721T>C	p.Ser241Pro	missense_variant	MODERATE	0.132	0.003918
chr1	158652616	G	A	SPTA1	c.3226G>T	p.Arg1076Cys	missense_variant	MODERATE	0.131	0.005589
chr1	154104117	G	T	NUP210L	c.1714C>A	p.His572Asn	missense_variant	MODERATE	0.125	0.006481
chr1	203307216	C	T	BTG2	c.255C>T	.	structural_interaction_variant	HIGH	0.122	0.003128
chr1	154104168	G	C	NUP210L	c.1663C>G	p.His555Asp	missense_variant	MODERATE	0.12	0.007611
chr1	197328693	T	A	CR81	c.342T>A	p.Cys114*	stop_gained	HIGH	0.119	0.003029
chr1	153261308	G	C	LOR	c.359G>C	p.Gly120Ala	missense_variant	MODERATE	0.106	0.004299
chr1	200606771	C	A	KIF14	c.1582G>T	p.Gly528*	stop_gained	HIGH	0.104	0.005575
chr1	173800511	ACACAGAATCTG	A	CENPL	c.1102-3_1109delCAGATTCTGTG	p.Ile368fs	_acceptor_variant&splice_regi	HIGH	0.084	0.008771
chr2	108846832	C	G	CDC138	c.1418C>G	p.Ser473Cys	missense_variant	MODERATE	0.232	0.008016
chr2	73449438	G	C	ALMS1	c.2911G>C	p.Asp971His	missense_variant	MODERATE	0.192	0.00313
chr2	74101563	T	A	TET3	c.4775T>A	p.Leu1592Gln	missense_variant	MODERATE	0.191	0.003119
chr2	209873801	A	G	UNC80	c.3677>A	p.Ala1226Asp	missense_variant	MODERATE	0.163	0.006133
chr2	61348007	T	G	USP34	c.2148A>C	p.Gln716His	missense_variant	MODERATE	0.162	0.004426
chr2	29227676	A	T	ALK	c.2816-4T>A	.	ice_region_variant&intron_vari	LOW	0.161	0.00284
chr2	61347999	TGAGAGC	T	USP34	c.2150_2156delGAGTCTC	717_Gln719delinl	disruptive_inframe_deletion	MODERATE	0.159	0.004233
chr2	27234598	C	A	CAD	c.3699C>A	p.Asp1233Glu	missense_variant	MODERATE	0.135	0.005313
chr2	174141968	C	T	OLA1	c.406G>A	p.Glu136Lys	missense_variant	MODERATE	0.12	0.007729
chr3	171843390	C	C	TMEM212	c.7G>C	p.Gly3Arg	missense_variant	MODERATE	0.337	0.006955
chr3	42223630	AGCTTCCCACCATGGTGGGATCTAGCAT	A	TRAK1	c.2758_2785delTTCCCCACCATGGTGGGATCTAGCATGC	p.Phe920fs	frameshift_variant	HIGH	0.279	0.003318
chr3	35721763	G	A	ARPP21	c.1052G>A	p.Gly351Glu	missense_variant	MODERATE	0.273	0.003646
chr3	27496535	C	T	SLC4A7	c.44G>A	p.Gly14Asp	missense_variant	MODERATE	0.224	0.006806
chr3	31990959	G	C	ZNF860	c.1880G>C	p.Arg627Pro	missense_variant	MODERATE	0.197	0.004839
chr3	19919967	G	C	EFHB	c.862C>G	p.Pro288Ala	missense_variant	MODERATE	0.183	0.008449
chr3	17406537	G	C	TBC1D5	c.168-11C>G	.	sequence_feature	LOW	0.168	0.004719
chr3	138946478	T	A	FON2	c.245A>T	p.Gln82Leu	missense_variant	MODERATE	0.152	0.003078
chr3	108633004	A	G	D2IP3	c.748A>G	p.Thr250Ala	missense_variant	MODERATE	0.144	0.014
chr3	157159786	A	G	CCNL1	c.303+6T>C	.	ice_region_variant&intron_vari	LOW	0.127	0.004918
chr3	157159783	AG	C	CCNL1	c.303+8delpC	.	ice_region_variant&intron_vari	LOW	0.124	0.004999
chr4	17709590	G	T	FAM184B	c.196C>A	p.Leu66Met	missense_variant	MODERATE	0.308	0.003524
chr4	48527587	C	A	FRYL	c.7207G>T	p.Glu2403*	stop_gained	HIGH	0.161	0.007412
chr5	40936478	G	C7		c.421G>T	p.Gly141*	stop_gained	HIGH	0.221	0.006084
chr5	177294806	G	A	NSD1	c.7438G>A	p.Asp2480Asn	missense_variant	MODERATE	0.206	0.002606
chr5	149847557	G	A	PPARGC1B	c.3071G>A	p.Ter1024Ter	stop_retained_variant	LOW	0.182	0.004954
chr5	102270761	T	G	SLCO4C1	c.665C>A	p.Thr222Asn	missense_variant	MODERATE	0.181	0.004516
chr5	141350808	C	A	PCDHGB1	c.548C>A	p.Pro183His	missense_variant	MODERATE	0.162	0.003155
chr5	119116251	G	A	DMXL1	c.6586>A	p.Glu2201Lys	missense_variant	MODERATE	0.114	0.009533
chr5	14479268	G	T	TRIO	c.6181G>C	p.Arg2054Thr	missense_variant	MODERATE	0.082	0.01
chr6	152151654	G	A	SYNE1	c.24349C>T	p.Arg8117Trp	missense_variant	MODERATE	0.21	0.005954
chr6	46653189	C	T	SLC25A27	c.-4C>T	.	ITR_premature_start_codon_ga	LOW	0.208	0.003959
chr6	43206230	G	C	CUL9	c.5017G>C	p.Glu1673Gln	missense_variant	MODERATE	0.201	0.004932
chr6	152365545	C	T	SYNE1	c.9577G>A	p.Glu3193Lys	missense_variant	MODERATE	0.192	0.003833
chr6	29086546	GC	G	OR2B3	c.702delG	p.Gln235fs	frameshift_variant	HIGH	0.184	0.002816
chr6	26216608	C	A	HIST1H2BG	c.36G>T	p.Lys12Asn	missense_variant	MODERATE	0.183	0.004064
chr6	31632184	A	G	PRRC2A	c.3511G>A	p.Glu1171Ser	missense_variant	MODERATE	0.181	0.00223
chr6	31154584	G	A	CCHCR1	c.713C>T	p.Ala238Val	missense_variant	MODERATE	0.171	0.002282
chr6	117319951	T	G	ROS1	c.5857A>C	p.Ser1953Arg	missense_variant	MODERATE	0.165	0.003202
chr6	136233404	G	T	MTFR2	c.965C>A	p.Ala322Glu	missense_variant	MODERATE	0.143	0.008299
chr6	107921915	GAAAAAC	G	SEC63	c.340-12_340-7delGTTTTT	.	ice_region_variant&intron_vari	LOW	0.114	0.017
chr6	142761484	T	A	HIVEP2	c.5600A>T	p.Asp1867Val	missense_variant	MODERATE	0.113	0.006779
chr7	113878024	C	C	PPP1R3A	c.2188A>G	p.Ile729Gly	missense_variant	MODERATE	0.257	0.004152
chr7	66771902	G	T	RABGEF1	c.456>T	p.Met151Ile	missense_variant	MODERATE	0.207	0.009396
chr7	17875709	C	A	SNX13	c.522G>T	p.Lys174Asn	missense_variant	MODERATE	0.198	0.006226
chr7	98233672	G	C	TICRR1	c.2421C>G	p.Thr474Arg	missense_variant	MODERATE	0.186	0.003587
chr8	24485282	A	C	ADAM7	c.881A>C	p.Lys294Thr	missense_variant	MODERATE	0.467	0.006016
chr8	143727762	C	T	FAM83H	c.1699G>A	p.Glu567Lys	missense_variant	MODERATE	0.353	0.003506
chr8	144517440	C	G	RECQL4	c.1876>C	p.Glu63Gln	missense_variant	MODERATE	0.328	0.003697
chr8	124061897	G	A	FER1L6	c.3193G>A	p.Val1065Met	missense_variant	MODERATE	0.168	0.004365
chr8	42708752	G	A	CHRNB3	c.88G>A	p.Asp30Asn	missense_variant	MODERATE	0.121	0.004459
chr8	96231381	TTGCCTAGTTTCAA	T	UQCRB	c.380_392delTTGAAACTAGGCA	p.Ile127fs	frameshift_variant	HIGH	0.113	0.00327
chr8	72936077	T	C	KCNB2	c.7227>C	p.Ile2417Thr	missense_variant	MODERATE	0.108	0.003195
chr9	137231730	G	A	SLC34A3	c.286>A	p.Val10Ile	missense_variant	MODERATE	0.214	0.004474
chr9	78304849	G	T	PSAT1	c.306G>T	.	structural_interaction_variant	HIGH	0.147	0.003861
chr9	35310750	C	CA	UNC13B	c.1050dupA	p.Asp351fs	frameshift_variant	HIGH	0.137	0.00467
chr9	94374921	C	A	MFSD14B	c.102C>A	p.Ser34Arg	missense_variant	MODERATE	0.115	0.008915
chr9	133031068	GCGGGAGCGACGCATGGTGTGCGTGGAGTACC	G	GTF3C5	c.64_94delCGACGCATGGTGTGCGTGGAGTACCCGGGAG	p.Arg22fs	frameshift_variant	HIGH	0.091	0.002599
chr10	46390863	A	G	ANXA8L1	c.925-8A>G	.	ice_region_variant&intron_vari	LOW	0.548	0.037
chr10	95069297	G	C	CYP2C8	c.106C>G	p.Leu36Val	missense_variant	MODERATE	0.33	0.004769
chr10	79310945	G	A	ZMIZ1	c.2857G>A	p.Asp953Asn	missense_variant	MODERATE	0.316	0.003705
chr10	15837196	G	A	FAM188A	c.576>BC>G	.	ice_region_variant&intron_vari	LOW	0.253	0.00706
chr10	93793309	ACC	A	LGI1	c.798_799delCC	p.Asp266fs	frameshift_variant	HIGH	0.202	0.005266
chr10	93793312	ATGTGG	A	LGI1	c.801_805delTGTGG	p.His267fs	frameshift_variant	HIGH	0.202	0.005284
chr11	1243461	T	C	MUC5B	c.65817C>T	p.Me2194Thr	missense_variant	MODERATE	0.63	0.07
chr11	95979772	A	A	MAML2	c.2647G>T	p.Val883Phe	missense_variant	MODERATE	0.25	0.005932
chr11	119678752	C	A	NECTIN1	c.936>T	p.Gln31His	missense_variant	MODERATE	0.222	0.004764

chr11	71929077	G	C	RNF121	c.16G>C	p.Glu6Gln	missense_variant	MODERATE	0.22	0.003657
chr11	68908323	C	G	IGHMBP2	c.435C>G	p.Tyr145*	stop_gained	HIGH	0.204	0.004971
chr11	66845205	A	AATAATCTT	RCE1	c.659_660insATAATCTT	p.Ser221fs	ameshift_variant&stop_gaine	HIGH	0.176	0.004055
chr11	66845203	C	CT	RCE1	c.657_658insT	p.Gln220fs	frameshift_variant	HIGH	0.174	0.004081
chr11	66845211	GCGTGGGGA	G	RCE1	c.666_673delCGTGGGGA	p.Ser222fs	frameshift_variant	HIGH	0.169	0.003939
chr11	48149446	G	A	PTPRJ	c.3000-1G>A	e_acceptor_variant&intron_va	HIGH	0.09	0.007062
chr12	101764542	GCAGGAAAAGTCAACCTCTGCAATCTTT	G	GNPTAB	c.2348_2374delAAAGATTGCAGAGGTTGACTTTTCCTG	Glu783_Pro791de	disruptive_inframe_deletion	MODERATE	0.316	0.003129
chr12	40309214	C	A	LRRK2	c.4298C>A	p.Pro1433His	missense_variant	MODERATE	0.222	0.007706
chr12	6329898	C	G	TNFRSF1A	c.937G>C	p.Glu313Gln	missense_variant	MODERATE	0.21	0.00274
chr12	49634573	G	A	PRPF40B	c.9720>A	p.Met3240Ile	missense_variant	MODERATE	0.203	0.003865
chr12	49033864	G	C	KMT2D	c.10843C>G	p.Ser3614*	stop_gained	HIGH	0.178	0.003541
chr12	129337759	C	A	TMEM132D	c.1174G>T	p.Asp392Tyr	missense_variant	MODERATE	0.156	0.004507
chr12	49021858	ATAGTCATAGGT	A	KMT2D	c.16525_16535delACTATGACTA	p.Thr5509fs	frameshift_variant	HIGH	0.154	0.004179
chr12	55822447	C	G	DNAJC14	c.1824C>G	p.Ile608Met	missense_variant	MODERATE	0.138	0.006001
chr12	56253391	C	A	ANKRD52	c.9976>T	p.Asp3337Tyr	missense_variant	MODERATE	0.104	0.004722
chr13	102861561	C	A	BIVM-ERCC5	c.2089C>A	p.Leu697Met	missense_variant	MODERATE	0.238	0.004332
chr14	20118434	C	G	OR4K17	c.1028C>G	p.Thr343Ser	missense_variant	MODERATE	0.535	0.011
chr14	75084568	A	T	NEK9	c.2972T>A	p.Leu991His	missense_variant	MODERATE	0.34	0.006319
chr14	20118376	C	A	OR4K17	c.9700>C	p.Glu324Gln	missense_variant	MODERATE	0.285	0.007973
chr15	36645220	C	T	C15orf41	c.148-3C>T	.	ce_region_variant&intron_vari	LOW	0.253	0.007502
chr15	41876155	C	T	SPTBN5	c.4081G>A	p.Glu1361Lys	missense_variant	MODERATE	0.253	0.005021
chr15	43523017	C	G	MAP1A	c.1544C>G	p.Pro515Arg	missense_variant	MODERATE	0.247	0.003107
chr15	48760164	C	T	CEP152	c.2665G>A	p.Glu889Lys	missense_variant	MODERATE	0.232	0.006376
chr15	41523971	C	G	RPAP1	c.2236G>C	p.Asp746His	inse_variant&splice_region_va	MODERATE	0.226	0.004541
chr15	66781169	G	C	SMAD6	c.1125G>C	p.Gln375His	missense_variant	MODERATE	0.219	0.002294
chr15	42686337	G	A	STARD9	c.4759G>A	p.Asp1587Asn	missense_variant	MODERATE	0.217	0.003836
chr15	52196449	G	A	MYO5C	c.4855G>C	p.Asp1619His	missense_variant	MODERATE	0.194	0.00464
chr15	73368145	G	T	HCN4	c.126C>A	p.Asp42Glu	missense_variant	MODERATE	0.152	0.005118
chr15	24678196	T	C	NPAP1	c.2329D>T	p.Pro777Ser	missense_variant	MODERATE	0.138	0.002952
chr16	89596557	G	T	CPNE7	c.1838G>T	p.Arg613Ile	missense_variant	MODERATE	0.455	0.002617
chr16	71027836	C	A	HYDIN	c.2808G>T	p.Lys936An	missense_variant	MODERATE	0.432	0.014
chr16	72793598	G	A	ZFHX3	c.9084G>C	p.Leu3028Phe	missense_variant	MODERATE	0.376	0.003845
chr16	30988084	G	T	HSD3B7	c.1011G>T	p.Lys337An	missense_variant	MODERATE	0.162	0.003478
chr16	31372636	C	T	ITGAX	c.2332D>T	p.Gln778*	stop_gained	HIGH	0.159	0.003126
chr16	16125849	C	A	ABCC1	c.3757G>A	p.Glu1253Lys	missense_variant	MODERATE	0.144	0.004556
chr16	1198713	G	A	CACNA1H	c.7426>A	p.Gly2485er	missense_variant	MODERATE	0.125	0.005008
chr16	1791099	T	A	IGFALS	c.1433A>T	p.Asp478Val	missense_variant	MODERATE	0.121	0.003429
chr16	1952952	G	A	RPL3L	c.267D>T	p.Pro96Leu	missense_variant	MODERATE	0.112	0.005055
chr16	2043626	ACACCCGGCAGGGC	A	NTHL1	c.637_649delGCGCTGCCGGGTG	p.Ala213fs	frameshift_variant	HIGH	0.111	0.002446
chr16	2461125	GAGCCCGAACCCCCAGGCCTGGGGCGGGGCCTCAGGGACCA	G	C16orf59	c.507_545delAGCCCGAACCCCCAGGCCTGGGGCGGGCCTCAGGGACCA	Ala170_Gln182de	disruptive_inframe_deletion	MODERATE	0.085	0.002519
chr17	35978192	G	T	CCL16	c.148C>A	p.Leu50Ile	missense_variant	MODERATE	0.329	0.003679
chr17	73472195	G	T	SOX2	c.248D>A	p.Arg83His	missense_variant	MODERATE	0.23	0.012
chr17	47122482	G	T	CDC27	c.2372C>A	p.Pro791Gln	missense_variant	MODERATE	0.208	0.006233
chr17	66302948	G	A	PRKCA	c.97G>A	p.Glu33Lys	missense_variant	MODERATE	0.188	0.003962
chr17	50501454	C	A	CACNA1G	c.2473C>A	p.Gln825Lys	missense_variant	MODERATE	0.153	0.003661
chr18	69599419	A	T	DOK6	c.210A>T	p.Arg70Ser	missense_variant	MODERATE	0.703	0.004866
chr18	58387481	G	A	NEDD4L	c.2530G>A	p.Asp844Asn	missense_variant	MODERATE	0.624	0.025
chr18	49837639	G	A	MYO5B	c.5016D>T	.	structural_interaction_variant	HIGH	0.318	0.057
chr19	804381	C	G	PTBP1	c.378C>G	p.Ile126Met	missense_variant	MODERATE	0.341	0.003071
chr19	38849781	C	G	HNRNPL	c.186G>C	p.Lys62Asn	missense_variant	MODERATE	0.249	0.004747
chr19	49654393	G	C	SCAF1	c.3361C>G	p.Arg1121Gly	missense_variant	MODERATE	0.218	0.005855
chr19	32991901	T	A	RHPN2	c.1566A>T	p.Glu522Asp	missense_variant	MODERATE	0.212	0.004269
chr19	18854936	C	G	UPF1	c.1356C>G	p.Ile452Met	missense_variant	MODERATE	0.202	0.003758
chr19	19501327	C	G	GATAD2A	c.1414G>C	p.Glu472Gln	missense_variant	MODERATE	0.202	0.003376
chr19	15239430	G	GTTTGTCC	BRD4	c.3531_3537dupGGACAAA	p.Gln1180fs	frameshift_variant	HIGH	0.2	0.003075
chr19	57639965	C	A	ZNF211	c.310C>A	p.Pro104Thr	missense_variant	MODERATE	0.197	0.0053
chr19	53068281	G	T	ZNF160	c.2253A>C	p.His751Gln	missense_variant	MODERATE	0.196	0.004501
chr19	49746762	T	C	TSK5	c.700G>A	p.Glu234Lys	missense_variant	MODERATE	0.137	0.003917
chr20	18137992	G	A	PET117	c.37G>A	p.Val13Met	missense_variant	MODERATE	0.123	0.004434
chr20	36613895	C	A	SLA2	c.757G>T	p.Asp253Tyr	missense_variant	MODERATE	0.109	0.005444
chr20	34845445	G	C	GGT7	c.1872C>G	p.His624Gln	missense_variant	MODERATE	0.107	0.004079
chr21	31705475	G	C	SCAF4	c.115-8C>G	.	ce_region_variant&intron_vari	LOW	0.305	0.013
chr21	41991130	G	A	ZBTB21	c.2966D>T	p.Pro988Leu	missense_variant	MODERATE	0.158	0.003593
chr21	43010106	T	C	PKNOX1	c.233C>T	p.Thr78Ile	missense_variant	MODERATE	0.125	0.00527
chr22	37182690	C	G	C1QTNF6	c.335G>C	p.Gly112Ala	missense_variant	MODERATE	0.276	0.003095
chr22	35746477	C	T	RBFOX2	c.1234G>A	p.Asp412Asn	missense_variant	MODERATE	0.268	0.004276
chr22	49794210	G	T	BRD1	c.2183>A	p.Thr728Asn	missense_variant	MODERATE	0.227	0.00342
chr22	26483893	GG	TC	SRRD	c.3_4delGGinsTC	p.MetAla17	start_lost	HIGH	0.21	0.019
chrX	13278508	T	C	IGSF1	c.2009A>G	p.Glu670Gly	missense_variant	MODERATE	0.288	0.002982
chrX	103274280	T	G	TCEAL5	c.284A>C	p.Lys95Thr	missense_variant	MODERATE	0.212	0.003168
chrX	106928505	C	A	CLDN2	c.277C>A	p.Leu93Met	missense_variant	MODERATE	0.202	0.002484
chrX	116172338	T	A	AGTR2	c.58T>A	p.Phe20Ile	missense_variant	MODERATE	0.196	0.004013
chrX	119845218	TT	AA	UPF3B	c.448_449delAinsTT	p.Lys150Leu	missense_variant	MODERATE	0.158	0.008188
chrX	119845220	GGT	G	UPF3B	c.445_446delAC	p.Thr149fs	frameshift_variant	HIGH	0.157	0.008103
chrX	51408003	G	T	Oforf67	c.987G>T	p.Arg329Ser	missense_variant	MODERATE	0.153	0.002214
chrX	70204947	C	A	DGAT2L6	c.860-5C>A	.	ce_region_variant&intron_vari	LOW	0.151	0.004417
chrX	111162978	G	A	PAK3	c.640G>A	p.Glu214Lys	missense_variant	MODERATE	0.145	0.004315
chrX	111901893	C	A	TRPCSOS	c.44C>A	p.Ala15Asp	missense_variant	MODERATE	0.136	0.005213
chrX	153869874	C	T	L1CAM	c.1052G>A	p.Arg351His	missense_variant	MODERATE	0.129	0.003376
chrX	130066809	C	T	ELF4	c.1904G>A	p.Gly635Glu	missense_variant	MODERATE	0.128	0.002586
chrX	153788134	G	C	IDH3G	c.348C>G	p.Gly116Gly	region_variant&synonymous_	LOW	0.099	0.003863
chrX	78432651	A	T	VCX	c.62A>T	p.Lys21Met	missense_variant	MODERATE	0.078	0.003149

Supplementary table 6: Variants in patient 4. Identified by WES. Green: shared mutations between tumor at baseline and tumor at progression.

Yellow: unique mutations to baseline tumor. Blue: Unique mutations to progression tumor

CHROM	POS	REF	ALT	GENE	c_change	p_change	Effect	Impact	AF_baseline	AF_progression	Ratio
chr1	228370193	GGCCCGGCCTAGTGCGGCCCAGT	G	OBSCN	c.22996_23017delCGGCCTAGTGCGGCCCAGTGCC	p.Arg7666fs	frameshift_variant	HIGH	0.224	0.322	1.44
chr1	177278694	C	A	BRINP2	c.1144C>A	p.Leu382Met	missense_variant	MODERATE	0.171	0.196	1.15
chr1	237423073	TCCTAACTGTTTTCATTAGGTGGAGTGGAAG	T	RYR2	c.849-16_862delTAACTGTTTTCATTAGGTGGAGTGGAAGCC	p.Trp284fs	_acceptor_variant&splice_regi	HIGH	0.206	0.214	1.04
chr1	248847417	G	C	ZNF672	c.143G>C	p.Gly48Ala	missense_variant	MODERATE	0.198	0.19	0.96
chr1	160748206	C	A	SLAMF7	c.68C>A	p.Ser23Tyr	missense_variant	MODERATE	0.227	0.19	0.84
chr1	207474890	TTCTATATGGAAATGAAGTCTCTTA	T	CR2	c.2392_2415delCTATATGGAAATGAAGTCTCTTAT	Leu798_Tyr805d	conservative_inframe_deletion	MODERATE	0.227	0.18	0.79
chr1	102961912	A	G	COL11A1	c.3158C>T	p.Pro1053Leu	missense_variant	MODERATE	0.306	0.239	0.78
chr1	171541186	G	A	PRRC2C	c.3724A>G	p.Ser1242Gly	missense_variant	MODERATE	0.301	0.221	0.73
chr1	54814942	C	T	LEXM	c.953C>T	p.Pro318Leu	missense_variant	MODERATE	0.311	0.212	0.68
chr1	175354433	CCTGTGCTGCCTGCAGGAGCA	C	TNR	c.3320_3339delTGCTGCTGCAGGCAGCACAG	p.Val1107fs	frameshift_variant	HIGH	0.208	0.133	0.64
chr1	22802361	C	A	EPHB2	c.1336C>A	p.Pro446Thr	inse_variant&splice_region_va	MODERATE	0.447	0.278	0.62
chr1	170992190	C	T	MRDH9	c.1055C>T	p.Ala352Val	missense_variant	MODERATE	0.239	0.141	0.59
chr1	132783065	C	G	NOXAP5	c.3746G>C	p.Arg1249Thr	missense_variant	MODERATE	0.136	0.211	1.55
chr2	176188998	C	A	HOXD1	c.197C>A	p.Pro66Gln	missense_variant	MODERATE	0.156	0.196	1.26
chr2	1267495	T	A	SNTG2	c.1208T>A	p.Val403Glu	missense_variant	MODERATE	0.178	0.167	0.94
chr2	43556355	G	C	THADA	c.2664>G	p.Asn888Lys	missense_variant	MODERATE	0.274	0.193	0.70
chr2	5692774	G	C	SOX11	c.53C>G	p.Ala18Gly	missense_variant	MODERATE	0.357	0.224	0.63
chr2	208350819	GAGAGTTTCATAAGATGCGTGA	G	PIKFYVE	c.5486_5506delTAGTTTCATAAGATGCGTGAAG	Ile1829_Glu1835	disruptive_inframe_deletion	MODERATE	0.304	0.177	0.58
chr2	141019986	G	A	LRP1B	c.1906C>T	p.Arg636Trp	missense_variant	MODERATE	0.429	0.235	0.55
chr2	127566671	T	A	MYO7B	c.314T>A	p.Val105Asp	missense_variant	MODERATE	0.468	0.226	0.48
chr3	75741673	C	T	ZNF717	c.1216>A	p.Asp416Asn	missense_variant	MODERATE	0.077	0.062	0.81
chr3	35721611	C	G	ARIP21	c.900C>G	p.Asn300Lys	missense_variant	MODERATE	0.268	0.198	0.74
chr3	12160890	C	A	SYN2	c.1292C>A	p.Thr431Lys	missense_variant	MODERATE	0.277	0.179	0.65
chr3	32534525	G	A	DYNC1I1	c.954G>C	p.Lys318Asn	missense_variant	MODERATE	0.354	0.218	0.62
chr3	50381063	C	T	CACNA2D2	c.716G>A	p.Arg239His	missense_variant	MODERATE	0.356	0.215	0.60
chr3	14907681	G	T	FGD5	c.3306G>T	.	structural_interaction_variant	HIGH	0.357	0.185	0.52
chr4	86732628	G	T	PTPN13	c.1720G>T	p.Val574Leu	missense_variant	MODERATE	0.191	0.159	0.83
chr4	155915890	G	A	TDO2	c.874G>A	p.Ala292Thr	missense_variant	MODERATE	0.261	0.208	0.80
chr4	88459411	GATTCTCTC	A	HERC5	c.333_340delTCTCTCAT	p.Leu112fs	frameshift_variant	HIGH	0.202	0.147	0.73
chr4	625978	G	A	FBXL5	c.352D>A	p.Val118Ile	missense_variant	MODERATE	0.403	0.251	0.62
chr4	42398130	G	C	SHISA3	c.74G>C	p.Gly25Ala	missense_variant	MODERATE	0.567	0.33	0.58
chr5	24492839	G	T	CDH10	c.1602C>A	p.AsnS34Lys	missense_variant	MODERATE	0.211	0.191	0.91
chr5	34868928	C	T	TTC23L	c.891G>C	p.Leu297Phe	missense_variant	MODERATE	0.219	0.197	0.90
chr5	73578745	T	C	UTP15	c.1045-6T>C	.	ce_region_variant&intron_vari	LOW	0.285	0.242	0.85
chr5	172926511	C	A	ERGIC1	c.483C>A	p.Val161Val	region_variant&synonymous_	LOW	0.201	0.164	0.82
chr6	177994300	C	G	PRDP1	c.148G>C	p.Gly50Arg	missense_variant	MODERATE	0.229	0.162	0.71
chr6	45422846	G	T	RUNX2	c.312G>T	p.Glu104Asp	missense_variant	MODERATE	0.242	0.258	1.07
chr6	165298082	TTGAGTTGAGCCAGAAAGCTAGGCAGGACCAGGTACA	T	C6orf118	c.937-19_955delTGTACCTGGTCCTGCCTAGGCTCTTCTGGCTCAACTCA	p.Ala313fs	_acceptor_variant&splice_regi	HIGH	0.633	0.533	0.84
chr6	29306922	A	C	OR14J1	c.233A>C	p.Gln78Pro	missense_variant	MODERATE	0.271	0.227	0.84
chr6	109979430	CATGTTCGTGCTGGTAGGCAGCCTGGCCACCGCTG	C	EPB6	c.365_398delTGTTCGTGCTGGTAGGCAGCCTGGCCACCGCTGA	p.Met122fs	frameshift_variant	HIGH	0.482	0.39	0.81
chr6	70242026	C	A	COL9A1	c.1936G>T	p.Gly646Cys	missense_variant	MODERATE	0.29	0.201	0.69
chr6	35959591	C	T	SLC26A8	c.1732G>A	p.Val578Ile	inse_variant&splice_region_va	MODERATE	0.325	0.225	0.69
chr6	131676756	G	A	ENPP3	c.893G>A	p.Arg298Lys	missense_variant	MODERATE	0.22	0.15	0.68
chr6	26190075	C	G	HIST1H2AD	c.169G>C	p.Glu57Gln	missense_variant	MODERATE	0.344	0.227	0.66
chr6	51754925	C	G	PKHD1	c.8656G>C	p.Asp2886His	missense_variant	MODERATE	0.324	0.205	0.63
chr6	17777273	TTACATTA	T	HIST1H3A	c.4167_4173delTAATGTA	p.His1388fs	e_donor_variant&splice_regio	HIGH	0.342	0.211	0.62
chr6	27871905	TTA	T	HIST1H3I	c.409_410delTA	p.Ter137fs	frameshift_variant&stop_lost	HIGH	0.362	0.197	0.54
chr7	99547699	C	T	FAM200A	c.709G>A	p.Val237Ile	missense_variant	MODERATE	0.261	0.223	0.85
chr7	44581444	C	G	TMED4	c.387+5G>C	.	ce_region_variant&intron_vari	LOW	0.265	0.208	0.78
chr7	151055548	C	T	CDK5	c.467G>A	.	protein_protein_contact	HIGH	0.544	0.412	0.76
chr7	44145195	G	A	GCK	c.1342>T	p.Arg448Trp	missense_variant	MODERATE	0.336	0.234	0.70
chr7	12688572	A	C	ARL4A	c.318A>C	p.Glu106Asp	missense_variant	MODERATE	0.352	0.223	0.63
chr7	5997386	C	A	PMS2	c.743G>T	p.Ser248Ile	missense_variant	MODERATE	0.366	0.167	0.46
chr8	143539155	C	G	ZCIH3	c.212G>C	p.Arg71Pro	missense_variant	MODERATE	0.375	0.383	1.02
chr8	143539152	T	A	ZCIH3	c.215A>T	p.Lys72Met	missense_variant	MODERATE	0.376	0.376	1.00
chr8	143867895	C	A	EPPK1	c.5359G>T	p.Gly1787Trp	missense_variant	MODERATE	0.219	0.172	0.79
chr8	103318624	C	G	FZD6	c.212C>G	p.Pro71Arg	missense_variant	MODERATE	0.502	0.356	0.71
chr8	143918885	G	A	PLEC	c.11347C>T	p.Arg3783Cys	missense_variant	MODERATE	0.478	0.328	0.69
chr9	99020437	G	A	COL15A1	c.1696G>A	p.Glu566Lys	missense_variant	MODERATE	0.253	0.213	0.84
chr9	86040732	C	A	GOLM1	c.597+7G>T	.	ce_region_variant&intron_vari	LOW	0.267	0.211	0.79
chr9	98985780	G	A	COL15A1	c.3166>A	p.Val1069Met	missense_variant	MODERATE	0.307	0.234	0.76
chr9	124482894	A	T	NR5A1	c.1160A>T	p.His387Leu	missense_variant	MODERATE	0.413	0.22	0.53
chr10	70145710	A	C	TYSND1	c.877T>G	p.Phe293Val	missense_variant	MODERATE	0.44	0.43	0.98
chr10	27119290	CTACCCATTAGAATTT	C	YME1L1	c.1727_1738+3delAAATTCTAATGGGTA	S76_Gly580delin	ve_inframe_deletion&splice_	HIGH	0.296	0.208	0.70
chr11	56743259	T	C	OR6G4	c.553G>A	p.Gly185Ser	missense_variant	MODERATE	0.301	0.297	0.99
chr11	32932774	A	C	QSER1	c.629A>C	p.His210Pro	missense_variant	MODERATE	0.31	0.263	0.85
chr11	78101171	C	T	ALG8	c.1374G>A	p.Trp458*	stop_gained	HIGH	0.344	0.25	0.73
chr11	74138970	G	GT	C2CD3	c.708-4dupA	.	ce_region_variant&intron_vari	LOW	0.349	0.231	0.66
chr11	67279833	C	T	GRK2	c.442-6C>T	.	ce_region_variant&intron_vari	LOW	0.363	0.237	0.62
chr12	120149921	C	T	GCN1	c.4431+1G>A	.	ice_donor_variant&intron_vari	HIGH	0.291	0.357	1.23
chr12	70521490	C	G	PTPRB	c.6647G>C	p.Ter2216Serext*	stop_lost	HIGH	0.21	0.229	1.09
chr12	54500555	G	A	NCKAP1L	c.2136G>A	p.Arg79His	missense_variant	MODERATE	0.243	0.19	0.78
chr12	52054310	GTCTCCTC	G	NR4A1	c.161-12_161-6delCTCTCTC	.	ce_region_variant&intron_vari	LOW	0.345	0.228	0.66
chr12	40340378	CATTGCAAAG	C	LRRK2	c.6039_6047delAAAGATTGC	Lys2014_Ala2016d	disruptive_inframe_deletion	MODERATE	0.317	0.189	0.60
chr14	104775168	C	A	AKT1	c.475G>T	p.Gly159Cys	missense_variant	MODERATE	0.225	0.213	0.95
chr14	20014429	G	T	OR4K14	c.765C>A	p.Cys255*	stop_gained	HIGH	0.271	0.208	0.77
chr14	20429328	C	T	KLHL33	c.1123G>A	p.Gly375Ser	missense_variant	MODERATE	0.303	0.23	0.76
chr14	63982781	T	C	SYNE2	c.1988D>T	p.Ser663Leu	missense_variant	MODERATE	0.325	0.243	0.75
chr14	37592623	G	C	FOXA1	c.161C>G	p.Thr54Ser	missense_variant	MODERATE	0.343	0.249	0.73
chr16	30555761	T	A	ZNF764	c.660A>T	p.Lys220Asn	missense_variant	MODERATE	0.326	0.262	0.80
chr16	20419230	A	T	ACSM5	c.418A>T	p.Thr140Ser	inse_variant&splice_region_va	MODERATE	0.34	0.242	0.71
chr16	69114610	C	T	HAS3	c.1006C>T	p.Arg336Cys	missense_variant	MODERATE	0.511	0.319	0.62
chr16	30651851	G	T	PRR14	c.79G>T	p.Ala27Ser	missense_variant	MODERATE	0.357	0.221	0.62
chr16	24825760	G	A	TNRC6A	c.5842G>A	p.Ala1948Thr	missense_variant	MODERATE	0.347	0.211	0.61
chr17	40140769	A	G	CASC3	c.2214>G	p.Glu746Gly	missense_variant	MODERATE	0.108	0.305	2.82
chr17	63536069	G	T	KCNH6	c.1501+1G>T	.	ice_donor_variant&intron_vari	HIGH	0.255	0.271	1.06
chr17	43074365	C	CAA	BRCA1	c.4702_4703dupTT	p.Leu1568fs	frameshift_variant	HIGH	0.325	0.323	0.99
chr17	39924228	G	T	ORMDL3	c.-22-3C>A	.	ce_region_variant&intron_vari	LOW	0.326	0.314	0.96
chr17	35193994	A	T	SLC35G3	c.314T>A	p.Phe105Tyr	missense_variant	MODERATE	0.248	0.196	0.79
chr17	35193976	T	C	SLC35G3	c.332A>G	p.Asn111Ser	missense_variant	MODERATE	0.256	0.196	0.77
chr17	69089457	C	T	ABCA6	c.3606+8G>A	.	ce_region_variant&intron_vari	LOW	0.171	0.122	0.71
chr17	30464602	G	A	CPD	c.3931G>A	p.Ala1311Thr	missense_variant	MODERATE	0.323	0.211	0.65
chr17	80332324	A	T	RNF213	c.3836A>T	p.Tyr1279Phe	missense_variant	MODERATE	0.197	0.127	0.64
chr17	43090944	C	G	BRCA1	c.4185G>C	p.Gln1395His	inse_variant&splice_region_va	MODERATE	0.458	0.295	0.64
chr17	28748575	T	C	TRAF4	c.689T>C	p.Val230Ala	missense_variant	MODERATE	0.362	0.186	0.51
chr17	7770255	C	A	DNAH2	c.3945C>A	p.His1315Gln	missense_variant	MODERATE	0.563	0.273	0.48
chr18	26548113	G	A	KCTD1	c.424C>T	p.Pro142Ser	missense_variant	MODERATE	0.26	0.286	1.10
chr18	5969443	C	A	L3MBTL4	c.1591G>T	p.Gly531Cys	missense_variant	MODERATE	0.378	0.353	0.93
chr18	51078408	C	T	SMAD4	c.1600D>T	p.Gln534*	stop_gained	HIGH	0.441	0.289	0.66
chr18	2732294	G	C	SMCHD1	c.3078G>C	p.Lys1026Asn	missense_variant	MODERATE	0.262	0.162	0.62
chr19	55694823	C	T	EPN1	c.1620>T	.	sequence_feature	MODERATE	0.311	0.272	0.87
chr19	10454848	G	A	POE4A	c.8036>A	p.Arg2681His	missense_variant	MODERATE	0.263	0.228	0.87

chr19	48464384	GG	AT	KCNJ14	c.918_919delGGinsAT	.MetVal306IlePh	missense_variant	MODERATE	0.273	0.217	0.79
chr19	49857120	CC	TA	PTOV1	c.704_705delCCinsTA	p.Thr235Ile	missense_variant	MODERATE	0.291	0.215	0.74
chr19	12113386	C	T	ZNF788	n.2476C>T	.	n_coding_transcript_exon_varia	MODIFIER	0.316	0.23	0.73
chr19	18451858	C	T	RYR1	c.12170>T	p.Thr4061e	missense_variant	MODERATE	0.281	0.195	0.69
chr19	10682574	G	C	ILF3	c.1418G>C	p.Gly473Ala	missense_variant	MODERATE	0.371	0.249	0.67
chr19	40570667	CA	C	SPTBN4	c.7259delA	p.Gln2420fs	frameshift_variant	HIGH	0.26	0.17	0.65
chr19	40570669	G	C	SPTBN4	c.7260G>C	p.Gln2420His	missense_variant	MODERATE	0.26	0.17	0.65
chr19	3179531	C	T	S1PR4	c.739C>T	p.Arg247Cys	missense_variant	MODERATE	0.386	0.25	0.65
chr19	32738848	T	C	TDRD12	c.184-8T>C	.	ice_region_variant&intron_vari	LOW	0.314	0.201	0.64
chr19	36054128	CGCTCACTTGTAGAA	C	THAP8	c.76_83+6delTTCTACAAGTGAGC	p.Phe26fs	e_donor_variant&splice_regio	HIGH	0.315	0.193	0.61
chr19	41811233	C	T	CEACAM3	c.755C>T	p.Ser252Phe	missense_variant	MODERATE	0.335	0.198	0.59
chr19	48739383	CG	C	RASIP1	c.399delC	p.Glu134fs	frameshift_variant	HIGH	0.48	0.279	0.58
chr19	2423352	C	T	TMPRSS9	c.2882-5C>T	.	ice_region_variant&intron_vari	LOW	0.428	0.232	0.54
chr19	56663788	C	T	ZNF835	c.1411G>A	p.Glu471Lys	missense_variant	MODERATE	0.386	0.168	0.44
chr20	62193449	G	T	MTG2	c.290>T	p.Arg10Ile	missense_variant	MODERATE	0.301	0.222	0.74
chr20	62335118	G	GCC	LAMA5	c.2383_2384dupGG	p.Gln796fs	frameshift_variant	HIGH	0.337	0.211	0.63
chr22	50224223	C	T	TUBGCP6	c.218BG>A	p.Asp730Asn	missense_variant	MODERATE	0.126	0.317	2.52
chr22	18169929	G	A	USP18	c.713G>A	p.Arg238His	missense_variant	MODERATE	0.321	0.237	0.74
chr22	42640258	C	T	ATP5L2	c.17G>A	p.Arg6His	missense_variant	MODERATE	0.298	0.212	0.71
chr22	42127617	T	A	CYP2D6	c.1003A>T	p.Ile335Phe	missense_variant	MODERATE	0.327	0.22	0.67
chr22	20457963	A	C	KLHL22	c.1150T>G	p.Ser384Ala	missense_variant	MODERATE	0.396	0.251	0.63
chrX	18730257	CC	AA	PREF1	c.123_124delCCinsAA	p.Leu42Ile	missense_variant	MODERATE	0.239	0.233	0.97
chrX	72140054	G	T	NHS12	c.2506G>T	p.Val836Phe	missense_variant	MODERATE	0.276	0.258	0.93
chrX	145824160	C	T	SLITRK2	c.1735C>T	p.Pro579Ser	missense_variant	MODERATE	0.289	0.222	0.77
chrX	110452756	A	T	RGAG1	c.2139A>T	p.Lys713Asn	missense_variant	MODERATE	0.333	0.229	0.69
chrX	155939716	A	T	VAMP7	c.449A>T	p.Asn150Ile	missense_variant	MODERATE	0.276	0.185	0.67
chrX	53559030	G	T	HUWE1	c.7946C>A	p.Thr2649Asn	missense_variant	MODERATE	0.304	0.2	0.66
chrX	37686076	C	A	XK	c.115C>A	p.Leu39Met	missense_variant	MODERATE	0.298	0.196	0.66
chrX	153866682	T	G	L1CAM	c.2398C>A	p.Pro800Thr	missense_variant	MODERATE	0.364	0.235	0.65
chrX	136349948	C	T	ADGRG4	c.624ZCT	p.Thr208Ile	missense_variant	MODERATE	0.382	0.204	0.53

Chrom	POS	REF	ALT	Gene	c_Change	p_Change	Effect	Impact	AF_Tumor	AF_BC	
chr1	32695450	G	SYNC	c.648A>C	p.Gln216His	missense_variant	MODERATE	0.393	0.003595		
chr1	247434133	C	A	NLRP3	c.2358C>A	p.Cys786*	stop_gained	HIGH	0.391	0.005076	
chr1	23337030	T	C	MLK4	c.1553-8T>C	.	ice_region_variant&intron_vari	LOW	0.354	0.005444	
chr1	152304234	T	A	FLG	c.10652A>T	p.Asp3551Val	missense_variant	MODERATE	0.329	0.001921	
chr1	10095453	C	A	UBE4B	c.212-8C>A	.	ice_region_variant&intron_vari	LOW	0.322	0.006045	
chr1	28474078	G	A	PHACTR4	c.1378G>A	p.Asp460Asn	missense_variant	MODERATE	0.279	0.003444	
chr1	38045448	CCCA	CCA	POU3F1	c.1295_1296insTGG	ro432_Pro433insIdisruptive_inframe_insertion		MODERATE	0.278	0.004759	
chr1	38045449	G	CACTGCAC	POU3F1	c.1294_1295insTGCCCGGCTCAGTGCAGTGACCCCGCGG	p.Pro432fs	rameshift_variant&stop_gaine	HIGH	0.278	0.004781	
chr1	15730630	G	T	PLEKHM2	c.2307G>T	p.Glu769Asp	missense_variant	MODERATE	0.249	0.002594	
chr1	33014531	A	C	AK2	c.488G>T	p.Met163Ile	missense_variant	MODERATE	0.245	0.009958	
chr1	54200266	CAAGG	C	MRPL37	c.24_27delAAGG	p.Arg9fs	frameshift_variant	HIGH	0.241	0.002905	
chr1	54200271	CGGG	C	MRPL37	c.29_31delGGG	tg10_Ala11delins	disruptive_inframe_deletion	MODERATE	0.236	0.002838	
chr1	46286313	C	T	LRRC41	c.544G>A	p.Gly182Lys	missense_variant	MODERATE	0.235	0.002667	
chr1	176710166	C	A	PAPPA2	c.3641C>A	p.Pro1214His	missense_variant	MODERATE	0.218	0.004593	
chr1	186070755	C	A	HMCN1	c.8137C>A	p.Gln2713Lys	nse_variant&splice_region_va	MODERATE	0.215	0.005	
chr1	222543531	C	T	HHIPL2	c.974+6A>G	.	ice_region_variant&intron_vari	LOW	0.17	0.006987	
chr1	10650933	C	T	CASZ1	c.2816+8G>A	.	ice_region_variant&intron_vari	LOW	0.129	0.0046	
chr1	165896320	C	A	UCK2	c.487C>A	p.Leu163Ile	missense_variant	MODERATE	0.12	0.003538	
chr1	211793074	G	T	LPGAT1	c.355C>A	p.Leu119Met	nse_variant&splice_region_va	MODERATE	0.111	0.006329	
chr1	27613356	G	A	FGR	c.1250-6C>T	.	ice_region_variant&intron_vari	LOW	0.107	0.005969	
chr1	26188312	G	A	CNKSR1	c.1549+5G>A	.	ice_region_variant&intron_vari	LOW	0.104	0.00475	
chr1	17632314	C	T	ARHGEF10L	c.1585-7C>T	.	ice_region_variant&intron_vari	LOW	0.103	0.006674	
chr1	1486103	C	T	ATAD3B	c.964-7C>T	.	ice_region_variant&intron_vari	LOW	0.102	0.003446	
chr1	11037704	C	T	MASP2	c.997G>A	.	structural_interaction_variant	HIGH	0.098	0.006792	
chr1	10644911	C	T	CASZ1	c.3868+6G>A	.	ice_region_variant&intron_vari	LOW	0.095	0.00439	
chr1	11784461	C	T	C1orf167	c.529ZC>T	p.Ala109Val	missense_variant	MODERATE	0.092	0.003402	
chr1	1313520	C	T	CPSF3L	c.1048G>A	p.Glu350Lys	missense_variant	MODERATE	0.091	0.003607	
chr1	204954392	G	A	NFASC	c.412+8G>A	.	ice_region_variant&intron_vari	LOW	0.089	0.00704	
chr1	27362649	T	C	MAP3K6	c.1247G>A	p.Arg416Gln	missense_variant	MODERATE	0.087	0.004634	
chr1	6636116	C	T	DNAJC11	c.1654+1G>A	.	ice_donor_variant&intron_vari	HIGH	0.085	0.006053	
chr1	3476069	G	A	ARHGEF16	c.1473+7G>A	.	ice_region_variant&intron_vari	LOW	0.083	0.004954	
chr1	37794279	G	A	MANEAL	c.670>A	p.Asp33Asn	missense_variant	MODERATE	0.083	0.015	
chr1	9723127	T	G	PIK3CD	c.2429T>G	p.Met810Arg	nse_variant&splice_region_va	MODERATE	0.082	0.004519	
chr1	45035803	C	T	ZSWIM5	c.2176G>A	p.Gly726Arg	missense_variant	MODERATE	0.081	0.003974	
chr1	17270235	T	C	PADI3	c.65SC>T	p.Pro219Ser	nse_variant&splice_region_va	MODERATE	0.08	0.004969	
chr1	21602811	C	T	RAP1GAP	c.1723G>A	p.Glu575Lys	missense_variant	MODERATE	0.08	0.004244	
chr1	33013358	C	G	AK2	c.543G>C	p.Lys181Asn	missense_variant	MODERATE	0.079	0.005401	
chr1	11768094	G	A	C1orf167	c.1361G>A	p.Arg454Lys	missense_variant	MODERATE	0.078	0.004011	
chr1	11776473	T	C	C1orf167	c.2174C>T	p.Ala725Val	missense_variant	MODERATE	0.078	0.003913	
chr1	980539	G	A	PERM1	c.491C>T	p.Thr164Ile	missense_variant	MODERATE	0.076	0.002675	
chr1	19270518	G	C	AKR7L	n.440C>G	.	n_coding_transcript_exon_varia	MODIFIER	0.075	0.00239	
chr1	10417117	G	A	PGD	c.975G>A	.	structural_interaction_variant	HIGH	0.073	0.00638	
chr1	20648989	G	A	PINK1	c.1252-6G>A	.	ice_region_variant&intron_vari	LOW	0.073	0.004375	
chr1	11858258	C	T	NPPB	c.344G>A	p.Arg115Lys	missense_variant	MODERATE	0.072	0.002988	
chr1	18228003	A	T	IGSF21	c.1760>A	p.Tyr59*	stop_gained	HIGH	0.072	0.00527	
chr1	22576778	G	A	EPHA8	c.721G>A	p.Asp241Asn	missense_variant	MODERATE	0.071	0.00174	
chr1	22912439	C	T	EPHB2	c.2697-5C>T	.	ice_region_variant&intron_vari	LOW	0.071	0.004385	
chr1	43311682	C	T	TIE1	c.1345C>T	p.Pro449Ser	missense_variant	MODERATE	0.071	0.00748	
chr1	5904617	C	T	NPHP4	c.2143G>A	p.Gly715Arg	nse_variant&splice_region_va	MODERATE	0.07	0.006308	
chr1	48761471	C	T	BEND5	c.227-1G>A	.	ze_acceptor_variant&intron_vai	HIGH	0.07	0.007665	
chr1	5874998	C	T	NPHP4	c.2920G>A	p.Ala974Thr	missense_variant	MODERATE	0.069	0.003066	
chr1	11230924	C	T	MTOR	c.2779+1G>A	.	ice_donor_variant&intron_vari	HIGH	0.068	0.004362	
chr1	11520756	C	T	DISP3	c.2270C>T	p.Pro757Leu	missense_variant	MODERATE	0.066	0.002763	
chr1	5867845	C	T	NPHP4	c.3367G>A	p.Val1123Met	missense_variant	MODERATE	0.065	0.002752	
chr1	230843347	C	T	C1orf198	c.927+7G>A	.	ice_region_variant&intron_vari	LOW	0.065	0.003868	
chr1	12276979	C	T	VPS13D	c.3391C>T	p.Pro1131Ser	missense_variant	MODERATE	0.064	0.006416	
chr1	32898125	C	T	TMEM54	c.210+1G>A	.	ice_donor_variant&intron_vari	HIGH	0.064	0.003983	
chr1	156910386	G	A	PEAR1	c.1825+6G>A	.	ice_region_variant&intron_vari	LOW	0.064	0.003953	
chr1	21857320	C	T	HSPG2	c.5362G>A	p.Ala1788Thr	missense_variant	MODERATE	0.063	0.004276	
chr1	56876054	C	T	CBA	c.317-8C>T	.	ice_region_variant&intron_vari	LOW	0.063	0.005582	
chr1	16137867	C	T	EPHA2	c.1298G>A	p.Ser433Asn	missense_variant	MODERATE	0.061	0.003394	
chr1	21238129	C	T	ECE1	c.1389+5G>A	.	ice_region_variant&intron_vari	LOW	0.061	0.004165	
chr1	55171679	C	T	USP24	c.703-1G>A	.	ze_acceptor_variant&intron_vai	HIGH	0.061	0.008002	
chr1	228378629	A	G	OBSCN	c.26606G>A	p.Cys8869Tyr	missense_variant	MODERATE	0.061	0.004421	
chr1	9733986	C	T	CLSTN1	c.2267G>A	p.Gly756Asp	missense_variant	MODERATE	0.06	0.004079	
chr1	33559476	G	A	CSMD2	c.8381-3C>T	.	ice_region_variant&intron_vari	LOW	0.06	0.005226	
chr1	228288446	T	C	OBSCN	c.12947-8C>T	.	ice_region_variant&intron_vari	LOW	0.06	0.005389	
chr1	15725386	C	T	PLEKHM2	c.782C>T	p.Ser261Phe	missense_variant	MODERATE	0.059	0.002208	
chr1	33013382	G	A	AK2	c.519C>T	.	structural_interaction_variant	HIGH	0.059	0.006484	
chr1	20776591	C	T	HP1BP3	c.350+6G>A	.	ice_region_variant&intron_vari	LOW	0.058	0.00709	
chr1	27415977	C	T	WASF2	c.537+8G>A	.	ice_region_variant&intron_vari	LOW	0.058	0.007808	
chr1	28532325	G	A	RCC1	c.509G>A	p.Arg170His	missense_variant	MODERATE	0.058	0.004028	
chr1	45507360	C	T	MMACHC	c.86C>T	p.Ala29Val	missense_variant	MODERATE	0.058	0.011	
chr1	20087353	A	G	GPR25	c.716G>A	p.Arg239Gln	missense_variant	MODERATE	0.058	0.002908	
chr1	3511612	G	A	MEGF6	c.1052C>T	p.Ala351Val	missense_variant	MODERATE	0.057	0.003706	
chr1	15567136	C	T	DNAJC16	c.1816C>T	p.Leu606Phe	missense_variant	MODERATE	0.057	0.006795	
chr1	23431696	C	T	ASAP3	c.2546G>A	p.Ser849Asn	nse_variant&splice_region_va	MODERATE	0.057	0.003925	
chr1	43339264	C	T	MPL	c.392-7C>T	.	ice_region_variant&intron_vari	LOW	0.057	0.005956	
chr1	46408452	C	T	FAAH	c.952-7C>T	.	ice_region_variant&intron_vari	LOW	0.057	0.004766	
chr1	156210236	C	T	SLC25A44	c.778-4C>T	.	ice_region_variant&intron_vari	LOW	0.057	0.00472	
chr1	201889032	C	T	SHISA4	c.38C>T	p.Thr13Ile	missense_variant	MODERATE	0.057	0.003335	
chr1	9609894	G	A	TMEM201	c.1448G>A	p.Gly483Glu	missense_variant	MODERATE	0.056	0.004657	
chr1	27263236	G	A	WDTC1	c.132+1G>A	.	ice_donor_variant&intron_vari	HIGH	0.056	0.006035	
chr1	205774830	C	T	RAB29	c.124+3G>A	.	ice_region_variant&intron_vari	LOW	0.056	0.008493	
chr1	236558258	A	G	HEATR1	c.51837>C	p.Leu1728Pro	missense_variant	MODERATE	0.056	0.004386	
chr1	40835099	G	A	KCNQ4	c.1745+1G>A	.	ice_donor_variant&intron_vari	HIGH	0.055	0.005252	
chr1	202144445	C	T	ARL8A	c.123+5G>A	.	ice_region_variant&intron_vari	LOW	0.055	0.00885	
chr1	11259244	G	A	MTOR	c.162+4C>T	.	ice_region_variant&intron_vari	LOW	0.054	0.004121	
chr1	17359299	G	A	PADI4	c.1649G>A	p.Arg550His	missense_variant	MODERATE	0.054	0.0045	
chr1	24464121	G	A	NIPAL3	c.1021+1G>A	.	ice_donor_variant&intron_vari	HIGH	0.054	0.005752	
chr1	24814086	C	T	CLIC4	c.183-8C>T	.	ice_region_variant&intron_vari	LOW	0.054	0.006005	
chr1	11026989	C	T	MASP2	c.1957G>A	p.Val653Met	missense_variant	MODERATE	0.053	0.003327	
chr1	26469013	G	A	DHDDS	c.887G>A	p.Arg296Gln	missense_variant	MODERATE	0.053	0.003305	
chr1	31730886	C	T	ADGRB2	c.4294G>A	p.Ala1432Thr	missense_variant	MODERATE	0.053	0.00299	
chr1	40240433	G	A	RLF	c.5731G>A	p.Val1911Ile	missense_variant	MODERATE	0.053	0.006757	
chr1	46818165	C	T	CYP4B1	c.1307C>T	p.Ala436Val	missense_variant	MODERATE	0.053	0.003891	
chr1	86455109	G	A	CLCA2	c.2414G>A	p.Ser805Asn	missense_variant	MODERATE	0.053	0.007791	
chr1	90714534	C	T	BARHL2	c.84BG>A	p.Arg28His	missense_variant	MODERATE	0.053	0.004781	
chr1	100539906	T	C	GPR88	c.940C>T	p.Pro314Ser	missense_variant	MODERATE	0.053	0.003345	
chr1	118055728	C	T	SPAG17	c.2722+5G>A	.	ice_region_variant&intron_vari	LOW	0.053	0.012	
chr1	153549930	G	A	S100A4	c.142-7C>T	.	ice_region_variant&intron_vari	LOW	0.053	0.005238	
chr1	155137972	C	T	SLC50A1	c.445-7C>T	.	ice_region_variant&intron_vari	LOW	0.053	0.004834	
chr1	155197486	C	T	THBS3	c.2476G>A	p.Ala826Thr	missense_variant	MODERATE	0.053	0.003435	
chr1	208052328	C	T	PLXNA2	c.2992G>A	p.Gly998Arg	nse_variant&splice_region_va	MODERATE	0.053	0.008973	
chr1	227845612	G	A	PRSS38	c.726G>A	p.Glu242Glu	region_variant&synonymous_v	LOW	0.053	0.003735	
chr1	11189916	C	T	ANGPTL7	c.337C>T	p.Gln113*	stop_gained	HIGH	0.052	0.004266	
chr1	12268699	C	T	VPS13D	c.1802-7C>T	.	ice_region_variant&intron_vari	LOW	0.052	0.006997	
chr1	15034802	C	T	KAZN	c.4720C>T	p.Gln1558*	stop_gained	HIGH	0.052	0.003093	
chr1	30723484	C	T	MATN1	c.680-4A>G	p.Ser23Asn	missense_variant	MODERATE	0.052	0.003449	
chr1	31736316	C	T	ADGRB2	c.3200+5G>A	.	ice_region_variant&intron_vari	LOW	0.052	0.005442	
chr1	42738241	G	A	CLDN19	c.461C>T	p.Pro154Leu	missense_variant	MODERATE	0.052	0.005568	
chr1	43439634	G	A	SZT2	c.6736G>A	p.Asp2246Asn	missense_variant	MODERATE	0.052	0.004372	
chr1	52404763	C	T	PRPF38A	c.14C>T	p.Thr5Ile	missense_variant	MODERATE	0.052	0.005973	
chr1	70353971	C	T	ANKRD13C	c.430+8G>A	.	ice_region_variant&intron_vari	LOW	0.052	0.009807	
chr1	15476546	A	G	CELA2B	c.129+1G>A	.	ice_donor_variant&intron_vari	HIGH	0.051	0.003981	
chr1	15934575	G	A	SPEN	c.8335G>A	p.Ala2778Thr	missense_variant	MODERATE	0.051	0.002248	
chr1	21471563	C	T	NBPF3	c.447-6C>T	.	ice_region_variant&intron_vari	LOW	0.051	0.003264	
chr1	40488214	G	A	ZFP69	c.346G>A	p.Ala116Thr	nse_variant&splice_region_va	MODERATE	0.051	0.007536	
chr1	203175554	C	T	MYBPH	c.202G>A	p.Glu68Lys	missense_variant	MODERATE	0.051	0.004224	
chr1	3505262	C	T	MEGF6	c.2134G>A	p.Gly712Ser	missense_variant	MODERATE	0.05	0.004046	
chr1	11080890	A	G	EXOSC10	c.1460C>T	p.Thr487Met	missense_variant	MODERATE	0.05	0.004634	
chr1	110380886	C	T	SLC16A4	c.522G>A	p.Trp174*	stop_gained	HIGH	0.05	0.006919	
chr2	11450058	A	T	E2F6	c.605T>A	p.Val202Asp	missense_variant	MODERATE	0.263	0.004443	
chr2	107671074	G	C	RGPD4	c.3070G>C	p.Asp1024His	missense_variant	MODERATE	0.244	0.003111	
chr2	133130082	C	A	NCKAP5	c.2376>T	p.Gly792up	missense_variant	MODERATE	0.234	0.003741	
chr2	26470588	C	T	OTOF	c.4023+5G>A	.	ice_region_variant&intron_vari	LOW	0.231	0.005379	
chr2	24298721	C	G	ITSN2	c.1438G>C	p.Glu480Gln	missense_variant	MODERATE	0.21	0.004866	
chr2	208338544	T	C	PKP1YVE	c.4648C>T	p.Pro1550Ser	missense_variant	MODERATE	0.206	0.00613	
chr2	229388308	G	C	DNER	c.1812C>G	p.Asn604Lys	missense_variant	MODERATE	0.196	0.003627	
chr2	174459869	AG	A	GPR155	c.1771+8delC	.	ice_region_variant&intron_vari	LOW	0.109	0.006628	
chr2	86861837	G	A	CD88	c.29C>T	p.Ala10Val	missense_variant	MODERATE	0.097	0.004892	
chr2	20670814	C	T	GDF7	c.742C>T	p.Arg248Trp	missense_variant	MODERATE	0.095	0.006173	
chr2	240875209	G	A	AGXT	c.776+5G>A	.	ice_region_variant&intron_vari	LOW	0.088	0.0066	
chr2	128268286	C	T	HS6ST1	c.1112G>A	p.Arg371His	missense_variant	MODERATE	0.087	0.009946	
chr2	3197024	G	A	TSSC1	c.517-7C>T	.	ice_region_variant&intron_vari	LOW	0.077	0.012	
chr2	112322899	G	A	ZC3H6	c.1337G>A	p.Arg446Lys	missense_variant	MODERATE	0.076	0.009766	
chr2	63055503	C	T	OTX1	c.252C>T	p.Val84Val	region_variant&synonymous_v	LOW	0.075	0.003803	
chr2	219421347	C	T	DES	c.1031C>T	p.Ser344Phe	missense_variant	MODERATE	0.074	0.006853	
chr2	241230752	G	A	HDLBP	c.3474+7C>T	.	ice_region_variant&intron_vari	LOW	0.072	0.012	
chr2	238060298	C	T	SCLY	c.329C>T	p.Ser110Leu	nse_variant&splice_region_va	MODERATE	0.071	0.00762	
chr2	176151842	G	A	HOXD4	c.209G>A	p.Gly70Asp	missense_variant	MODERATE	0.07	0.005313	
chr2	74536933	G	A	LOXL3	c.693-5C>T	.	ice_region_variant&intron_vari	LOW	0.068	0.004562	
chr2	71660554	C	T	DYSF	c.4912-6C>T	.	ice_region_variant&intron_vari	LOW	0.067	0.007447	
chr2	218070746	C	T	RUFY4	c.47-7C>T	.	ice_region_variant&intron_vari	LOW	0.067	0.006006	
chr2	84701343	G	A	DNAH6	c.8061+4G>A	.	ice_region_variant&intron_vari	LOW	0.066	0.008585	
chr2	219557342	C	T	OBSL1	c.4066+1G>A	.	ice_donor_variant&intron_vari	HIGH	0.065	0.003417	
chr2	132783939	C	T	NCKAP5	c.4871+1G>A	.	ice_donor_variant&intron_vari	HIGH	0.064	0.005532	
chr2	240767029	G	A	KIF1A	c.1578-8C>T	.	ice_region_variant&intron_vari	LOW	0.063	0.007148	
chr2	232891357	C	T	NGEF	c.1272+1G>A	.	ice_donor_variant&intron_vari	HIGH	0.062	0.004934	
chr2	173364986	G	A	CDCA7	c.891G>A	p.Met297Ile	missense_variant	MODERATE	0.061	0.005632	
chr2	202090934	G	A	KIAA2012	c.529+5G>A	.	ice_region_variant&intron_vari	LOW	0.061	0.0038	
chr2	135132888	C	T	RAB3GAP1	c.1237-7C>T	.	ice_region_variant&intron_vari	LOW	0.06	0.01	
chr2	178535846	G	A	TTN	c.100769C>T	p.Pro33590Leu	missense_variant	MODERATE	0.06	0.006816	
chr2	74247029	C	T	SLC4A5	c.2059+7G>A	.	ice_region_variant&intron_vari	LOW	0.059	0.005539	
chr2	75696199	C	T	GCFC2	c.833+1G>A	.	ice_donor_variant&intron_vari	HIGH	0.059	0.012	
chr2	96867773	C	T	SEMA4C	c.109+5G>A	.	ice_region_variant&intron_vari	LOW	0.059	0.004533	
chr2	132154675	C	T	ANKRD30BL	n.848G>A	.	n_coding_transcript_exon_varia	MODIFIER	0.059	0.013	
chr2	201582208	G	A	ALS2CR11	c.526C>T	p.Arg176Cys	missense_variant	MODERATE	0.059	0.011	

chr2	217813819	G	A	TNS1	c.4418-3C>T	-	ce_region_variant&intron_vari	LOW	0.059	0.006443
chr2	43813116	C	T	ABCG5	c.1956G>A	p.Ter652Ter	stop_retained_variant	LOW	0.058	0.006722
chr2	231113729	C	T	HTR2B	c.553G>A	p.Gly185Ser	inse_variant&splice_region_va	MODERATE	0.058	0.007464
chr2	84709337	C	T	DNAH6	c.9049-6C>T	-	ce_region_variant&intron_vari	LOW	0.057	0.005637
chr2	108484149	G	A	GCC2	c.3451G>A	p.Asp1151Asn	inse_variant&splice_region_va	MODERATE	0.057	0.01
chr2	240572541	G	A	RNPEPL1	c.647G>A	p.Cys216Tyr	missense_variant	MODERATE	0.057	0.0057
chr2	232524739	C	T	PRSS56	c.1416C>T	p.Gly472Gly	region_variant&synonymous_v	LOW	0.056	0.004061
chr2	29152680	C	T	CLIP4	c.1022-5C>T	-	ce_region_variant&intron_vari	LOW	0.055	0.007591
chr2	96498261	C	T	NEURL3	c.772G>A	p.Val258Ile	missense_variant	MODERATE	0.055	0.004017
chr2	158621052	C	T	PKP4	c.343C>T	p.Leu115Phe	missense_variant	MODERATE	0.055	0.003871
chr2	169198783	C	T	LRP2	c.8578+3G>A	-	ce_region_variant&intron_vari	LOW	0.054	0.009373
chr2	68537891	C	T	APLF	c.824C>T	p.Ser275Phe	missense_variant	MODERATE	0.053	0.008557
chr2	135772427	C	T	UBXN4	c.830C>T	p.Ala277Val	missense_variant	MODERATE	0.053	0.007312
chr2	218073259	C	T	RUFY4	c.403C>T	p.Arg135Trp	missense_variant	MODERATE	0.053	0.003721
chr2	95286476	C	T	PROM2	c.1948-3C>T	-	ce_region_variant&intron_vari	LOW	0.052	0.005974
chr2	99078654	C	T	TSGA10	c.882+5G>A	-	ce_region_variant&intron_vari	LOW	0.052	0.008383
chr2	218403325	G	A	CTDSP1	c.565G>A	p.Val189Met	missense_variant	MODERATE	0.052	0.002254
chr2	21010879	C	T	APOB	c.5989G>A	p.Asp1997Asn	missense_variant	MODERATE	0.051	0.00428
chr2	27729427	C	T	MRPL33	c.149-6C>T	-	ce_region_variant&intron_vari	LOW	0.051	0.011
chr2	73902359	G	A	ACTG2	c.127-1G>A	-	e_acceptor_variant&intron_va	HIGH	0.051	0.004155
chr2	137094895	C	T	THSD7B	c.973C>T	p.Pro325Ser	missense_variant	MODERATE	0.051	0.006091
chr2	233813782	A	A	MROH2A	c.2769+4G>A	-	ce_region_variant&intron_vari	LOW	0.051	0.0047
chr2	238081844	G	A	UBE2F-SCLY	n.1188+8G>A	-	ce_region_variant&intron_vari	LOW	0.051	0.00411
chr2	240746087	C	T	KIF1A	c.3154G>A	p.Ala1052Thr	missense_variant	MODERATE	0.051	0.002009
chr2	3192407	C	T	TSSC1	c.989+7G>A	-	ce_region_variant&intron_vari	LOW	0.05	0.00516
chr2	3741952	C	T	DCDC2C	c.449C>T	p.Pro150Leu	missense_variant	MODERATE	0.05	0.008224
chr2	27222655	G	A	CAD	c.6326>A	p.Ser2114sn	missense_variant	MODERATE	0.05	0.004254
chr2	95901512	C	T	ANKRD36C	c.197G>A	p.Arg66Lys	inse_variant&splice_region_va	MODERATE	0.05	0.006931
chr2	128127453	G	A	UGGT1	c.1226+1G>A	-	ice_donor_variant&intron_vari	HIGH	0.05	0.008194
chr2	135265533	C	T	ZRANB3	c.1539+1G>A	-	ice_donor_variant&intron_vari	HIGH	0.05	0.006922
chr2	218650529	G	A	ZNF142	c.281-3C>T	-	ce_region_variant&intron_vari	LOW	0.05	0.007756
chr2	233842212	G	A	HUIRP	c.575-7C>T	-	ce_region_variant&intron_vari	LOW	0.05	0.012
chr2	240873979	C	T	AGXT	c.597C>T	-	structural_interaction_variant	HIGH	0.05	0.003044
chr3	70965985	T	A	FOXP1	c.1842A>T	p.Leu614Phe	missense_variant	MODERATE	0.348	0.002697
chr3	36855175	G	C	TRANK1	c.4547C>G	p.Ser1516*	p_gained&splice_region_varia	HIGH	0.263	0.005053
chr3	185689353	A	T	IGF2BP2	c.695+2T>A	-	ice_donor_variant&intron_vari	HIGH	0.255	0.003771
chr3	187370955	C	A	RTP4	c.323C>A	p.Ser108*	stop_gained	HIGH	0.239	0.002863
chr3	154421401	C	T	GPR149	c.1261G>A	p.Asp421Asn	missense_variant	MODERATE	0.228	0.005268
chr3	49358049	G	C	EPX1	c.230C>G	p.Pro77Arg	missense_variant	MODERATE	0.221	0.014
chr3	179218294	G	A	PIK3CA	c.1624G>A	-	protein_protein_contact	HIGH	0.214	0.005607
chr3	49110947	C	T	USP19	c.3539+3G>A	-	ce_region_variant&intron_vari	LOW	0.111	0.002933
chr3	186720186	G	C	KNG1	c.277G>C	p.Asp93His	missense_variant	MODERATE	0.109	0.004162
chr3	52802519	G	A	ITIH3	c.1569G>A	p.Gly523Gly	region_variant&synonymous_v	LOW	0.092	0.00393
chr3	13571358	A	G	FBLN2	c.1003A>G	p.Arg335Gly	missense_variant	MODERATE	0.09	0.002285
chr3	48422118	C	T	PLXNB1	c.1507G>A	p.Val503Met	missense_variant	MODERATE	0.085	0.004162
chr3	129091351	G	A	RAB43	c.389-5C>T	-	ce_region_variant&intron_vari	LOW	0.081	0.004295
chr3	38726608	G	A	SCN10A	c.3085C>T	p.Gln1029*	p_gained&splice_region_varia	HIGH	0.08	0.004966
chr3	48459917	G	A	ATRIP	c.1855+1G>A	-	ice_donor_variant&intron_vari	HIGH	0.079	0.005404
chr3	52806413	C	T	ITIH3	c.2056+7C>T	-	ce_region_variant&intron_vari	LOW	0.076	0.005235
chr3	52388341	G	A	DNAH1	c.9171+7G>A	-	ce_region_variant&intron_vari	LOW	0.075	0.008907
chr3	49311640	G	A	USP4	c.710C>T	p.Pro237Leu	missense_variant	MODERATE	0.074	0.007555
chr3	48402025	G	A	PLXNB1	c.2081C>T	p.Pro694Leu	missense_variant	MODERATE	0.072	0.004267
chr3	49241394	G	A	CCDC36	c.395+5G>A	-	ce_region_variant&intron_vari	LOW	0.071	0.00733
chr3	53228051	C	T	TKT	c.1597+5G>A	-	ce_region_variant&intron_vari	LOW	0.071	0.006607
chr3	48649121	C	T	CELSR3	c.6567G>A	p.Leu2189Leu	region_variant&synonymous_v	LOW	0.069	0.004327
chr3	49033113	C	T	QRICH1	c.1895+7G>A	-	ce_region_variant&intron_vari	LOW	0.069	0.004614
chr3	184060145	C	T	HTR3C	c.1142-5C>T	-	ce_region_variant&intron_vari	LOW	0.067	0.00321
chr3	50367492	G	A	CACNA2D2	c.2324C>T	p.Ala775Val	missense_variant	MODERATE	0.065	0.00401
chr3	50273909	C	T	SEMA3B	c.1008-4C>T	-	ce_region_variant&intron_vari	LOW	0.064	0.005165
chr3	53288057	C	T	DCP1A	c.1668+8G>A	-	ce_region_variant&intron_vari	LOW	0.064	0.007895
chr3	136259243	G	A	PCCB	c.432+8G>A	-	ce_region_variant&intron_vari	LOW	0.063	0.009315
chr3	48627991	G	A	SLC26A6	c.1848C>T	-	sequence_feature	MODERATE	0.062	0.003962
chr3	50646818	G	A	MAPKAPK3	c.908G>A	p.Trp303*	stop_gained	HIGH	0.062	0.003795
chr3	52786848	G	T	ITIH3	c.386+5G>T	-	ce_region_variant&intron_vari	LOW	0.062	0.004911
chr3	127677706	C	T	ABTB1	c.892C>T	p.Arg298*	stop_gained	HIGH	0.061	0.002889
chr3	43052564	G	A	FAM198A	c.3016>A	p.Val1010Met	missense_variant	MODERATE	0.06	0.003081
chr3	49119019	C	T	USP19	c.124+3G>A	-	ce_region_variant&intron_vari	LOW	0.06	0.005162
chr3	133390323	G	A	TMEM108	c.1596G>A	p.Glu532Lys	missense_variant	MODERATE	0.06	0.003714
chr3	58333008	C	T	PXK	c.20C>T	p.Pro7Leu	missense_variant	MODERATE	0.059	0.005566
chr3	9943071	C	T	CRELD1	c.818-6C>T	-	ce_region_variant&intron_vari	LOW	0.058	0.005031
chr3	47265727	C	T	KIF9	c.916+3G>A	-	ce_region_variant&intron_vari	LOW	0.058	0.004102
chr3	49013768	C	T	WDR6	c.2324C>T	p.Thr775Ile	missense_variant	MODERATE	0.058	0.002289
chr3	52383987	G	A	DNAH1	c.8278G>A	p.Glu2760Lys	missense_variant	MODERATE	0.058	0.003575
chr3	12816002	G	A	CAND2	c.1435G>A	p.Val479Ile	missense_variant	MODERATE	0.057	0.00439
chr3	47007073	G	A	NBEAL2	c.7142G>A	p.Ser2381Asn	missense_variant	MODERATE	0.057	0.002992
chr3	48416163	G	A	PLXNB1	c.348SC>T	p.Pro1162Leu	missense_variant	MODERATE	0.057	0.003334
chr3	50273782	C	T	SEMA3B	c.961C>T	p.Arg321Trp	missense_variant	MODERATE	0.056	0.002447
chr3	132690528	C	T	NPHP3	c.2693G>A	p.Arg898Lys	inse_variant&splice_region_va	MODERATE	0.056	0.007264
chr3	151443887	G	A	IGSF10	c.5063-3C>T	-	ce_region_variant&intron_vari	LOW	0.056	0.006128
chr3	184354096	C	T	CLDN2	c.1721+5G>A	-	ce_region_variant&intron_vari	LOW	0.056	0.005334
chr3	49793829	G	A	CDH84	c.1457C>T	p.Thr486Ile	missense_variant	MODERATE	0.055	0.002847
chr3	56296429	G	A	ERC2	c.664C>T	p.Gln222*	stop_gained	HIGH	0.055	0.005199
chr3	108688596	C	T	DZIP3	c.3274C>T	p.Gln1092*	stop_gained	HIGH	0.055	0.004819
chr3	3053978	G	A	CNTN4	c.2980+3G>A	-	ce_region_variant&intron_vari	LOW	0.054	0.004276
chr3	14525453	C	T	GRIP2	c.241G>A	p.Gly81Arg	missense_variant	MODERATE	0.054	0.005311
chr3	39128937	A	A	TTC21A	c.1917+5G>A	-	ce_region_variant&intron_vari	LOW	0.054	0.003445
chr3	47404668	C	T	PTPN23	c.176C>T	p.Pro59Leu	missense_variant	MODERATE	0.054	0.003758
chr3	48600083	C	T	UQCRC1	c.128ZG>A	p.Glu428Lys	missense_variant	MODERATE	0.054	0.004079
chr3	123330888	C	T	ADCY5	c.1646+1G>A	-	ice_donor_variant&intron_vari	HIGH	0.054	0.005158
chr3	127668598	G	A	PODN2	c.1363+1G>A	-	ice_donor_variant&intron_vari	HIGH	0.054	0.011
chr3	136250544	G	A	PCCB	c.169G>A	p.Ala57Thr	missense_variant	MODERATE	0.054	0.003306
chr3	158105993	G	A	SHOX2	c.32C>T	p.Ser11Phe	missense_variant	MODERATE	0.054	0.006959
chr3	10074524	C	T	FAND2	c.2716-6C>T	-	ce_region_variant&intron_vari	LOW	0.053	0.005723
chr3	14926194	G	A	FGD5	c.4193G>A	p.Ser1398Asn	missense_variant	MODERATE	0.053	0.005854
chr3	49913220	C	T	MON1A	c.418G>A	p.Gly140Ser	inse_variant&splice_region_va	MODERATE	0.053	0.0043
chr3	190609186	G	A	IL1RAP	c.537+5G>A	-	ce_region_variant&intron_vari	LOW	0.053	0.007509
chr3	12924593	C	T	IQSEC1	c.1718G>A	p.Arg573His	missense_variant	MODERATE	0.052	0.003177
chr3	33516138	G	A	CLASP2	c.4022>T	p.Ala1341Val	missense_variant	MODERATE	0.052	0.007702
chr3	44900861	G	A	TGM4	c.1088G>A	p.Cys363Tyr	missense_variant	MODERATE	0.052	0.005056
chr3	46685593	G	A	ALS2CL	c.718C>T	p.Pro240Ser	missense_variant	MODERATE	0.052	0.007363
chr3	47442999	G	A	SCAP	c.-6C>T	-	TR_premature_start_codon_ga	LOW	0.052	0.004142
chr3	114018677	C	T	CCDC191	c.1163+1G>A	-	ice_donor_variant&intron_vari	HIGH	0.052	0.00806
chr3	114159750	C	T	DRD3	c.383+5G>A	-	ce_region_variant&intron_vari	LOW	0.052	0.005591
chr3	123793847	G	A	MYLK	c.-3-3C>T	-	ce_region_variant&intron_vari	LOW	0.052	0.008725
chr3	47435009	C	T	SCAP	c.2516>A	p.Trp84*	p_gained&splice_region_varia	HIGH	0.051	0.004534
chr3	47680492	G	A	SMARCC1	c.1402C>T	p.Arg468Trp	missense_variant	MODERATE	0.051	0.007701
chr3	45011334	G	A	EXOSC7	c.871G>A	p.Gly291Arg	missense_variant	MODERATE	0.05	0.005007
chr3	123347906	G	A	ADCY5	c.1285-3C>T	-	ce_region_variant&intron_vari	LOW	0.05	0.004273
chr3	130401040	C	T	COL6A5	c.4001C>T	p.Ala1334Val	missense_variant	MODERATE	0.05	0.006463
chr3	158710733	C	T	RARRES1	c.535+5G>A	-	ce_region_variant&intron_vari	LOW	0.05	0.006847
chr4	154589402	C	T	FGA	c.125G>A	p.Arg42Lys	missense_variant	MODERATE	0.215	0.003705
chr4	108014509	G	A	HADH	c.340G>A	p.Asp144Asn	missense_variant	MODERATE	0.214	0.003673
chr4	157078109	A	G	GLRB	c.85A>G	p.Lys29Glu	missense_variant	MODERATE	0.156	0.007527
chr4	6716348	G	A	BLOC1S4	c.139G>A	p.Glu47Lys	missense_variant	MODERATE	0.142	0.007231
chr4	657012	A	A	PDE6B	c.1246G>A	p.Val416Ile	missense_variant	MODERATE	0.111	0.003452
chr4	2238603	C	T	HAUS3	c.1349+1G>A	-	ice_donor_variant&intron_vari	HIGH	0.094	0.011
chr4	25377421	C	T	ANAPC4	c.-7C>T	-	TR_premature_start_codon_ga	LOW	0.094	0.009288
chr4	38988078	G	A	TMEM156	c.620-8C>T	-	ce_region_variant&intron_vari	LOW	0.085	0.012
chr4	10540494	C	T	CLNK	c.602G>A	p.Ser201Asn	inse_variant&splice_region_va	MODERATE	0.079	0.005342
chr4	5731658	G	A	EVC	c.617+1G>A	-	ice_donor_variant&intron_vari	HIGH	0.077	0.004109
chr4	47515671	G	A	ATP10D	c.485+1G>A	-	ice_donor_variant&intron_vari	HIGH	0.075	0.008881
chr4	38988012	G	A	TMEM156	c.89-3C>T	-	ce_region_variant&intron_vari	LOW	0.069	0.009166
chr4	185267163	G	A	SNX25	c.599+8G>A	-	ce_region_variant&intron_vari	LOW	0.065	0.012
chr4	3188943	C	T	HTT	c.5226-8C>T	-	ce_region_variant&intron_vari	LOW	0.061	0.007242
chr4	761275	G	A	PDCF3	c.463-4G>A	-	ce_region_variant&intron_vari	LOW	0.06	0.007947
chr4	88390879	G	A	HERC6	c.664G>A	p.Val222Met	inse_variant&splice_region_va	MODERATE	0.06	0.005011
chr4	153788340	C	T	SFRP2	c.496G>A	p.Glu166Lys	missense_variant	MODERATE	0.06	0.004549
chr4	3316232	G	A	RGS12	c.62G>A	p.Arg21Gln	missense_variant	MODERATE	0.059	0.002776
chr4	84410358	G	A	ACOX3	c.544-3C>T	-	ce_region_variant&intron_vari	LOW	0.058	0.005782
chr4	39863350	C	T	PDSSA	c.2752G>A	p.Ala918Thr	missense_variant	MODERATE	0.057	0.008351
chr4	186609176	C	T	FAT1	c.10206+7G>A	-	ce_region_variant&intron_vari	LOW	0.057	0.00495
chr4	5618495	C	T	EVC2	c.2689G>A	p.Ala897Thr	missense_variant	MODERATE	0.056	0.008338
chr4	98420151	G	A	RAP1GDS1	c.1303+7G>A	-	ce_region_variant&intron_vari	LOW	0.056	0.01
chr4	36210385	C	T	ARAP2	c.1487+5G>A	-	ce_region_variant&intron_vari	LOW	0.055	0.006379
chr4	52076784	C	T	SPATA18	c.764C>T	p.Ser255Phe	missense_variant	MODERATE	0.055	0.004231
chr4	20488983	G	A	SLIT2	c.775+1G>A	-	ice_donor_variant&intron_vari	HIGH	0.053	0.008318
chr4	39862868	C	T	PDSSA	c.2971+1G>A	-	ice_donor_variant&intron_vari	HIGH	0.053	0.006959
chr4	24529596	C	T	DHX15	c.2270+5G>A	-	ce_region_variant&intron_vari	LOW	0.051	0.005572
chr4	83295511	G	A	HPSE	c.1473-8C>T	-	ce_region_variant&intron_vari	LOW	0.051	0.006346
chr4	121925029	C	T	TRPC3	c.1165G>A	p.Glu389Lys	missense_variant	MODERATE	0.051	0.005315
chr4	184408283	G	A	IRF2	c.412-8C>T	-	ce_region_variant&intron_vari	LOW	0.051	0.005332
chr4	185339505	G	A	SNX25	c.1549G>A	p.Gly517Arg	missense_variant	MODERATE	0.051	0.007081
chr4	119268280	C	T	USP53	c.1148C>T	p.Pro383Leu	missense_variant	MODERATE	0.05	0.012
chr4	140823972	C	T	PCDHA5	c.2197C>T	p.Arg733Trp	missense_variant	MODERATE	0.514	0.00187
chr5	141864056	C	T	PCDH1	c.2275G>A	p.Gly759Ser	missense_variant	MODERATE	0.286	0.002582
chr5	159972229	G	A	ADRA1B	c.1300G>A	p.Gly434Ser	missense_variant	MODERATE	0.255	0.011
chr5	178886665	ATCT	A	GRM6	c.1586_1588delAGA	p.Lys529del	disruptive_inframe_deletion	MODERATE	0.246	0.001787
chr5	13931104	T	A	DNAH5	c.192+6A>T	-	ce_region_variant&intron_vari	LOW	0.155	0.005234
chr5	35871115	G	C	IL7R	c.439G>C	p.Val147Leu	missense_variant	MODERATE	0.101	0.003955
chr5	153646934	C	T	GRIA1	c.257C>T	p.Ser86Phe	missense_variant	MODERATE	0.089	0.007122
chr5	179733224	G	A	MAML1	c.1126>A	p.Glu38Lys	missense_variant	MODERATE	0.086	0.005285
chr5	179153626	G	A	ADAMTS2	c.1383-3C>T	-	ce_region_variant&intron_vari	LOW	0.085	0.004785
chr5	179140038	G	A	ADAMTS2	c.1630-3C>T	-	ce_region_variant&intron_vari	LOW	0.08	0.003833
chr5	153770420	G	A	GRIA1	c.2300+5G>A	-	ce_region_variant&intron_vari	LOW	0.078	0.00588
chr5	134306617	G	A	CDK3	c.1450C>T	p.Pro484Ser	missense_variant	MODERATE	0.075	0.005912
chr5	138018519	G	A	FAM13B	c.158-5C>T	-	ce_region_variant&intron_vari	LOW	0.073	0.01
chr5	140641659	C	T	TMCO6	c.199-6C>T	-	ce_region_variant&intron_vari	LOW	0.068	0.005005
chr5	50441094	G	A	EMB	c.58C>T	p.Leu20Phe	missense_variant	MODERATE	0.066	0.004545
chr5	132603914	C	T	RADSO	c.2398-6C>T	-	ce_region_variant&intron_vari	LOW	0.066	0.006643
chr5	154935842	C	T	GEMIN5	c.5086>A	p.Gly1705er	inse_variant&splice_region_va	MODERATE	0.065	0.007145
chr5	140659167	G	A	IK	c.1176+3G>A	-	ce_region_variant&intron_vari	LOW	0.064	0.005401
chr5	127422663	C	T	MEGF10	c.1591-7C>T	-	ce_region_variant&intron_vari	LOW	0.063	0.006413
chr5	150256763	C	T	CAMK2A	c.338+3G>A	-	ce_region_variant&intron_vari	LOW	0.062	0.004033
chr5	151803979	G	A	G3BP1	c.1289G>A	p.Gly430Glu	missense_variant	MODERATE	0.062	0.003298
chr5	157326168	C	T	CYFIP2	c.2058-3C>T	-	ce_region_variant&intron_vari	LOW	0.062	0.005215
chr5	138091541	G	A	WNTBA	c.*1G>A	-	splice_region_variant	LOW	0.061	0.007988
chr5	146060117	G	A	SH3RF2	c.1807G>A	p.Glu603Lys	missense_variant	MODERATE	0.06	0.00613
chr5	3600677	G	A	IRX1	c.1381G>A	p.Asp461Asn	missense_variant	MODERATE	0.059	0.00545
chr5	146691232	C	T	PPP2R2B	c.661G>A	p.Val221Met	missense_variant	MODERATE	0.059	0.005305
chr5	120685954	G	A	PRR16	c.160G>A	p.Val54Met	inse_variant&splice_region_va	MODERATE	0.058	0.005389
chr5	149996354	G	A	TIGD6	c.-6C>T	-	TR_premature_start_codon_ga	LOW	0.058	0.004804
chr5	129704240	G	A	ADAMTS19	c.3161G>A	p.Cys1054Tyr	inse_variant&splice_region_va	MODERATE	0.057	0.005081
chr5	132604829	C	T	RADSO	c.2548C>T	p.Arg850Cys	missense_variant	MODERATE	0.057	0.004905
chr5	128141824	C	T	SLC12A2	c.1622-6C>T	-	ce_region_variant&intron_vari	LOW	0.056	0.008011
chr5	132642175	C	T	RADSO	c.3753-3C>T	-	ce_region_variant&intron_vari	LOW	0.056	0.006095
chr5	160606765	C	T	ATP10B	c.3160G>A	p.Gly1054Ser	inse_variant&splice_region_va	MODERATE	0.056	0.00672
chr5	180616905	G	A	FLT4	c.3091C>T	p.Arg1031*	stop_gained	HIGH	0.056	0.003126
chr5	81068037	C	T	RASGRF2	c.401C>T	p.Ala134Val	missense_variant	MODERATE	0.055	0.005971
chr5	140807239	C	T	PCDHA4	c.52C>T	p.Leu18Phe	missense_variant	MODERATE	0.055	0.002557
chr5	140807312	G	A	PCDHA4	c.125G>A	p.Gly42Asp	missense_variant	MODERATE	0.054	0.005182
chr5	132708906	C	T	KIF3A	c.1300+1G>A	-	ice_donor_variant&intron_vari	HIGH	0.053	0.007516
chr5	13792326	G	A	PKD12	c.1551+5G>A	-	ce_region_variant&intron_vari	LOW	0.053	0.018
chr5	138165153	G	A	BRD8	c.1292C>T	p.Pro431Leu	missense_variant	MODERATE	0.053	0.005183
chr5	139308313	G	A	MATR3	c.898G>A	p.Val300Ile	missense_variant	MODERATE	0.053	0.005407
chr5	151804080	G	A	G3BP1	c.1400G>A	p.Ter467Ter	stop_retained_variant	LOW	0.053	0.004438
chr5	72197847	G	A	MAP1B	c.4492G>A	p.Gly1498Arg	missense_variant	MODERATE	0.052	0.003527
chr5	80202895	C	T	SERINC5	c.186G>A	p.Met62Ile	missense_variant	MODERATE	0.052	0.005106
chr5	119496653	G	A	HSD17B4	c.1047>7G>A	-	ce_region_variant&intron_vari	LOW	0.052	0.006419
chr5	140562414	C	T	APBB3	c.437G>A	p.Cys146Tyr	missense_variant	MODERATE	0.052	0.002954
chr5	72186752	G	A	MAP1B	c.508G>A	p.Glu170Lys	inse_variant&splice_region_va	MODERATE	0.051	0.005669

chr5	147351062	C	T	STK32A	c.473-3C>T	.	ice_region_variant&intron_vari	LOW	0.051	0.004508
chr5	109362842	C	T	PIAS	c.1650G>A	p.Trp550*	op_gained&splice_region_varia	HIGH	0.05	0.005031
chr5	138568920	C	T	HSPA9	c.535+5G>A	.	ice_region_variant&intron_vari	LOW	0.05	0.006443
chr5	151543094	C	T	FAT2	c.8033G>A	p.Arg2678Gln	missense_variant	MODERATE	0.05	0.004487
chr6	139260410	C	T	TXLNB	c.910G>A	p.Glu304Lys	missense_variant	MODERATE	0.26	0.005413
chr6	32129494	A	C	FKBPL.4	c.287T>G	p.Leu96Arg	missense_variant	MODERATE	0.243	0.002221
chr6	30898070	C	G	DDR1	c.2235-3C>G	.	ice_region_variant&intron_vari	LOW	0.231	0.003028
chr6	34133367	G	A	GRM4	c.130C>T	p.Arg44Cys	missense_variant	MODERATE	0.229	0.002355
chr6	2890514	C	T	SERPINB9	c.780G>A	p.Met260Ile	missense_variant	MODERATE	0.227	0.003543
chr6	30897115	A	T	DDR1	c.1971A>T	p.Leu657Phe	missense_variant	MODERATE	0.223	0.003136
chr6	43132143	G	T	PTK7	c.964G>T	p.Glu322*	stop_gained	HIGH	0.213	0.004219
chr6	100848354	ACTT	A	ASCC3	c.592_594delAAG	p.Lys198del	onservative_inframe_deletion	MODERATE	0.207	0.00468
chr6	31645444	G	A	BAG6	c.1087C>T	p.Thr363Ile	missense_variant	MODERATE	0.203	0.001986
chr6	137044634	C	T	IL20RA	c.88+7G>A	.	ice_region_variant&intron_vari	LOW	0.111	0.013
chr6	30589976	T	A	ABCF1	c.2233+2T>A	.	ice_donor_variant&intron_vari	HIGH	0.081	0.002787
chr6	43645106	C	T	RSPH9	c.8C>T	p.Ala3Val	missense_variant	MODERATE	0.078	0.003772
chr6	73408102	G	A	DDX43	c.1179+1G>A	.	ice_donor_variant&intron_vari	HIGH	0.073	0.007512
chr6	83921180	G	A	CYB5R4	c.658+5G>A	.	ice_region_variant&intron_vari	LOW	0.073	0.008928
chr6	169636507	G	A	WDR27	c.1870-3C>T	.	ice_region_variant&intron_vari	LOW	0.072	0.011
chr6	52053094	C	T	PKHD1	c.2122G>A	p.Ala708Thr	missense_variant	MODERATE	0.071	0.00658
chr6	36717420	G	A	RAB44	c.641+1G>A	.	ice_donor_variant&intron_vari	HIGH	0.07	0.011
chr6	32068819	C	T	TNXB.2	c.5902+3G>A	.	ice_region_variant&intron_vari	LOW	0.066	0.004289
chr6	158608329	C	T	TMEM181	c.1085-4C>T	.	ice_region_variant&intron_vari	LOW	0.066	0.005888
chr6	50715132	C	T	TFAP2D	c.56C>T	p.Ser19Leu	missense_variant	MODERATE	0.065	0.004489
chr6	73395155	G	A	DDX43	c.2500>A	p.Gly845Ser	nse_variant&splice_region_va	MODERATE	0.065	0.004931
chr6	31507105	C	T	MICB	c.697C>T	p.Arg233Trp	missense_variant	MODERATE	0.064	0.003255
chr6	33398026	C	T	KIFC1	c.13-3C>T	.	ice_region_variant&intron_vari	LOW	0.064	0.004096
chr6	33682525	C	T	ITPR3	c.4478C>T	p.Thr1493Ile	nse_variant&splice_region_va	MODERATE	0.062	0.004216
chr6	15496718	A	G	IARS1D2	c.1483G>A	p.Asp495Gln	missense_variant	MODERATE	0.059	0.001987
chr6	33695090	G	A	ITPR3	c.7947+5G>A	.	ice_region_variant&intron_vari	LOW	0.059	0.005074
chr6	87616432	G	A	ORC3	c.987+5G>A	.	ice_region_variant&intron_vari	LOW	0.059	0.013
chr6	160509944	C	T	LPA	c.3787G>A	p.Ala1263Thr	nse_variant&splice_region_va	MODERATE	0.059	0.004244
chr6	31507121	C	G	MICB	c.713C>G	p.Thr238Ser	missense_variant	MODERATE	0.058	0.00327
chr6	70281027	G	A	COL9A1	c.889C>T	p.Pro297Ser	missense_variant	MODERATE	0.056	0.004935
chr6	30546080	C	T	GNL1	c.1816G>A	p.Glu606Lys	missense_variant	MODERATE	0.054	0.003324
chr6	152232136	C	T	SYNE1	c.20842G>A	p.Glu6948Lys	missense_variant	MODERATE	0.054	0.008594
chr6	31032586	G	A	MUC22	c.5064+5G>A	.	ice_region_variant&intron_vari	LOW	0.053	0.003374
chr6	160736882	C	T	PLG	c.1682-5C>T	.	ice_region_variant&intron_vari	LOW	0.053	0.007391
chr6	37011057	A	G	FGD2	c.378+7G>A	.	ice_region_variant&intron_vari	LOW	0.052	0.004135
chr6	46689134	C	T	TDRD6	c.1006C>T	p.Arg336Trp	missense_variant	MODERATE	0.052	0.003669
chr6	24134522	G	A	NR5N1	c.189+6G>A	.	ice_region_variant&intron_vari	LOW	0.051	0.005829
chr6	24873804	G	A	FAM65B	c.102-5C>T	.	ice_region_variant&intron_vari	LOW	0.051	0.007629
chr6	44404024	G	A	CDC5L	c.755G>A	p.Arg252Lys	missense_variant	MODERATE	0.051	0.011
chr6	53273219	C	T	ELOVL5	c.702+1G>A	.	ice_donor_variant&intron_vari	HIGH	0.051	0.005532
chr6	89695616	C	T	MDN1	c.97606>A	p.Val13541le	missense_variant	MODERATE	0.05	0.005063
chr6	144539446	G	A	UTRN	c.6519+3G>A	.	ice_region_variant&intron_vari	LOW	0.05	0.011
chr7	121130194	G	T	CPED1	c.1477G>T	p.Gly493*	stop_gained	HIGH	0.464	0.004883
chr7	73682909	T	G	DNAJC30	c.515A>C	p.Tyr172Ser	missense_variant	MODERATE	0.254	0.002868
chr7	103635528	G	T	RELN	c.2362C>A	p.Pro788Thr	missense_variant	MODERATE	0.252	0.004066
chr7	44073775	C	:TGCCTACC	POLM	c.1073_1074+7dupAGGTAGGCA	.	ice_region_variant&intron_vari	LOW	0.25	0.003165
chr7	44073805	AG	A	POLM	c.1051delC	p.Leu351fs	frameshift_variant	HIGH	0.247	0.002851
chr7	71665403	A	T	WBSCR17	c.1081-8A>T	.	ice_region_variant&intron_vari	LOW	0.219	0.004808
chr7	21687241	C	A	DNAH11	c.5764C>A	p.Gln1922Lys	missense_variant	MODERATE	0.208	0.004595
chr7	137846455	C	T	DGKI	c.401+7G>A	.	ice_region_variant&intron_vari	LOW	0.174	0.006924
chr7	4860400	G	T	PAPOLB	c.1411C>A	p.Gln471Lys	missense_variant	MODERATE	0.129	0.00323
chr7	100822656	C	T	EPHB4	c.423G>A	.	structural_interaction_variant	HIGH	0.102	0.00458
chr7	67083465	G	A	TYW1	c.1310G>A	p.Trp437*	stop_gained	HIGH	0.101	0.00783
chr7	143703259	C	T	TCAF2	c.265C>T	p.Pro89Ser	missense_variant	MODERATE	0.1	0.012
chr7	151632122	G	A	PRKAG2	c.701C>T	p.Ala234Val	missense_variant	MODERATE	0.1	0.007276
chr7	44110012	C	T	AEBP1	c.1151-3C>T	.	ice_region_variant&intron_vari	LOW	0.097	0.00446
chr7	6622828	C	T	ZNF853	c.1837C>T	p.Arg613Cys	missense_variant	MODERATE	0.092	0.003561
chr7	50057989	C	T	ZPBP	c.487G>A	p.Ala163Thr	nse_variant&splice_region_va	MODERATE	0.091	0.011
chr7	102466275	G	A	LRWD1	c.432+5G>A	.	ice_region_variant&intron_vari	LOW	0.089	0.007203
chr7	128840540	C	T	FLNC	c.1550-8C>T	.	ice_region_variant&intron_vari	LOW	0.088	0.003869
chr7	149278521	G	A	ZNF783	c.796G>A	p.Glu266Lys	missense_variant	MODERATE	0.088	0.005092
chr7	33905753	G	A	BMPER	c.133+7G>A	.	ice_region_variant&intron_vari	LOW	0.084	0.007823
chr7	130041041	A	C	ZCHC1	c.319T>G	p.Trp107Gly	missense_variant	MODERATE	0.082	0.003496
chr7	102300653	G	A	SH2B2	c.232G>A	p.Ala78Thr	missense_variant	MODERATE	0.078	0.009186
chr7	130385139	C	T	CPA1	c.788-7C>T	.	ice_region_variant&intron_vari	LOW	0.078	0.004367
chr7	127694953	G	A	SND1	c.349+5G>A	.	ice_region_variant&intron_vari	LOW	0.075	0.005015
chr7	31873562	G	A	PTPN21	c.58+5G>A	.	ice_region_variant&intron_vari	LOW	0.074	0.004501
chr7	111741540	C	T	DOCK4	c.4892G>A	p.Ser1631Asn	nse_variant&splice_region_va	MODERATE	0.073	0.007643
chr7	100030383	G	A	ZKSCAN1	c.799+8G>A	.	ice_region_variant&intron_vari	LOW	0.071	0.005393
chr7	99710732	C	T	9'3A7-CYP3A5	c.1026G>A	p.Lys342Lys	region_variant&synonymous_v	LOW	0.07	0.00443
chr7	132210960	G	A	PLXNA4	c.2281C>T	p.Gln761*	stop_gained	HIGH	0.07	0.004254
chr7	139596716	C	T	HIPK2	c.2717+1G>A	.	ice_donor_variant&intron_vari	HIGH	0.07	0.005337
chr7	2314358	C	T	SNX8	c.64G>A	p.Ala22Thr	missense_variant	MODERATE	0.069	0.004104
chr7	141935958	G	A	CLECSA	c.209-8C>T	.	ice_region_variant&intron_vari	LOW	0.067	0.006321
chr7	151235615	G	A	CHPF2	c.828+3G>A	.	ice_region_variant&intron_vari	LOW	0.067	0.004467
chr7	99951426	C	T	CDK13	c.785C>T	p.Ser262Leu	missense_variant	MODERATE	0.065	0.003159
chr7	75021919	G	A	GATSL2	c.792G>A	p.Trp264*	stop_gained	HIGH	0.064	0.004933
chr7	135721513	C	T	SLC13A4	c.1100>A	p.Cys371Tyr	missense_variant	MODERATE	0.064	0.004012
chr7	144188360	ACGC	A	ARHGEF35	c.23_24insGCG	.His8GlnfsinsGlnfs	disruptive_inframe_insertion	MODERATE	0.064	0.004311
chr7	144188361	T	:TCCTCAGC	ARHGEF35	c.22_23insGTGGAGGCTGAGGAGGCCC	p.His8fs	rameshift_variant&stop_gaine	HIGH	0.064	0.004311
chr7	149777988	G	A	SSPO	c.778G>A	p.Gly260Arg	missense_variant	MODERATE	0.064	0.003572
chr7	139283026	G	A	UBN2	c.2121G>A	p.Glu707Glu	region_variant&synonymous_v	LOW	0.063	0.008958
chr7	138504408	G	A	TRIM24	c.483G>A	p.Gln161Gln	region_variant&synonymous_v	LOW	0.062	0.009709
chr7	149806868	C	T	SSPO	c.8783C>T	p.Thr2928Ile	missense_variant	MODERATE	0.062	0.003524
chr7	108182701	C	T	NRCAM	c.2524G>A	p.Gly842Lys	missense_variant	MODERATE	0.061	0.005669
chr7	130173824	C	T	TMEM209	c.1459+1G>A	.	ice_donor_variant&intron_vari	HIGH	0.061	0.005726
chr7	132130492	C	T	PLXNA4	c.5672G>A	p.Ser1891Asn	missense_variant	MODERATE	0.061	0.005573
chr7	64979264	G	A	ZNF117	c.307C>T	p.His103Tyr	missense_variant	MODERATE	0.06	0.006756
chr7	93252783	G	A	VPS50	c.225+8G>A	.	ice_region_variant&intron_vari	LOW	0.06	0.008791
chr7	100562324	G	A	AGFG2	c.943G>A	p.Ala315Thr	missense_variant	MODERATE	0.06	0.003773
chr7	512462	G	A	P0GFA	c.161-7C>T	.	ice_region_variant&intron_vari	LOW	0.059	0.00446
chr7	102467348	C	T	LRWD1	c.442C>T	p.His148Tyr	missense_variant	MODERATE	0.059	0.004476
chr7	111741543	C	T	DOCK4	c.4889G>A	p.Arg1630His	missense_variant	MODERATE	0.058	0.007528
chr7	130672884	G	A	TSGA13	c.388-8C>T	.	ice_region_variant&intron_vari	LOW	0.058	0.006111
chr7	102446811	C	T	ORAI2	c.524C>T	p.Pro175Leu	missense_variant	MODERATE	0.057	0.002119
chr7	77908955	G	A	PHTF2	c.5066>A	p.Arg1695Lys	missense_variant	MODERATE	0.056	0.005643
chr7	140426098	G	A	RAB19	c.602G>A	p.Ser201Asn	missense_variant	MODERATE	0.056	0.003296
chr7	135573098	C	T	NUP205	c.29-7C>T	.	ice_region_variant&intron_vari	LOW	0.055	0.017
chr7	139281999	C	T	UBN2	c.2068-6C>T	.	ice_region_variant&intron_vari	LOW	0.055	0.00823
chr7	154954255	C	T	PAXIP1	c.2821G>A	p.Asp941Asn	nse_variant&splice_region_va	MODERATE	0.055	0.005941
chr7	32169945	G	A	PDE1C	c.148C>T	p.Gln50*	stop_gained	HIGH	0.054	0.003878
chr7	8284751	G	A	PCLO	c.13655-4C>T	.	ice_region_variant&intron_vari	LOW	0.054	0.006813
chr7	99648330	C	T	CYP3A5	c.1484G>A	p.Arg495Lys	missense_variant	MODERATE	0.054	0.006987
chr7	99707978	G	A	9'3A7-CYP3A5	c.1254-4C>T	.	ice_region_variant&intron_vari	LOW	0.054	0.005556
chr7	127582466	C	T	GCC1	c.1876G>A	p.Gly626Ser	missense_variant	MODERATE	0.054	0.00242
chr7	149801791	C	T	SSPO	c.7334C>T	p.Thr2445Ile	missense_variant	MODERATE	0.054	0.004145
chr7	24863285	G	A	OSBPL3	c.785C>T	p.Ser262Phe	missense_variant	MODERATE	0.053	0.006898
chr7	44404587	G	A	NUDCD3	c.643-4C>T	.	ice_region_variant&intron_vari	LOW	0.053	0.004613
chr7	127590061	C	T	ARFS	c.259-5C>T	.	ice_region_variant&intron_vari	LOW	0.053	0.005313
chr7	74109017	G	A	LIMK1	c.1265G>A	.	structural_interaction_variant	HIGH	0.052	0.006234
chr7	87585688	G	A	ABCB1	c.118-8C>T	.	ice_region_variant&intron_vari	LOW	0.052	0.005018
chr7	142869125	C	T	EPHB6	c.2438C>T	p.Ala813Val	missense_variant	MODERATE	0.052	0.002725
chr7	149266337	C	T	ZNF783	c.27C>T	p.Asp9Asp	region_variant&synonymous_v	LOW	0.052	0.00846
chr7	151194006	G	A	IQCA1L	c.1595C>T	p.Ser532Phe	missense_variant	MODERATE	0.052	0.004268
chr7	4761059	C	T	FOXK1	c.1697-5C>T	.	ice_region_variant&intron_vari	LOW	0.051	0.004572
chr7	47943516	G	A	PKD1L1	c.45-5C>T	.	ice_region_variant&intron_vari	LOW	0.051	0.007184
chr7	50674662	C	T	GRB10	c.140-4G>A	.	ice_region_variant&intron_vari	LOW	0.051	0.00508
chr7	110663622	T	C	IMMP2L	c.508G>A	p.Val170Ile	missense_variant	MODERATE	0.051	0.005368
chr7	118224895	G	A	ANKRD7	c.65G>A	p.Arg22Gln	missense_variant	MODERATE	0.051	0.00451
chr7	123119080	C	T	SLC13A1	c.1512+1G>A	.	ice_donor_variant&intron_vari	HIGH	0.051	0.005829
chr7	135734322	G	A	FAM18BA	c.178-3C>T	.	ice_region_variant&intron_vari	LOW	0.051	0.005671
chr7	143444072	C	T	TAS2R60	c.620C>T	p.Ala207Val	missense_variant	MODERATE	0.051	0.003238
chr7	152144713	C	T	KMT2C	c.14343G>A	p.Gln4781Gln	region_variant&synonymous_v	LOW	0.051	0.004428
chr7	47885701	T	C	PKD1L1	c.3190G>A	p.Asp1064Asn	missense_variant	MODERATE	0.05	0.003922
chr7	48248449	G	A	ABCA13	c.1865+5G>A	.	ice_region_variant&intron_vari	LOW	0.05	0.005645
chr7	73831803	G	A	CLDN4	c.602G>A	p.Arg201His	missense_variant	MODERATE	0.05	0.00294
chr7	92097583	C	T	AKAP9	c.10399-3C>T	.	ice_region_variant&intron_vari	LOW	0.05	0.006494
chr7	117791175	G	A	CTTNBP2	c.2021C>T	p.Ser674Leu	missense_variant	MODERATE	0.05	0.004488
chr7	151222531	C	T	ABCF2	c.808G>A	p.Glu270Lys	missense_variant	MODERATE	0.05	0.006022
chr7	6815904	G	A	XRN1	c.8220>C	p.Glu2740sp	missense_variant	MODERATE	0.237	0.004724
chr8	58576051	C	G	SDCBP	c.392>CG	p.Ser131*	stop_gained	HIGH	0.208	0.006584
chr8	27610467	C	T	CLU	c.974+8G>A	.	ice_region_variant&intron_vari	LOW	0.095	0.004137
chr8	144358155	G	A	FBXL6	c.2936>T	p.Ala298Val	missense_variant	MODERATE	0.089	0.006707
chr8	2219252	G	A	BMP1	c.1180+1G>A	.	ice_donor_variant&intron_vari	HIGH	0.085	0.005903
chr8	20147398	G	A	SLC18A1	c.1331-7C>T	.	ice_region_variant&intron_vari	LOW	0.07	0.004836
chr8	144472596	G	A	KIFC2	c.1751G>A	p.Ser584Asn	missense_variant	MODERATE	0.069	0.00318
chr8	143872823	C	T	EPPK1	c.4310>A	p.Arg1441ys	missense_variant	MODERATE	0.066	0.002915
chr8	27451042	G	A	PTK2B	c.2488-1G>A	.	'e_acceptor_variant&intron_var	HIGH	0.064	0.003376
chr8	21995489	C	T	XPO7	c.2238-3C>T	.	ice_region_variant&intron_vari	LOW	0.061	0.007357
chr8	3189907	C	T	CSMD1	c.5398+5G>A	.	ice_region_variant&intron_vari	LOW	0.059	0.005124
chr8	7973223	C	A	USP17L8	c.31G>T	p.Glu11*	stop_gained	HIGH	0.059	0.043
chr8	22004035	G	A	XPO7	c.3170+5G>A	.	ice_region_variant&intron_vari	LOW	0.058	0.00769
chr8	28029384	C	T	NUGGC	c.2036G>A	p.Gly679Asp	missense_variant	MODERATE	0.057	0.003809
chr8	93758535	C	T	TMEM67	c.365C>T	p.Thr122Ile	missense_variant	MODERATE	0.057	0.006475
chr8	64596671	C	T	CYP7B1	c.1492G>A	p.Val498Ile	missense_variant	MODERATE	0.056	0.009057
chr8	28716405	A	G	EXT1.3	c.1346G>A	p.Arg116Thr	missense_variant	MODERATE	0.055	0.002846
chr8	144317927	C	T	DGAT1	c.842G>A	p.Arg281Gln	missense_variant	MODERATE	0.054	0.003766
chr8	100706650	C	T	PABPC1	c.1602+1G>A	.	ice_donor_variant&intron_vari	HIGH	0.053	0.009922
chr8	2966754	A	G	CSMD1	c.8924-8C>T	.	ice_region_variant&intron_vari	LOW	0.051	0.006762
chr8	70608076	C	T	TRAM1	c.123+1G>A	.	ice_donor_variant&intron_vari	HIGH	0.051	0.004343
chr9	19369988	G	GT	DENND4C	c.5528+2dupT	.	ice_region_variant&intron_vari	LOW	0.486	0.007857
chr9	95915660	C	A	ERCC6L2	c.822-8C>A	.	ice_region_variant&intron_vari	LOW	0.29	0.005797
chr9	130362897	G	T	HMCN2	c.6139G>T	p.Ala20475er	missense_variant	MODERATE	0.25	0.003532
chr9	128508900	C	G	GLE1	c.124C>G	p.Leu42Val	missense_variant	MODERATE	0.243	0.004744
chr9	74642467	G	T	RORB	c.289G>T	p.Val97Leu	missense_variant	MODERATE	0.24	0.003565
chr9	133733942	C	G	SARDH	c.2326>C	p.Gln776Arg	missense_variant	MODERATE	0.227	0.002757
chr9	123097815	G	C	RABGAP1	c.2703G>C	p.Glu901Asp	missense_variant	MODERATE	0.222	0.004635
chr9	131482368	C	T	PRRC2B	c.4984-3C>T	.	ice_region_variant&intron_vari	LOW	0.217	0.005765
chr9	114307780	A	T	COL27A1	c.5217+2T>A	.	ice_donor_variant&intron_vari	HIGH	0.202	0.004813
chr9	5832841	C	T	ERMP1	c.1876>A	p.Gly635er	missense_variant	MODERATE	0.125	0.0026
chr9	128456191	A	G	ODF2	c.100A>G	p.Thr34Ala	missense_variant	MODERATE	0.124	0.00284
chr9	136837857	C	T	RABL6	c.1130-5C>T	.	ice_region_variant&intron_vari	LOW	0.087	0.004556
chr9	92718536	C	T	BICD2	c.2106+3G>A	.	ice_region_variant&intron_vari	LOW	0.085	0.005215
chr9	35710820	C	T	TLN1	c.41800>A	p.Asp1394Asn	missense_variant	MODERATE	0.082	0.004496
chr9	37777594	C	T	TRMT10B	c.845-7C>T	.	ice_region_variant&intron_vari	LOW	0.079	0.006566
chr9	128434230	G	A	CERCAM	c.1331+1G>A	.	ice_donor_variant&intron_vari	HIGH	0.077	0.004878
chr9	137097823	C	T	MAN1B1	c.621-5C>T	.	ice_region_variant&intron_vari	LOW	0.077	0.005467
chr9	114096482	G	A	KIF12	c.233-4C>T	.	ice_region_variant&intron_vari	LOW	0.075	0.006337
chr9	131075970	G	A	LAMC3	c.3629+5G>A	.	ice_region_variant&intron_vari	LOW	0.073	0.004612
chr9	19078279	G	A	HAUS6	c.1088C>T	p.Thr363Ile	missense_variant	MODERATE	0.071	0.006957
chr9	37025942	C	T	PAXS	c.47-5143G>A	.	sequence_feature	LOW	0.071	0.00571
chr9	136334455	C	T	GPSM1	c.77C>T	p.Ala26Val	missense_variant	MODERATE	0.07	0.003423
chr9	14868740	C	T	FREM1	c.2344>4G>A	.	ice_region_variant&intron_vari	LOW	0.068	0.006029
chr9	136370293	C	T	CARD9	c.951+1G>A	.	ice_donor_variant&intron_vari	HIGH	0.067	0.002841
chr9	33465362	A	G	NOL6	c.2529-3C>T	.	ice_region_variant&intron_vari	LOW	0.066	0.01
chr9	137812998	C	T	EHMT1	c.2868-8C>T	.	ice_region_variant&intron_vari	LOW	0.066	0.005655
chr9	122378908	G	A	PTGS1	c.486G>A	p.Met162Ile	missense_variant	MODERATE	0.065	0.005339
chr9	19102546	C	T	HAUS6	c.1036>A	p.Val368Met	missense_variant	MODERATE	0.064	0.004478
chr9	35042370	C	T	C9orf131	c.116C>T	p.Pro39Leu	missense_variant	MODERATE	0.064	0.002982
chr9	114169384	C	T	COL27A1	c.1829C>T	p.Ser610Leu	missense_variant	MODERATE	0.064	0.003017
chr9	132499373	C	T	CFAP77	c.405C>T	p.Ala135Ala	region_variant&synonymous_v	LOW	0.063	0.00353
chr9	111442430	G	A	KIAA0368	c.805-6C>T	.	ice_region_variant&intron_vari	LOW	0.062	0.017
chr9	135945998	C	T	UBAC1	c.545-1G>A	.	'e_acceptor_variant&intron_var	HIGH	0.062	0.003982
chr9	137232569	C	T	SLC34A3	c.176-6C>T	.	ice_region_variant&intron_vari	LOW	0.061	0.004444
chr9	121318674	C	T	GSN	c.1138C>T	p.Leu380Phe	missense_variant	MODERATE	0.06	0.00511
chr9	130402783	C	T	HMCN2	c.11771-6C>T	.	ice_region_variant&intron_vari	LOW	0.06	0.005018

chr9	4583043	C	T	SLC1A1	c.1199C>T	p.Thr400Met	missense_variant	MODERATE	0.059	0.004891
chr9	14842315	C	T	FREM1	c.1738+1G>A		ice_donor_variant&intron_vari	HIGH	0.059	0.00527
chr9	98770898	G	A	ANKS6	c.1970C>T	p.Ser657Leu	nse_variant&splice_region_va	MODERATE	0.059	0.004998
chr9	129869777	C	T	USP20	c.1498C>T	p.Pro500Ser	missense_variant	MODERATE	0.059	0.004103
chr9	72805505	G	A	TMC1	c.1690G>A	p.Gly564Arg	missense_variant	MODERATE	0.058	0.01
chr9	137256828	C	T	NELFB	c.515C>T	p.Pro172Leu	missense_variant	MODERATE	0.058	0.005488
chr9	33313651	C	T	NFX1	c.1449-3C>T		ce_region_variant&intron_vari	LOW	0.056	0.007016
chr9	35869618	G	A	OR13J1	c.784C>T	p.Pro262Ser	missense_variant	MODERATE	0.056	0.006145
chr9	83887185	C	T	KIF27	c.2095G>A	p.Asp699Asn	missense_variant	MODERATE	0.056	0.011
chr9	137175744	C	T	ANAPC2	c.1984G>A	p.Val662Ile	missense_variant	MODERATE	0.056	0.004233
chr9	731179	C	T	KANK1	c.2918C>T	p.Thr973Ile	missense_variant	MODERATE	0.055	0.007347
chr9	14868764	C	T	FREM1	c.214G>A	p.Val72Ile	missense_variant	MODERATE	0.055	0.004689
chr9	35698369	C	T	TLN1	c.7325G>A	p.Cys2442Tyr	missense_variant	MODERATE	0.055	0.003581
chr9	136980030	C	T	PTGDS	c.416C>T	p.Pro139Leu	missense_variant	MODERATE	0.054	0.003864
chr9	16435550	C	T	BNC2	c.2639+5G>A	-	ce_region_variant&intron_vari	LOW	0.053	0.00484
chr9	137506084	C	T	PNPLA7	c.1226-1G>A		e_acceptor_variant&intron_va	HIGH	0.053	0.00305
chr9	6990518	G	A	KDM4C	c.1780G>A	p.Asp594Asn	missense_variant	MODERATE	0.052	0.013
chr9	37441056	C	T	ZBTB5	c.1496G>A	p.Gly499Glu	missense_variant	MODERATE	0.052	0.002818
chr9	114438715	G	A	TMEM268	c.838G>A	p.Ala280Thr	missense_variant	MODERATE	0.052	0.004548
chr9	130400946	G	A	HMCN2	c.11769G>A	p.Ser3923Ser	region_variant&synonymous_	LOW	0.052	0.005341
chr9	128577274	G	A	SPTAN1	c.930+1G>A		ice_donor_variant&intron_vari	HIGH	0.051	0.003531
chr9	128716805	C	T	PKN3	c.1867C>T	p.Leu623Phe	missense_variant	MODERATE	0.051	0.003362
chr9	131198784	C	T	NUP214	c.5290C>T	p.Pro1764Ser	missense_variant	MODERATE	0.051	0.00482
chr9	131638789	G	A	RAPGEF1	c.500C>T	p.Ser167Leu	nse_variant&splice_region_va	MODERATE	0.051	0.006706
chr9	97669707	G	A	NCBP1	c.2259+1G>A		ice_donor_variant&intron_vari	HIGH	0.05	0.005025
chr10	27434189	G	A	PTCH53	c.62C>T	p.Pro21Leu	missense_variant	MODERATE	0.336	0.002308
chr10	119826921	C	G	INPP5F	c.2540C>G	p.Ser847Cys	missense_variant	MODERATE	0.259	0.003492
chr10	43200667	C	T	RASGEF1A	c.705G>A	p.Leu235Leu	region_variant&synonymous_	LOW	0.114	0.004981
chr10	92508896	G	A	IDE	c.898-6C>T	-	ce_region_variant&intron_vari	LOW	0.093	0.008262
chr10	689494	C	T	DIP2C	c.85G>A	p.Gly29Ser	nse_variant&splice_region_va	MODERATE	0.087	0.01
chr10	98252461	G	A	LOXL4	c.1843C>T	p.His615Tyr	missense_variant	MODERATE	0.079	0.004907
chr10	70736677	T	C	ADAMTS14	c.1495-3C>T		ce_region_variant&intron_vari	LOW	0.078	0.004808
chr10	79613925	G	A	SFTPA1	c.604G>A	p.Val202Ile	missense_variant	MODERATE	0.077	0.005995
chr10	30047794	G	A	KIAA1462	c.19C>T	p.Leu7Phe	missense_variant	MODERATE	0.075	0.003723
chr10	49746827	T	C	OGDHL	c.1219G>A	p.Val407Ile	missense_variant	MODERATE	0.074	0.004246
chr10	73802477	C	T	NDST2	c.2626G>A	p.Glu876Lys	missense_variant	MODERATE	0.074	0.003618
chr10	103767093	C	T	SH3PXD2A	c.229+1G>A		ice_donor_variant&intron_vari	HIGH	0.074	0.007749
chr10	48778622	C	T	WDFY4	c.3187C>T	p.Pro1063Ser	missense_variant	MODERATE	0.071	0.00393
chr10	119042014	C	T	EIF3A	c.3506G>A	p.Trp1169*	stop_gained	HIGH	0.071	0.003899
chr10	47348539	C	T	RBP3	c.55C>T	p.Pro19Ser	missense_variant	MODERATE	0.07	0.003903
chr10	75388990	G	A	ZNF503	c.1700C>T	p.Ala567Val	missense_variant	MODERATE	0.07	0.006202
chr10	97379395	G	A	RRP12	c.1696C>T	p.Arg566Trp	missense_variant	MODERATE	0.069	0.005126
chr10	13195269	G	A	MCM10	c.1977G>A	p.Lys659Lys	region_variant&synonymous_	LOW	0.067	0.011
chr10	88583104	G	A	RNLS	c.87C>T		structural_interaction_variant	HIGH	0.066	0.003532
chr10	112376400	G	A	ACSL5	c.1210>A	p.Asp414Asn	missense_variant	MODERATE	0.066	0.003441
chr10	127023317	G	A	DOCK1	c.1445G>A	p.Arg482Gln	missense_variant	MODERATE	0.066	0.005113
chr10	48828771	C	T	WDFY4	c.6222-7C>T	-	ce_region_variant&intron_vari	LOW	0.065	0.007593
chr10	97656284	A	G	PI4K2A	c.637-1G>A		e_acceptor_variant&intron_va	HIGH	0.065	0.006096
chr10	113578622	C	T	HABP2	c.569-5C>T	-	ce_region_variant&intron_vari	LOW	0.065	0.005856
chr10	91485177	C	T	HECTD2	c.983-3C>T	-	ce_region_variant&intron_vari	LOW	0.064	0.01
chr10	103089912	G	A	NTSC2	c.1450-4C>T	-	ce_region_variant&intron_vari	LOW	0.063	0.00574
chr10	132198463	G	A	DPYSL4	c.670G>A	p.Val224Met	missense_variant	MODERATE	0.063	0.003311
chr10	132404663	C	T	PWWP2B	c.163C>T	p.Pro55Ser	missense_variant	MODERATE	0.063	0.002766
chr10	132697924	G	A	INPP5A	c.474+5G>A	-	ce_region_variant&intron_vari	LOW	0.063	0.004662
chr10	49740768	C	T	OGDHL	c.2082G>A	p.Trp694*	stop_gained	HIGH	0.062	0.003495
chr10	71702680	G	A	CDH23	c.2719G>A	p.Val907Ile	missense_variant	MODERATE	0.062	0.004644
chr10	84425898	G	A	CCSER2	c.1868+5G>A	-	ce_region_variant&intron_vari	LOW	0.062	0.00667
chr10	45765675	C	T	FAM21C	c.1738-4C>T	-	ce_region_variant&intron_vari	LOW	0.061	0.005378
chr10	71779315	C	T	CDH23	c.5236C>T	p.Arg1746Trp	missense_variant	MODERATE	0.061	0.004781
chr10	73637744	C	T	MYO21	c.252G>A	p.Met84Ile	nse_variant&splice_region_va	MODERATE	0.061	0.005816
chr10	60064149	C	T	ANK3	c.12451+8G>A	-	ce_region_variant&intron_vari	LOW	0.06	0.007922
chr10	128114927	C	T	MKI67	c.1480+1G>A	-	ice_donor_variant&intron_vari	HIGH	0.06	0.00574
chr10	67988838	G	A	HERC4	c.1634-3C>T		ce_region_variant&intron_vari	LOW	0.059	0.008926
chr10	70150396	G	A	AIFM2	c.794C>T	p.Ala265Val	missense_variant	MODERATE	0.059	0.00402
chr10	98400227	G	A	PYROXD2	c.346C>T	p.Pro116Ser	missense_variant	MODERATE	0.059	0.004219
chr10	99723951	C	T	CDH15	c.750+5G>A		ce_region_variant&intron_vari	LOW	0.059	0.005776
chr10	73639948	C	T	MYO21	c.70G>A	p.Gly24Arg	missense_variant	MODERATE	0.058	0.006301
chr10	94259144	G	A	PLCE1	c.3808G>A	p.Asp1270Asn	missense_variant	MODERATE	0.058	0.004971
chr10	88764406	C	T	LIPN	c.227-4C>T		ce_region_variant&intron_vari	LOW	0.057	0.004463
chr10	91261424	G	A	PCGF5	c.573G>A	p.Glu191Glu	region_variant&synonymous_	LOW	0.057	0.011
chr10	97617207	C	T	MORN4	c.182+1G>A	-	ice_donor_variant&intron_vari	HIGH	0.057	0.004597
chr10	122283918	G	A	BTBD16	c.238G>A	p.Glu80Lys	missense_variant	MODERATE	0.057	0.005308
chr10	26203107	G	A	MYO3A	c.4730G>A	p.Arg1577Lys	nse_variant&splice_region_va	MODERATE	0.056	0.008525
chr10	73539600	G	A	USP54	c.826-7C>T		ce_region_variant&intron_vari	LOW	0.056	0.0073
chr10	60208221	G	A	ANK3	c.1009C>T	p.Pro337Ser	missense_variant	MODERATE	0.055	0.005209
chr10	68965499	G	A	DDX21	c.904+5G>A		ce_region_variant&intron_vari	LOW	0.055	0.009362
chr10	86691945	C	T	LDB3	c.943C>T	p.Gln315*	stop_gained	HIGH	0.055	0.003727
chr10	30047779	C	T	KIAA1462	c.34G>A	p.Gly12Arg	missense_variant	MODERATE	0.054	0.003268
chr10	48232119	C	T	FRMPD2	c.1164G>A	p.Met388Ile	missense_variant	MODERATE	0.054	0.011
chr10	127354665	C	T	DOCK1	c.3225-4C>T		ce_region_variant&intron_vari	LOW	0.054	0.007117
chr10	72336641	C	T	DNAJB12	c.991G>A	p.Val331Met	missense_variant	MODERATE	0.053	0.004372
chr10	73500650	G	A	USP54	c.4495+5C>T		ce_region_variant&intron_vari	LOW	0.053	0.011
chr10	97430603	C	T	PGAM1	c.364C>T	p.Pro122Ser	missense_variant	MODERATE	0.053	0.003832
chr10	277584	G	A	DIP2C	c.4419-7C>T		ce_region_variant&intron_vari	LOW	0.052	0.00532
chr10	7170927	C	T	SFMBT2	c.2544+1G>A	-	ice_donor_variant&intron_vari	HIGH	0.052	0.005283
chr10	50235887	C	T	ASAH2	c.687+1G>A	-	ice_donor_variant&intron_vari	HIGH	0.052	0.007329
chr10	96157056	C	T	ZNF518A	c.734C>T	p.Thr245Ile	missense_variant	MODERATE	0.052	0.005488
chr10	103910522	C	T	OBFC1	c.229+5G>A	-	ce_region_variant&intron_vari	LOW	0.052	0.007342
chr10	125772687	C	T	MMP21	c.761G>A	p.Arg254His	missense_variant	MODERATE	0.052	0.002864
chr10	133285166	C	T	TUBGCP2	c.2027G>A	p.Cys676Tyr	missense_variant	MODERATE	0.052	0.005161
chr10	97396255	C	T	RRP12	c.416G>A	p.Gly139Glu	missense_variant	MODERATE	0.051	0.005556
chr10	125770362	C	T	MMP21	c.1209G>A	p.Trp403*	stop_gained	HIGH	0.051	0.004481
chr11	80090916	G	A	TMEM254	c.4433>A	p.Ter1487Ter	stop_retained_variant	LOW	0.05	0.0065
chr11	88678667	G	A	LIPF	c.1213G>A	p.Glu405Lys	missense_variant	MODERATE	0.05	0.007855
chr11	5389570	C	G	OR51M1	c.172C>G	p.Leu58Val	missense_variant	MODERATE	0.345	0.002839
chr11	61008651	AC	A	CD6	c.588delC	p.His196Fs	frameshift_variant	HIGH	0.33	0.002358
chr11	1189030	A	G	MUC5AC	c.10885A>G	p.Thr3629Ala	missense_variant	MODERATE	0.323	0.035
chr11	124895084	G	T	ROBO4	c.1146C>A	p.Tyr382*	stop_gained	HIGH	0.309	0.004462
chr11	47724475	GT	G	FNBP4	c.2317delA	p.Thr773fs	frameshift_variant	HIGH	0.298	0.004439
chr11	65396934	G	C	FRMD8	c.717G>C	p.Glu239Asp	missense_variant	MODERATE	0.255	0.002911
chr11	126413625	C	G	ST3GAL4	c.892C>G	p.Gln298Glu	missense_variant	MODERATE	0.254	0.003151
chr11	1771970	T	C	MYOD1	c.188C>T	p.Ser63Leu	missense_variant	MODERATE	0.249	0.001932
chr11	17169142	C	A	PIK3C2A	c.6000>T	p.Leu2000Phe	missense_variant	MODERATE	0.238	0.003169
chr11	70486857	G	T	SHANK2	c.3436C>A	p.Pro1146Thr	missense_variant	MODERATE	0.217	0.002548
chr11	64912188	C	A	ATG2A	c.984G>T	p.Trp328Cys	missense_variant	MODERATE	0.214	0.002883
chr11	7790761	C	T	INTS4	c.1972G>A	p.Asp658Asn	missense_variant	MODERATE	0.205	0.006966
chr11	88525351	G	T	GRM5	c.2684C>A	p.Pro895His	missense_variant	MODERATE	0.205	0.004127
chr11	88525358	A	T	GRM5	c.2677T>A	p.Phe893Ile	missense_variant	MODERATE	0.205	0.004025
chr11	75667651	C	T	MAP6	c.719G>A	p.Arg240Lys	missense_variant	MODERATE	0.139	0.006024
chr11	6623617	A	C	DCHS1	c.8059T>G	p.Phe2687Val	missense_variant	MODERATE	0.116	0.002754
chr11	1054398	G	A	LOC101927503	c.375+6G>A	-	ce_region_variant&intron_vari	LOW	0.114	0.004402
chr11	8111143	G	A	RIC3	c.671-6C>T	-	ce_region_variant&intron_vari	LOW	0.111	0.006263
chr11	5841243	G	T	OR52E6	c.655C>A	p.His219Asn	missense_variant	MODERATE	0.106	0.003351
chr11	66545718	C	T	ZDHHC24	c.281+5G>A	-	ce_region_variant&intron_vari	LOW	0.104	0.007521
chr11	75429743	C	T	KLHL35	c.881+6G>A	-	ce_region_variant&intron_vari	LOW	0.103	0.004903
chr11	65953745	G	A	TSGA10IP	c.1322+8G>A	-	ce_region_variant&intron_vari	LOW	0.097	0.005122
chr11	64600946	G	A	SLC22A12	c.1598+8G>A	-	ce_region_variant&intron_vari	LOW	0.09	0.004232
chr11	291111	C	T	PGGHG	c.904C>T	p.Gln302*	p_gained&splice_region_varia	HIGH	0.087	0.004556
chr11	883195	C	T	CHID1	c.9870>A	p.Met329Ile	missense_variant	MODERATE	0.086	0.003122
chr11	114242168	C	T	ZBTB16	c.1455C>T	p.Gly485Gly	region_variant&synonymous_	LOW	0.086	0.003648
chr11	74467444	G	A	KDM3	c.-236C>T	-	TR_premature_start_codon_ga	LOW	0.082	0.003728
chr11	69073002	G	A	TPCN2	c.1230+1G>A	-	ice_donor_variant&intron_vari	HIGH	0.081	0.01
chr11	122796284	G	A	UBASH3B	c.1234+8G>A	-	ce_region_variant&intron_vari	LOW	0.081	0.007312
chr11	64751318	C	T	PYGM	c.1969>7G>A	-	ce_region_variant&intron_vari	LOW	0.079	0.004338
chr11	64796394	C	G	MAP4K2	c.1634-4G>C	-	ce_region_variant&intron_vari	LOW	0.077	0.002647
chr11	92834869	G	A	FAT3	c.9872-1G>A		e_acceptor_variant&intron_va	HIGH	0.077	0.011
chr11	5643153	C	T	TRIM6-TRIM34	c.1973>T	p.Thr658Ile	missense_variant	MODERATE	0.076	0.01
chr11	55260331	G	A	TRIM48	c.176G>A	p.Trp59*	stop_gained	HIGH	0.075	0.005346
chr11	70433282	C	T	CTTN	c.1333+4C>T	-	ce_region_variant&intron_vari	LOW	0.075	0.004236
chr11	132436773	G	A	OPCML	c.673C>T	p.Pro224Leu	missense_variant	MODERATE	0.074	0.005468
chr11	60942028	C	T	SLC15A3	c.1107>7G>A	-	ce_region_variant&intron_vari	LOW	0.071	0.008208
chr11	122959241	C	T	C11orf63	c.2140-7C>T	-	ce_region_variant&intron_vari	LOW	0.071	0.006604
chr11	126435271	C	T	KIRREL3	c.1585G>A	p.Ala529Thr	missense_variant	MODERATE	0.071	0.00444
chr11	1841140	C	T	TNNI2	c.386C>T	p.Ser129Leu	missense_variant	MODERATE	0.067	0.003809
chr11	17387170	C	G	KCNJ11	c.922G>C	p.Glu308Gln	missense_variant	MODERATE	0.067	0.002519
chr11	34154385	G	A	ABTB2	c.2767-7C>T		ce_region_variant&intron_vari	LOW	0.067	0.011
chr11	72578907	C	T	POLR2A	c.2459G>A	p.Arg820Lys	missense_variant	MODERATE	0.066	0.005505
chr11	85983865	C	T	PICALM	c.1516+1G>A		ice_donor_variant&intron_vari	HIGH	0.066	0.006756
chr11	119054499	C	T	HYOU1	c.673G>A	p.Ala225Thr	missense_variant	MODERATE	0.066	0.004684
chr11	5046924	T	G	ORS2J3	c.399T>G	p.His133Gln	missense_variant	MODERATE	0.065	0.003297
chr11	103147886	G	A	DYNC2H1	c.2817G>A	p.Gln939Gln	region_variant&synonymous_	LOW	0.063	0.00782
chr11	4990592	C	T	MMP26	c.321-6C>T	-	ce_region_variant&intron_vari	LOW	0.061	0.007228
chr11	20093197	G	A	NAV2	c.6091G>A	p.Glu2031Lys	nse_variant&splice_region_va	MODERATE	0.061	0.005985
chr11	61487241	G	A	PPP1R32	c.1043+1G>A		ice_donor_variant&intron_vari	HIGH	0.06	0.006158
chr11	72205509	C	T	CLPB	c.1559G>A	p.Arg520His	missense_variant	MODERATE	0.06	0.009797
chr11	125908504	G	A	DDX25	c.507+1G>A		ice_donor_variant&intron_vari	HIGH	0.06	0.007569
chr11	126276492	G	A	FOXRED1	c.1070G>A	p.Ser357Asn	missense_variant	MODERATE	0.06	0.006393
chr11	129942625	G	A	PRDM10	c.767C>T	p.Ser256Phe	missense_variant	MODERATE	0.06	0.00804
chr11	134177460	G	A	NCAPD3	c.2783-3C>T	-	ce_region_variant&intron_vari	LOW	0.06	0.004315
chr11	15221649	G	A	INSC	c.1132+1G>A	-	ice_donor_variant&intron_vari	HIGH	0.059	0.00374
chr11	62141047	G	A	INCENP	c.1593+3G>A	-	ce_region_variant&intron_vari	LOW	0.059	0.003396
chr11	65849473	C	T	SNX32	c.37-5C>T	-	ce_region_variant&intron_vari	LOW	0.059	0.004079
chr11	66066736	G	A	SF3B2	c.2330+7G>A	-	ce_region_variant&intron_vari	LOW	0.059	0.005054
chr11	89698407	C	T	FOLH1B	c.1140-3C>T	-	ce_region_variant&intron_vari	LOW	0.059	0.00443
chr11	117203777	C	T	TAGLN	c.359-5C>T	-	ce_region_variant&intron_vari	LOW	0.059	0.004165
chr11	34646442	C	T	EHF	c.167C>T	p.Ser56Phe	missense_variant	MODERATE	0.058	0.005499
chr11	66545765	C	T	ZDHHC24	c.239G>A	p.Arg80His	missense_variant	MODERATE	0.058	0.009983
chr11	126274924	C	T	FOXRED1	c.537-3C>T	-	ce_region_variant&intron_vari	LOW	0.058	0.005462
chr11	4991503	G	A	MMP26	c.595>7G>A	-	ce_region_variant&intron_vari	LOW	0.057	0.008444
chr11	47347861	G	A	MYBPC3	c.817C>T	p.Arg273Cys	missense_variant	MODERATE	0.057	0.00466
chr11	6401073	C	T	APBB1	c.1589-1G>A		e_acceptor_variant&intron_va	HIGH	0.056	0.004315
chr11	11621431	C	T	GALNT18	c.163G>A	p.Asp55Asn	missense_variant	MODERATE	0.055	0.004066
chr11	46894588	C	T	LRP4	c.1540+1G>A	-	ice_donor_variant&intron_vari	HIGH	0.055	0.004762
chr11	59195369	G	A	DTX4	c.1536G>A	p.Gln512Gln	region_variant&synonymous_	LOW	0.055	0.00375
chr11	65585004	C	T	EHBP1L1	c.3346C>T	p.Pro1116Ser	missense_variant	MODERATE	0.055	0.006825
chr11	65618963	C	T	PCNX3	c.1601C>T	p.Ala534Val	missense_variant	MODERATE	0.055	0.002688
chr11	14474618	G	A	COPB1	c.1617-3C>T	-	ce_region_variant&intron_vari	LOW	0.054	0.007605
chr11	17634269	G	A	OTOG	c.7504G>A	p.Gly2502Arg	missense_variant	MODERATE	0.054	0.003257
chr11	65131044	G	A	SYVN1	c.825-8C>T	-	ce_region_variant&intron_vari	LOW	0.054	0.002885
chr11	67521130	G	A	CABP2	c.292C>T	p.Arg98*	stop_gained	HIGH	0.054	0.002802
chr11	108257497	C	T	ATM	c.2267>T	p.Ala756Val	missense_variant	MODERATE	0.054	0.005629
chr11	119020253	G	A	TRAPPC4	c.454G>A	p.Gly152Arg	nse_variant&splice_region_va	MODERATE	0.054	0.005059
chr11	125903199	G	A	PUS3	c.-76C>T	-	TR_premature_start_codon_ga	LOW	0.054	0.005048
chr11	125905598	G	A	DDX25	c.175+1G>A		ice_donor_variant&intron_vari	HIGH	0.054	0.008107
chr11	134184749	G	A	NCAPD3	c.2339C>T	p.Ala780Val	missense_variant	MODERATE	0.054	0.005641
chr11	12294836	CCTCCTA	C	MICALCL	c.1407_1412delTCCTAC	Pro470_Thr471del	disruptive_inframe_deletion	MODERATE	0.053	0.01
chr11	46890282	C	T	LRP4	c.1910G>A	p.Ser637Asn	missense_variant	MODERATE	0.053	0.004828
chr11	67405174	G	A	TBC1D10C	c.242G>A	p.Arg81Gln	missense_variant	MODERATE	0.053	0.00448
chr11	113817844	G	A	USP28	c.1284-7C>T		ce_region_variant&intron_vari	LOW	0.053	0.005829
chr11	119335613	C	T	RNF26	c.491C>T	p.Ser164Phe	missense_variant	MODERATE	0.053	0.002527
chr11	2919378	C	T	SLC22A18	c.1090C>T	p.Leu364Phe	missense_variant	MODERATE	0.052	0.00648
chr11	47815474	C	T	NUP160	c.1686+5G>A		ce_region_variant&intron_vari	LOW	0.052	0.006901
chr11	57485136	C	T	SLC43A1	c.1640G>A	p.Gly547Asp	missense_variant	MODERATE	0.052	0.00452
chr11	67610397	C	T	NDUFV1	c.527C>T	p.Ala176Val	missense_variant	MODERATE	0.052	0.004464
chr11	82733492	C	T	FAM181B	c.238G>A	p.Ala80Thr	missense_variant	MODERATE	0.052	0.003099
chr11	103468591	C	T	DYNC2H1	c.12672>T	p.Ile4224Ile	region_variant&synonymous_	LOW	0.052	0.01
chr11	674715	C	T	DEAF1	c.1324G>A	p.Val442Ile	missense_variant	MODERATE	0.051	0.003888
chr11	5719431	C	T	NUP98	c.2380G>A	p.Val794Met	missense_variant	MODERATE	0.051	0.008132
chr11	20636300	C	T	SLC6A5	c.1625-7C>T		ce_region_variant&intron_vari	LOW	0.051	0.004947
chr11	101963881	G	A	CEP126	c.2845+1G>A	-	ice_donor_variant&intron_vari	HIGH	0.051	0.006824

chr11	124754269		C	T	ESAM	c.802G>A	p.Val268Ile	missense_variant	MODERATE	0.051	0.003803
chr11	22193517		G	A	ANOS	c.2G>A	p.Val9Met	missense_variant	MODERATE	0.05	0.003777
chr11	70343895		G	A	PPFIA1	c.1931+3G>A	.	ice_region_variant&intron_vari	LOW	0.05	0.006188
chr11	85631815		G	A	TMEM126B	c.203+7G>A	.	ice_region_variant&intron_vari	LOW	0.05	0.012
chr11	94583570		G	A	PIWIL4	c.635+1G>A	.	ice_donor_variant&intron_vari	HIGH	0.05	0.006272
chr11	111882377		C	A	C11orf1	c.55C>A	p.Leu19Ile	missense_variant	MODERATE	0.05	0.005337
chr12	13258500		C	T	FBRS1L	c.2860C>T	p.Pro954Ser	missense_variant	MODERATE	0.364	0.019
chr12	55221665		T	G	OR10A7	c.641T>G	p.Ile214Ser	missense_variant	MODERATE	0.269	0.00442
chr12	10723096		C	T	YBX3	c.16G>A	p.Glu6Lys	missense_variant	MODERATE	0.258	0.006005
chr12	6774670		A	G	LAG3	c.587G>A	p.Arg196His	missense_variant	MODERATE	0.22	0.004403
chr12	53195684		G	C	ITGB7	c.1013C>G	p.Ser338Cys	missense_variant	MODERATE	0.219	0.002987
chr12	14511508		T	A	PLBD1	c.1045+3A>T	.	ice_region_variant&intron_vari	LOW	0.215	0.003721
chr12	22471492		C	A	CICOS	c.2308-4G>T	.	ice_region_variant&intron_vari	LOW	0.211	0.007371
chr12	52848810		G	T	KRT78	c.121C>A	p.Leu41Ile	missense_variant	MODERATE	0.182	0.002303
chr12	101901357		C	G	DRAM1	c.266C>G	p.Thr89Ser	missense_variant	MODERATE	0.176	0.003825
chr12	113386931		C	T	PLBD2	c.1287-6C>T	.	ice_region_variant&intron_vari	LOW	0.108	0.005505
chr12	12164268		C	T	LRP6	c.2052+5G>A	.	ice_region_variant&intron_vari	LOW	0.1	0.008454
chr12	57191314		C	T	LRP1	c.7237-6C>T	.	ice_region_variant&intron_vari	LOW	0.097	0.004068
chr12	3281190		C	T	TSPAN9	c.433-8C>T	.	ice_region_variant&intron_vari	LOW	0.083	0.00505
chr12	5969394		G	A	VWF	c.7549-3C>T	.	ice_region_variant&intron_vari	LOW	0.083	0.00476
chr12	111729820		C	T	ACAD10	c.1351C>T	p.Arg451Cys	missense_variant	MODERATE	0.074	0.005163
chr12	130437089		G	A	RIMBP2	c.1808C>T	p.Ala603Val	missense_variant	MODERATE	0.073	0.002193
chr12	57031035		C	A	MYO1A	c.2484+5G>T	.	ice_region_variant&intron_vari	LOW	0.072	0.006767
chr12	57160890		C	T	LRP1	c.1980-3C>T	.	ice_region_variant&intron_vari	LOW	0.072	0.004241
chr12	51820453		C	T	FIGNL1	c.1961G>A	p.Ter654Ter	stop_retained_variant	LOW	0.07	0.00537
chr12	121309701		C	T	ANAPC5	c.2056G>A	p.Ala686Thr	inse_variant&splice_region_va	MODERATE	0.07	0.006035
chr12	6025582		G	A	VWF	c.3220C>T	p.Leu1074Leu	region_variant&synonymous_v	LOW	0.069	0.006185
chr12	52771870		C	T	KRT76	c.1263+1G>A	.	ice_donor_variant&intron_vari	HIGH	0.069	0.004904
chr12	122187696		C	T	LRRC43	c.523-5C>T	.	ice_region_variant&intron_vari	LOW	0.069	0.004705
chr12	124953876		G	A	DHX37	c.2695+4C>T	.	ice_region_variant&intron_vari	LOW	0.069	0.006703
chr12	20879454		C	T	SLCO1B3	c.1154C>T	p.Thr385Met	missense_variant	MODERATE	0.067	0.007127
chr12	6977006		T	C	LPCAT3	c.1180G>A	p.Glu394Lys	missense_variant	MODERATE	0.066	0.004701
chr12	120214991		G	A	PXN	c.1154C>T	p.Thr385Ile	missense_variant	MODERATE	0.066	0.005785
chr12	57728366		T	A	AGAP2	c.2569A>T	p.Met857Leu	missense_variant	MODERATE	0.065	0.01
chr12	120516791		A	G	COQ5	c.353-3C>T	.	ice_region_variant&intron_vari	LOW	0.065	0.006179
chr12	5921042		C	T	ANO2	c.5329G>A	p.Glu1784Lys	inse_variant&splice_region_va	MODERATE	0.064	0.005031
chr12	26122131		C	T	BHLHE41	c.1384G>A	p.Glu462Lys	missense_variant	MODERATE	0.064	0.005105
chr12	7921631		G	A	SLC2A3	c.1273C>T	p.His425Tyr	inse_variant&splice_region_va	MODERATE	0.062	0.005423
chr12	2859131		A	T	FOXM1	c.1913C>T	p.Thr638Ile	missense_variant	MODERATE	0.061	0.003054
chr12	52056039		C	T	NR4A1	c.1048C>T	p.Gln350*	stop_gained	HIGH	0.061	0.005763
chr12	96647868		C	T	CFAP54	c.4548-7C>T	.	ice_region_variant&intron_vari	LOW	0.061	0.009521
chr12	26663678		C	T	ITPR2	c.1713+7G>A	.	ice_region_variant&intron_vari	LOW	0.06	0.005343
chr12	3038103		G	A	TEAD4	c.1033G>A	p.Val345Ile	missense_variant	MODERATE	0.059	0.004116
chr12	14506161		C	T	PLBD1	c.1479+1G>A	.	ice_donor_variant&intron_vari	HIGH	0.059	0.005516
chr12	31097882		C	T	DDX11	c.1763-3C>T	.	ice_region_variant&intron_vari	LOW	0.059	0.007374
chr12	53102157		G	A	IGFBP6	c.713G>A	p.Ser238Asn	missense_variant	MODERATE	0.059	0.004767
chr12	125415678		G	A	TMEM132B	c.1091+1G>A	.	ice_donor_variant&intron_vari	HIGH	0.058	0.004277
chr12	26621118		C	T	ITPR2	c.3462+5G>A	.	ice_region_variant&intron_vari	LOW	0.057	0.007762
chr12	29345535		G	A	ERGIC2	c.733C>T	p.Gln245*	stop_gained	HIGH	0.057	0.007302
chr12	40446623		G	A	MUC19	c.4871G>A	p.Arg1624Lys	missense_variant	MODERATE	0.057	0.007912
chr12	112941565		C	T	OAS3	c.178-5C>T	.	ice_region_variant&intron_vari	LOW	0.057	0.011
chr12	8933357		G	A	PHC1	c.1893+7G>A	.	ice_region_variant&intron_vari	LOW	0.056	0.005383
chr12	109258970		C	T	ACACB	c.6361-3C>T	.	ice_region_variant&intron_vari	LOW	0.056	0.004408
chr12	122481654		G	A	ZCCHC8	c.886C>T	p.Gln296*	stop_gained	HIGH	0.056	0.007391
chr12	133226441		G	A	ANKH	c.719-3C>T	.	ice_region_variant&intron_vari	LOW	0.056	0.003539
chr12	13068299		C	T	FAM234B	c.1143-5C>T	.	ice_region_variant&intron_vari	LOW	0.055	0.005942
chr12	57620455		G	A	SLC26A10	c.232+3G>A	.	ice_region_variant&intron_vari	LOW	0.055	0.00653
chr12	70746092		G	A	PTPRR	c.739-6C>T	.	ice_region_variant&intron_vari	LOW	0.055	0.005051
chr12	132776955		C	T	GOLGA3	c.3855+3G>A	.	ice_region_variant&intron_vari	LOW	0.055	0.005021
chr12	21378234		C	T	IAPP	c.81-3C>T	.	ice_region_variant&intron_vari	LOW	0.054	0.004974
chr12	44299746		G	A	TMEM117	c.768+7G>A	.	ice_region_variant&intron_vari	LOW	0.054	0.006117
chr12	101365626		G	A	UTP20	c.6125+1G>A	.	ice_donor_variant&intron_vari	HIGH	0.054	0.007559
chr12	121817029		C	T	SETD1B	c.2716-4C>T	.	ice_region_variant&intron_vari	LOW	0.054	0.004057
chr12	132021079		C	T	EP400	c.4448C>T	p.Ala1483Val	inse_variant&splice_region_va	MODERATE	0.054	0.005144
chr12	4811630		G	A	KCNA6	c.1589G>A	p.Ter530Ter	stop_retained_variant	LOW	0.053	0.004362
chr12	10064854		G	A	CLEC9A	c.593+1G>A	.	ice_donor_variant&intron_vari	HIGH	0.053	0.006942
chr12	12125298		T	C	LRP6	c.4447G>A	p.Ala1483Thr	inse_variant&splice_region_va	MODERATE	0.053	0.004935
chr12	125025003		C	T	BRI3BP	c.329C>T	p.Ser110Phe	missense_variant	MODERATE	0.053	0.004111
chr12	21477822		C	T	RECQL	c.848G>A	.	structural_interaction_variant	HIGH	0.052	0.007424
chr12	48569231		G	A	LALBA	c.143C>T	p.Thr48Ile	missense_variant	MODERATE	0.052	0.005993
chr12	53722180		G	A	CALCOCO1	c.454C>T	p.Gln152*	stop_gained	HIGH	0.052	0.00447
chr12	3020768		G	A	TEAD4	c.718G>A	p.Asp240Asn	missense_variant	MODERATE	0.051	0.003422
chr12	10015249		C	T	CLEC12B	c.410-3C>T	.	ice_region_variant&intron_vari	LOW	0.051	0.008146
chr12	45409488		G	A	ANO6	c.2074+1G>A	.	ice_donor_variant&intron_vari	HIGH	0.051	0.007519
chr12	51982809		G	A	ACVR1B	c.934+1G>A	.	ice_donor_variant&intron_vari	HIGH	0.051	0.006677
chr12	77029824		C	T	E2F7	c.1884+7G>A	.	ice_region_variant&intron_vari	LOW	0.051	0.012
chr12	80610830		G	A	PTPRQ	c.4918+5G>A	.	ice_region_variant&intron_vari	LOW	0.051	0.007894
chr12	120157947		C	T	GCN1	c.2989G>A	p.Gly997Lys	missense_variant	MODERATE	0.051	0.00282
chr12	22255280		C	T	ST8SIA1	c.491G>A	p.Arg164Gln	inse_variant&splice_region_va	MODERATE	0.05	0.004166
chr12	120052493		C	T	RNF10	c.355-6C>T	.	ice_region_variant&intron_vari	LOW	0.05	0.006273
chr12	113219051		A	G	CUL4A	c.368+3A>G	.	ice_region_variant&intron_vari	LOW	0.344	0.00532
chr13	77296606		C	A	MYCBP2	c.371G>T	p.Arg124Ile	missense_variant	MODERATE	0.276	0.006874
chr13	41568244		G	A	VWA8	c.5671C>T	p.Gln1891*	stop_gained	HIGH	0.276	0.003678
chr13	77662146		C	T	LOC100129307	c.481G>A	p.Glu161Lys	missense_variant	MODERATE	0.222	0.008185
chr13	24477701		C	T	PARP4	c.1789G>A	p.Asp597Asn	inse_variant&splice_region_va	MODERATE	0.067	0.009278
chr13	30227411		C	T	KATNAL1	c.1147+1G>A	.	ice_donor_variant&intron_vari	HIGH	0.062	0.006607
chr13	52845420		C	T	PCDH8	c.2839+5G>A	.	ice_region_variant&intron_vari	LOW	0.062	0.003771
chr13	46895490		C	T	HTR2A	c.412+5G>A	.	ice_region_variant&intron_vari	LOW	0.059	0.007184
chr13	46368255		G	A	RUBCNL	c.619-6C>T	.	ice_region_variant&intron_vari	LOW	0.058	0.009621
chr13	24909792		G	A	CENPJ	c.883C>T	p.Thr288Ile	inse_variant&splice_region_va	MODERATE	0.057	0.01
chr13	95970107		C	T	UGGT2	c.1335+5G>A	.	ice_region_variant&intron_vari	LOW	0.056	0.009251
chr13	99529599		G	A	TMEM5F2	c.461+5G>A	.	ice_region_variant&intron_vari	LOW	0.053	0.011
chr13	77603072		A	T	SCEL	c.1038-4A>T	.	ice_region_variant&intron_vari	LOW	0.052	0.009208
chr13	98016728		G	A	IPO5	c.2548-1G>A	.	ice_acceptor_variant&intron_vari	HIGH	0.051	0.01
chr13	113631742		C	T	TFDP1	c.306C>T	p.Ala102Ala	region_variant&synonymous_v	LOW	0.05	0.003463
chr14	104944211		C	T	AHNAK2	c.112404>G	p.Lys3747Arg	missense_variant	MODERATE	0.218	0.00174
chr14	59367510		C	G	DAAM1	c.2938C>G	p.Leu980Val	missense_variant	MODERATE	0.213	0.00506
chr14	75003139		G	A	EIF2B2	c.149G>A	p.Arg50His	missense_variant	MODERATE	0.074	0.006498
chr14	77465648		G	A	AHSA1	c.671G>A	p.Arg224Lys	missense_variant	MODERATE	0.073	0.005858
chr14	74676741		G	A	AREL1	c.493C>T	p.Pro165Ser	missense_variant	MODERATE	0.069	0.006997
chr14	95686472		C	T	TCL1B	c.5C>T	p.Ala2Val	missense_variant	MODERATE	0.069	0.004998
chr14	21327618		C	T	RPGRIP1	c.2711-5C>T	.	ice_region_variant&intron_vari	LOW	0.067	0.006894
chr14	74676575		C	T	AREL1	c.651+8G>A	.	ice_region_variant&intron_vari	LOW	0.067	0.005723
chr14	93928944		G	A	FAM181A	c.845G>A	p.Gly282Glu	missense_variant	MODERATE	0.065	0.002326
chr14	23373395		G	A	IL25	c.277G>A	p.Glu93Lys	inse_variant&splice_region_va	MODERATE	0.064	0.004563
chr14	23129733		C	T	TNFAIP2	c.861-7C>T	.	ice_region_variant&intron_vari	LOW	0.064	0.006252
chr14	21082279		G	A	ARHGEF40	c.3287G>A	p.Cys1096Tyr	missense_variant	MODERATE	0.063	0.003363
chr14	24412994		C	T	NYNRIN	c.2643-3C>T	.	ice_region_variant&intron_vari	LOW	0.06	0.007362
chr14	31150228		A	G	HECTD1	c.1933-7C>T	.	ice_region_variant&intron_vari	LOW	0.06	0.007836
chr14	92932664		G	A	CHGA	c.1103G>A	p.Arg368Gln	missense_variant	MODERATE	0.059	0.002661
chr14	103104762		G	A	EXOC3L4	c.1309G>A	p.Ala437Thr	missense_variant	MODERATE	0.059	0.004112
chr14	70978648		G	A	PCNX1	c.2311G>A	p.Ala771Thr	inse_variant&splice_region_va	MODERATE	0.056	0.006904
chr14	69237571		C	T	EXD2	c.1293-4C>T	.	ice_region_variant&intron_vari	LOW	0.055	0.004307
chr14	81497892		C	T	SEL1L	c.1128G>A	p.Gln376Gln	region_variant&synonymous_v	LOW	0.055	0.006064
chr14	100539248		A	G	BEGAIN	c.5Q5C>T	p.Pro168Leu	missense_variant	MODERATE	0.055	0.00206
chr14	21082351		G	A	ARHGEF40	c.3359G>A	p.Arg1120Gln	missense_variant	MODERATE	0.054	0.003122
chr14	23522027		C	T	ZFHX2	c.7654G>A	p.Ala2552Thr	missense_variant	MODERATE	0.054	0.009584
chr14	75097099		C	T	NID2	c.2209+1G>A	.	ice_donor_variant&intron_vari	HIGH	0.054	0.005139
chr14	64048003		T	A	SYNE2	c.7225T>A	p.Ser2409Thr	missense_variant	MODERATE	0.053	0.009715
chr14	90312394		C	T	NRXE2	c.557G>A	p.Arg186Lys	inse_variant&splice_region_va	MODERATE	0.053	0.0082
chr14	92712863		G	A	LGMN	c.552C>T	.	structural_interaction_variant	HIGH	0.053	0.005492
chr14	20386610		G	A	TEP1	c.2698C>T	p.Arg900Trp	missense_variant	MODERATE	0.052	0.003879
chr14	20385116		G	A	TEP1	c.2983-7C>T	.	ice_region_variant&intron_vari	LOW	0.051	0.007467
chr14	77723174		C	T	SNW1	c.1130+7G>A	.	ice_region_variant&intron_vari	LOW	0.051	0.004223
chr14	20634418		C	T	PRKD1	c.1338G>A	p.Leu446Leu	region_variant&synonymous_v	LOW	0.05	0.005836
chr15	23334124		T	A	GOLGA6L22	c.18A>T	p.Gln6His	missense_variant	MODERATE	0.671	0.055
chr15	64691536		G	T	OAZ2	c.76C>A	p.Pro26Thr	missense_variant	MODERATE	0.277	0.003111
chr15	90904287		A	T	MAN2A2	c.80A>T	p.Asp27Val	missense_variant	MODERATE	0.271	0.003864
chr15	50492758		C	A	USP8	c.2292C>A	p.Asn764Lys	missense_variant	MODERATE	0.257	0.037
chr15	74937925	GCCGGGGGT	G	CCKSA	c.82_89delACCCCCGG	p.Thr28fs	frameshift_variant	HIGH	0.25	0.004979
chr15	40930670		G	DLL4	c.38D>T	p.Asp12Tyr	missense_variant	MODERATE	0.155	0.003905
chr15	73367478		C	T	HCN4	c.785+8G>A	.	ice_region_variant&intron_vari	LOW	0.153	0.00492
chr15	42695134		C	T	STARD9	c.12963-6C>T	.	ice_region_variant&intron_vari	LOW	0.125	0.006011
chr15	65982237		C	T	MEGF11	c.641+5G>A	.	ice_region_variant&intron_vari	LOW	0.105	0.006316
chr15	40335165		C	T	C15orf52	c.1598G>A	p.Arg533Lys	missense_variant	MODERATE	0.089	0.005132
chr15	82709593		C	T	AP3B2	c.113+1G>A	.	ice_donor_variant&intron_vari	HIGH	0.089	0.017
chr15	42669343		G	A	STARD9	c.1497+6G>A	.	ice_region_variant&intron_vari	LOW	0.083	0.005566
chr15	40657351		C	T	KNL1	c.6673-4C>T	.	ice_region_variant&intron_vari	LOW	0.075	0.006859
chr15	42001180		C	T	PLA2G4E	c.650G>A	p.Arg217Lys	missense_variant	MODERATE	0.075	0.003743
chr15	29093068		C	T	APBA2	c.1070-7C>T	.	ice_region_variant&intron_vari	LOW	0.072	0.00314
chr15	40281485		G	A	ANKRD63	c.1102C>T	p.Gln368*	stop_gained	HIGH	0.072	0.008304
chr15	65463911		G	A	DPP8	c.1874-5C>T	.	ice_region_variant&intron_vari	LOW	0.072	0.0089
chr15	50258401		C	T	HDC	c.318+3G>A	.	ice_region_variant&intron_vari	LOW	0.071	0.006262
chr15	56391419		G	A	TEX9	c.571+1G>A	.	ice_donor_variant&intron_vari	HIGH	0.071	0.011
chr15	34948383		G	A	AQR	c.211C>T	p.Gln71*	stop_gained&splice_region_varia	HIGH	0.07	0.01
chr15	89666933		C	T	PLIN1	c.1209+3G>A	.	ice_region_variant&intron_vari	LOW	0.07	0.005295
chr15	55319413		A	G	PIGB	c.16G>A	p.Asp55Asn	inse_variant&splice_region_va	MODERATE	0.068	0.006228
chr15	34897706		C	T	AQR	c.2244-1G>A	.	ice_acceptor_variant&intron_vari	HIGH	0.066	0.006341
chr15	40471356		C	T	CHST14	c.143C>T	p.Ala48Val	missense_variant	MODERATE	0.066	0.005846
chr15	52364557		C	T	MYO5A	c.3306G>A	p.Met1102Ile	missense_variant	MODERATE	0.065	0.00637
chr15	62736874		C	T	TLN2	c.3359-4C>T	.	ice_region_variant&intron_vari	LOW	0.065	0.004752
chr15	39939498		C	T	EIF2AK4	c.145-7C>T	.	ice_region_variant&intron_vari	LOW	0.063	0.007814
chr15	91984008		C	T	VPS13C	c.1726G>A	p.Glu576Lys	missense_variant	MODERATE	0.063	0.005635
chr15	89666937		G	A	PLIN1	c.1208C>T	p.Pro403Leu	inse_variant&splice_region_va	MODERATE	0.063	0.005026
chr15	101029232		G	A	LRRK1	c.2963G>A	p.Ser988Asn	inse_variant&splice_region_va	MODERATE	0.062	0.005173
chr15	53732992		C	T	WDR72	c.153+5G>A	.	ice_region_variant&intron_vari	LOW	0.061	0.00704
chr15	61929501		C	T	VPS13C	c.6286G>A	p.Asp2096Asn	inse_variant&splice_region_va	MODERATE	0.061	0.007679
chr15	42001156		C	T	PLA2G4E	c.673+1G>A	.	ice_donor_variant&intron_vari	HIGH	0.06	0.003932
chr15	52260862		C	T	MYO5C	c.1313G>A	p.Gly438Asp	inse_variant&splice_region_va	MODERATE	0.059	0.006875
chr15	62820611		A	G	TLN2	c.7002+1G>A	.	ice_donor_variant&intron_vari	HIGH	0.059	0.005822
chr15	41870499		C	T	SPTBN5	c.5509G>A	p.Glu1837Lys	missense_variant	MODERATE	0.058	0.004347
chr15	43211508		C	T	EPB42	c.547G>A	p.Ala183Thr	missense_variant	MODERATE	0.058	0.004047
chr15	40472168		A	G	CHST14	c.955G>A	p.Val319Ile	missense_variant	MODERATE	0.057	0.00274
chr15	56446840		C	T	MNS1	c.456+1G>A	.	ice_donor_variant&intron_vari	HIGH	0.057	0.012
chr15	99993048		C	T	ADAMTS17	c.2949G>A	p.Thr983Thr	region_variant&synonymous_v	LOW	0.057	0.004057
chr15	27886650		A	G	OCA2	c.1183-7C>T	.	ice_region_variant&intron_vari	LOW	0.056	0.005578
chr15	31229335		G	A	LOC283710	c.44C>T	p.Ser15Phe	missense_variant	MODERATE	0.055	0.005224
chr15	28115421		G	A	HERC2	c.13722+8C>T	.	ice_region_variant&intron_vari	LOW	0.054	0.003592
chr15	63605742		C	T	HERC1	c.10084G>A	p.Gly3362Ser	inse_variant&splice_region_va	MODERATE	0.054	0.005508
chr15	90878291		G	A	FURIN	c.827G>A	p.Arg276His	missense_variant	MODERATE	0.054	0.007237
chr15	26580331		C	T	GABRB3	c.670G>A	p.Val224Ile	missense_variant	MODERATE	0.053	0.00517
chr15	42330677		G	A	GANC	c.1741+5G>A	.	ice_region_variant&intron_vari	LOW	0.053	0.005813
chr15	88841866		G	A	ACAN	c.7546>A	p.Glu2525Glu	region_variant&synonymous_v	LOW	0.053	0.004035
chr15	28280068		C	T	HERC2	c.542G>A	p.Ser181Asn	inse_variant&splice_region_va	MODERATE	0.052	0.004849
chr15	43209399		G	A	EPB42	c.797C>T	p.Thr266Ile	missense_variant	MODERATE	0.052	0.002811
chr15	52225531		A	G	MYO5C	c.3209C>T	p.Thr1070Ile	inse_variant&splice_region_va	MODERATE	0.052	0.009025
chr15	72760406		C	T	ADPGK	c.643+1G>A	.	ice_donor_variant&intron_vari	HIGH	0.052	0.008255
chr15	57992701		C	T	ALDH1A2	c.798+4G>A	.	ice_region_variant&intron_vari	LOW	0.051	0.004446
chr15	64118247		A	G	SNX1	c.399+3G>A	.	ice_region_variant&intron_vari	LOW	0.051	0.006476
chr15	78341056		G	A	CRABP1	c.84G>A	p.Met28Ile	missense_variant	MODERATE	0.051	0.004919
chr15	88859170		G	C	ACAN	c.6585G>C	p.Arg2195Ser	missense_variant	MODERATE	0.051	0.002715
chr15	90893933		C	T	FES	c.2204-3C>T	.	ice_region_variant&intron_vari	LOW	0.051	0.003766
chr15	34359711		C	T	LPCAT4	c.1277G>A	p.Arg426His	missense_variant	MODERATE	0.05	0.00328
chr15	59492380		G	A	FAM81A	c.413G>A	p.Arg138Lys	inse_variant&splice_region_va	MODERATE	0.05	0.007969
chr15	63696124		C	T	HERC1	c.5121G>A	p.Gln1707Gln	region_variant&synonymous_v	LOW	0.05	0.005861
chr15	66444650		C	T	MAP2K1	c.517-6C>T	.	ice_region_variant&intron_vari	LOW	0.05	0.007267
chr15	88860323		C	T	ACAN	c.6833-3C>T	.	ice_region_variant&intron_vari	LOW	0.05	0.006677
chr16	3557857		T	C	NLRC3	c.2035A>G	p.Ser679Gly	missense_variant	MODERATE	0.26	0.004917
chr16	31109736		T	C	BCKDK	c.328C>T	p.Arg110Cys	missense_variant	MODERATE	0.17	0.003239
chr16	87491803		T	A	ZCCHC14	c.25A>T	p.Ser9Cys	missense_variant	MODERATE	0.146	0.011

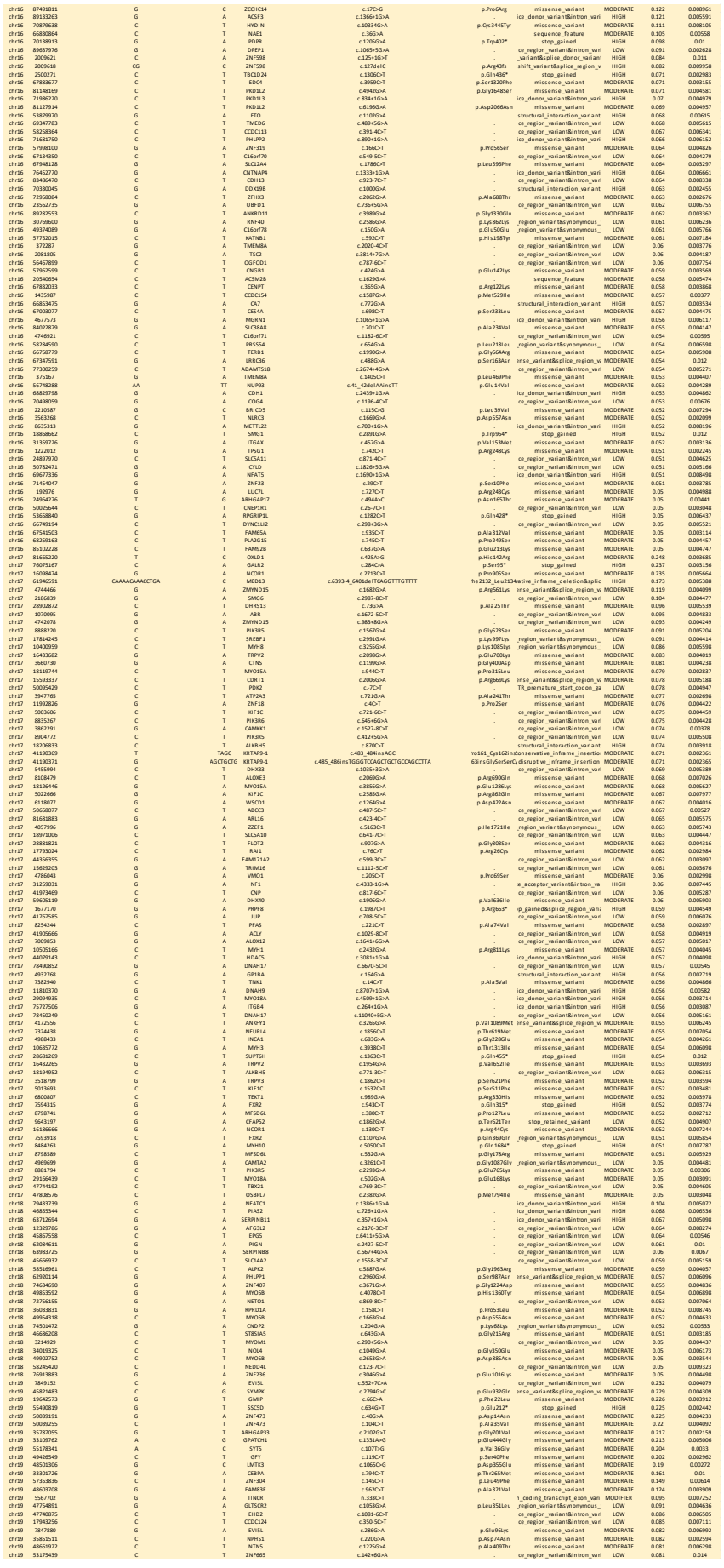

chr16	87491811	G	C	ZCCHC14	c.17C>G	p.Pro6Arg	missense_variant	MODERATE	0.122	0.008961
chr16	89133263	G	A	ACSF3	c.1366+1G>A		ice_donor_variant&intron_vari	HIGH	0.121	0.005591
chr16	70879638	C	T	HYDIN	c.10334G>A	p.Cys3445Tyr	missense_variant	MODERATE	0.111	0.008105
chr16	66830864	C	T	NAE1	c.36G>A		sequence_feature	MODERATE	0.105	0.00558
chr16	70138913	G	A	PDPR	c.1205G>A	p.Trp402*	stop_gained	HIGH	0.098	0.01
chr16	89637976	G	A	DPEP1	c.1065+5G>A	-	ce_region_variant&intron_vari	LOW	0.091	0.002628
chr16	2009621	C	T	ZNF598	c.125+1G>T	-	_variant&splice_donor_variant	HIGH	0.084	0.011
chr16	2009618	CG	C	ZNF598	c.127delC	p.Arg43fs	shift_variant&splice_region_v	HIGH	0.082	0.009958
chr16	2500271	C	T	TBC1D24	c.1306C>T	p.Gln436*	stop_gained	HIGH	0.071	0.002983
chr16	67883677	C	T	CES4	c.3959C>T	p.Ser1320Phe	missense_variant	MODERATE	0.071	0.003155
chr16	81148169	C	T	PKD1L2	c.4942G>A	p.Gly1648Ser	missense_variant	MODERATE	0.071	0.004581
chr16	71986220	C	T	PKD1L3	c.834+1G>A		ice_donor_variant&intron_vari	HIGH	0.07	0.004979
chr16	81127914	C	T	PKD1L2	c.619G>A	p.Asp206Asn	missense_variant	MODERATE	0.069	0.004957
chr16	53879970	G	A	FTO	c.1102G>A		structural_interaction_variant	HIGH	0.068	0.00615
chr16	69347783	C	T	TMED6	c.489+5G>A	-	ce_region_variant&intron_vari	LOW	0.068	0.005615
chr16	58258364	C	T	CDC113	c.391-4C>T	-	ce_region_variant&intron_vari	LOW	0.067	0.006341
chr16	71681750	C	T	PHLPP2	c.890+1G>A	-	ice_donor_variant&intron_vari	HIGH	0.066	0.006152
chr16	57998100	G	A	ZNF319	c.166C>T	p.Pro56Ser	missense_variant	MODERATE	0.064	0.004826
chr16	67134350	C	T	C16orf70	c.549-5G>T	-	ce_region_variant&intron_vari	LOW	0.064	0.004279
chr16	67948128	G	A	SLC12A4	c.1786C>T	p.Leu596Phe	missense_variant	MODERATE	0.064	0.003297
chr16	76452770	G	A	CNTNAP4	c.1333+1G>A	-	ice_donor_variant&intron_vari	HIGH	0.064	0.006661
chr16	83486470	C	T	CDH13	c.923-7C>T	-	ce_region_variant&intron_vari	LOW	0.064	0.008338
chr16	70330045	G	A	DDX19B	c.1000G>A		structural_interaction_variant	HIGH	0.063	0.002455
chr16	72958084	C	T	ZFHX3	c.2062G>A	p.Ala688Thr	missense_variant	MODERATE	0.063	0.002676
chr16	23562735	G	A	UBFD1	c.736+5G>A	-	ce_region_variant&intron_vari	LOW	0.062	0.006755
chr16	89282553	C	T	ANKRD11	c.3989G>A	p.Gly1330Glu	missense_variant	MODERATE	0.062	0.003362
chr16	30769600	G	A	RNF40	c.2586G>A	p.Lys862Lys	region_variant&synonymous_	LOW	0.061	0.006236
chr16	49374089	G	A	C16orf78	c.150G>A	p.Glu50Glu	region_variant&synonymous_	LOW	0.061	0.005766
chr16	57752015	C	T	KATNB1	c.592C>T	p.His198Tyr	missense_variant	MODERATE	0.061	0.007184
chr16	372287	G	A	TMEM8A	c.2020-4C>T	-	ce_region_variant&intron_vari	LOW	0.06	0.003776
chr16	2081805	G	A	TSC2	c.3814+7G>A	-	ce_region_variant&intron_vari	LOW	0.06	0.004187
chr16	56467899	C	T	DGFOD1	c.787-6C>T	-	ce_region_variant&intron_vari	LOW	0.06	0.007754
chr16	57962599	C	T	CNGB1	c.4246>A	p.Glu1142Lys	missense_variant	MODERATE	0.059	0.003569
chr16	20540654	C	T	ACSM2B	c.1629G>A		sequence_feature	MODERATE	0.058	0.005474
chr16	67832033	C	T	CENPT	c.365G>A	p.Arg122Lys	missense_variant	MODERATE	0.058	0.003868
chr16	1435987	C	T	CCDC154	c.1587G>A	p.Met529Ile	missense_variant	MODERATE	0.057	0.00377
chr16	66851475	G	A	CA7	c.772G>A		structural_interaction_variant	HIGH	0.057	0.003534
chr16	67003077	C	T	CES4A	c.698C>T	p.Ser233Leu	missense_variant	MODERATE	0.057	0.004475
chr16	4677573	G	A	MGRN1	c.1065+1G>A	-	ice_donor_variant&intron_vari	HIGH	0.056	0.006117
chr16	84022879	G	A	SLC38A8	c.701C>T	p.Ala234Val	missense_variant	MODERATE	0.055	0.004147
chr16	4746921	C	T	C16orf71	c.1182-6C>T	-	ce_region_variant&intron_vari	LOW	0.054	0.00595
chr16	58284590	C	T	PRSS54	c.654G>A	p.Leu218Leu	region_variant&synonymous_	LOW	0.054	0.006598
chr16	66758779	C	T	TERB1	c.1990G>A	p.Gly664Arg	missense_variant	MODERATE	0.054	0.005908
chr16	67347591	G	A	LRRC36	c.488G>A	p.Ser163Asn	nse_variant&splice_region_v	MODERATE	0.054	0.012
chr16	77300259	C	T	ADAMTS18	c.2674+4G>A	-	ce_region_variant&intron_vari	LOW	0.054	0.005271
chr16	375167	G	A	TMEM8A	c.1405C>T	p.Leu469Phe	missense_variant	MODERATE	0.053	0.004407
chr16	56748288	AA	TT	NUP93	c.41_42delAAinsTT	p.Glu14Val	missense_variant	MODERATE	0.053	0.004289
chr16	68829798	G	A	CDH1	c.2439+1G>A	-	ice_donor_variant&intron_vari	HIGH	0.053	0.004862
chr16	70498059	G	A	COG4	c.1196-4C>T	-	ce_region_variant&intron_vari	LOW	0.053	0.00676
chr16	2210587	G	C	BRICD5	c.115C>G	p.Leu39Val	missense_variant	MODERATE	0.052	0.007294
chr16	3563268	T	G	NLRC3	c.1669G>A	p.Asp557Asn	missense_variant	MODERATE	0.052	0.002099
chr16	8635313	G	A	METTL22	c.700+1G>A	-	ice_donor_variant&intron_vari	HIGH	0.052	0.008196
chr16	18868662	C	T	SMG1	c.2891G>A	p.Trp964*	stop_gained	HIGH	0.052	0.012
chr16	31359726	G	A	ITGAX	c.457G>A	p.Val153Met	missense_variant	MODERATE	0.052	0.003136
chr16	1222012	G	A	TPSG1	c.742C>T	p.Arg248Cys	missense_variant	MODERATE	0.051	0.002245
chr16	24897970	C	T	SLC5A11	c.871-4C>T	-	ce_region_variant&intron_vari	LOW	0.051	0.004625
chr16	50782471	G	A	CYLD	c.1826+5G>A	-	ce_region_variant&intron_vari	LOW	0.051	0.005166
chr16	69677336	G	A	NFAT5	c.1690+1G>A	-	ice_donor_variant&intron_vari	HIGH	0.051	0.008498
chr16	71454047	G	A	ZNF23	c.29C>T	p.Ser10Phe	missense_variant	MODERATE	0.051	0.003785
chr16	192976	G	A	LUC7L	c.727C>T	p.Arg243Cys	missense_variant	MODERATE	0.05	0.004988
chr16	24964276	T	G	ARHGAP17	c.494A>C	p.Asn165Thr	missense_variant	MODERATE	0.05	0.00441
chr16	50025644	C	T	CNEP1R1	c.26-7C>T	-	ce_region_variant&intron_vari	LOW	0.05	0.003048
chr16	53658840	G	A	RPGRIP1L	c.1282C>T	p.Gln428*	stop_gained	HIGH	0.05	0.006437
chr16	66749194	C	T	DYNC1LI2	c.288+3G>A	-	ce_region_variant&intron_vari	LOW	0.05	0.005521
chr16	67541503	C	T	FAM65A	c.935C>T	p.Ala312Val	missense_variant	MODERATE	0.05	0.003114
chr16	68259163	C	T	PLA2G15	c.745C>T	p.Pro249Ser	missense_variant	MODERATE	0.05	0.004457
chr16	85102228	C	T	FAM92B	c.637G>A	p.Glu213Lys	missense_variant	MODERATE	0.05	0.004747
chr17	81665220	T	C	OXLD1	c.425A>G	p.His142Arg	missense_variant	MODERATE	0.248	0.003685
chr17	76075167	C	A	GALR2	c.284C>A	p.Ser95*	stop_gained	HIGH	0.237	0.003156
chr17	16098474	G	A	NCOR1	c.2713C>T	p.Pro905Ser	missense_variant	MODERATE	0.235	0.005664
chr17	61946591	CAAAACAAACCTGA	C	MED13	c.6393-4_6401delTCAGGTTTGTTTT	fre2132_Leu2134ative_inframe_deletion&splic		HIGH	0.173	0.005388
chr17	4744466	G	A	ZMYND15	c.1682G>A	p.Arg561Lys	nse_variant&splice_region_v	MODERATE	0.119	0.004099
chr17	2186839	G	A	SMG6	c.2987-8C>T	-	ce_region_variant&intron_vari	LOW	0.104	0.004477
chr17	28902872	C	T	DHRS13	c.73C>A	p.Ala25Thr	missense_variant	MODERATE	0.096	0.005339
chr17	1070095	G	A	ABR	c.1672-5C>T	-	ce_region_variant&intron_vari	LOW	0.095	0.004833
chr17	4742078	G	A	ZMYND15	c.983+8G>A	-	ce_region_variant&intron_vari	LOW	0.093	0.004249
chr17	8888220	C	T	PHF8	c.1567G>A	p.Gly523Ser	missense_variant	MODERATE	0.091	0.005204
chr17	17814245	C	T	SREBF1	c.2991G>A	p.Lys997Lys	region_variant&synonymous_	LOW	0.091	0.004414
chr17	10409959	C	T	MYH8	c.3255G>A	p.Lys1085Lys	region_variant&synonymous_	LOW	0.086	0.005598
chr17	16433682	G	A	TRPV2	c.2098G>A	p.Glu700Lys	missense_variant	MODERATE	0.083	0.004019
chr17	3660730	G	A	CTNS	c.1199G>A	p.Gly400Asp	missense_variant	MODERATE	0.081	0.004238
chr17	18119744	C	T	MYO15A	c.944C>T	p.Pro315Leu	missense_variant	MODERATE	0.079	0.002837
chr17	15593337	C	T	CDRT1	c.2006G>A	p.Arg669Lys	nse_variant&splice_region_v	MODERATE	0.078	0.005188
chr17	50095429	C	T	PDK2	c.-7C>T	-	TR_premature_start_codon_ga	LOW	0.078	0.004947
chr17	3947765	C	T	ATP2A3	c.721G>A	p.Ala241Thr	missense_variant	MODERATE	0.077	0.002698
chr17	11902826	G	A	ZNF18	c.4C>T	p.Pro2Ser	missense_variant	MODERATE	0.076	0.004422
chr17	5003606	C	T	KIF1C	c.721-6C>T	-	ce_region_variant&intron_vari	LOW	0.075	0.004459
chr17	8835267	C	T	PIK3R6	c.645+6G>A	-	ce_region_variant&intron_vari	LOW	0.075	0.004428
chr17	3862291	G	A	CAMKK1	c.1527-8C>T	-	ce_region_variant&intron_vari	LOW	0.074	0.00378
chr17	8904772	C	T	PIK3R5	c.442+5G>A	-	ce_region_variant&intron_vari	LOW	0.074	0.005508
chr17	18206833	C	T	ALKBH5	c.870C>T		structural_interaction_variant	HIGH	0.074	0.003918
chr17	41190369	T	TAGC	KRTAP9-1	c.483_484insAGC	to161_Cys162insConservative_inframe_insertion		MODERATE	0.071	0.002361
chr17	41190371	AGCTGCTG	KRTAP9-1	c.485_486insTGCGCTGCTGCTGCAGCCTTA		63insGlySerSerCysdisruptive_inframe_insertion		MODERATE	0.071	0.002365
chr17	5455994	C	T	DHX33	c.1035+3G>A	-	ce_region_variant&intron_vari	LOW	0.069	0.005389
chr17	8108479	C	T	ALOXE3	c.2069G>A	p.Arg690Gln	missense_variant	MODERATE	0.068	0.007026
chr17	18126446	G	A	MYO15A	c.3856G>A	p.Glu1286Lys	missense_variant	MODERATE	0.068	0.005627
chr17	5022666	G	A	KIF1C	c.2585G>A	p.Arg862Gln	missense_variant	MODERATE	0.067	0.007977
chr17	6118077	G	A	WSCD1	c.1264G>A	p.Asp422Asn	missense_variant	MODERATE	0.067	0.004016
chr17	59658077	C	T	ABCC3	c.487-5C>T	-	ce_region_variant&intron_vari	LOW	0.067	0.00527
chr17	81681883	G	A	ARL16	c.423-4C>T	-	ce_region_variant&intron_vari	LOW	0.065	0.005575
chr17	4057996	G	A	ZZEF1	c.5163C>T	p.Ile1721Ile	region_variant&synonymous_	LOW	0.063	0.005743
chr17	18971006	C	T	SLC5A10	c.641-7C>T	-	ce_region_variant&intron_vari	LOW	0.063	0.004447
chr17	28881821	C	T	FLOT2	c.907G>A	p.Gly303Ser	missense_variant	MODERATE	0.063	0.004316
chr17	17793024	C	T	RAI1	c.76C>T	p.Arg26Cys	missense_variant	MODERATE	0.062	0.002984
chr17	44356355	G	A	FAM171A2	c.599-3G>T	-	ce_region_variant&intron_vari	LOW	0.062	0.003097
chr17	15629203	G	A	TRIM16	c.1112-5C>T	-	ce_region_variant&intron_vari	LOW	0.061	0.003676
chr17	4786043	G	A	VMO1	c.205G>T	p.Pro69Ser	missense_variant	MODERATE	0.06	0.002998
chr17	31259031	G	A	NF1	c.4333-1G>A	-	ar_acceptor_variant&intron_va	HIGH	0.06	0.007445
chr17	41973469	C	T	CNP	c.817-8C>T	-	ce_region_variant&intron_vari	LOW	0.06	0.005287
chr17	59605119	G	A	DHX40	c.1906G>A	p.Val636Ile	missense_variant	MODERATE	0.06	0.005903
chr17	1677170	G	A	PRPF8	c.1987C>T	p.Arg663*	tp_gained&splice_region_vari	HIGH	0.059	0.004549
chr17	41767585	G	A	JUP	c.708-5C>T	-	ce_region_variant&intron_vari	LOW	0.059	0.006076
chr17	8254244	C	T	PFAS	c.221C>T	p.Ala74Val	missense_variant	MODERATE	0.058	0.002897
chr17	41905666	G	A	ACLY	c.1029-8C>T	-	ce_region_variant&intron_vari	LOW	0.058	0.004919
chr17	7009853	G	A	ALOX12	c.1641+6G>A	-	ce_region_variant&intron_vari	LOW	0.057	0.005017
chr17	10505166	C	T	MYH1	c.2432G>A	p.Arg811Lys	missense_variant	MODERATE	0.057	0.004045
chr17	44079143	C	T	HDAC5	c.3081+1G>A	-	ice_donor_variant&intron_vari	HIGH	0.057	0.004098
chr17	78400852	G	A	DNAH17	c.6670-5C>T	-	ce_region_variant&intron_vari	LOW	0.057	0.00545
chr17	4932768	G	A	GP1BA	c.1640>A		structural_interaction_variant	HIGH	0.056	0.002719
chr17	7382940	C	T	TNK1	c.14C>T	p.Ala5Val	missense_variant	MODERATE	0.056	0.004866
chr17	11810370	G	A	DNAH9	c.8707+1G>A	-	ice_donor_variant&intron_vari	HIGH	0.056	0.00582
chr17	29094935	C	T	MYO18A	c.4509+1G>A	-	ice_donor_variant&intron_vari	HIGH	0.056	0.003714
chr17	75727506	G	A	ITGB4	c.264+1G>A	-	ice_donor_variant&intron_vari	HIGH	0.056	0.003087
chr17	78450249	C	T	DNAH17	c.11040+5G>A	-	ce_region_variant&intron_vari	LOW	0.056	0.005161
chr17	4172556	C	T	ANKFY1	c.3265G>A	p.Val1089Met	nse_variant&splice_region_v	MODERATE	0.055	0.006245
chr17	7324438	G	A	NEURL4	c.1856C>T	p.Thr619Met	missense_variant	MODERATE	0.055	0.007054
chr17	4988433	C	T	INCA1	c.683G>A	p.Gly228Glu	missense_variant	MODERATE	0.054	0.004261
chr17	10635772	A	T	MYH3	c.3938C>T	p.Thr1313Ile	missense_variant	MODERATE	0.054	0.006098
chr17	28681269	C	T	SUPT6H	c.1363C>T	p.Gln455*	stop_gained	HIGH	0.054	0.012
chr17	16432265	G	A	TRPV2	c.1954G>A	p.Val652Ile	missense_variant	MODERATE	0.053	0.003693
chr17	18194952	C	T	ALKBH5	c.771-3C>T	-	ce_region_variant&intron_vari	LOW	0.053	0.006315
chr17	3518799	G	A	TRPV3	c.1862C>T	p.Ser621Phe	missense_variant	MODERATE	0.052	0.003594
chr17	5013693	C	T	KIF1C	c.1532C>T	p.Ser511Phe	missense_variant	MODERATE	0.052	0.003481
chr17	6800807	C	T	TEKT1	c.989G>A	p.Arg330His	missense_variant	MODERATE	0.052	0.003978
chr17	7594315	G	A	FXR2	c.943C>T	p.Gln315*	stop_gained	HIGH	0.052	0.003774
chr17	8798741	G	A	MFSD6L	c.380C>T	p.Pro127Leu	missense_variant	MODERATE	0.052	0.002712
chr17	9643197	G	A	CFAP52	c.1862G>A	p.Ter621Ter	stop_retained_variant	LOW	0.052	0.004907
chr17	16186666	G	A	NCOR1	c.130C>T	p.Arg44Cys	missense_variant	MODERATE	0.052	0.007244
chr17	7503918	C	T	FXR2	c.1107G>A	p.Gln369Gln	region_variant&synonymous_	LOW	0.051	0.005854
chr17	8484263	G	A	MYH10	c.5050C>T	p.Gln1684*	stop_gained	HIGH	0.051	0.007787
chr17	8798580	T	C	MFSD6L	c.532G>A	p.Gly178Arg	missense_variant	MODERATE	0.051	0.005929
chr17	4969699	G	A	CAMTA2	c.3261C>T	p.Gly1087Gly	region_variant&synonymous_	LOW	0.05	0.004481
chr17	8881794	C	T	PIK3R5	c.2293G>A	p.Glu765Lys	missense_variant	MODERATE	0.05	0.00306
chr17	29166439	C	T	MYO18A	c.5026>A	p.Glu168Lys	missense_variant	MODERATE	0.05	0.003091
chr17	47744192	C	T	TBX21	c.769-3C>T	-	ce_region_variant&intron_vari	LOW	0.05	0.004605
chr17	47808576	C	T	OSBPL7	c.2382G>A	p.Met794Ile	missense_variant	MODERATE	0.05	0.003048
chr18	79433739	G	A	NFATC1	c.1386+1G>A	-	ice_donor_variant&intron_vari	HIGH	0.104	0.005072
chr18	46855344	C	T	PIAS2	c.726+1G>A	-	ice_donor_variant&intron_vari	HIGH	0.068	0.006536
chr18	63712694	G	A	SERPINB11	c.357+1G>A	-	ice_donor_variant&intron_vari	HIGH	0.067	0.005098
chr18	12329786	G	A	AFG3L2	c.2176-3C>T	-	ce_region_variant&intron_vari	LOW	0.064	0.008274
chr18	45867558	C	T	EPG5	c.6411+5G>A	-	ce_region_variant&intron_vari	LOW	0.064	0.00546
chr18	62084611	G	A	PIGN	c.2427-5C>T	-	ce_region_variant&intron_vari	LOW	0.061	0.01
chr18	63983725	G	A	SERPINB8	c.567+4G>A	-	ce_region_variant&intron_vari	LOW	0.06	0.0067
chr18	45666932	C	T	SLC14A2	c.1558-3C>T	-	ce_region_variant&intron_vari	LOW	0.059	0.005159
chr18	58516961	C	T	ALPK2	c.5887G>A	p.Gly1963Arg	missense_variant	MODERATE	0.059	0.004057
chr18	62920114	G	A	PHLPP1	c.2960G>A	p.Ser987Asn	nse_variant&splice_region_va	MODERATE	0.057	0.006096
chr18	74634690	G	A	ZNF407	c.3671G>A	p.Gly1224Asp	missense_variant	MODERATE	0.055	0.004836
chr18	49853592	G	A	MYO5B	c.4078C>T	p.His1360Tyr	missense_variant	MODERATE	0.054	0.006898
chr18	72756155	G	A	NETO1	c.869-8C>T	-	ce_region_variant&intron_vari	LOW	0.053	0.007064
chr18	36033831	G	A	RPH3A	c.158C>T	p.Pro53Leu	missense_variant	MODERATE	0.052	0.008745
chr18	49954318	C	T	MYO5B	c.1663G>A	p.Asp555Asn	missense_variant	MODERATE	0.052	0.004633
chr18	74501472	G	A	CNDP2	c.204G>A	p.Lys68Lys	region_variant&synonymous_	LOW	0.052	0.00533
chr18	46686208	C	T	STBD1	c.643G>A	p.Gly215Arg	missense_variant	MODERATE	0.051	0.003185
chr18	3214929	C	T	MYOM1	c.290+5G>A	-	ce_region_variant&intron_vari	LOW	0.05	0.004437
chr18	34019325	C	T	NOL4	c.1049G>A	p.Gly350Glu	missense_variant	MODERATE	0.05	0.006173
chr18	49902752	C	T	MYO5B	c.2653G>A	p.Asp885Asn	missense_variant	MODERATE	0.05	0.003544
chr18	58245420	C	T	NEDD4L	c.123-7C>T	-	ce_region_variant&intron_vari	LOW	0.05	0.009323
chr18	76913883	G	A	ZNF236	c.3046G>A	p.Glu1016Lys	missense_variant	MODERATE	0.05	0.004498
chr19	7849152	C	A	EVI5L	c.552+7C>A	-	ce_region_variant&intron_vari	LOW	0.232	0.004079
chr19	45821483	C	G	SYMPK	c.2794G>C	p.Glu932Gln	nse_variant&splice_region_v	MODERATE	0.229	0.004309
chr19	19642573	G	T	GMIP	c.66C>A	p.Phe22Leu	missense_variant	MODERATE	0.226	0.003912
chr19	55490819	G	T	SSC5D	c.634G>T	p.Glu212*	stop_gained	HIGH	0.225	0.002442
chr19	50039191	G	A	ZNF473	c.40G>A	p.Asp14Asn	missense_variant	MODERATE	0.225	0.004233
chr19	50039255	C	T	ZNF473	c.104C>T	p.Ala35Val	missense_variant	MODERATE	0.22	0.004092
chr19	35787055	G	T	ARHGAP33	c.2102G>T	p.Gly701Val	missense_variant	MODERATE	0.217	0.002159
chr19	33109762	A	G	GPATCH1	c.1331A>G	p.Glu444Gly	missense_variant	MODERATE	0.213	0.005006
chr19	55178341	A	C	SYT5	c.1077>G	p.Val36Gly	missense_variant	MODERATE	0.204	0.0033
chr19	49426549	C	T	GFY	c.119C>T	p.Ser40Phe	missense_variant	MODERATE	0.202	0.002962
chr19	48501306	G	C	LMTK3	c.1065C>G	p.Asp355Glu	missense_variant	MODERATE	0.19	0.00272
chr19	33301726	G	A	CEBPA	c.794C>T	p.Thr265Met	missense_variant	MODERATE	0.161	0.01
chr19	57353836	C	T	ZNF304	c.145C>T	p.Leu49Phe	missense_variant	MODERATE	0.149	0.00614
chr19	48603708	G	A	FAM83E	c.962C>T	p.Ala321Val	missense_variant	MODERATE	0.124	0.003909
chr19	5567702	G	A	TINCR	n.333C>T	n_coding_transcript_exon_vari	MODIFIER		0.095	0.007252
chr19	47754891	G	A	GLTSCR2	c.1053G>A	p.Leu351Leu	region_variant&synonymous_	LOW	0.091	0.004636
chr19	47740875	C	T	EHD2	c.1081-6C>T	-	ce_region_variant&intron_vari	LOW	0.086	0.006505
chr19	17943256	C	T	CCDC124	c.350-5C>T	-	ce_region_variant&intron_vari	LOW	0.085	0.007111
chr19	7847880	G	A	EVI5L	c.286G>A	p.Glu96Lys	missense_variant	MODERATE	0.082	0.006992
chr19	35851511	C	T	NPHS1	c.220G>A	p.Asp74Asn	missense_variant	MODERATE	0.082	0.002594
chr19	48661922	C	T	NTN5	c.1225G>A	p.Ala409Thr	missense_variant	MODERATE	0.081	0.006298
chr19	53175439	C	T	ZNF665	c.142+6G>A	-	ce_region_variant&intron_vari	LOW	0.081	0.014

chr19	49829090	.	G	A	MED25	c.525G>A	p.Glu175Glu	region_variant&synonymous_	LOW	0.079	0.007358	.
chr19	10285108	.	C	T	ICAM1	c.1427-7C>T	.	ce_region_variant&intron_vari	LOW	0.078	0.004183	.
chr19	42134739	.	C	T	TMEM145	c.1404C>T	p.Pro468Pro	region_variant&synonymous_	LOW	0.078	0.004977	.
chr19	17282148	.	C	T	ANKLE1	c.316C>T	p.His106Tyr	missense_variant	MODERATE	0.077	0.004573	.
chr19	17577951	.	C	T	COLGALT1	c.1134-6C>T	.	ce_region_variant&intron_vari	LOW	0.074	0.004277	.
chr19	46838806	.	G	A	AP2S1	c.316-7C>T	.	ce_region_variant&intron_vari	LOW	0.072	0.005765	.
chr19	4324448	.	T	STAP2	c.1285+7G>A	.	ce_region_variant&intron_vari	LOW	0.071	0.005271	.	
chr19	47112509	TTGATGGGCGGCGGCGGGCGATGGCGGCGGCGGCGACTC	T	ZGM4	c.40_75delGATGGCGCCGCCGCCATCGCCGCCGCCGCCATCA	p.Glu14_Ser25delconservative_inframe_deletion	MODERATE	0.069	0.005512	.		
chr19	51416650	.	C	T	LOC100129083	c.236C>T	p.Ser79Phe	missense_variant	MODERATE	0.069	0.002164	.
chr19	16797889	.	G	A	NWD1	c.3459+3G>A	.	ce_region_variant&intron_vari	LOW	0.068	0.0061	.
chr19	42250323	.	G	A	ERF	c.257+8C>T	.	ce_region_variant&intron_vari	LOW	0.068	0.003973	.
chr19	51643998	.	G	A	SIGLEC14	c.793C>T	p.Gln265*	stop_gained	HIGH	0.068	0.006388	.
chr19	35510259	.	G	A	DMKN	c.919-7C>T	.	ce_region_variant&intron_vari	LOW	0.067	0.004656	.
chr19	54930659	.	G	A	NLRP7	c.2650C>T	p.Gln884*	stop_gained	HIGH	0.067	0.005297	.
chr19	2226197	.	G	A	DOT1L	c.3676G>A	p.Gly1226Arg	missense_variant	MODERATE	0.066	0.003278	.
chr19	17647265	.	C	T	UNC13A	c.2044G>A	p.Val682Met	nse_variant&splice_region_va	MODERATE	0.066	0.003836	.
chr19	1108239	.	C	T	SBNO2	c.4082G>A	p.Gly1361Asp	missense_variant	MODERATE	0.065	0.005326	.
chr19	35269599	.	C	T	USF2	c.128C>T	p.Ala43Val	missense_variant	MODERATE	0.065	0.006198	.
chr19	36039315	.	C	T	THAP8	c.672+8G>A	.	ce_region_variant&intron_vari	LOW	0.065	0.004155	.
chr19	5746064	.	G	A	CATSPERD	c.808+1G>A	.	ce_donor_variant&intron_vari	HIGH	0.064	0.004624	.
chr19	45800569	.	G	A	RSPH6A	c.1799-6C>T	.	ce_region_variant&intron_vari	LOW	0.064	0.004067	.
chr19	6375788	.	C	T	PSPN	c.62G>A	p.Gly21Asp	missense_variant	MODERATE	0.063	0.002398	.
chr19	13825719	.	G	A	ZSWIM4	c.2028+6G>A	.	ce_region_variant&intron_vari	LOW	0.063	0.008449	.
chr19	13982114	.	C	T	RFX1	c.621+7G>A	.	ce_region_variant&intron_vari	LOW	0.063	0.006127	.
chr19	40371874	.	G	A	PLD3	c.879+1G>A	.	ce_donor_variant&intron_vari	HIGH	0.063	0.004283	.
chr19	8822091	.	G	A	ZNF558	c.32C>T	p.Ala11Val	nse_variant&splice_region_va	MODERATE	0.062	0.004849	.
chr19	10492265	.	G	A	KEAP1	c.640-3C>T	.	ce_region_variant&intron_vari	LOW	0.062	0.003673	.
chr19	15124925	.	C	T	ILVBL	c.135G>A	p.Lys45Lys	region_variant&synonymous_	LOW	0.062	0.003597	.
chr19	9157363	.	A	G	ZNF317	c.258G>A	p.Met186Ile	missense_variant	MODERATE	0.061	0.005263	.
chr19	12691458	.	C	T	FBXW9	c.679-4G>A	.	ce_region_variant&intron_vari	LOW	0.061	0.005197	.
chr19	18539544	.	C	T	FKBP8	c.462+7G>A	.	ce_region_variant&intron_vari	LOW	0.061	0.005945	.
chr19	50255212	.	C	T	MYH14	c.1946-8C>T	.	ce_region_variant&intron_vari	LOW	0.061	0.006223	.
chr19	46623455	.	C	T	PTGIR	c.768+3G>A	.	ce_region_variant&intron_vari	LOW	0.06	0.004062	.
chr19	48052998	.	C	T	PLA2G4C	c.1609G>A	p.Gly537Arg	nse_variant&splice_region_va	MODERATE	0.06	0.004722	.
chr19	19647600	.	C	T	ATP1A1	c.2792G>A	p.Arg931Lys	nse_variant&splice_region_va	MODERATE	0.059	0.00421	.
chr19	48182759	.	G	A	C19orf68	c.580G>A	p.Glu194Lys	missense_variant	MODERATE	0.059	0.004497	.
chr19	49428101	.	G	A	GFY	c.1339G>A	p.Asp447Asn	missense_variant	MODERATE	0.059	0.003499	.
chr19	2434401	.	C	T	LMNB2	c.1096G>A	p.Val366Met	missense_variant	MODERATE	0.058	0.003044	.
chr19	3747983	.	C	T	TJP3	c.2539C>T	p.Pro847Ser	missense_variant	MODERATE	0.058	0.002762	.
chr19	17989713	.	C	T	KCNN1	c.1171-3C>T	.	ce_region_variant&intron_vari	LOW	0.058	0.004147	.
chr19	35023319	.	G	A	GRAMD1A	c.218G>A	p.Trp728*	stop_gained	HIGH	0.058	0.003544	.
chr19	48022337	.	G	A	ELSPBP1	c.*7+3G>A	.	ce_region_variant&intron_vari	LOW	0.058	0.005933	.
chr19	55809739	.	C	T	NLRP11	c.871G>A	p.Glu291Lys	missense_variant	MODERATE	0.058	0.005215	.
chr19	2987781	.	G	A	TLE6	c.616G>A	p.Asp206Asn	missense_variant	MODERATE	0.057	0.003744	.
chr19	19569443	.	C	T	PBX4	c.768+6G>A	.	ce_region_variant&intron_vari	LOW	0.057	0.005493	.
chr19	48196693	.	C	T	C19orf68	c.2629C>T	p.Arg877Cys	missense_variant	MODERATE	0.057	0.002393	.
chr19	619212	.	G	A	POLRMT	c.3153C>T	p.Gln1051*	tp_gained&splice_region_varia	HIGH	0.056	0.002789	.
chr19	6375765	.	C	T	PSPN	c.85G>A	p.Val29Ile	missense_variant	MODERATE	0.056	0.002212	.
chr19	7485837	.	C	T	PEX11G	c.249+1G>A	.	ce_donor_variant&intron_vari	HIGH	0.056	0.005754	.
chr19	7847743	.	C	T	EVI5L	c.1467C>T	p.Ala450Val	missense_variant	MODERATE	0.056	0.003862	.
chr19	10908131	.	G	A	CARM1	c.439G>A	p.Val147Met	missense_variant	MODERATE	0.056	0.0048	.
chr19	12691161	.	C	T	FBXW9	c.883+5G>A	.	ce_region_variant&intron_vari	LOW	0.056	0.012	.
chr19	18369833	.	C	T	PGPEP1	c.565C>T	p.Leu189Phe	missense_variant	MODERATE	0.056	0.006666	.
chr19	43080926	.	C	T	PSG2	c.385G>A	p.Asp129Asn	missense_variant	MODERATE	0.056	0.002444	.
chr19	49646831	.	G	A	SCAF1	c.478+1G>A	.	ce_donor_variant&intron_vari	HIGH	0.056	0.006152	.
chr19	12799986	.	G	A	PRDX2	c.384C>T	.	structural_interaction_variant	HIGH	0.055	0.006317	.
chr19	15022899	.	C	T	CCDC105	c.1280C>T	p.Thr427Met	missense_variant	MODERATE	0.055	0.006633	.
chr19	45351657	.	C	T	ERCC2	c.2255G>A	p.Arg752Lys	missense_variant	MODERATE	0.055	0.002591	.
chr19	50963308	.	C	T	KLK6	c.439G>A	p.Ala147Thr	missense_variant	MODERATE	0.055	0.004458	.
chr19	54536890	.	C	T	KIR3DX1	n.782C>T	.	n_coding_transcript_exon_vari	MODIFIER	0.055	0.007746	.
chr19	11243334	.	G	A	DOCK6	c.1310C>T	p.Ala437Val	missense_variant	MODERATE	0.054	0.005321	.
chr19	35752169	.	G	A	LIN37	c.35-7G>A	.	ce_region_variant&intron_vari	LOW	0.054	0.006324	.
chr19	40607380	.	C	T	LTBP4	c.1208C>T	p.Ser403Leu	missense_variant	MODERATE	0.054	0.003616	.
chr19	50658044	.	C	T	C19orf81	c.317C>T	p.Pro106Leu	missense_variant	MODERATE	0.054	0.004102	.
chr19	58511265	.	C	T	SLC27A5	c.688+3G>A	.	ce_region_variant&intron_vari	LOW	0.054	0.004007	.
chr19	4428752	.	C	T	OHAF1A	c.1468C>T	p.Pro488Leu	missense_variant	MODERATE	0.053	0.003883	.
chr19	35812472	.	C	T	PRDM12	c.487G>A	p.Gly163Ser	missense_variant	MODERATE	0.053	0.002589	.
chr19	35848405	.	G	A	NPHS1	c.1171-8C>T	.	ce_region_variant&intron_vari	LOW	0.053	0.005299	.
chr19	44793471	.	C	T	CBLC	c.1138-3C>T	.	ce_region_variant&intron_vari	LOW	0.053	0.003981	.
chr19	45093399	.	C	T	PPP1R37	c.74C>T	p.Ala25Val	missense_variant	MODERATE	0.053	0.003253	.
chr19	6746569	.	G	A	TRIP10	c.1262+8G>A	.	ce_region_variant&intron_vari	LOW	0.052	0.007388	.
chr19	10093343	.	C	T	ANGPTL6	c.1222+6G>A	.	ce_region_variant&intron_vari	LOW	0.052	0.006633	.
chr19	13890057	.	C	T	C19orf57	c.799G>A	p.Gly267Arg	missense_variant	MODERATE	0.052	0.002243	.
chr19	15228105	.	G	A	EPHX3	c.617-5C>T	.	ce_region_variant&intron_vari	LOW	0.052	0.006766	.
chr19	19120002	.	C	T	TMEM161A	c.1368G>A	p.Trp456*	stop_gained	HIGH	0.052	0.002958	.
chr19	38426084	.	C	T	RASGRP4	c.80>A	p.Arg3Lys	missense_variant	MODERATE	0.052	0.003763	.
chr19	49614530	.	C	T	PRR12	c.4774-3C>T	.	ce_region_variant&intron_vari	LOW	0.052	0.00609	.
chr19	8601076	.	C	T	ADAMTS10	c.662G>A	p.Gly221Glu	missense_variant	MODERATE	0.051	0.003277	.
chr19	8916613	.	G	A	MUC16	c.36605-8C>T	.	ce_region_variant&intron_vari	LOW	0.051	0.003477	.
chr19	39333069	.	C	T	GMFG	c.200+8G>A	.	ce_region_variant&intron_vari	LOW	0.051	0.008041	.
chr19	49763091	.	C	T	TSKS	c.157G>A	p.Val53Met	missense_variant	MODERATE	0.051	0.004024	.
chr19	804657	.	C	T	PTBP1	c.56G>T	.	structural_interaction_variant	HIGH	0.05	0.002588	.
chr19	7520551	.	C	T	ZNF358	c.1309C>T	p.Leu437Phe	missense_variant	MODERATE	0.05	0.00403	.
chr19	10552878	.	C	T	ATG4D	c.1243-7C>T	.	ce_region_variant&intron_vari	LOW	0.05	0.004084	.
chr19	12138545	.	C	T	ZNF30	c.643G>A	p.Cys214Tyr	missense_variant	MODERATE	0.05	0.004557	.
chr19	63977236	.	C	T	SAMD10	c.262G>A	p.Asp88Asn	missense_variant	MODERATE	0.238	0.003884	.
chr20	57391640	.	C	T	RBM38	c.59C>T	p.Ala20Val	missense_variant	MODERATE	0.136	0.006533	.
chr20	3746032	.	G	A	HSPA12B	c.675+1G>A	.	ce_donor_variant&intron_vari	HIGH	0.095	0.004434	.
chr20	62391251	.	C	T	CABLES2	c.1294G>A	p.Asp432Asn	nse_variant&splice_region_va	MODERATE	0.072	0.004061	.
chr20	49094148	.	G	A	CSE1L	c.2456G>A	p.Gly819Glu	missense_variant	MODERATE	0.071	0.011	.
chr20	51618954	.	C	T	ATP9A	c.2205G>A	p.Glu735Glu	region_variant&synonymous_	LOW	0.069	0.004275	.
chr20	62760037	.	C	T	NTSR1	c.1027C>T	p.His343Tyr	missense_variant	MODERATE	0.069	0.004932	.
chr20	25296364	.	C	T	PYGB	c.2380-6C>T	.	ce_region_variant&intron_vari	LOW	0.067	0.004567	.
chr20	44054529	.	G	A	TOX2	c.879+3G>A	.	ce_region_variant&intron_vari	LOW	0.067	0.006586	.
chr20	46037386	.	G	A	SLC12A5	c.681+5G>A	.	ce_donor_variant&intron_vari	HIGH	0.067	0.005864	.
chr20	33417922	.	G	A	SNTA1	c.498C>T	p.Val166Val	region_variant&synonymous_	LOW	0.066	0.005412	.
chr20	33679750	.	C	T	E2F1	c.572+5G>A	.	ce_region_variant&intron_vari	LOW	0.064	0.004563	.
chr20	34993471	.	G	A	MYH7B	c.2570+1G>A	.	ce_donor_variant&intron_vari	HIGH	0.062	0.004387	.
chr20	37129170	.	G	A	MROH8	c.1650-3C>T	.	ce_region_variant&intron_vari	LOW	0.061	0.007823	.
chr20	49221449	.	C	T	DDX27	c.187-3C>T	.	ce_region_variant&intron_vari	LOW	0.06	0.005769	.
chr20	2394485	.	C	T	TGM6	c.41G>T	p.Ser14Leu	missense_variant	MODERATE	0.058	0.003419	.
chr20	5983170	.	G	A	MCMB	c.1853+5G>A	.	ce_region_variant&intron_vari	LOW	0.058	0.006672	.
chr20	3110164	.	G	A	UBOX5	c.1568C>T	p.Thr523Met	missense_variant	MODERATE	0.057	0.002919	.
chr20	62412837	.	C	T	RBBP8NL	c.1739G>A	p.Gly580Asp	missense_variant	MODERATE	0.057	0.0031	.
chr20	5176642	.	C	T	CDS2	c.292-6C>T	.	ce_region_variant&intron_vari	LOW	0.056	0.00627	.
chr20	33002595	.	C	T	SUN5	c.203G>A	p.Gly68Glu	missense_variant	MODERATE	0.056	0.004944	.
chr20	25284099	.	C	T	PYGB	c.1621-5C>T	.	ce_region_variant&intron_vari	LOW	0.055	0.006606	.
chr20	33008689	.	C	T	BPIFB2	c.109+6C>T	.	ce_region_variant&intron_vari	LOW	0.054	0.00447	.
chr20	1318353	.	G	A	SDCBP2	c.190C>T	p.Gln64*	stop_gained	HIGH	0.053	0.00633	.
chr20	46375661	.	C	T	ELMO2	c.930+7G>A	.	ce_region_variant&intron_vari	LOW	0.053	0.006654	.
chr20	43534374	.	G	A	L3MBTL1	c.1624G>A	p.Val542Met	missense_variant	MODERATE	0.052	0.007384	.
chr20	391356	.	G	A	TRIB3	c.442G>A	p.Ala148Thr	missense_variant	MODERATE	0.051	0.002799	.
chr20	5106297	.	G	A	TMEM230	c.302C>T	p.Pro101Leu	missense_variant	MODERATE	0.051	0.00598	.
chr20	33002588	.	C	T	SUN5	c.210G>A	p.Val70Val	region_variant&synonymous_	LOW	0.05	0.005132	.
chr20	52166032	.	G	A	ZFP64	c.287-7C>T	.	ce_region_variant&intron_vari	LOW	0.05	0.005994	.
chr21	37013544	.	G	A	RIPPLY3	c.172-7G>A	.	ce_region_variant&intron_vari	LOW	0.244	0.006168	.
chr21	43030055	.	C	T	PKNOX1	c.1226C>T	p.Ala422Val	missense_variant	MODERATE	0.179	0.003671	.
chr21	45475495	.	G	A	COL18A1	c.2003G>A	p.Ser668Asn	missense_variant	MODERATE	0.15	0.003109	.
chr21	44324656	.	G	A	PFKL	c.1965+1G>A	.	ce_donor_variant&intron_vari	HIGH	0.087	0.003859	.
chr21	29067573	.	A	C	CCT8	c.364G>T	p.Gly122Cys	missense_variant	MODERATE	0.077	0.009535	.
chr21	37228346	.	G	A	DSCR3	c.535C>T	p.Arg179*	stop_gained	HIGH	0.066	0.008462	.
chr21	42088474	.	G	A	UMODL1	c.784G>A	p.Val262Met	missense_variant	MODERATE	0.065	0.005184	.
chr21	44397742	.	C	T	TRPM2	c.1933-5C>T	.	ce_region_variant&intron_vari	LOW	0.065	0.004528	.
chr21	46311449	.	C	T	C21orf58	c.721+7G>A	.	ce_region_variant&intron_vari	LOW	0.058	0.008879	.
chr21	26844810	.	C	T	ADAMTS1	c.145G>A	p.Ala49Thr	missense_variant	MODERATE	0.052	0.004902	.
chr21	44423646	.	G	A	TRPM2	c.3613G>A	p.Val1205Ile	nse_variant&splice_region_va	MODERATE	0.051	0.005324	.
chr21	37121814	.	C	T	ITCH	c.967-3C>T	.	ce_region_variant&intron_vari	LOW	0.05	0.006273	.
chr21	43970807	.	G	A	AGPAT3	c.664+1G>A	.	ce_donor_variant&intron_vari	HIGH	0.05	0.006462	.
chr22	45009463	CCCCGGCCCCGGGCCCGGCCCCGGCCA	C	PHF21B	c.54+6_54+32delTGGCCGGGGGCCGGGCCCGGGCCGGG	.	ce_region_variant&intron_vari	LOW	0.324	0.006082	.	
chr22	26483906	.	G	T	SRRD	c.16G>T	p.Ala6Ser	missense_variant	MODERATE	0.25	0.02	.
chr22	43143234	.	G	T	MCAT	c.115C>A	p.Leu39Met	missense_variant	MODERATE	0.093	0.002718	.
chr22	49777033	.	C	T	BRD1	c.3121+1G>A	.	ce_donor_variant&intron_vari	HIGH	0.087	0.007396	.
chr22	43838999	.	A	G	SULT4A1	c.382-6C>T	.	ce_region_variant&intron_vari	LOW	0.08	0.00625	.
chr22	41237176	.	C	T	CHADL	c.1896G>A	p.Gln632Gln	region_variant&synonymous_	LOW	0.074	0.004909	.
chr22	41238456	.	G	A	CHADL	c.616C>T	p.Pro206Ser	missense_variant	MODERATE	0.072	0.00263	.
chr22	24177525	.	C	T	CABIN1	c.6227C>T	p.Pro2076Leu	missense_variant	MODERATE	0.069	0.003935	.
chr22	41325566	.	C	T	ZCH7B	c.56C>T	p.Ser19Leu	nse_variant&splice_region_va	MODERATE	0.069	0.007878	.
chr22	37832953	.	C	T	ANKRD54	c.720+5G>A	.	ce_region_variant&intron_vari	LOW	0.068	0.004776	.
chr22	36936653	.	A	G	CSF2RB	c.1568+1G>A	.	ce_donor_variant&intron_vari	HIGH	0.067	0.003815	.
chr22	45197784	.	C	T	KIAA0930	c.1189+6G>A	.	ce_region_variant&intron_vari	LOW	0.066	0.003977	.
chr22	50582293	.	C	T	CHKB	c.289G>A	.	structural_interaction_variant	HIGH	0.065	0.005448	.
chr22	50226060	.	C	T	TUBGCP6	c.1823G>A	p.Cys608Tyr	missense_variant	MODERATE	0.064	0.003266	.
chr22	39664159	.	G	A	CACNA1I	c.3666G>A	p.Lys1222Lys	region_variant&synonymous_	LOW	0.062	0.006745	.
chr22	41897086	.	C	T	SREBF2	c.2530C>T	p.Leu844Phe	missense_variant	MODERATE	0.061	0.009246	.
chr22	41905473	.	G	A	SREBF2	c.3229G>A	p.Arg1080Gln	missense_variant	MODERATE	0.061	0.004899	.
chr22	42079761	.	C	T	SMDT1	c.-8C>T	.	TR_premature_start_codon_ga	LOW	0.061	0.005435	.
chr22	19820614	.	C	T	GNB1L	c.238G>A	p.Gly80Arg	missense_variant	MODERATE	0.06	0.00315	.
chr22	29792538	.	G	A	ASCC2	c.1920-3C>T	.	ce_region_variant&intron_vari	LOW	0.06	0.005613	.
chr22	49777722	.	A	C	BRD1	c.2949C>T	.	sequence_feature	MODERATE	0.058	0.001906	.
chr22	42062840	.	C	T	NAGA	c.944G>A	.	structural_interaction_variant	HIGH	0.057	0.007122	.
chr22	38123096	.	G	A	PLA2G6	c.1590C>T	p.His530His	region_variant&synonymous_	LOW	0.056	0.004676	.
chr22	31088586	.	G	A	SMTN	c.436G>A	p.Val146Met	missense_variant	MODERATE	0.055	0.004599	.
chr22	37244118	.	C	T	RAC2	c.31G>A	.	structural_interaction_variant	HIGH	0.055	0.003532	.
chr22	19919543	.	C	T	TXNRD2	c.229G>A	p.Gly77Ser	nse_variant&splice_region_va	MODERATE	0.054	0.004186	.
chr22	20464892	.	C	T	KLHL22	c.1078G>A	p.Val360Ile	missense_variant	MODERATE	0.054	0.004416	.
chr22	32868962	.	C	T	SYN3	c.621+4G>A	.	ce_region_variant&intron_vari	LOW	0.054	0.005732	.
chr22	19981446	.	C	T	ARVCF	c.661G>A	p.Gly221Ser	missense_variant	MODERATE	0.053	0.002348	.
chr22	23980998	.	C	T	GSTT2_2	c.163C>T	p.Pro55Ser	missense_variant	MODERATE	0.052	0.005299	.
chr22	33604557	.	G	A	LARGE1	c.493C>T	p.Arg165Trp	nse_variant&splice_region_va	MODERATE	0.05	0.005355	.
chr22	36476864	.	G	A	TXN2	c.264-8C>T	.	ce_region_variant&intron_vari	LOW	0.05	0.005346	.
chr22	42432279	.	A	G	NF4M1	c.79C>T	p.Leu27Phe	missense_variant	MODERATE	0.05	0.002883	.
chrX	3674638	.	A	C	PRKX	c.295T>G	p.Ser99Ala	missense_variant	MODERATE	0.361	0.00267	.
chrX	15287929	.	G	A	ASB11	c.799C>T	.	structural_interaction_variant	HIGH	0.348	0.002836	.
chrX	19515152	.	G	A	MAP3K15	c.110C>T	p.Pro37Leu	missense_variant	MODERATE	0.202	0.039	.
chrX	6534127	.	G	A	VCX3A	c.179C>T	p.Ala60Val	missense_variant	MODERATE	0.228	0.003433	.
chrX	53087871	.	G	T	TSPYL2	c.2014G>T	p.Asp672Tyr	missense_variant	MODERATE	0.214	0.00204	.
chrX	119759112	.	T	A	SOWAHD	c.445T>A	p.Tyr149Asn	missense_variant	MODERATE	0.213	0.001787	.
chrX	150649811	.	A	T	MTM1	c.963A>T	p.Leu321Phe	missense_variant	MODERATE	0.2	0.003762	.
chrX	124481752	.	G	T	TENM1	c.3929C>A	p.Ala1310Asp	missense_variant	MODERATE	0.183	0.006055	.
chrX	53194136	.	C	T	KDM5C	c.4038+3G>A	.	ce_region_variant&intron_vari	LOW	0.082	0.002963	.
chrX	17375785	.	C	T	NHS	c.28C>T	p.Pro10Ser	missense_variant	MODERATE	0.075	0.008026	.
chrX	55488942	.	G	A	USP51	c.-3C>T	.	TR_premature_start_codon_ga	LOW	0.069	0.004562	.
chrX	153781139	.	G	A	SRPK3	c.53G>A	p.Ser18Asn	missense_variant	MODERATE	0.066	0.002846	.
chrX	37810783	.	C	T	CYBB	c.1587-8C>T	.	ce_region_variant&intron_vari	LOW	0.062	0.007615	.
chrX	53255942	.	G	A	IQSEC2	c.857C>T	p.Ala286Val	missense_variant	MODERATE	0.061	0.002176	.
chrX	135556300	.	G	A	INTS6L	c.1192G>A	p.Asp398Asn	nse_variant&splice_region_va	MODERATE	0.061	0.009013	.
chrX	153794579	.	C	T	SSR4	c.13C>T	p.Pro5Ser	missense_variant	MODERATE	0.061	0.004985	.
chrX	154546801	.	G	A	G6PD	c.70C>T	p.Arg24*	stop_gained	HIGH	0.06	0.011	.
chrX	55090495	.	C	T	PAGE2	c.85-7C>T	.	ce_region_variant&intron_vari	LOW	0.059	0.005633	.
chrX	35953726	.	G	A	CFAP47	c.1174+7G>A	.	ce_region_variant&intron_vari	LOW	0.057	0.007528	.
chrX	48823676	.	C	T	HDAC6	c.3236C>T	p.Ala1079Val	missense_variant	MODERATE	0.057	0.002775	.
chrX	53428279	.	C	T	RIBC1	c.200-4C>T	.	ce_region_variant&intron_vari	LOW	0.057	0.003585	.
chrX	36099744	.	C	T	CFAP47	c.4999-7C>T	.	ce_region_variant&intron_vari	LOW	0.053	0.00898	.
chrX	49123562	.	C	T	GPKOW	c.161G>A	p.Gly54Glu	missense_variant	MODERATE	0.053	0.003378	.
chrX	31147352	.	C	T	DMD	c.10720G>A	p.Ala3574Thr	missense_variant	MODERATE	0.052	0.00543	.
chrX	29954523	.	C	T	ILIRAPL1	c.1202C>T	p.Asp401Asp	region_variant&synonymous_	LOW	0.051	0.005285	.
chrX	43731235	.	C	T	MAOA	c.646-6C>T	.	ce_region_variant&intron_vari	LOW	0.051	0.003706	.
chrX	74304372	.	T	A	ZCCHC13	c.106T>A	p.Ser36Thr	missense_variant	MODERATE	0.051	0.002113	.
chrX	18908796	.	C	T	PHKA2	c.2360+5G>A	.	ce_region_variant&intron_vari	LOW	0.05	0.006718	.
chrX	48993425	.	C	T	GRIPAP1	c.457+3G>A	.	ce_region_variant&intron_vari	LOW	0.05	0.003198	.
chrX	53194509	.	G	A	KDM5C	c.3668C>T	p.Pro1223Leu	missense_variant	MODERATE	0.05	0.001703	.

chr1	247434133	C	A	NLRP3	c.2358C>A	p.Cys786*	stop_gained	HIGH	0.391	0.005076
chr1	54200266	CAAGG	C	MRPL37	c.24_27delAAGG	p.Arg9fs	frameshift_variant	HIGH	0.241	0.002905
chr1	233372030	T	C	MLK4	c.1553-8T>C	.	ice_region_variant&intron_vari	LOW	0.354	0.005444
chr1	10095453	C	A	UBE4B	c.212-8C>A	.	ice_region_variant&intron_vari	LOW	0.322	0.006045
chr1	15730630	G	T	PLEKHM2	c.2307G>T	p.Glu769Asp	missense_variant	MODERATE	0.249	0.002594
chr1	33014531	C	A	AK2	c.489G>T	p.Met163Ile	missense_variant	MODERATE	0.245	0.009958
chr1	54200271	CGGG	C	MRPL37	c.29_31delGGG	sp10_Ala11delins	disruptive_inframe_deletion	MODERATE	0.236	0.002838
chr1	46286313	C	T	LRRC41	c.544G>A	p.Glu182Lys	missense_variant	MODERATE	0.235	0.002667
chr1	186070755	C	A	HMCN1	c.8137C>A	p.Gln2713Lys	nse_variant&splice_region_va	MODERATE	0.215	0.005
chr1	65636493	C	A	LEPR	c.2976C>A	p.Asn992Lys	missense_variant	MODERATE	0.199	0.003403
chr1	243191402	C	T	CEP170	c.724G>A	p.Glu242Lys	missense_variant	MODERATE	0.191	0.005631
chr1	42927650	G	T	SLC2A1	c.1233C>A	p.Asn411Lys	missense_variant	MODERATE	0.188	0.004297
chr1	46197815	C	T	POMGNT1	c.7G>A	p.Asp3Asn	missense_variant	MODERATE	0.188	0.004538
chr1	186346213	C	G	TPR	c.3018G>C	p.Lys1006Asn	missense_variant	MODERATE	0.14	0.005204
chr2	26470588	C	T	OTOF	c.4023+5G>A	.	ice_region_variant&intron_vari	LOW	0.231	0.005379
chr2	107871074	G	C	RGPD4	c.3070G>C	p.Asp1024His	missense_variant	MODERATE	0.244	0.003111
chr2	133130082	C	A	NCKAP5	c.237G>T	p.Glu79Asp	missense_variant	MODERATE	0.234	0.003741
chr2	24298721	C	G	ITSN2	c.1438G>C	p.Glu480Gln	missense_variant	MODERATE	0.21	0.004866
chr2	208338544	C	T	PIKFYVE	c.4648C>T	p.Pro1550Ser	missense_variant	MODERATE	0.206	0.00613
chr3	36855175	G	C	TRANK1	c.4547C>G	p.Ser1516*	p_gained&splice_region_varia	HIGH	0.263	0.005053
chr3	187370955	C	A	RTP4	c.323C>A	p.Ser108*	stop_gained	HIGH	0.239	0.002863
chr3	179218294	G	A	PIK3CA	c.1624G>A	.	protein_protein_contact	HIGH	0.214	0.005607
chr3	122606056	G	T	PARP15	c.306+1G>T	.	ice_donor_variant&intron_vari	HIGH	0.066	0.009096
chr3	154421401	C	T	GPR149	c.1261G>A	p.Asp421Asn	missense_variant	MODERATE	0.228	0.005268
chr4	55115042	T	G	KDR	c.490A>C	.	protein_protein_contact	HIGH	0.192	0.005499
chr4	743544	GACCTGCTCTGCAAAACAGCACTTAGATTCCC	G	PCGF3	c.335_365delCCTGCTCTGCAAAACAGCACTTAGATTCCCA	p.Thr112fs	frameshift_variant	HIGH	0.174	0.003764
chr4	154589492	C	T	FGA	c.125G>A	p.Arg42Lys	missense_variant	MODERATE	0.215	0.003705
chr4	108014509	G	A	HADH	c.340G>A	p.Asp114Asn	missense_variant	MODERATE	0.214	0.003673
chr4	61983577	C	A	ADGRL3	c.3210C>A	p.Asp1070Glu	missense_variant	MODERATE	0.198	0.004788
chr4	79406957	C	A	GK2	c.1244G>T	p.Cys415Phe	missense_variant	MODERATE	0.166	0.002841
chr5	90724850	TTTCCGTATTTCAAAGTTTTTTGGATGAATCAG	T	ADGRV1	c.9768_9799delTTCCGTATTTCAAAGTTTTTTGGATGAATCAG	p.Ser3257fs	frameshift_variant	HIGH	0.198	0.006358
chr5	177409042	T	A	F12	c.115+4A>T	.	ice_region_variant&intron_vari	LOW	0.153	0.003987
chr5	141864056	C	T	PCDH1	c.2275G>A	p.Gly759Ser	missense_variant	MODERATE	0.286	0.002582
chr5	159972229	G	A	ADRA1B	c.1300G>A	p.Gly434Ser	missense_variant	MODERATE	0.255	0.011
chr5	178986665	ATCT	A	GRM6	c.1586_1588delAGA	p.Lys529del	disruptive_inframe_deletion	MODERATE	0.246	0.001787
chr5	271797	G	C	PDCD6	c.77G>C	p.Ser26Thr	missense_variant	MODERATE	0.168	0.00419
chr6	43132143	G	T	PTK7	c.964G>T	p.Glu322*	stop_gained	HIGH	0.213	0.004219
chr6	34857370	CCTTTCCTGCAGTCGGAAACTTCA	C	UHRF1BP1	c.1475_1497delTTTCCTGCAGTCGGAAACTTCAC	p.Leu492fs	frameshift_variant	HIGH	0.162	0.003208
chr6	42684839	CA	C	UBR2	c.4822delA	p.Ser1608fs	frameshift_variant	HIGH	0.16	0.007527
chr6	125855018	A	C	NCOA7	c.51-2A>C	.	e_acceptor_variant&intron_var	HIGH	0.119	0.009452
chr6	30898070	C	G	DDR1	c.2235-3C>G	.	ice_region_variant&intron_vari	LOW	0.231	0.003028
chr6	119248360	A	C	MAN1A1	c.898-6T>G	.	ice_region_variant&intron_vari	LOW	0.159	0.006513
chr6	32129494	A	C	FKBPL4	c.287T>G	p.Leu96Arg	missense_variant	MODERATE	0.243	0.002221
chr6	34133367	G	A	GRM4	c.130C>T	p.Arg44Cys	missense_variant	MODERATE	0.229	0.002355
chr6	2890514	C	T	SERPINB9	c.780G>A	p.Met260Ile	missense_variant	MODERATE	0.227	0.003543
chr6	30897115	A	T	DDR1	c.1971A>T	p.Leu657Phe	missense_variant	MODERATE	0.223	0.003136
chr6	100848354	ACTT	A	ASCC3	c.592_594delAAG	p.Lys198del	conservative_inframe_deletion	MODERATE	0.207	0.00468
chr6	31645444	G	A	BAG6	c.1097C>T	p.Thr366Ile	missense_variant	MODERATE	0.203	0.001986
chr6	26045695	G	C	HIST1H3C	c.285G>C	p.Glu95Asp	missense_variant	MODERATE	0.122	0.0021
chr7	44073805	AG	A	POLM	c.1051delC	p.Leu351fs	frameshift_variant	HIGH	0.247	0.002851
chr7	44073775	C	:TGCCTACC	POLM	c.1073_1074+7dupAGGTAGGCA	.	ice_region_variant&intron_vari	LOW	0.25	0.003165
chr7	71665403	A	T	WBSCR17	c.1081-8A>T	.	ice_region_variant&intron_vari	LOW	0.219	0.004808
chr7	73682909	T	G	DNAJC30	c.515A>C	p.Tyr172Ser	missense_variant	MODERATE	0.254	0.002868
chr7	103635528	G	T	RELN	c.2362C>A	p.Pro788Thr	missense_variant	MODERATE	0.252	0.004066
chr7	12229698	A	G	TMEM106B	c.461A>G	p.Asn154Ser	missense_variant	MODERATE	0.194	0.008765
chr7	7360402	C	A	COL28A1	c.3193G>T	p.Asp1065Tyr	missense_variant	MODERATE	0.185	0.003913
chr7	20402072	T	G	ITGB8	c.1633T>G	p.Tyr545Asp	missense_variant	MODERATE	0.151	0.006235
chr7	5902718	G	C	CCZ1	c.496G>C	p.Glu166Gln	missense_variant	MODERATE	0.139	0.004654
chr8	58576051	C	G	SDCBP	c.392C>G	p.Ser131*	stop_gained	HIGH	0.208	0.006584
chr8	109430014	TC	T	PKHD1L1	c.3207delC	p.Leu1070fs	frameshift_variant	HIGH	0.153	0.004613
chr8	140541243	TGGATGA	T	AGO2	c.1949_1954delTCATCC	.	structural_interaction_variant	HIGH	0.146	0.002598
chr8	6815904	C	G	XKR5	c.822G>C	p.Glu274Asp	missense_variant	MODERATE	0.237	0.004724
chr8	3187876	GCTTCCCAGT	G	CSMD1	c.5604_5612delACTGGGAAG	rg1868_Gly1870d	disruptive_inframe_deletion	MODERATE	0.197	0.004634
chr8	109441374	A	G	PKHD1L1	c.4199A>G	p.Asp1400Gly	missense_variant	MODERATE	0.184	0.009799
chr8	109968235	C	A	KCNV1	c.1356G>T	p.Lys452Asn	missense_variant	MODERATE	0.168	0.003618
chr9	114307780	T	A	COL27A1	c.5217+2T>A	.	ice_donor_variant&intron_vari	HIGH	0.202	0.004813
chr9	95915660	C	A	ERCC6L2	c.822-8C>A	.	ice_region_variant&intron_vari	LOW	0.29	0.005797
chr9	131482368	C	T	PRRC2B	c.4984-3C>T	.	ice_region_variant&intron_vari	LOW	0.217	0.005765
chr9	130362897	G	T	HMCN2	c.6139G>T	p.Ala2047Ser	missense_variant	MODERATE	0.25	0.003532
chr9	128508900	C	G	GLE1	c.124C>G	p.Leu42Val	missense_variant	MODERATE	0.243	0.004744
chr9	74642467	G	T	RORB	c.289G>T	p.Val97Leu	missense_variant	MODERATE	0.24	0.003565
chr9	133733942	C	G	SARDH	c.232G>C	p.Gly78Arg	missense_variant	MODERATE	0.227	0.002757
chr9	123097815	G	C	RABGAP1	c.2703G>C	p.Glu901Asp	missense_variant	MODERATE	0.222	0.004635
chr10	119826921	C	G	INPP5F	c.2540C>G	p.Ser847Cys	missense_variant	MODERATE	0.259	0.003492
chr10	69157045	A	G	VPS26A	c.268A>G	p.Asn90Asp	missense_variant	MODERATE	0.09	0.007745
chr11	61008651	AC	A	CD6	c.588delC	p.His196fs	frameshift_variant	HIGH	0.33	0.002358
chr11	124895084	G	T	ROBO4	c.1146C>A	p.Tyr382*	stop_gained	HIGH	0.309	0.004462
chr11	5389570	C	G	ORS1M1	c.172C>G	p.Leu58Val	missense_variant	MODERATE	0.345	0.002839
chr11	65396934	G	C	FRMD8	c.717G>C	p.Glu239Asp	missense_variant	MODERATE	0.255	0.002911
chr11	126413625	C	G	ST3GAL4	c.892C>G	p.Gln298Glu	missense_variant	MODERATE	0.254	0.003151
chr11	17719970	C	T	MYOD1	c.188C>T	p.Ser63Leu	missense_variant	MODERATE	0.249	0.001932
chr11	17169142	C	A	PIK3C2A	c.600G>T	p.Leu200Phe	missense_variant	MODERATE	0.238	0.003169
chr11	70486857	G	T	SHANK2	c.3436C>A	p.Pro1146Thr	missense_variant	MODERATE	0.217	0.002548
chr11	64912188	C	A	ATG2A	c.984G>T	p.Trp328Cys	missense_variant	MODERATE	0.214	0.002883
chr11	77907761	C	T	INTS4	c.1972G>A	p.Asp658Asn	missense_variant	MODERATE	0.205	0.006966
chr11	88525351	G	T	GRM5	c.2684C>A	p.Pro895His	missense_variant	MODERATE	0.205	0.004127
chr11	88525358	A	T	GRM5	c.2677T>A	p.Phe893Ile	missense_variant	MODERATE	0.205	0.004025
chr11	54603094	C	A	OR4C46	c.905G>T	p.Arg302Ile	missense_variant	MODERATE	0.143	0.005567
chr12	22471492	C	A	C2CD5	c.2308-4G>T	.	ice_region_variant&intron_vari	LOW	0.211	0.007371
chr12	55221665	T	G	OR10A7	c.641T>G	p.Ile214Ser	missense_variant	MODERATE	0.269	0.00442
chr12	10723096	C	T	YBX3	c.16G>A	p.Glu6Lys	missense_variant	MODERATE	0.258	0.006005
chr12	6774670	G	A	LAG3	c.587G>A	p.Arg196His	missense_variant	MODERATE	0.22	0.004403
chr12	53195684	G	C	ITGB7	c.1013C>G	p.Ser338Cys	missense_variant	MODERATE	0.219	0.002987
chr12	50467078	G	C	LARP4	c.1503G>C	p.Glu501Asp	missense_variant	MODERATE	0.197	0.005143
chr12	12584396	C	G	KNTC1	c.3382C>G	p.Leu1128Val	missense_variant	MODERATE	0.182	0.003599
chr13	41568244	G	A	VWA8	c.5671C>T	p.Gln1891*	stop_gained	HIGH	0.276	0.003678
chr13	44949840	T	A	NUFIP1	c.1022-2A>T	.	e_acceptor_variant&intron_var	HIGH	0.063	0.017
chr14	71624131	AGAAGTGC	A	SIPA1L1	c.1714_1720delGAAGTGC	p.Glu572fs	frameshift_variant	HIGH	0.145	0.00369
chr14	104944211	T	C	AHNAK2	c.11240A>G	p.Lys3747Arg	missense_variant	MODERATE	0.218	0.00174
chr14	59367510	C	G	DAAM1	c.2938C>G	p.Leu980Val	missense_variant	MODERATE	0.213	0.00506
chr14	19876386	T	G	OR4K2	c.119T>G	p.Val40Gly	missense_variant	MODERATE	0.143	0.004491
chr14	44505051	A	T	FSCB	c.1937T>A	p.Val646Asp	missense_variant	MODERATE	0.074	0.005765
chr15	64691536	G	T	OIP2	c.76C>A	p.Pro26Thr	missense_variant	MODERATE	0.277	0.003111
chr15	90904287	A	T	MAN2A2	c.80A>T	p.Asp27Val	missense_variant	MODERATE	0.271	0.003864
chr16	3557657	T	C	NLRC3	c.2035A>G	p.Ser679Gly	missense_variant	MODERATE	0.26	0.004917
chr17	43492757	C	T	DHX8	c.580C>T	p.Arg194*	stop_gained	HIGH	0.15	0.002966
chr17	77213917	G	C	SEC14L1	c.2043-1G>C	.	e_acceptor_variant&intron_var	HIGH	0.147	0.00505
chr17	64562970	G	C	SMURF2	c.1017-4C>G	.	ice_region_variant&intron_vari	LOW	0.146	0.006908
chr17	39706966	G	C	ERBB2	c.74-24G>C	.	sequence_feature	LOW	0.075	0.002434
chr17	81665220	T	C	OXLD1	c.425A>G	p.His142Arg	missense_variant	MODERATE	0.248	0.003685
chr17	1609874	G	A	NCOR1	c.2713C>T	p.Pro905Ser	missense_variant	MODERATE	0.235	0.005664
chr17	51155743	A	G	NME1-NME2	c.89A>G	p.Gln30Arg	missense_variant	MODERATE	0.17	0.005696
chr17	76021905	G	T	EVPL	c.769C>A	p.Leu257Ile	missense_variant	MODERATE	0.152	0.002222
chr17	81720195	G	A	SLC25A10	c.899G>A	p.Arg300His	missense_variant	MODERATE	0.152	0.003029
chr17	39471507	G	T	CDK12	c.1675G>T	p.Ala559Ser	missense_variant	MODERATE	0.145	0.00291
chr17	63761264	C	G	CCDC47	c.635G>C	p.Arg212Pro	missense_variant	MODERATE	0.141	0.004033
chr17	75898961	G	T	MRPL38	c.1032C>A	p.Phe344Leu	missense_variant	MODERATE	0.137	0.002923
chr17	43074364	TCAAATC	T	BRCA1	c.4699_4704delGATTTG	sp1567_Leu1568	conservative_inframe_deletion	MODERATE	0.13	0.003754
chr17	82442546	G	A	HEXDC	c.1712G>A	p.Arg571Lys	missense_variant	MODERATE	0.115	0.002977
chr17	6925824	C	A	ABCA5	c.3885G>T	p.Leu1295Phe	missense_variant	MODERATE	0.097	0.008493
chr19	55490819	G	T	SSCSD	c.634G>T	p.Glu212*	stop_gained	HIGH	0.225	0.002442
chr19	11227414	AGCGCAGCTTGCGGGGGTGTGTCTAGTC	A	DOCK6	c.2852_2877delGACTAGACACACCCGCAAGCTGCGC	p.Arg951fs	frameshift_variant	HIGH	0.19	0.003302
chr19	7849152	C	A	EVI5L	c.552+7C>A	.	ice_region_variant&intron_vari	LOW	0.232	0.004079
chr19	45821483	C	G	SYMPK	c.2794G>C	p.Glu932Gln	nse_variant&splice_region_va	MODERATE	0.229	0.004309
chr19	19642573	G	T	GMIP	c.66C>A	p.Phe22Leu	missense_variant	MODERATE	0.226	0.003912
chr19	50039191	G	A	ZNF473	c.40G>A	p.Asp14Asn	missense_variant	MODERATE	0.225	0.004233
chr19	50039255	C	T	ZNF473	c.104C>T	p.Ala35Val	missense_variant	MODERATE	0.22	0.004092
chr19	35787055	G	T	ARHGAP33	c.2102G>T	p.Gly701Val	missense_variant	MODERATE	0.217	0.002159
chr19	55178341	A	C	SYT5	c.107T>G	p.Val36Gly	missense_variant	MODERATE	0.204	0.0033
chr19	10924142	T	C	YIPF2	c.418A>G	p.Asn140Asp	missense_variant	MODERATE	0.068	0.003599
chr20	63977236	C	T	SAMD10	c.262G>A	p.Asp88Asn	missense_variant	MODERATE	0.238	0.003884
chr20	17481666	G	C	PCSK2	c.1513G>C	p.Glu505Gln	missense_variant	MODERATE	0.163	0.003025
chr20	46054990	G	C	SLC12A5	c.2823G>C	p.Gln941His	missense_variant	MODERATE	0.163	0.004638
chr21	44333261	C	T	C21orf2	c.145G>A	p.Val49Ile	nse_variant&splice_region_va	MODERATE	0.165	0.002463
chr22	45009463	CCCCGGCCCCGGGCCCGGCCCCCGGCCA	C	PHF21B	c.54+6_54+32delTGGCCGGGGCCGGGCCCGGGCCGGG	.	ice_region_variant&intron_vari	LOW	0.324	0.006082
chr22	26483906	G	T	SRRD	c.186G>T	p.Ala62Ser	missense_variant	MODERATE	0.25	0.02
chr22	41636764	G	A	XRCC6	c.583G>A	p.Asp195Asn	missense_variant	MODERATE	0.198	0.00802
chrX	15287929	G	A	ASB11	c.799C>T	.	structural_interaction_variant	HIGH	0.348	0.002836
chrX	124042640	G	C	STAG2	c.457G>C	.	structural_interaction_variant	HIGH	0.16	0.006058
chrX	3674638	A	C	PRKX	c.295T>G	p.Ser99Ala	missense_variant	MODERATE	0.361	0.00267
chrX	19515152	G	A	MAP3K15	c.110C>T	p.Pro37Leu	missense_variant	MODERATE	0.292	0.039
chrX	6534127	G	A	VCX3A	c.179C>T	p.Ala60Val	missense_variant	MODERATE	0.228	0.003433
chrX	53087871	G	T	TSPYL2	c.2014G>T	p.Asp672Tyr	missense_variant	MODERATE	0.214	0.00204
chrX	119759112	T	A	SOWAHD	c.445T>A	p.Tyr149Asn	missense_variant	MODERATE	0.213	0.001787
chrX	150649811	A	T	MTM1	c.963A>T	p.Leu321Phe	missense_variant	MODERATE	0.2	0.003762
chrX	75070501	A	T	ABCB7	c.1232T>A	p.Leu411Gln	missense_variant	MODERATE	0.199	0.003998
chrX	48983091	G	T	GRIPAP1	c.1487C>A	p.Ala496Asp	nse_variant&splice_region_va	MODERATE	0.198	0.00282
chrX	124042593	G	C	STAG2	c.410G>C	p.Arg137Thr	missense_variant	MODERATE	0.17	0.005565
chrX	17727327	C	T	NHS	c.3221C>T	p.Ser1074Leu	missense_variant	MODERATE	0.128	0.00293

Supplementary table 7: Variants in patient 5. Identified by TSO500. Green: shared mutations between tumor at baseline and tumor at progression.

Yellow: unique mutations to baseline tumor. Blue: Unique mutations to progression tumor

CHROM	POS	REF	ALT	GENE	c_change	p_change	Effect	AF_baseline	AF_progression	Ratio
chr8	37686456	G	A	ADGRA2	c.389G>A	p.Gly130Asp	missense_variant	0.0556	0.051	0.92
chr17	16068377	C	G	NCOR1	c.534G>C	p.Lys178Asn	missense_variant	0.0364	0.0408	1.12
chr17	62006662	G	C	CD79B	c.617C>G	p.Ala206Gly	missense_variant	0.0152	0.0179	1.18

Chrom	POS	REF	ALT	Gene	c_Change	p_Change	Effect	AF
chr2	25469985	CACTGCAAA	C	DNMT3A	c.1049_1056del	.Phe350CysfsTer4	frameshift_variant	0.0133
chr3	71247356	TTGC	T	FOXP1	c.174_176del	p.Gln60del	inframe_deletion	0.0217
chr6	94068078	C	T	EPHA7	c.884G>A	p.Arg295His	missense_variant	0.025
chr22	23654012	C	G	BCR	c.3311C>G	p.Ala1104Gly	missense_variant	0.0093
chr3	178936091	G	A	PIK3CA	c.1633G>A	p.Glu545Lys	missense_variant	0.0227
chr16	68862134	TACTG	T	CDH1	c.2223_2226del	Leu741PhefsTer2	frameshift_variant	0.0174
chr17	7577539	G	A	TP53	c.742C>T	p.Arg248Trp	missense_variant	0.012

Supplementary table 8: Variants in patient 6. Identified by TSO500. Green: shared mutations between tumor at baseline and tumor at progression.

Yellow: unique mutations to baseline tumor. Blue: Unique mutations to progression tumor

CHROM	POS	REF	ALT	GENE	c_change	p_change	Effect	AF_baseline	AF_progression	Ratio
chr8	41791414	C	T	KAT6A	NM_006766.4:c.4324G>A	36757.2:p.(Ala144	missense_variant	0.2717	0.4973	1.83
chr17	16068377	C	G	NCOR1	NM_006311.3:c.534G>C	06302.2:p.(Lys178	missense_variant	0.0393	0.0489	1.24
chr20	31022292	A	G	ASXL1	NM_015338.5:c.1777A>G	56153.2:p.(Ile593	missense_variant	0.0086	0.0119	1.38

Chrom	POS	REF	ALT	Gene	c_Change	p_Change	Effect	AF
chr2	198266834	T	C	SF3B1	c.2098A>G	p.Lys700Glu	missense_variant	0.0746
chr3	49724183	C	G	MST1	c.781G>C	p.Glu261Gln	missense_variant	0.0426
chr6	111983041	CT	C	FYN	c.1514del	.Lys505ArgfsTer5	frameshift_variant	0.0111
chr6	137519504	ACT	A	IFNGR1	c.1132_1133del	.Ser378PhefsTer6	frameshift_variant	0.0168
chr6	152419926	A	G	ESR1	c.1613A>G	p.Asp538Gly	missense_variant	0.0551
chr8	41790746	TGGC	T	KAT6A	c.4989_4991del	p.Pro1664del	inframe_deletion	0.0125
chr17	7577094	G	A	TP53	c.844C>T	p.Arg282Trp	missense_variant	0.1192
chr19	47735796	T	A	BBC3	c.64A>T	p.Thr22Ser	missense_variant	0.0993
chr2	25463308	G	A	DNMT3A	c.2185C>T	p.Arg729Trp	missense_variant	0.014
chr11	69624256	G	T	FGF3			downstream_gene_variant	0.0165
chr20	31024452	ACCCTTCAG	A	ASXL1	c.3939_3946del	Leu1314ProfsTer	frameshift_variant	0.0106

Supplementary table 9: Variants in patient 7. Identified by TSO500. Green: shared mutations between tumor at baseline and tumor at progression.

Yellow: unique mutations to baseline tumor. Blue: Unique mutations to progression tumor

CHROM	POS	REF	ALT	GENE	c_change	p_change	Effect	AF_baseline	AF_progression	Ratio
chr1	150000000	G	T	HIST2H3D	c.291C>A	p.Ser97Arg	missense_variant	0.1157	0.136	1.18
chr3	49724172	C	T	MST1	c.792G>A	p.Trp264Ter	stop_gained	0.0332	0.0469	1.41
chr3	49724183	C	G	MST1	c.781G>C	p.Glu261Gln	missense_variant	0.0363	0.0334	0.92
chr17	16068340	C	T	NCOR1	c.571G>A	p.Glu191Lys	missense_variant	0.1429	0.0452	0.32
chr17	16068377	C	G	NCOR1	c.534G>C	p.Lys178Asn	missense_variant	0.1124	0.0682	0.61

Chrom	POS	REF	ALT	Gene	c_Change	p_Change	Effect	AF
chr16	2137924	TCCCTGCAGTGCAGGAAAGGTAGGGCCGGGTGGGG	T	TSC2	c.5068+27_5069-47del		intron_variant	0.0109
chr11	76227182	G	A	EMSY	c.1559-4G>A		intron_variant	0.5061
chr17	58027205	TA	T	RPS6KB1	c.*3058del		3_prime_UTR_variant	0.5127

Supplementary table 10: Variants in patient 8. Identified by TSO500. Green: shared mutations between tumor at baseline and tumor at progression.

Yellow: unique mutations to baseline tumor. Blue: Unique mutations to progression tumor

CHROM	POS	REF	ALT	GENE	c_change	p_change	Effect	AF_baseline	AF_progression	Ratio
chr3	179000000	A	G	PIK3CA	c.3140A>G	p.His1047Arg	missense_variant	0.0444	0.0091	0.20
chr11	119000000	C	G	CBL	c.1250C>G	p.Pro417Arg	missense_variant	0.0814	0.0249	0.31
chr12	25380309	G	A	KRAS	c.149C>T	p.Thr50Ile	missense_variant	0.073	0.0292	0.40
chr17	16068377	C	G	NCOR1	c.534G>C	p.Lys178Asn	missense_variant	0.0429	0.0419	0.98
chr18	39613922	G	A	PIK3C3	:c.1839+1G>A		splice_donor_variant	0.0221	0.0128	0.58

Chrom	POS	REF	ALT	Gene	c_Change	p_Change	Effect	AF
chr1	16259615	G	A	SPEN	c.6880G>A	p.Gly2294Ser	missense_variant	0.0392
chr3	138453522	G	C	PIK3CB	c.926C>G	p.Ser309Cys	missense_variant	0.0468
chr5	79974840	C	T	MSH3	c.1268C>T	p.Pro423Leu	missense_variant	0.0331
chr11	108129785	G	A	ATM	c.2449G>A	p.Asp817Asn	missense_variant	0.0318
chr16	72831196	GTGC	G	ZFHX3	c.5382_5384del	p.Gln1794del	inframe_deletion	0.0139
chr17	16068340	C	T	NCOR1	c.571G>A	p.Glu191Lys	missense_variant	0.0326
chr3	49724183	C	G	MST1	c.781G>C	p.Glu261Gln	missense_variant	0.0331
chr7	106509387	C	T	PIK3CG	c.1381C>T	p.Leu461Phe	missense_variant	0.0104
chr12	31944883	T	C	H3F3C	c.218A>G	p.Glu73Gly	missense_variant	0.0104
chr16	3778302	CGCT	C	CREBBP	c.6743_6745del	p.Gln2248del	inframe_deletion	0.0208
chr21	42837091	G	C	TMPRSS2	c.*978C>G		3_prime_UTR_variant	0.01

Supplementary table 11: Variants in patient 9. Identified by TSO500. Green: shared mutations between tumor at baseline and tumor at progression.

Yellow: unique mutations to baseline tumor. Blue: Unique mutations to progression tumor

CHROM	POS	REF	ALT	GENE	c_change	p_change	Effect	AF_baseline	AF_progression	Ratio
chr3	49724172	C	T	MST1	c.792G>A	p.Trp264Ter	stop_gained	0.0448	0.0546	1.22
chr3	49724183	C	G	MST1	c.781G>C	p.Glu261Gln	missense_variant	0.0441	0.0836	1.90
chr4	185000000	G	A	IRF2	c.991C>T	p.Arg331Trp	missense_variant	0.0505	0.0353	0.70
chr16	68845645	T	TG	CDH1	c.892dup	.Ala298GlyfsTer1	frameshift_variant	0.0397	0.0296	0.75
chr17	15995176	C	A	NCOR1	c.3016+1G>T		splice_donor_variant	0.0395	0.0334	0.85
chr17	16068377	C	A	NCOR1	c.534G>T	p.Lys178Asn	missense_variant	0.0219	0.0283	1.29
chr17	37880261	G	T	ERBB2	c.2305G>T	p.Asp769Tyr	splice_region_variant	0.2369	0.2052	0.87
chr20	46281683	C	T	NCOA3	c.4130C>T	p.Ser1377Phe	missense_variant	0.0486	0.0263	0.54

Chrom	POS	REF	ALT	Gene	c_Change	p_Change	Effect	AF
chr1	158656281	T	C	SPTA1	c.24+3A>G		intron_variant	0.9975
chr6	137519504	ACT	A	IFNGR1	c.1132_1133del	.Ser378PhefsTer6	frameshift_variant	0.0156
chr17	58740623	CA	C	PPM1D	c.1535del	.Asn512IlefsTer2	frameshift_variant	0.0202

References

1. Cardoso F, et al. 5th ESO-ESMO international consensus guidelines for advanced breast cancer (ABC 5). Ann Oncol. 2020;31(12):1623-49.
2. Finn RS, et al. PD 0332991, a selective cyclin D kinase 4/6 inhibitor, preferentially inhibits proliferation of luminal estrogen receptor-positive human breast cancer cell lines in vitro. Breast Cancer Research. 2009;11(5):R77.
3. Johnston S, et al. MONARCH 3 final PFS: a randomized study of abemaciclib as initial therapy for advanced breast cancer. NPJ Breast Cancer. 2019;5:5.
4. Rugo HS, et al. Palbociclib plus letrozole as first-line therapy in estrogen receptor-positive/human epidermal growth factor receptor 2-negative advanced breast cancer with extended follow-up. Breast Cancer Res Treat. 2019;174(3):719-29.
5. Tripathy D, et al. Ribociclib plus endocrine therapy for premenopausal women with hormone-receptor-positive, advanced breast cancer (MONALEESA-7): a randomised phase 3 trial. Lancet Oncol. 2018;19(7):904-15.
6. Herrera-Abreu MT, et al. Early Adaptation and Acquired Resistance to CDK4/6 Inhibition in Estrogen Receptor-Positive Breast Cancer. Cancer Res. 2016;76(8):2301-13.
7. Condorelli R, et al. Polyclonal RB1 mutations and acquired resistance to CDK 4/6 inhibitors in patients with metastatic breast cancer. Ann Oncol. 2018;29(3):640-5.
8. O'Leary B, et al. The Genetic Landscape and Clonal Evolution of Breast Cancer Resistance to Palbociclib plus Fulvestrant in the PALOMA-3 Trial. Cancer Discov. 2018;8(11):1390-403.
9. Wander SA, et al. The Genomic Landscape of Intrinsic and Acquired Resistance to Cyclin-Dependent Kinase 4/6 Inhibitors in Patients with Hormone Receptor-Positive Metastatic Breast Cancer. Cancer Discov. 2020;10(8):1174-93.
10. Formisano L, et al. Aberrant FGFR signaling mediates resistance to CDK4/6 inhibitors in ER+ breast cancer. Nature Communications. 2019;10(1).
11. Dean JL, et al. Therapeutic response to CDK4/6 inhibition in breast cancer defined by ex vivo analyses of human tumors. Cell Cycle. 2012;11(14):2756-61.
12. Alves CL, et al. Co-targeting CDK4/6 and AKT with endocrine therapy prevents progression in CDK4/6 inhibitor and endocrine therapy-resistant breast cancer. Nat Commun. 2021;12(1):5112.
13. Eisenhauer EA, et al. New response evaluation criteria in solid tumours: revised RECIST guideline (version 1.1). Eur J Cancer. 2009;45(2):228-47.
14. Erdi YE. Limits of Tumor Detectability in Nuclear Medicine and PET. Mol Imaging Radionucl Ther. 2012;21(1):23-8.
15. Ulz P, et al. Inferring expressed genes by whole-genome sequencing of plasma DNA. Nat Genet. 2016;48(10):1273-8.
16. Bettegowda C, et al. Detection of circulating tumor DNA in early- and late-stage human malignancies. Sci Transl Med. 2014;6(224):224ra24.
17. Abbosh C, et al. Phylogenetic ctDNA analysis depicts early-stage lung cancer evolution. Nature. 2017;545(7655):446-51.
18. Heitzer E, et al. Establishment of tumor-specific copy number alterations from plasma DNA of patients with cancer. Int J Cancer. 2013;133(2):346-56.
19. Heidary M, et al. The dynamic range of circulating tumor DNA in metastatic breast cancer. Breast Cancer Res. 2014;16(4):421.
20. Diehl F, et al. Circulating mutant DNA to assess tumor dynamics. Nature Medicine. 2008;14(9):985-90.
21. Cingolani P, et al. A program for annotating and predicting the effects of single nucleotide polymorphisms, SnpEff: SNPs in the genome of Drosophila melanogaster strain w1118; iso-2; iso-3. Fly (Austin). 2012;6(2):80-92.
22. Tate JG, et al. COSMIC: the Catalogue Of Somatic Mutations In Cancer. Nucleic Acids Research. 2018;47(D1):D941-D7.
23. Christensen UB, et al. Intercalating Nucleic Acids: The Influence of Linker Length and Intercalator Type on Their Duplex Stabilities. Nucleosides, Nucleotides & Nucleic Acids. 2004;23(1-2):207-25.
24. Riva A, et al. SensiScreen® KRAS exon 2-sensitive simplex and multiplex real-time PCR-based assays for detection of KRAS exon 2 mutations. PLOS ONE. 2017;12(6):e0178027.
25. AACR Project GENIE: Powering Precision Medicine through an International Consortium. Cancer Discov. 2017;7(8):818-31.

26. Jansen VM, et al. Kinome-Wide RNA Interference Screen Reveals a Role for PDK1 in Acquired Resistance to CDK4/6 Inhibition in ER-Positive Breast Cancer. Cancer Research. 2017;77(9):2488-99.
27. Tolosa Ortega P, et al. 57P Benefit of CDK4/6 inhibitors beyond PIK3CA mutations in metastatic breast cancer patients. Annals of Oncology. 2020;31:S35.
28. O'Leary B, et al. Early circulating tumor DNA dynamics and clonal selection with palbociclib and fulvestrant for breast cancer. Nat Commun. 2018;9(1):896.
29. Cristofanilli M, et al. Fulvestrant plus palbociclib versus fulvestrant plus placebo for treatment of hormone-receptor-positive, HER2-negative metastatic breast cancer that progressed on previous endocrine therapy (PALOMA-3): final analysis of the multicentre, double-blind, phase 3 randomised controlled trial. Lancet Oncol. 2016;17(4):425-39.
30. Bai F, et al. PDGFRβ is an essential therapeutic target for BRCA1-deficient mammary tumors. Breast Cancer Research. 2021;23(1):10.
31. Jansson S, et al. The PDGF pathway in breast cancer is linked to tumour aggressiveness, triple-negative subtype and early recurrence. Breast Cancer Res Treat. 2018;169(2):231-41.
32. Su W, et al. ARAF protein kinase activates RAS by antagonizing its binding to RASGAP NF1. Mol Cell. 2022;82(13):2443-57.e7.
33. Xie G, et al. UTX promotes hormonally responsive breast carcinogenesis through feed-forward transcription regulation with estrogen receptor. Oncogene. 2017;36(39):5497-511.
34. Ogino M, et al. Implications of Topoisomerase (TOP1 and TOP2α) Expression in Patients With Breast Cancer. In Vivo. 2020;34(6):3483-7.
35. Luo J, et al. SRC kinase-mediated signaling pathways and targeted therapies in breast cancer. Breast Cancer Research. 2022;24(1):99.
36. Prat A, et al. Circulating tumor DNA reveals complex biological features with clinical relevance in metastatic breast cancer. Nature Communications. 2023;14(1):1157.
37. Hallermayr A, et al. Somatic copy number alteration and fragmentation analysis in circulating tumor DNA for cancer screening and treatment monitoring in colorectal cancer patients. Journal of Hematology & Oncology. 2022;15(1):125.
38. Heitzer E, et al. Tumor-associated copy number changes in the circulation of patients with prostate cancer identified through whole-genome sequencing. Genome Medicine. 2013;5(4):30.
39. Goncalves MD, et al. Phosphatidylinositol 3-Kinase, Growth Disorders, and Cancer. The New England Journal of Medicine. 2018;379(21):2052-62.
40. André F, et al. Alpelisib for PIK3CA-Mutated, Hormone Receptor–Positive Advanced Breast Cancer. New England Journal of Medicine. 2019;380(20):1929-40.
41. Martínez-Sáez O, et al. Frequency and spectrum of PIK3CA somatic mutations in breast cancer. Breast Cancer Research. 2020;22(1):45.
42. Kalinsky K, et al. PIK3CA mutations rarely demonstrate genotypic intratumoral heterogeneity and are selected for in breast cancer progression. Breast Cancer Res Treat. 2011;129(2):635-43.
43. Bertucci F, et al. Comparative genomic analysis of primary tumors and metastases in breast cancer. Oncotarget. 2016;7(19):27208-19.

Chapter 7: General discussion and future perspectives

The treatment of ER+ metastatic breast cancer has been revolutionized by the addition of CDK4/6 inhibitors to endocrine therapy as standard-of-care therapy. Several studies have demonstrated the efficacy of CDK4/6 inhibitors in improving PFS and, for some CDK4/6i, also overall survival in this patient population(1-3). Despite their success, the development of CDK4/6 inhibitor resistance poses a significant clinical challenge, as patients inevitably experience disease progression. As a result, there is a pressing need for a better understanding of the mechanisms of resistance to combined CDK4/6i and endocrine therapy, identification of personalized treatment strategies upon progression, and implementation of strategies for monitoring treatment response.

In manuscript 1, we investigate the mechanisms of resistance to combined CDK4/6i and endocrine therapy in ER+ breast cancer cell lines with acquired resistance to this combined therapy, whereas in manuscript 2 we used tissue and blood samples from ER+ advanced breast cancer patients. The different source material used in the two manuscripts has both advantages and disadvantages. Although cell lines are widely accessible, abundant, reproducible, and low cost, these models do not capture tumor heterogeneity and are usually not clinically relevant (4, 5). In contrast, patient samples are patient specific and clinically relevant however the amount of material available is very limited, particularly with tumor biopsies.

Resistance mechanisms to combined CDK4/6i and endocrine therapy

In manuscript 1, we found that RET overexpression, but not fusions, is likely associated with resistance to combined CDK4/6i and endocrine therapy in two ER+ breast cancer cell lines resistant to combined CDK4/6i and endocrine therapy. RET expression has previously been linked to tamoxifen and AI resistance in ER+ breast cancers by estrogen-independent activation of ER transcriptional activity via the MAPK/ERK and PI3K/AKT pathways, and likely mediated by mTOR (6, 7). Vandetanib, a multikinase inhibitor targeting RET, has been shown to improve the efficacy of tamoxifen resulting in greater reduction of tumor growth in ER+ breast cancer cells (8). Moreover, combined RET inhibitor NVP-AST487 and letrozole synergically inhibited breast cancer cell motility and growth (9). Our findings indicate that blocking RET through siRNA-mediated knockdown or using the specific RET inhibitor selpercatinib restores sensitivity of tumor cells to CDK4/6 inhibitors and fulvestrant treatment. Interestingly, RET inhibition caused downregulation of modulators of G2-M phase progression of the cell cycle. Previous studies have shown that RET upregulates the transcription of cyclin D1, leading to cell cycle

progression and tamoxifen resistance, and this effect was blocked by the addition of a CDK4/6i (10). However, the effect of RET on cell cycle progression in tumor cells resistant to CDK4/6i has not yet been described. To gain further insight into how RET is involved in cell cycle progression, we plan to investigate specific regulators of the cell cycle that are impaired upon RET inhibition, with focus on proteins involved in the regulation of later stages of cell cycle progression. Furthermore, we will investigate these changes following treatment with RETi in combination with CDK4/6i and endocrine therapy to assess the effect of different combinations on cell cycle progression. Additionally, we plan to investigate the efficacy of RETi in xenograft models transplanted with cell lines resistant to combined CDK4/6i and endocrine therapy. Notably, *RET* mutations or amplifications were not identified in tumors and blood samples from patients who progressed on combined CDK4/6i and endocrine therapy (manuscript 2).

Current treatment options following progression on combined CDK4/6i and endocrine therapy are limited. Many patients will receive chemotherapy which often lead to a severe decrease in quality of life. RETi are already approved for patients with thyroid and NSCLC with either activating *RET* mutations or activating *RET* fusions. Importantly, results from a recent clinical trial evaluating the multikinase inhibitor Lenvatinib, which has potent activity against RET, in combination with the AI letrozole showed manageable toxicity profile and promising efficacy in heavily pretreated ER+ advanced breast cancer patients, including patients who progressed on previous combined CDK4/6i and endocrine therapy (11). Notably, ongoing clinical trials are comparing the efficacy of combined RETi lenvatinib or multikinase inhibitors vandetinib or anlotinib with letrozole or fulvestrant, respectively, in patients with AI-resistant ER+ metastatic breast cancer (NCT05181033, NCT02530411, NCT05075512). Another clinical trial is assessing the efficacy of combined lenvatinib, letrozole and the PD-1 inhibitor pembrolizumab in patients with endocrine-resistant ER+ metastatic breast cancer (NCT05286437). Specifically, the RETi selpercatinib is currently being evaluated in solid tumors, including advanced breast cancer, with RET mutations or fusions (NCT03157128). In total, five clinical trials are investigating the use of RETi in the metastatic setting of ER+ breast cancer; however, these mainly include multikinase inhibitors that target other receptor tyrosine kinases besides RET, and only one study investigates RETi in patients who have progressed on combined CDK4/6i and endocrine therapy. Initially we used lenvatinib in our study, but this did not have a significant effect, and we switched to selpercatinib, since this is the most specific and selective RETi.

In manuscript 2, we investigated SNVs in tumor and blood samples from ER+ advanced breast cancer patients to identify mechanisms of resistance and monitor response to

combined CDK4/6i and endocrine therapy. Previous studies have identified *RB* and *FGFR1/2* mutations to be associated with resistance to CDK4/6i (12-14). In our limited study we found *TP53* and *PIK3CA* mutation increased or solely in the progression samples of six patients suggesting that these alterations could be associated with resistance to the treatment in specific patients. Additionally, CNVs have been linked to metastasis in ER+ breast cancer and may be involved in the mechanism of resistance to combined CDK4/6i and endocrine therapy (15). We identified more shared CNVs than SNVs in all patients. For instance, an increase in *PDK1* copy number was observed in three of the four patients with paired tumor samples, following progression on combined CDK4/6i and endocrine therapy, which indicates that *PDK1* amplification may be involved in the resistance mechanisms to combined CDK4/6i and endocrine therapy. As resistance might not depend on the amplification of a single gene, it would be important to assess CNVs of multiple genes, as recently described (16). In this study, the authors have shown that ER+ breast cancer patients exhibiting retinoblastoma loss of heterozygosity (RB-LOH-positive)had worse prognosis on combined CDK4/6i and endocrine therapy than RB-LOH negative patients. RB-LOH status depends on a signature based on DNA copy numbers of chromosomal regions that encompass 345 genes including important cell cycle regulators such as *RB, E2F, CCND1/2/3, CDK6*, and *MYC* (16). The RB-LOH signature was increased in blood samples following progression on combined CDK4/6i and endocrine therapy compared to samples prior to therapy initiation. It would be interesting to investigate the role of other alterations, including as epigenetic modifications (methylation), gene expression (RNA-sequencing), or larger gene insertions/deletions (copy number alteration) in the drug resistance mechanisms in tumor and blood samples from this patient population. A recent study has shown that CDK4/6i treatment induces enhancer activity through AP-1 transcriptional changes and extensive chromatin remodeling in ER+ breast cancer, which may be involved in early adaptations leading to resistance (17). Hydroxymethylation is an epigenetic modification produced by ten-eleven translocation (TET) methylcytosine dioxygenases during cytosine demethylation and it acts as a marker of active promoters (18). New techniques to assess regions with 5-hydroxymethyl cytosines have been developed, and these approaches may reveal surrogates of gene expression that could confer resistance to combined CDK4/6i and endocrine therapy (19, 20).

Monitoring disease progression in liquid biopsies

In manuscript 2, we investigated the potential of using *PIK3CA* mutations in tumor DNA and ctDNA from blood samples to monitor treatment response to combined CDK4/6i and

endocrine therapy in ER+ advanced breast cancer patients. Due to the high inter-patient heterogeneity in breast cancer, we chose to monitor the treatment response by following the variant allele frequency (VAF) of specific *PIK3CA* mutations present in either blood or tissue samples from these patients. Development of assays to detect other patient-specific mutations identified in the cohort included in this study is currently ongoing. Notably, monitoring the *PIK3CA* mutation was indicative of tumor growth in almost all patients. Indeed, an increase in the variant allele frequency (VAF) of the *PIK3CA* mutation was observed either significantly earlier or at the same time as progression diagnosis by imaging techniques. The only case, where it was not observed an increased in *PIK3CA* mutation VAF may indicate that the *PIK3CA* mutation is not present in the resistant cancer subclone that is growing during treatment, even though *PIK3CA* mutations are frequently clonal (21, 22). Multiple assays for detection of a panel of patient-specific mutations could have been used for each patient.

Importantly, numerous new drugs are being developed that target SNP. Indeed, alpelisib has been recently approved for treating ER+ advanced breast cancers with a *PIK3CA* mutation after progression on endocrine therapy with or without CDK4/6i (23). It is unknown whether variants with low frequency are as responsive to targeted therapy as those with high frequency, but some studies indicate that oncogenic drivers with low VAF do respond to targeted therapy, which emphasizes the advantage of monitoring targetable variations and using highly sensitive tests (24).

However, monitoring patient-specific alterations is expensive and time-consuming, and the majority of the ctDNA released into bloodstream is not mutated. Better monitoring of disease burden with emerging methods not tumor-specific such as the LIFE-CNA method which combines fragmentation size, epigenetic signatures, copy number alterations, and machine learning to monitor colorectal cancer and predict progressive disease up to four months before clinical diagnosis (25).

Impact on clinical decision making

In manuscript 1, we found overexpression of RET to be a possible mechanism of resistance to combined CDK4/6i and endocrine therapy. Thus, RET inhibition could be a potential option for patients who progress on combined CDK4/6i and endocrine therapy, but further research is needed to determine which patients are eligible for this therapy. ctDNA monitoring is a promising approach for disease progression and has shown to predict progression earlier than imaging techniques in multiple studies (26-28). In manuscript 2, *PIK3CA* mutation detection in ctDNA allowed detection of progression 4-17 months before clinical diagnosis of disease progression with PET-CT, which could ena-

ble an earlier switch to a potentially more effective treatment, such as alpelisib. However, if no alternative treatments are available, relying on ctDNA analysis alone can be challenging, as clinicians may choose to continue current treatment based on radiological evidence of progression. PET-CT is highly accurate in detecting disease progression in metastatic breast cancer (29), but monitoring progression using patient-specific clonal alterations in ctDNA could complement PET/CT for earlier detection of progression.

Conclusion

The work described in this thesis provides novel insight into the role of RET expression, *TP53* and *PIK3CA* mutations in resistance to combined CDK4/6i and endocrine therapy. Additionally, it contributes to the increasing evidence supporting the potential use of serial ctDNA analysis for real-time monitoring of CDK4/6i response and earlier detection of progressive disease.

References

1. Finn RS, et al. Overall survival (OS) with first-line palbociclib plus letrozole (PAL+LET) versus placebo plus letrozole (PBO+LET) in women with estrogen receptor–positive/human epidermal growth factor receptor 2–negative advanced breast cancer (ER+/HER2− ABC): Analyses from PALOMA-2. Journal of Clinical Oncology. 2022;40(17_suppl):LBA1003-LBA.
2. Llombart-Cussac A, et al. Abstract PD13-11: PD13-11 Final Overall Survival Analysis of Monarch 2 : A Phase 3 trial of Abemaciclib Plus Fulvestrant in Patients with Hormone Receptor-Positive, HER2-Negative Advanced Breast Cancer. Cancer Research. 2023;83(5_Supplement):PD13-1-PD-1.
3. Turner NC, et al. Overall Survival with Palbociclib and Fulvestrant in Advanced Breast Cancer. New England Journal of Medicine. 2018;379(20):1926-36.
4. Burdall SE, et al. Breast cancer cell lines: friend or foe? Breast Cancer Res. 2003;5(2):89-95.
5. Vargo-Gogola T, Rosen JM. Modelling breast cancer: one size does not fit all. Nat Rev Cancer. 2007;7(9):659-72.
6. Plaza-Menacho I, et al. Targeting the receptor tyrosine kinase RET sensitizes breast cancer cells to tamoxifen treatment and reveals a role for RET in endocrine resistance. Oncogene. 2010;29(33):4648-57.
7. Morandi A, et al. GDNF-RET signaling in ER-positive breast cancers is a key determinant of response and resistance to aromatase inhibitors. Cancer Res. 2013;73(12):3783-95.
8. Spanheimer PM, et al. Inhibition of RET increases the efficacy of antiestrogen and is a novel treatment strategy for luminal breast cancer. Clin Cancer Res. 2014;20(8):2115-25.
9. Andreucci E, et al. Targeting the receptor tyrosine kinase RET in combination with aromatase inhibitors in ER positive breast cancer xenografts. Oncotarget. 2016;7(49):80543-53.
10. Marks BA, et al. GDNF-RET signaling and EGR1 form a positive feedback loop that promotes tamoxifen resistance via cyclin D1. BMC Cancer. 2023;23(1):138.
11. Lim JSJ, et al. Phase Ib/II Dose Expansion Study of Lenvatinib Combined with Letrozole in Postmenopausal Women with Hormone Receptor–Positive Breast Cancer. Clinical Cancer Research. 2022;28(11):2248-56.
12. Dean JL, et al. Therapeutic response to CDK4/6 inhibition in breast cancer defined by ex vivo analyses of human tumors. Cell Cycle. 2012;11(14):2756-61.
13. O'Leary B, et al. The Genetic Landscape and Clonal Evolution of Breast Cancer Resistance to Palbociclib plus Fulvestrant in the PALOMA-3 Trial. Cancer Discov. 2018;8(11):1390-403.
14. Formisano L, et al. Aberrant FGFR signaling mediates resistance to CDK4/6 inhibitors in ER+ breast cancer. Nature Communications. 2019;10(1).
15. Bao L, et al. Coexisting genomic aberrations associated with lymph node metastasis in breast cancer. J Clin Invest. 2018;128(6):2310-24.
16. Prat A, et al. Circulating tumor DNA reveals complex biological features with clinical relevance in metastatic breast cancer. Nature Communications. 2023;14(1):1157.
17. Watt AC, et al. CDK4/6 inhibition reprograms the breast cancer enhancer landscape by stimulating AP-1 transcriptional activity. Nature Cancer. 2021;2(1):34-48.
18. Branco MR, et al. Uncovering the role of 5-hydroxymethylcytosine in the epigenome. Nat Rev Genet. 2011;13(1):7-13.
19. Song C-X, et al. 5-Hydroxymethylcytosine signatures in cell-free DNA provide information about tumor types and stages. Cell Research. 2017;27(10):1231-42.
20. Li W, et al. 5-Hydroxymethylcytosine signatures in circulating cell-free DNA as diagnostic biomarkers for human cancers. Cell Res. 2017;27(10):1243-57.
21. Kalinsky K, et al. PIK3CA mutations rarely demonstrate genotypic intratumoral heterogeneity and are selected for in breast cancer progression. Breast Cancer Res Treat. 2011;129(2):635-43.
22. Bertucci F, et al. Comparative genomic analysis of primary tumors and metastases in breast cancer. Oncotarget. 2016;7(19):27208-19.
23. André F, et al. Alpelisib for PIK3CA-Mutated, Hormone Receptor–Positive Advanced Breast Cancer. New England Journal of Medicine. 2019;380(20):1929-40.
24. Jacobs MT, et al. Use of low-frequency driver mutations detected by cell-free circulating tumor DNA to guide targeted therapy in non-small-cell lung cancer: A multicenter case series. JCO Precision Oncology. 2018;2:1-10.

25. Hallermayr A, et al. Somatic copy number alteration and fragmentation analysis in circulating tumor DNA for cancer screening and treatment monitoring in colorectal cancer patients. Journal of Hematology & Oncology. 2022;15(1):125.
26. Chin YM, et al. Serial circulating tumor DNA monitoring of CDK4/6 inhibitors response in metastatic breast cancer. Cancer Sci. 2022;113(5):1808-20.
27. O'Leary B, et al. Early circulating tumor DNA dynamics and clonal selection with palbociclib and fulvestrant for breast cancer. Nat Commun. 2018;9(1):896.
28. Dawson SJ, et al. Analysis of circulating tumor DNA to monitor metastatic breast cancer. N Engl J Med. 2013;368(13):1199-209.
29. Vogsen M, et al. Response monitoring in metastatic breast cancer – a prospective study comparing ¹⁸F-FDG PET/CT with conventional CT. Journal of Nuclear Medicine. 2022:jnumed.121.263358.

Chapter 8: List of abbreviations

Abbreviation	Definition
2D	Two dimensional
3D	Three dimensional
AI	Aromatase Inhibitor
AKT	also known as protein kinase B (PKB)
ANOVA	Analysis of variance
ARAF	A-Raf Proto-Oncogene
AURKA	Aurora Kinase A
BC	Breast cancer
BCA	Bicinchoninic acid assay
BEAM	Beads, emulsion, amplification, and magnetics
CAPP-seq	Cancer personalized profiling by deep sequencing
CDK2	Cyclin dependent kinase 2
CDK4/6	Cyclin dependent kinase 4 and 6
CDK4/6i	CDK4/6 inhibitor
CE-CT	Contrast Enhanced Cranial Computerized Tomograph
cfDNA	Circulating free DNA
CNA	Copy number alteration
CNV	Copy number variation
CTB	CellTiter Blue
ctDNA	Circulating tumor DNA
CV	Crystal violet
ddPCR	Droplet digital PCR
DMEM/F-12	Dulbecco's Modified Eagle Medium
DMSO	Dimethyl sulfoxide
EMA	European Medicines Agency
EPCAM	Epithelial cell adhesion molecule
ER	Estrogen Receptor
ER+	Estrogen Receptor positive
ERK	Extracellular regulated kinaae
ESR1	Gene encoding estrogen receptor
FBS	Fetal bovine serum
FDA	Food and Drug Administration
FDR	False discovery rate
FFPE	Formalin fixed paraffin embedded
FGFR1/2	Fibroblast growth factor receptor 1 and 2
GAPDH	Glyceraldehyde-3-phosphate dehydrogenase
GDNF	Glial cell line-derived neurotrophic factor
GFL	GDNF family of ligands
GFRα1-4	GDNF receptor 1-4
GSEA	Gene set enrichment analysis
HER2	Human epidermal growth receptor 2
HRP	Horseradish peroxidase
IHC	Immunohistochemistry
JAK	Janus Kinase
KD	Knockdown

KDM6A	Lysine Demethylase 6A
LIFE-CNA	Liquid biopsy fragmentation, epigenetic signature and Copy Number Alteration analysis
MAPK	Mitogen-activated protein kinase
MEK/MAPKK	Mitogen-activated protein kinase kinase
MTC	Medullary thyroid cancer
mTOR	Mammalian target of rapamycin
NGS	Next-generation sequencing
NSCLC	Non-small cell lung cancer
OFS	Ovarian function suppression
OS	Overall survival
PDGFRA/B	Platelet derived growth factor receptor alpha/beta
PDK1	Phosphoinositide-dependent kinase-1
PET-CT	Positron emission tomography-computed tomography
PFS	Progression Free Survival
PI3K	Phospatidylinositol 3-kinase
PIK3CA	Phosphatidylinositol-4,5-bisphosphate 3-kinase catalytic subunit alpha
PR	Progesterone receptor
PTC	Papillary thyroid carcinoma
PTEN	Phosphatase and tensin homolog
PUM1	Pumilio RNA Binding Family Member 1
PVDF	Polyvinylidene fluoride
RAF	Rapidly Accelerated Fibrosarcoma
RAS	Rat sarcoma virus
Rb	Retinoblastoma
RET	Rearranged during transfection
RFS	Relapse free survival
RPMI	Roswell Park Memorial Institute Medium,
RT-qPCR	Quantitative real time polymerase chain reaction
SDS-PAGE	Sodium dodecyl sulfate polyacrylamide gel electrophoresis
SERD	Selective estrogen receptor degrader
SERM	Selective estrogen receptor modulater
siRNA	Small interfering RNA
SLIT2	Slit Guidance Ligand 2
SNV	Single nucleotide variation
SRC	SRC Proto-Oncogene, Non-Receptor Tyrosine Kinase
STAT	Signal transducer and activator of transcription
TARDIS	Targeted digital sequencing
TOP1	DNA Topoisomerase I
Tp53	Tumor protein 53
TSC2	Tuberous Sclerosis Complex 2
TSO500	Trusight oncology 500
WB	Western Blot
WES	Whole exome sequencing
WGS	Whole genome sequencing